

# **ENHANCEMENT OF HEAT TRANSFER USING TURBULENCE PROMOTERS**

**A Thesis  
Submitted to the College of Engineering  
of Nahrain University in Partial Fulfillment of the  
Requirements for the Degree of Master of Science  
in  
Chemical Engineering**

**by**

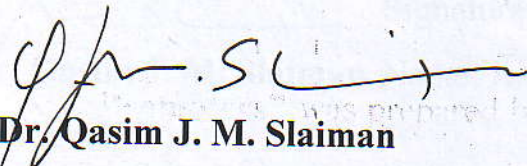
**ABBAS NAWAR ZNAD  
(B.Sc., 1995)**

**Rabee I 1432  
February 2011**

## Certification

I certify that this thesis entitled "**Enhancement of Heat Transfer Using Turbulence Promoters**" was prepared by **Abbas Nawar Znad** under my supervision at Nahrain University/College of Engineering in partial fulfillment of the requirements for the degree of Master of Science in Chemical Engineering..

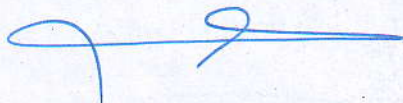
Signature:



Name: **Prof. Dr. Qasim J. M. Slaiman**  
(Supervisor)

Date: **13 / 2 / 2011**

Signature:

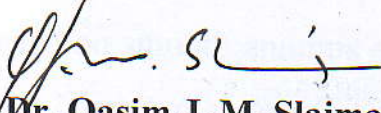


Name: **Asst. Prof. Dr. Basim O. Hasan**  
(Head of Department)

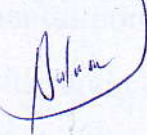
Date: **13 / 2 / 2011**

## Certificate

We certify, as an examining committee, that we have read the thesis entitled "**Enhancement of Heat Transfer Using Turbulence Promoters**", examined the student **Abbas Nawar Znad** in its content and found it meets the standard of thesis for the degree of Master of Science in Chemical Engineering..

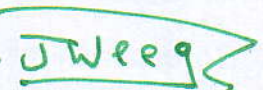
Signature:  Signature:   
Name: Prof. Dr. Qasim J. M. Slaiman Name: Asst. Prof. Dr. Basim O. Hasan  
(Supervisor) (Member)

Date: 13 / 2 / 2011 Date: 13 / 2 / 2011

Signature:  Signature:   
Name: Asst. Prof. Dr. Basma Abbas Name: Asst. Prof. Dr. Balasim A. Abid  
(Member) (Chairman)

Date: 13 / 2 / 2011 Date: 13 / 2 / 2011

Approval of the College of Engineering

Signature:   
Name: Prof. Dr. Muhsin J. Jweeg  
(Dean)  
Date: 21 / 2 / 2011

## ABSTRACT

Three cases of heat transfer enhancement by turbulence promoters were adopted in order to increase the thermal performance of a double pipe heat exchanger of 1245 mm effective length, 28 mm outer diameter and changeable inner diameter (11 or 14 mm). Wire coils of 1 mm diameter and 10, 20, 30 and 40 mm coiling pitches were used as turbulence promoters to augment heat transfer inside the inner tube of heat exchanger at a Reynolds number range of 5000 to 40000 based on smooth tube diameter. Two new types of turbulence promoters are used to enhance heat transfer in the annulus of the same double pipe heat exchanger for a Reynolds number range of 3000 to 10000 based on smooth annulus equivalent diameter. The first was by wire coils of 1 and 2.2 mm diameters and 10, 20, 30 and 40 mm coiling pitches set up on the outer surface of the inner tube. The second was by circular ribs of 2.2 mm diameter and the same pitches and position. Water was used as the working fluid in the two sides. Variation in the experimental conditions was attained by changing the mass flowrates of unenhanced side and changing the inlet temperature of hot fluid. These conditions were followed in order to increase the data points in addition to observe the effect of these conditions.

Heat transfer is increased inside the inner tube by 2.43 folds compared to smooth tube at the same Reynolds number accompanied by friction factor increase of 4.75 folds. For the annulus-side enhancement, heat transfer is increased by 3.25 folds, compared to smooth annulus with an increase of friction factor of 2.63 folds. New correlations of Nusselt number and friction factor for the tube and annulus sides were proposed as functions of Reynolds number, Prandtl number and geometrical characteristics of inserts and sizes of tubes and annuli. In addition, performance evaluation criteria (PEC) were applied to the results, in order to determine the most beneficial method.

# List of Contents

<u>Contents</u>	<u>Page</u>
Abstract	I
List of Contents	II
Notations	VI
List of Tables	IX
List of Figures	XIV
<b>CHAPTER ONE: Introduction</b>	<b>1</b>
1.1    Introduction	1
1.2    Classification of Heat Transfer Enhancement Techniques	1
1.3    Scope of the present work	3
<b>CHAPTER TWO: Literature Review</b>	<b>4</b>
2.1    The Problem of Turbulence	4
2.2    Enhancement of Heat Transfer	5
2.2.1    Enhancement of Heat Transfer by Turbulence Promoters	5
2.2.1.1    Wire coil inserts	5
2.2.1.2    Twisted tapes, helical inserts and twisted angles	8
2.2.1.3    Rod-pin inserts and louvered strips	11
2.2.1.4    Disk and mesh inserts	12
2.2.1.5    Conical nozzles	13
2.2.1.6    Twisted and corrugated tubes	13
2.2.1.7    Ribbed surfaces and channels	15
2.2.2    Enhancement of heat transfer in the annulus of a double-pipe heat exchanger	16
<b>CHAPTER THREE: Theoretical Background</b>	<b>18</b>
3.1    Introduction	18
3.2    Turbulent Fluid Flow and Heat Transfer	18
3.2.1    Fluid Flow and Heat Transfer in Circular Tubes	18

3.2.2	Fluid Flow and Heat Transfer in the Annulus of Concentric Tubes	21
3.2.3	Empirical Correlations of Turbulent Fluid Flow and Heat Transfer in Tubes Inserted with Wire Coils	24
3.3	Mechanisms of Heat Transfer Augmentation by Turbulence Promoters	26
3.4	Performance Evaluation Criteria (PEC)	29
3.4.1	Objective Functions and Constraints	30
3.4.2	Algebraic Formulation of the PEC	31
3.5	Thermal Design of the Double Pipe Heat Exchangers	33
<b>CHAPTER FOUR: Experimental Work</b>		<b>34</b>
4.1	Experimental Rig Design and Assembly	34
4.1.1	Components of the Experimental Rig	37
4.1.1.1	Hot Fluid Unit	37
4.1.1.2	Cold Fluid Unit	37
4.1.1.3	Flow Measurement Instrumentation	38
4.1.1.4	Pressure Measurement Instrumentation	39
4.1.1.5	Temperature Measurement Instrumentation	40
4.1.1.6	Pipes, Pumps, and Valves	40
4.1.1.7	Test Section (Double-Pipe Heat Exchanger)	40
4.1.2	Turbulence Promoter Selection and Fabrication	43
4.2	Operation of the System	44
4.2.1	Isothermal Pressure Drop Experiments	44
4.2.2	Heat Exchange Experiments	46
4.3	Calculation procedure	48
4.3.1	Prediction of Physical Properties	48
4.3.2	Isothermal Pressure Drop Calculations	49
4.3.3	Heat Transfer Calculations	49
4.4	Error Sources and Uncertainty	51

<b>CHAPTER FIVE: Experimental Results</b>	<b>52</b>
5.1        Introduction	52
5.2        Test of Authenticity of Using the Present Heat Exchanger	52
5.3        The Effect of Turbulence Promoters on Heat Transfer Rate and Pressure Drop	55
5.4        Effect of Turbulence Promoters on Friction Factor	60
5.4.1    Friction Factor in Heat Exchange Process	60
5.4.2    Friction Factor in Isothermal Process	62
5.5        Effect of Turbulence Promoters on Heat Transfer	65
5.6        Proposed Correlations of Friction Factor and Nusselt Number	70
5.6.1    Concise Description of Inserts	70
5.6.2    Proposed Correlations of Friction Factor	70
5.6.3    Proposed Correlations of Nusselt Number	74
<b>CHAPTER SIX: Discussion</b>	<b>77</b>
6.1        Introduction	77
6.2        The Influence of the Experimental Conditions	77
6.3        Friction Factor in Enhanced Tubes and Annuli	80
6.3.1    The Effect of the Wire or Rib Diameter and Coiling or Ribbing Pitch on Friction Factor	80
6.3.2    The Effect of the Annulus Diameter Ratio ( $D_i/D_o$ )	82
6.3.3    The Effect of Disruption Shape of Insert on Friction Factor	83
6.3.4    The Dependency of Friction Factor on Reynolds Number	83
6.3.5    Friction Factor Augmentation	84
6.3.5.1  Friction Factor Augmentation for Tube-Side Heat Transfer Enhancement	84
6.3.5.2  Friction Factor Augmentation for Annulus-Side Heat Transfer Enhancement by Wire Coil	87

6.3.5.3	Friction Factor Augmentation for Annulus-Side Heat Transfer Enhancement by Circular Ribs	89
6.4	Heat Transfer in Enhanced Tubes and Annuli	90
6.4.1	The Effect of the Wire or Rib Diameter and Coiling or Ribbing Pitch on Nusselt Number	91
6.4.2	The Effect of the Annulus Diameter Ratio ( $D_i/D_o$ )	93
6.4.3	The Dependency of Nusselt Number on Reynolds Number	94
6.4.4	The Effect of Prandtl Number on Heat Transfer	95
6.4.5	Nusselt Number Augmentation	95
6.4.5.1	Nusselt Number Augmentation for Tube-Side Heat Transfer Enhancement	95
6.4.5.2	Nusselt Number Augmentation for Annulus-Side Heat Transfer Enhancement by Wire Coil	99
6.4.5.3	Nusselt Number Augmentation for Annulus-Side Heat Transfer Enhancement by Circular Ribs	101
6.5	Performance Evaluation Criteria (PEC)	103
6.5.1	PEC Application for Tube-Side Heat Transfer Enhancement	104
6.5.2	PEC Application for Annulus-Side Heat Transfer Enhancement	112
<b>CHAPTER SEVEN: Conclusions and Recommendations</b>		120
7.1	Conclusions	120
7.2	Recommendations	121
<b>References</b>		122
<b>Appendix A</b>	Physical Properties of Liquid Water	A-1
<b>Appendix B</b>	Calibration of Measurement Instrumentations	B-1
<b>Appendix C</b>	Experimental and Predicted Results	C-1

## Notations

<b>Symbols</b>	<b>Description</b>
A	Heat exchange surface area [ $\text{m}^2$ ]
$A_c$	Cross-sectional area [ $\text{m}^2$ ]
$C_f$	Fanning friction factor [—]
$C_p$	Heat capacity [ $\text{J/kg.}^\circ\text{C}$ ]
d	Tube diameter [m]
$D_e$	Equivalent diameter of annulus based on fluid flow [m]
$D_e$	Equivalent of annulus [m]
$D_i$	Inner diameter of annulus[m]
$D_o$	Outer diameter of annulus [m]
e	Wire or rib diameter [m]
$E_h$	Enhancement ratio [—]
$f$	Darcy friction factor [—]
G	Mass flux [ $\text{kg}/\text{m}^2\text{s}$ ]
h	Convective heat transfer coefficient [ $\text{W}/\text{m}^2.^\circ\text{C}$ ]
j	Colburn factor ( $\text{Nu}/\text{Re Pr}^{1/3}$ ) [—]
k	Thermal conductivity [ $\text{W}/\text{m.}^\circ\text{C}$ ]
L	Length [m]
$\dot{m}$	Mass flowrate [ $\text{kg}/\text{s}$ ]
N	Number of tubes of shell and tube heat exchanger
Nu	Nusselt number ( $hd/k$ ) [—]
p	Coiling or ribbing pitch [m]
P	Pumping Power [W]
Pr	Prandtl number ( $C_p\mu/k$ ) [—]
q	Heat transfer rate [W]
r	Radius [m]
Re	Reynolds number ( $\rho d v/\mu$ ) [—]

$Re_o$	Reynolds number in smooth tube for PEC calculations [—]
St	Stanton number (Nu/Re Pr) [—]
T	Temperature [ $^{\circ}\text{C}$ ]
U	Overall heat transfer coefficient
y	Twist ratio (twisted tape insert) [—]
$\Delta H$	Enthalpy difference [kJ/kg]
$\Delta p$	Pressure drop [N/m <sup>2</sup> ]
$\Delta T_i$	Approach temperature difference [ $^{\circ}\text{C}$ ]
Q	Volumetric flowrate [m <sup>3</sup> /s]

### Greek Symbols

$\mu$	Dynamic viscosity [Pa.s]
$\beta$	Coiling angle (Bergles equation)
$\delta$	Tape thickness (twisted tape) [m]
$\theta$	Disruption shape corner (Bergles equation)
$v$	Fluid Velocity [m/s]
$\rho$	Density [kg/m <sup>3</sup> ]

### Subscripts

1,2,3,4	The four temperatures of the heat exchanger
a	Augmented
b	Bulk, both
c	Cold, cross-sectional, corrected
e	Equivalent
h	Hot, hydraulic
i	Inner, inlet
m	Mean
o	Outer, outlet, smooth in PEC calculations
p	Pass

s      Smooth  
w      Wall

### **Superscript**

n      exponent of Prandtl number

### **Abbreviations**

ID      Inner diameter of tube  
OD      Outer diameter of tube  
PEC      Performance Evaluation criteria  
LMTD      Logarithmic Mean Temperature Difference

## List of Tables

<u>Table No.</u>	<u>Title of Table</u>	<u>Page</u>
3-1	Performance Evaluation Criteria for Single-Phase Forced Convection in Enhanced Tubes	30
5-1	Deviations of Experimental Nusselt and Friction Factor from Theoretical Values for Smooth Inner Tubes and Annuli	55
A-1	Physical Properties of Liquid Water	A-1
B-1	Calibration of Thermocouples	B-1
B-2	Calibration of the Rotameter at 20, 40, 60 and 70 °C	B-2
B-3	Calibration of the Orifice Plate at 60 and 70 °C	B-4
C-1	Experimental Results of Tube-Side Heat Transfer Enhancement for Two Sizes of Inner Tube (Smooth Tube)	C-2
C-2	Experimental Results of Tube-Side Heat Transfer Enhancement for Two Sizes of Inner Tube (Wire coil, $e=1$ mm, $p = 10$ mm)	C-3
C-3	Experimental Results of Tube-Side Heat Transfer Enhancement for Two Sizes of Inner Tube (Wire coil, $e=1$ mm, $p = 20$ mm)	C-4
C-4	Experimental Results of Tube-Side Heat Transfer Enhancement for Two Sizes of Inner Tube (Wire coil, $e=1$ mm, $p = 30$ mm)	C-5
C-5	Experimental Results of Tube-Side Heat Transfer Enhancement for Two Sizes of Inner Tube (Wire coil, $e=1$ mm, $p = 40$ mm)	C-6
C-6	Experimental Results of Annulus-Side Heat Transfer Enhancement for Two Annulus Sizes (Smooth Annulus)	C-7
C-7	Experimental Results of Annulus-Side Heat Transfer Enhancement for Two Annulus Sizes (Wire Coil, $e = 1$ mm, $p = 10$ mm)	C-8

- C-8      Experimental Results of Annulus-Side Heat Transfer C-9  
          Enhancement for Two Annulus Sizes (Wire Coil,  $e = 1$   
          mm,  $p = 20$  mm)
- C-9      Experimental Results of Annulus-Side Heat Transfer C-10  
          Enhancement for Two Annulus Sizes (Wire Coil,  $e = 1$   
          mm,  $p = 30$  mm)
- C-10     Experimental Results of Annulus-Side Heat Transfer C-11  
          Enhancement for Two Annulus Sizes (Wire Coil,  $e = 1$   
          mm,  $p = 40$  mm)
- C-11     Experimental Results of Annulus-Side Heat Transfer C-12  
          Enhancement for Two Annulus Sizes (Wire Coil,  $e = 2.2$   
          mm,  $p = 10$  mm)
- C-12     Experimental Results of Annulus-Side Heat Transfer C-13  
          Enhancement for Two Annulus Sizes (Wire Coil,  $e = 2.2$   
          mm,  $p = 20$  mm)
- C-13     Experimental Results of Annulus-Side Heat Transfer C-14  
          Enhancement for Two Annulus Sizes (Wire Coil,  $e = 2.2$   
          mm,  $p = 30$  mm)
- C-14     Experimental Results of Annulus-Side Heat Transfer C-15  
          Enhancement for Two Annulus Sizes (Wire Coil,  $e = 2.2$   
          mm,  $p = 40$  mm)
- C-15     Experimental Results of Annulus-Side Heat Transfer C-16  
          Enhancement for Two Annulus Sizes (Circular Ribs,  
           $e = 2.2$  mm,  $p = 10$  mm)
- C-16     Experimental Results of Annulus-Side Heat Transfer C-17  
          Enhancement for Two Annulus Sizes (Circular Ribs,  $e$   
          = $2.2$  mm,  $p = 20$  mm)
- C-17     Experimental Results of Annulus-Side Heat Transfer C-18  
          Enhancement for Two Annulus Sizes (Ribs,  $e = 2.2$  mm,  
           $p = 30$  mm)
- C-18     Experimental Results of Annulus-Side Heat Transfer C-19  
          Enhancement for Two Annulus Sizes (Circular Ribs,  $e$   
          = $2.2$  mm,  $p = 40$  mm)

- C-19 Predicted Results ( $Re_{s,c}$ ,  $Pr$ ,  $f$ ,  $h$ ,  $Nu$  and empirical values of  $f_{s,i}$  and  $Nu_{s,i}$ ) for Tube-Side Heat Transfer Enhancement for Two Sizes of Inner Tube (Tube) C-20
- C-20 Predicted Results ( $Re_{s,c}$ ,  $Pr$ ,  $f$ ,  $h$ ,  $Nu$ ,  $f_a/f_s$  and  $Nu_a/Nu_s$ ) for Tube-Side Heat Transfer Enhancement for Two Sizes of Inner Tube (Wire Coil,  $e = 1$  mm,  $p = 10$  mm) C-21
- C-21 Predicted Results ( $Re_{s,c}$ ,  $Pr$ ,  $f$ ,  $h$ ,  $Nu$ ,  $f_a/f_s$  and  $Nu_a/Nu_s$ ) for Tube-Side Heat Transfer Enhancement for Two Sizes of Inner Tube (Wire Coil,  $e = 1$  mm,  $p = 20$  mm) C-22
- C-22 Predicted Results ( $Re_{s,c}$ ,  $Pr$ ,  $f$ ,  $h$ ,  $Nu$ ,  $f_a/f_s$  and  $Nu_a/Nu_s$ ) for Tube-Side Heat Transfer Enhancement for Two Sizes of Inner Tube (Wire Coil,  $e = 1$  mm,  $p = 30$  mm) C-23
- C-23 Predicted Results ( $Re_{s,c}$ ,  $Pr$ ,  $f$ ,  $h$ ,  $Nu$ ,  $f_a/f_s$  and  $Nu_a/Nu_s$ ) for Tube-Side Heat Transfer Enhancement for Two Sizes of Inner Tube (Wire Coil,  $e = 1$  mm,  $p = 40$  mm) C-24
- C-24 Predicted Results ( $Re_{s,h}$ ,  $Pr$ ,  $f$ ,  $h$ ,  $Nu$  and empirical values of  $f_{s,o}$  and  $Nu_{s,o}$ ) for Annulus-Side Heat Transfer Enhancement for Two Annulus Sizes (Smooth Annulus) C-25
- C-25 Predicted Results ( $Re_{s,h}$ ,  $Pr$ ,  $f$ ,  $h$ ,  $Nu$ ,  $f_a/f_s$  and  $Nu_a/Nu_s$ ) for Annulus-Side Heat Transfer Enhancement for Two Annulus Sizes (Wire Coil,  $e = 1$  mm,  $p = 10$  mm) C-26
- C-26 Predicted Results ( $Re_{s,h}$ ,  $Pr$ ,  $f$ ,  $h$ ,  $Nu$ ,  $f_a/f_s$  and  $Nu_a/Nu_s$ ) for Annulus-Side Heat Transfer Enhancement for Two Annulus Sizes (Wire Coil,  $e = 1$  mm,  $p = 20$  mm) C-27
- C-27 Predicted Results ( $Re_{s,h}$ ,  $Pr$ ,  $f$ ,  $h$ ,  $Nu$ ,  $f_a/f_s$  and  $Nu_a/Nu_s$ ) for Annulus-Side Heat Transfer Enhancement for Two Annulus Sizes (Wire Coil,  $e = 1$  mm,  $p = 30$  mm) C-28
- C-28 Predicted Results ( $Re_{s,h}$ ,  $Pr$ ,  $f$ ,  $h$ ,  $Nu$ ,  $f_a/f_s$  and  $Nu_a/Nu_s$ ) for Annulus-Side Heat Transfer Enhancement for Two Annulus Sizes (Wire Coil,  $e = 1$  mm,  $p = 40$  mm) C-29
- C-29 Predicted Results ( $Re_{s,h}$ ,  $Pr$ ,  $f$ ,  $h$ ,  $Nu$ ,  $f_a/f_s$  and  $Nu_a/Nu_s$ ) for Annulus-Side Heat Transfer Enhancement for Two Annulus Sizes (Wire Coil,  $e = 2.2$  mm,  $p = 10$  mm) C-30

- C-30 Predicted Results ( $Re_{s,h}$ ,  $Pr$ ,  $f$ ,  $h$ ,  $Nu$ ,  $f_a/f_s$  and  $Nu_a/Nu_s$ ) C-31  
for Annulus-Side Heat Transfer Enhancement for Two  
Annulus Sizes (Wire Coil,  $e = 2.2$  mm,  $p = 20$  mm)
- C-31 Predicted Results ( $Re_{s,h}$ ,  $Pr$ ,  $f$ ,  $h$ ,  $Nu$ ,  $f_a/f_s$  and  $Nu_a/Nu_s$ ) C-32  
for Annulus-Side Heat Transfer Enhancement for Two  
Annulus Sizes (Wire Coil,  $e = 2.2$  mm,  $p = 30$  mm)
- C-32 Predicted Results ( $Re_{s,h}$ ,  $Pr$ ,  $f$ ,  $h$ ,  $Nu$ ,  $f_a/f_s$  and  $Nu_a/Nu_s$ ) C-33  
for Annulus-Side Heat Transfer Enhancement for Two  
Annulus Sizes (Wire Coil,  $e = 2.2$  mm,  $p = 40$  mm)
- C-33 Predicted Results ( $Re_{s,h}$ ,  $Pr$ ,  $f$ ,  $h$ ,  $Nu$ ,  $f_a/f_s$  and  $Nu_a/Nu_s$ ) C-34  
for Annulus-Side Heat Transfer Enhancement for Two  
Annulus Sizes (Circular Ribs,  $e = 2.2$  mm,  $p = 10$  mm)
- C-34 Predicted Results ( $Re_{s,h}$ ,  $Pr$ ,  $f$ ,  $h$ ,  $Nu$ ,  $f_a/f_s$  and  $Nu_a/Nu_s$ ) C-35  
for Annulus-Side Heat Transfer Enhancement for Two  
Annulus Sizes (Circular Ribs,  $e = 2.2$  mm,  $p = 20$  mm)
- C-35 Predicted Results ( $Re_{s,h}$ ,  $Pr$ ,  $f$ ,  $h$ ,  $Nu$ ,  $f_a/f_s$  and  $Nu_a/Nu_s$ ) C-36  
for Annulus-Side Heat Transfer Enhancement for Two  
Annulus Sizes (Circular Ribs,  $e = 2.2$  mm,  $p = 30$  mm)
- C-36 Predicted Results ( $Re_{s,h}$ ,  $Pr$ ,  $f$ ,  $h$ ,  $Nu$ ,  $f_a/f_s$  and  $Nu_a/Nu_s$ ) C-37  
for Annulus-Side Heat Transfer Enhancement for Two  
Annulus Sizes (Circular Ribs,  $e = 2.2$  mm,  $p = 40$  mm)
- C-37 Isothermal Pressure Drop and Friction Factor for Smooth C-38  
and Augmented Tubes (Using a Wire Coil of  $e = 1$  mm  
and  $p = 10, 20, 30$ , and  $40$  mm) for Water Flowing at  $20$ ,  
 $40$ ,  $60$ , and  $70$  °C
- C-38 Isothermal Pressure Drop and Friction Factor for Smooth C-39  
and Augmented Annuli (Using a Wire Coil of  $e = 1$  mm  
and  $p = 10, 20, 30$ , and  $40$  mm) for Water Flowing at  $20$ ,  
 $40$ ,  $60$ , and  $70$  °C
- C-39 Isothermal Pressure Drop and Friction Factor for Smooth C-40  
and Augmented Annuli (Using a Wire Coil of  $e = 2.2$   
mm and  $p = 10, 20, 30$ , and  $40$  mm) for Water Flowing at  
 $20$ ,  $40$ ,  $60$ , and  $70$  °C

- C-40 Isothermal Pressure Drop and Friction Factor for Smooth C-41  
and Augmented Annuli (Using Circular Ribs of  $e = 2.2$   
mm and  $p = 10, 20, 30$ , and  $40$  mm) for Water Flowing at  
 $20, 40, 60$ , and  $70$  °C
- C-41 Description of Turbulence Promoters (Inserts) in Terms C-42  
of the Dimensionless Parameters ( $e/d_i$ ) and ( $p/d_i$ ) or  
( $e/D_e$ ) and ( $p/D_e$ )
- C-42 Application of FG-2a Criterion to the Tube-Side Heat C-43  
Transfer Enhancement for all Geometrical Characteristics  
and Conditions
- C-43 Application of FG-3 Criterion to the Tube-Side Heat C-44  
Transfer Enhancement for all Geometrical Characteristics  
and Conditions
- C-44 Application of FN-1 Criterion to the Tube-Side Heat C-45  
Transfer Enhancement for all Geometrical Characteristics  
and Conditions
- C-45 Application of FG-2a Criterion to the Annulus-Side Heat C-46  
Transfer Enhancement for all Geometrical Characteristics  
and Conditions
- C-46 Application of FG-3 Criterion to the Annulus-Side Heat C-47  
Transfer Enhancement for all Geometrical Characteristics  
and Conditions
- C-47 Application of FN-1 Criterion to the Annulus-Side Heat C-48  
Transfer Enhancement for all Geometrical Characteristics  
and Conditions

## List of Figures

<u><b>Figure No.</b></u>	<u><b>Title of Figure</b></u>	<u><b>Page</b></u>
1-1	Enhanced tubes for augmentation of single-phase heat transfer	2
2-1	compound wire coil/ twisted tape insert tested by Eiamsa-ard et al	8
2-2	Devices used by Promvonge, et al.	9
2-3	Test tube used by Eiamsa-ard and Promvonge	10
2-4	A twisted angle	11
2-5	Rod-pin inserts used by Nazrul Islam et al.	12
2-6	Louvered strips with forward and backward arrangements	12
2-7	Mesh inserts	13
2-8	Completed twisted tube bundle	14
2-9	The V corrugated plates used by Naphon	15
2-10	Enhanced annulus adopted by Agrawal et al.	16
2-11	Schematic representation of angled spiraling tape heat exchanger	17
3-1	Internal enhancement geometries and profile shapes considered by Ravigururajan and Bergles	25
3-2	An enhanced tube with the separation and reattachment mechanism	27
3-3	Recirculation flow patterns over transverse ribs as a function of rib spacing	28
4-1	A photograph of the experimental rig	35
4-2	A schematic flow diagram of the experimental rig	36
4-3	Sketch of the double-pipe heat exchanger used in the present work	41
4-4	Pressure taps	42
4-5	Turbulence promoters used in the present work	43

4-6	An algorithm for calculations of tube-side heat transfer enhancement	50
5-1	Comparison of empirical and experimental friction factor of smooth tubes used in tube-side heat transfer enhancement experiments for two tube sizes	53
5-2	Comparison of empirical and experimental Nusselt number inside the smooth tubes used in tube-side heat transfer enhancement experiments	53
5-3	Comparison of empirical and experimental friction factor of smooth annuli used in annulus-side heat transfer enhancement experiments	54
5-4	Comparison of empirical and experimental Nusselt number of smooth annuli used in annulus-side heat transfer enhancement experiments	54
5-5	Heat transfer rate (W) and pressure drop ( $\text{N}/\text{m}^2$ ) vs. Reynolds number for tube-side heat transfer enhancement using a wire coil of $e = 1 \text{ mm}$	56
5-6	Heat transfer rate (W) and pressure drop ( $\text{N}/\text{m}^2$ ) vs. Reynolds number for annulus-side heat transfer enhancement by wire coils of $e = 1 \text{ mm}$	57
5-7	Heat transfer rate (W) and pressure drop ( $\text{N}/\text{m}^2$ ) vs. Reynolds number for annulus-side heat transfer enhancement by wire coils of $e = 2.2 \text{ mm}$	58
5-8	Heat transfer rate (W) and pressure drop ( $\text{N}/\text{m}^2$ ) vs. Reynolds number for annulus-side heat transfer enhancement by circular ribs of $e = 2.2 \text{ mm}$	59
5-9	Friction factor vs. Reynolds number for heat exchange process inside the inner tube inserted with a wire coil of $e = 1 \text{ mm}$	60
5-10	Friction factor vs. Reynolds number for annulus-side heat transfer enhancement by wire coils of $e = 1 \text{ mm}$ (heat exchange process)	61
5-11	Friction factor vs. Reynolds number for annulus-side	61

	heat transfer enhancement by wire coils of $e = 2.2$ mm (heat exchange process)	
5-12	Friction factor vs. Reynolds number for annulus-side heat transfer enhancement by circular ribs of $e = 2.2$ mm (heat exchange process)	62
5-13	Friction factor vs. Reynolds number for smooth tube and roughened by a wire coil of $e = 1$ mm in isothermal conditions	63
5-14	Friction factor vs. Reynolds number for smooth annulus and with a wire coil of $e = 1$ mm in isothermal conditions	63
5-15	Friction factor vs. Reynolds number for smooth annulus and with a wire coil of $e = 2.2$ mm in isothermal conditions	64
5-16	Friction factor vs. Reynolds number for smooth annulus and with circular ribs of $e = 2.2$ mm in isothermal conditions	64
5-17	Nusselt number vs. Reynolds number for tube-side heat transfer enhancement using a wire coil of $e = 1$ mm	66
5-18	Nusselt number vs. Reynolds number for annulus-side heat transfer enhancement using a wire coil of $e = 1$ mm	67
5-19	Nusselt number vs. Reynolds number for annulus-side heat transfer enhancement using a wire coil of $e = 2.2$ mm	68
5-20	Nusselt number vs. Reynolds number for annulus-side heat transfer enhancement using circular ribs of $e = 2.2$ mm	69
6-1	Friction factor augmentation vs. Reynolds number for tube-side heat transfer enhancement using a wire coil of $e = 1$ mm	85
6-2	Comparison of present work friction factor with that of previous works for tube-side heat transfer enhancement by wire coil of $e/d_i = 0.1$ and $p/d_i = 1.2$	87

6-3	Friction factor augmentation vs. Reynolds number for annulus-side heat transfer enhancement using two wire coils of 1 and $e=2.2$ mm	88
6-4	Friction factor augmentation vs. Reynolds number for annulus-side heat transfer enhancement using circular ribs of $e = 2.2$ mm for two annulus sizes	90
6-5	Nusselt number augmentation vs. Reynolds number for inner tube-side heat transfer enhancement using a wire coil of $e=1$ mm	97
6-6	Comparison of Nusselt number resulted in the present work with that of previous works for tube-side heat transfer enhancement with wire coil of $e/d_i=0.1$ and $p/d_i= 1.2$ and $\text{Pr} = 3.0$	98
6-7	Nusselt number augmentation vs. Reynolds number for annulus-side heat transfer enhancement using two wire coils of $e = 1$ and $2.2$ mm for two annulus sizes	100
6-8	Nusselt number augmentation vs. Reynolds number for annulus-side heat transfer enhancement using circular ribs of $e= 2.2$ mm	102
6-9	Application of the performance evaluation criterion (FG-2a) to the tube-side heat transfer enhancement by wire coils	106
6-10	Application of the performance evaluation criterion (FG-3) to the tube-side heat transfer enhancement by wire coils	108
6-11	Application of the performance evaluation criterion (FN-1) to the tube-side heat transfer enhancement by wire coils	111
6-12	Application of the performance evaluation criterion (FG-2a) to the annulus-side heat transfer enhancement by wire coils and circular ribs	115
6-13	Application of the performance evaluation criterion (FG-3) to the annulus-side heat transfer enhancement	117

	by wire coils and circular ribs	
6-14	Application of the performance evaluation criterion (FN-1) to the annulus-side heat transfer enhancement by wire coils and circular ribs	119
A-1	Physical properties of liquid water	A-2
B-1	Calibration of the rotameter at 20, 40, 60 and 70 °C	B-2
B-2	An orifice plate design	B-3
B-3	Calibration of the orifice at 60 and 70 °C	B-4

# **CHAPTER ONE**

## **Introduction**

### **1.1 Introduction**

The conversion, utilization, and recovery of energy in every industrial, commercial, and domestic application involve a heat exchange process. Some common examples are steam generation in power plants; sensible heating and cooling of viscous media in thermal processing of chemical, pharmaceutical, and agricultural products; refrigerant evaporation and condensation in air conditioning and refrigeration; gas flow heating in manufacturing and waste-heat recovery; air and liquid cooling of engine and turbomachinery systems; and cooling of electrical machines and electronic devices. Improved heat exchange, can significantly improve the thermal efficiency in such applications as well as the economics of their design and operation.

Enhancement techniques essentially reduce the thermal resistance in a conventional heat exchanger by promoting higher convective heat transfer coefficient with or without surface area increases. As a result, the size of a heat exchanger can be reduced, or the heat duty of an existing exchanger can be increased, or the pumping power requirements can be reduced, or the exchanger's operating approach temperature difference can be decreased [1].

### **1.2 Classification of Heat Transfer Enhancement Techniques**

Generally, enhancement techniques can be classified either as passive or active methods. In the first class, no direct application of external power is required, but, to the surface configuration, the enhancement of heat transfer belongs. Treated or roughened surfaces are used for boiling and condensation

by coating the surface with fine-scale roughness which also might be beneficial, when its height is larger to enhance heat transfer in single-phase. The latter might be produced in many configurations ranging from random sand-grain type roughness to discrete protuberances, all to disturb the laminar sublayer rather than increasing the heat transfer surface area.

Displaced enhancement devices, such as in fig. 1-1 are inserted into the flow channel, in forced flow operation, so as indirectly to improve energy transport at the heated surface. A category of those is Swirl-flow devices which include a number of geometric arrangements or tube inserts that create rotating and secondary flow, for example coiled tubes, inlet vortex generators, twisted-tape inserts, wire coils.

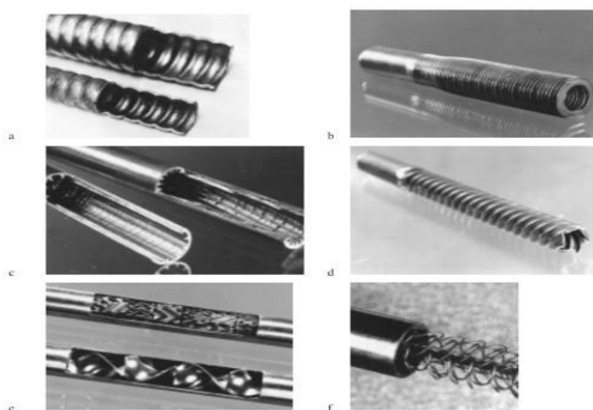


**Figure 1-1:** Enhanced tubes for augmentation of single-phase heat transfer.

The second class of enhancement techniques requires external power. It might include Mechanical aids which involve stirring the fluid by mechanical means or by rotating the surface especially in batch processing of viscous liquids in the chemical process industry; vibration of surface at either low or high frequency or vibration of fluid itself with a range from pulsations of about 1 Hz to ultrasound. Single-phase fluids are of primary concern; AC or

DC electrostatic fields; injection of particular gas to the stagnant or flowing liquids; and suction or removal of vapors in nucleate boiling [1, 2].

In many cases heat transfer enhancement in tubes can be supplemented by heat transfer enhancement on the outside wall of tubes, as for double pipe heat exchangers. An application is in vapor compression hot-water heat pumps. The condensing refrigerant may typically flow in the inner tube and the water to be heated in a counter flow direction in the annulus. In this case, heat transfer enhancement on the outer wall is also important. Like these heat exchangers are suitable when one or both of the fluids is at very high pressure because containment in the small-diameter pipe or tubing is less costly than containment in a large-diameter shell. Furthermore, double pipe exchangers are generally used for small-capacity applications where the total heat transfer surface area required is  $50 \text{ m}^2$  or less [3, 4].

### **1.3 Scope of the present work**

The present work aims to study the application of wire coil inserts and circular ribs as turbulence promoters to enhance heat transfer, with different conditions and assembling positions of a double pipe heat exchanger. It is comprised of three parts; the first is using the coiled wire insert as a turbulence promoter inside the inner tube of heat exchanger using a wire with one diameter; the second part is using a coiled wire with two diameters on the outer surface of the inner tube; and finally using circular rib turbulence promoters on the outer surface of the inner tube.

All experiments would be implemented using the same double pipe heat exchanger but with two inner tubes. Different experimental conditions and dimensions are employed to obtain large quantity of data to be used to obtain empirical correlations for heat transfer and pressure drop.

# CHAPTER TWO

## Literature Review

### 2.1 The Problem of Turbulence

Turbulent fluid flow is a complex, nonlinear multiscale phenomenon, which poses some of the most difficult and fundamental problems in classical physics. It is also of tremendous practical importance in making predictions, for example, about heat transfer in nuclear reactors, drag in oil pipelines, the weather, and the circulation of the atmosphere and the oceans. Many generations of scientists have struggled valiantly to understand both the physical essence and the mathematical structure of turbulent fluid motion. **Leonardo da Vinci in (1507)** named the phenomenon observed in swirling flow “la turbolenza” [5].

The scientific study of turbulence had generally begun with the work of **Osborne Reynolds in (1883)**. The problem that Reynolds had studied was the classic one of flow through long straight pipes of constant diameter and circular cross-section. Using his “method of color bands”, he was the first person to show that, for a given fluid and pipe, the flow would be orderly (laminar) for velocities below a certain critical speed. At the critical speed, the flow abruptly became turbulent at some distances from the pipe entrance.

Reynolds found that the criterion for the transition from laminar to turbulent flow could be expressed in universal form in the terms of the value taken by dimensionless group

$$\text{Re} = \frac{\rho dv}{\mu} \quad \dots (2.1)$$

where Re is what is now called the Reynolds number [6].

Reynolds noted that the main motion of the flow took place in the direction of the axis of the pipe. Because of the flow fluctuations, a great amount of mixing occurred in the turbulent flow, leading to a transverse motion perpendicular to the main motion. Reynolds discovered that the transition from laminar to turbulent flow always took place at almost exactly the same Reynolds number ( $Re_{crit}=2300$ ). For  $Re < Re_{crit}$ , the flow is laminar, and turbulent for  $Re > Re_{crit}$ . He already suspected that the critical Reynolds number will be larger if the disturbances in the incoming flow are smaller [7].

## **2.2 Enhancement of Heat Transfer.**

Here, a brief survey for the most recent works performed in the field of heat transfer enhancement in single-phase flow is included concentrating on those that depends on turbulence caused by devices or inserts installed in the flow passage which may be referred to as “turbulence promoters”. Some studies, stated here, ascribe the enhancement of heat transfer to vortices or swirls generated by these devices; the present survey will include, for the reason that such phenomena may occur together with turbulence.

### **2.2.1 Enhancement of Heat Transfer by Turbulence Promoters**

To make it easy to understand and compare the different types of turbulence promoters, a simple classification, built on the basis of similarity in configuration and the manner of work for each group, is introduced in the following sections.

#### **2.2.1.1 Wire coil inserts.**

Wire coils inserts are currently used in applications as oil cooling devices, preheaters or fire boilers. They showed several advantages with respect to other enhancement techniques:

1. Low cost.
2. Easy installation and removal.
3. Preservation of original plain tube mechanical strength.
4. Possibility of installation in an existing smooth tube heat exchanger [8].

Many correlations had been set for predicting the heat transfer and pressure drop. **Ravigururajan and Bergles in (1985)** [1, 2] proposed what might be the most famous method for predicting heat transfer and pressure drop inside internally ribbed tubes and plain tubes with coiled wire inserts.

**Kumar et al., in (1970)** [9] examined the influence of wire coils inserted in a tube on the heat transfer and the pressure drop. Water was used as the test fluid. The pitch ( $p/d_i=1.05-5.5$ ) and the wire size ( $e/d_i=0.1-0.15$ ) were employed. They had maximum increase of heat transfer of 280% with a large increase of pressure drop. They developed the following relation:

$$\frac{Nu_a}{Pr^{1/3}} = 0.0554(f Re^3)^{0.286} \quad \dots (2.2)$$

This equation was found to be independent of the tube diameter  $d_i$ , the wire diameter  $e$ , the pitch  $p$  and the test fluid [9].

**Zhang et al., in (1991)** [10] investigated heat transfer and friction factor of hot air, regarding the influence of pitches and wire diameter of the helical coils in tubes. They used air as the flowing fluid, heated to  $200\pm5^\circ\text{C}$ , and obtained the following correlation

$$Nu_a = 0.253 Re^{0.716} \left( \frac{e}{d_i} \right)^{0.372} \left( \frac{p}{d_i} \right)^{-0.171} \quad \dots (2.3)$$

which was considered to be valid for:  $6000 \leq Re \leq 100000$ ,  $0.037 \leq e/d_i \leq 0.10$  and  $0.35 \leq p/d_i \leq 2.50$ .

**Viedma, et al. in (2005) [8]**, had experimentally studied wire coils inserted in a round tube in order to obtain their thermodynamic behavior in laminar, transition and turbulent flows. They used water and propylene glycol mixtures at different concentrations, for a range of Reynolds number of 100 to 90,000 and Prandtl number from 2.8 to 200. They tested six wire coil inserts with different geometric range of helical pitch and wire diameter. Their results showed that the wire coil increased pressure drop up to 9 times and heat transfer up to 4 times compared to the empty smooth tube. Their proposed correlation for Nusselt number was:

$$Nu_a = 0.132(p/d_i)^{-0.372} Re^{0.72} Pr^{0.37} \dots (2.4)$$

They concluded that the wire coil diameter had a slight influence on heat transfer. The corresponding correlation of friction factor for Reynolds numbers from 2000 to 30000 was:

$$C_{f_a} = 5.76 (e/d_i)^{0.95} (p/d_i)^{1.21} Re^{-0.217} \dots (2.5)$$

They recommended that equation (2.5) might overpredict up to 15 % the experimental values.

**Eiamsa-ard et al., in (2010) [11]** studied experimentally heat transfer, friction factor and thermal performance behaviors in a tube equipped with the combined devices between the twisted tape and constant and periodically varying wire coil pitch ratio. The experiments were conducted in a turbulent flow regime with Reynolds numbers ranging from 4600 to 20000 using air as the test fluid. They found that heat transfer rate was further augmented by the compound devices by 3.65 times compared to plane tube, 1.39 times compared to wire coil insert and 2.34 times compared to tube inserted with twisted tape. Correspondingly, the friction factor augmentation was about 28.8, 2.24 and 8.37 respectively.



**Figure 2-1:** Compound wire coil/ twisted tape insert tested by Eiamsa-ard et al [11].

### 2.2.1.2 Twisted tapes, helical inserts and twisted angles.

Twisted tape inserts cause the flow to spiral along the tube. Their potential performance is diminished because the thermal contact of the tape and the tube wall is not ideal, so they do not perform as “wall-attached roughness”. They enhance the heat transfer due to the increased tangential velocity component and reduced flow cross section [51].

**Manglik and Bergles in 1992 [12]** proposed the following friction factor correlation for tubes with twisted tape inserts in turbulent flow regime:

$$C_{fa} = \frac{0.0791}{Re^{0.25}} \left[ \frac{\pi}{\pi - 4(\delta/d_i)} \right]^{1.75} \left[ \frac{\pi + 2 - 2(\delta/d_i)}{\pi - 4(\delta/d_i)} \right]^{1.25} \left[ 1 + \frac{2.752}{y^{1.29}} \right] \quad \dots (2.6)$$

where:

$$y = \frac{p}{2d_i} \quad \dots (2.7)$$

Their corresponding heat transfer correlation for turbulent flows was:

$$\frac{Nu_a}{Nu_{y=\infty}} = 1 + \frac{0.769}{y} \quad \dots (2.8)$$

and  $Nu_{y=\infty}$  for straight tape:

$$Nu_{y=\infty} = 0.023 Re^{0.8} Pr^{0.4} \left( \frac{\pi}{\pi - 4\delta/d_i} \right)^{0.8} \left( \frac{\pi + 2 - 2t/d_i}{\pi - 4\delta/d_i} \right)^{0.2} \left( \frac{\mu_b}{\mu_w} \right)^n \quad \dots (2.9)$$

where the exponent  $n$  is equal to 0.18 for heating and 0.30 for cooling.

**Promvonge, et al., in 2004 [13]** studied experimentally the influence of helical tapes inserted in a tube on heat transfer enhancement, fig. 2-2. Their swirling flow devices were a full-length helical tape with or without a centered-rod, and a regularly-spaced helical tape, inserted in the inner tube of a concentric tube heat exchanger. Hot air was passed through the inner tube, whereas cold water flowed in the annulus. They concluded that full-length helical tape with rod provides the highest heat transfer rate about 10% better than that without rod but with increased pressure drop. They found that regularly spaced helical tape inserts at spacing ratio=0.5 yielded the highest Nusselt number which was about 50% above the plain tube.

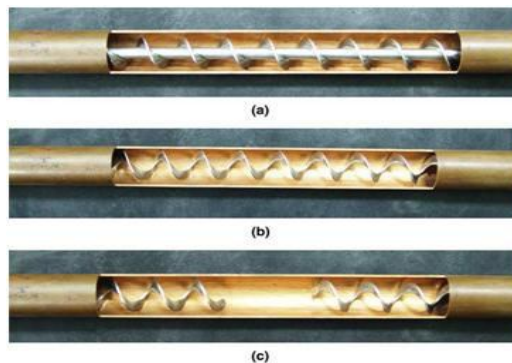


**Figure 2-2:** Devices used by Promvonge, et al., [13].

**Ahmed et al., in 2005 [14]** performed an experimental investigation on heat transfer and pressure drop characteristics in a circular tube fitted with twisted tape inserts, at three different twist ratios ( $y=23, 11.5$  and  $8$ ). They concluded that the average heat transfer coefficient was about 1.3 to 3 times higher than that of the smooth tube.

**Promvonge et al., in 2006 [15]** studied experimentally the influence of the twisted tape insertion on heat transfer and flow friction in double pipe heat exchanger. In the experiments, the swirling flow was introduced by using twisted tape placed inside the inner test tube of the heat exchanger with

different twist ratios,  $y=5$  and  $7$ . Over the range investigated, they found that the maximum increase in Nusselt number was for using the enhancement devices with  $y=5$  became 188% higher than that for plain tube.

**Eiamsa-ard and Promvonge in 2006 [16]** investigated the heat transfer and pressure drop characteristics in a circular wavy-surfaced tube with a helical-tape insert, fig. 2-3. In the experiment, the turbulence flow near the tube wall was produced by using wavy surfaced wall while the swirling flow was generated by inserting the helical-tape along the core region. The Nusselt numbers for the tube with wavy-surfaced wall was found 1.9 to 2.0 times that for the plain tube, while for the tube combined with wavy-surfaced wall and a helical-tape insert, were 2.48 to 2.67 times, and pressure drops were seen to be 9.3 to 22.3 times the plain tube.

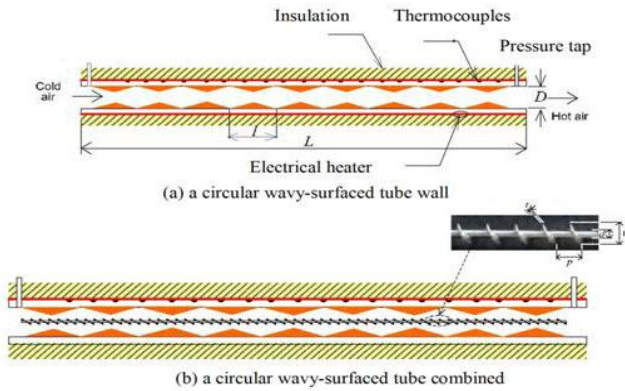


**Figure 2-3:** Test tube used by Eiamsa-ard and Promvonge [16].

**Kumar et al., in 2008 [17]**, studied the development and testing of modified solar water heater having twisted tape inserted inside the tubes along with plain one for the range of flow Reynolds number as  $4000 < Re < 20000$ , and twist pitch ratio of between 3 and 12. Experimental results showed that in the range of parameters investigated, thermal enhancement factor varied between 1.18 to 2.7 and the maximum value of collector efficiency increased by about 30% compared to that of plain ones at same operational conditions.

**Gouda and Bikram in 2008 [18]** studied the determination of friction factor and heat transfer coefficient for various twisted angles, fig. 2-4, having different twist ratios. They observed that the heat transfer coefficient could vary from 1.16 to 2.87 times the smooth tube value but the corresponding friction factor increased by 4 to 9.6 times the smooth tube values.



**Figure 2-4:** A twisted angle [18].

**Yadav in 2009 [19]** investigated experimentally influences of the half length twisted tape inserted inside the inner tube of a U-bend double pipe heat exchanger. The heat transfer coefficient was found to increase by 40% with half-length twisted tape inserts when compared with plain heat exchanger. It was found that on the basis of equal mass flow rate, the heat transfer performance of half-length twisted tape was better than plain heat exchanger.

**Thianpong et al. in 2009 [20]** investigated experimentally the friction factor heat transfer behaviors in a dimpled tube fitted with a twisted tape swirl generator using air as working fluid in the range of Reynolds number of 12000 to 44000. They found that both heat transfer coefficient and friction factor in the dimpled tube fitted with the twisted tape, were higher than those in the dimple tube acting alone and plain tube.

### **2.2.1.3 Rod-pin inserts and louvered strips.**

**Nazrul Islam et al., in 2007 [21]** investigated experimentally the pressure drop and heat transfer in a tube with rod-pin, fig. 2-5 with air as the working fluid. They indicated that heat transfer increased by three folds.

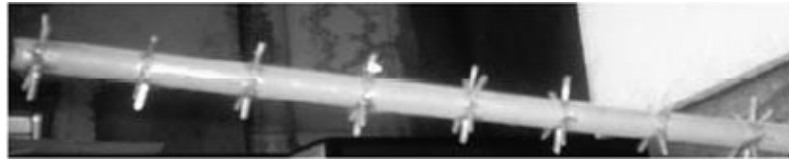


**Figure 2-5:** Rod-pin inserts used by Nazrul Islam et al., [21].

**Promvonge et al., in 2007** [22] investigated experimentally, heat transfer and friction characteristics, employing louvered strips inserted in a concentric tube heat exchanger, fig. 2-6 with water used as working fluid. They obtained increases in average Nusselt number and friction loss for the inclined forward louvered strip about 284% and 413% while those for the backward louvered strip were 263% and 233% over the plain tube, respectively.

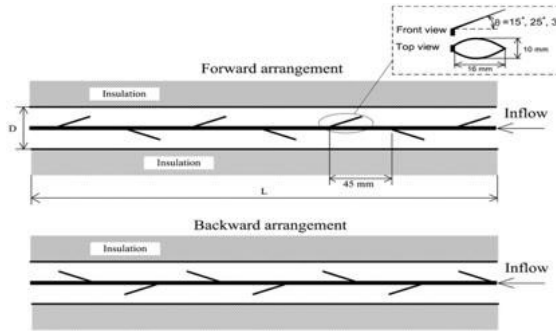


**Figure 2-6:** Louvered strips with forward and backward arrangements [22].

#### 2.2.1.4 Disk and mesh inserts

**Alemrajabi et al., in 2006** [23] studied experimentally the effects of insertion of disks with different geometries on heat transfer in the flow of air in a tube. The disks were elliptic in shape with an elliptical or rectangular hole in the center and were either perpendicular to the flow or at angle relative to the flow. They found that disks were more effective at higher Reynolds numbers.

**Raju et al., in 2009** [24] investigated experimentally the augmentation of turbulent flow heat transfer in a horizontal tube by means of mesh inserts, fig. 2-7, with air as the working fluid with different types of mesh inserts with

different screen diameters and distances between the screens in the porosity range of 99.73 to 99.98 were considered for experimentation. It was observed that the enhancement of heat transfer by using mesh inserts when compared to plain tube at the same mass flow rate was more by a factor of 2 times, whereas the pressure drop was only about a factor of 1.45 times.

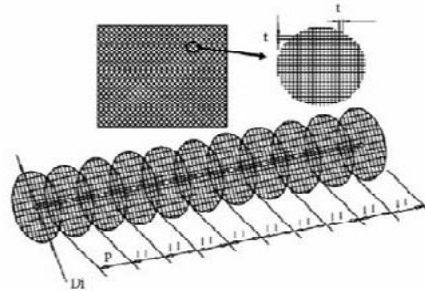


**Figure 2-7:** Mesh inserts [24].

#### 2.2.1.5 Conical nozzles.

**Promvonge et al., in 2009 [25]** investigated experimentally the enhancements of heat transfer characteristics in a uniform heat flux circular tube fitted with conical nozzles and swirl generator. The conical nozzles, assumed as a turbulator/reverse flow generator, were placed in a model pipe line through which air was flowing as working fluid. In addition, the snail was also employed to provide swirling flow at the inlet of the test tube. They found that application of the conical nozzle and the snail could help to increase heat transfer rate over that of the plain tube by about 278% and 206%, respectively. The use of the conical nozzle with the snail led to a maximum heat transfer rate that was up by 316%.

#### 2.2.1.6 Twisted and corrugated tubes

A new innovation or developed technology, known as twisted tube technology, fig. 2-8, which has been able to overcome the limitations of the conventional technology, and in addition, provide superior overall heat

transfer coefficients through tube side enhancement. The twisted tube exchanger consists of a bundle of uniquely formed tubes assembled in a bundle without the use of baffles. That type is giving 40% increase in heat transfer coefficient compared to a conventional shell and tube heat exchanger with the same pressure drop [26].



**Figure 2-8:** Completed twisted tube bundle [26].

**Rainieri, et al., [27]** investigated experimentally the effect of the internal helical ridging tubes on the heat transfer coefficient and friction factor for laminar flow forced convection to. They found that in the spirally enhanced geometries the transition to the turbulent flow might occur at Reynolds number values much lower than 2000. This early transition is accompanied by a significant heat transfer enhancement values between 1.1 and 6 in the Reynolds number range 300-1800.

**Zimparov et al., [28]**, studied performance evaluation criteria, used to assess the benefit of replacing the smooth tubes with deeper corrugated tubes in shell and-tube heat exchangers in the case of condensers with steam condensing on the outside of the vertically or horizontally mounted tubes and water in forced convection (non-boiling) flow being pumped through the tubes. It was concluded that in all the cases considered, corrugated tubes with large pitches and small helix angle have low thermal efficiency.

### 2.2.1.7 Ribbed surfaces and channels

**Kotcioglu et al., in 1998 [29]** studied experimentally heat transfer using winglet-type vortex generators in the range of Reynolds number between 3,000 and 30,000. The installation of wings was organized, in such a way that periodically interrupted enlarged and contracted channel flow domains could be established. Wings were aligned at various angles of 7-20° positively and negatively with the direction of main air flow direction. They concluded an increase of heat transfer coefficient was observed with accompanying large pressure drops, increasing with the inclination angle.

**Layek, et al., in 2006 [30]** studied the effect of compound turbulator on heat transfer coefficient and friction factor in rectangular ducts with repeated transverse integral chamfered rib groove roughness on one broad uniformly heated. They found that heat transfer performance of chamfered rib-groove roughened ducts was much better than the ribbed ducts only, and compared to smooth duct the chamfered rib-groove roughened walls enhanced the Nusselt number and friction factor 3.03 and 3.6 folds respectively.

**Naphon in 2006 [31]** tested the heat transfer characteristics and pressure drop in a channel with V corrugated upper and lower plates under constant heat flux, fig. 2-9. They concluded that the corrugated surface had higher heat transfer as well as pressure drop, and that was because of the presence of recirculation zones.

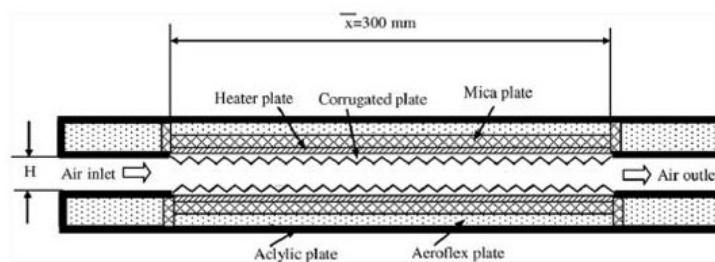


**Figure 2-9:** The V corrugated plates used by Naphon [31].

**Fletcher et al., in 2008 [32]** conducted an investigation to determine whether dimpled surfaces (spherical and elliptical or trenched dimples) could improve the heat transfer in a heat sink under laminar airflows. They found that heat transfer enhancement was up to a 6% relative to a flat plate were consistently observed for Reynolds number (based on channel height) in the range of 500 to 1650 on both circular and oval dimples. The pressure drop over the dimpled plates was either equivalent to or less than that of the flat plate with no dimples.

### 2.2.2 Enhancement of heat transfer in the annulus of a double-pipe heat exchanger.

**Agrawal et al., in 1992 [33]** investigated numerically the laminar forced convection in a double pipe heat exchanger which with an isothermal tube with periodic enhancements (promoters) placed concentrically inside an insulated circular tube; fig. 2-10. Comparing to an unenhanced tube annulus of identical length and heat transfer surface area and mass flow rate and Reynolds number kept the same, they found that the effects of promoter length and spacing on the pressure drop and heat transfer were small and the pressure drop was influenced significantly by the promoter height and the annular gap, while the promoter height was the only significant geometric parameter affecting the heat transfer.

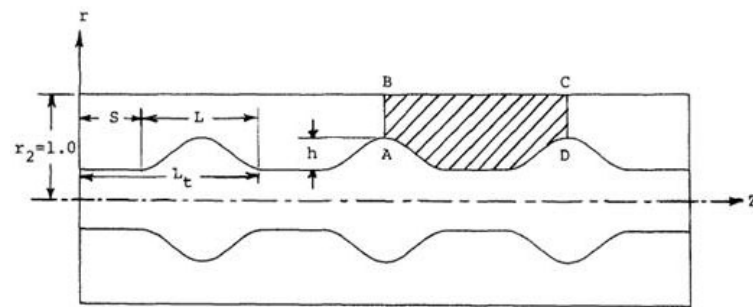


**Figure 2-10:** Enhanced annulus adopted by Agrawal et al. [33]

**Coetze in 2001** [34] studied the heat transfer and pressure drop characteristics of an angled spiraling tape used in the annulus of a double pipe heat exchanger, fig. 2-11 to induce swirl and then increase heat transfer. Three heat exchangers were tested with angled spiraling tape in the annulus with different pitches. It was determined that the heat exchanger with the smallest pitch of the angled spiraling tape and with flow against the curvature of the tape resulted in the highest increase in the Nusselt number of 206%. As penalty this heat exchanger also had the highest increase of the pressure drop of 203%.

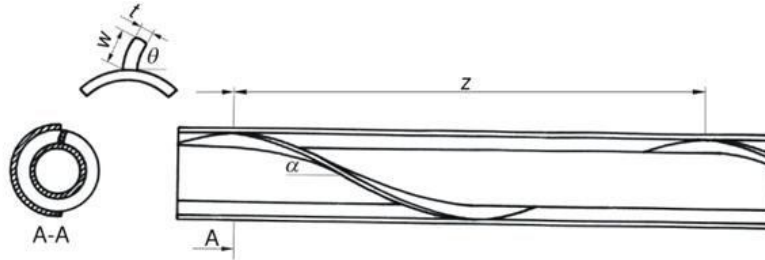


**Figure 2-11:** Schematic representation of angled spiraling tape heat exchanger [34].

The second and third parts of the present work fall into this type of enhancement inserts, where a wire coil and circular ribs with different diameters, different coiling pitches and different experimental conditions have been used to enhance heat transfer in the annulus of a double pipe heat exchanger. The first part is a conventional method which is the coiled wire insert in the inside of the inner tube of the double pipe heat exchanger but with new conditions and with exploiting the most recent correlations in calculating heat transfer and pressure drop in smooth tubes which had undergone numerous developments in the last decades.

# CHAPTER THREE

## Theoretical Background

### 3.1 Introduction

The subject of enhanced heat transfer has developed to the stage that it is of serious interest for heat exchanger application. The refrigeration and automotive industries routinely use enhanced surfaces in their heat exchangers. The process industry is aggressively working to incorporate enhanced heat transfer surfaces in its heat exchangers. Virtually, every heat exchanger is a potential candidate for enhanced heat transfer. However, each potential application must be tested to see if enhanced heat transfer “makes sense”. Heat exchangers were initially developed to use plain (or smooth) heat transfer surfaces. An “enhanced heat transfer surface” has a special surface geometry that provides a higher ( $hA$ ) value, per unit base surface area than a plain surface. The term “enhancement ratio” ( $E_h$ ), is the ratio of the ( $hA$ ) of an enhanced surface to that of a plain surface [35]. Thus:

$$E_h = \frac{hA}{(hA)_s} \quad \dots (3.1)$$

### 3.2 Turbulent Fluid Flow and Heat Transfer

#### 3.2.1 Fluid Flow and Heat Transfer in Circular Tubes

Turbulent flow is commonly utilized in practice because of the higher heat transfer coefficients that is associated with. Most correlations for the friction and heat transfer coefficients in turbulent flow are based on experimental studies because of the difficulty in dealing with turbulent flow theoretically.

For smooth tubes, the friction factor in turbulent flow can be determined from the first Petukhov equation [36]

$$f = (0.79 \ln Re - 1.64)^{-2} \quad \dots (3.3)$$

or from the well-known Moody diagram. The friction factor considered in equation (3.3) is the Darcy friction factor that is used to calculate the pressure drop using the equation

$$\Delta p = f \frac{L}{d_i} \rho \frac{v^2}{2} \quad \dots (3.4)$$

which is well-known as Darcy-Weisbach equation [37, 38].

The Nusselt number in turbulent flow is related to the friction factor through the Chilton–Colburn analogy [39] expressed as:

$$Nu = 0.125 f Re^{(1/3)} \quad \dots (3.5)$$

With the friction factor is available, equation (3.5) can be used conveniently to evaluate the Nusselt number for both smooth and rough tubes. For fully developed turbulent flow in smooth tubes, a simple relation for the Nusselt number can be obtained by substituting the simple power law relation

$$f = 0.184 Re^{-2} \quad \dots (3.6)$$

for the friction factor into equation (3.5), it gives

$$Nu = 0.023 Re^{0.8} Pr^{1/3} \quad (0.7 \leq Pr \leq 160, Re > 10,000) \quad \dots (3.7)$$

which is known as the Colburn equation. The accuracy of this equation can be improved by modifying it as:

$$Nu = 0.023 Re^{0.8} Pr^n \quad \dots (3.8)$$

where  $n = 0.4$  for heating and  $0.3$  for cooling of the fluid flowing through the tube. This equation is known as the Dittus–Boelter equation [40], with properties of the fluid concerned evaluated at the bulk mean fluid temperature  $T_b = (T_i - T_o)/2$ . When the temperature difference between the fluid and the

wall is very large, a correction factor is used to account for the different viscosities near the wall and at the tube center. **Sieder and Tate [41]** suggested a correction factor to be used with all the equations above

$$Nu_c = Nu \left( \frac{\mu_b}{\mu_w} \right)^{0.14} \quad \dots (3.9)$$

where  $\mu_b$  is evaluated at bulk mean temperature while  $\mu_w$  at the temperature of the wall. The Nusselt number relations above are fairly simple, but they may give errors as large as 25% [42].

Comparing a great number of experimental data on heat transfer in tubes with the correlations included in the literature, **Gnielinski [43]** found that a semiempirical type of equation similar to that proposed by Prandtl correlates the data best. The equation of Prandtl for fully developed turbulent flow is of the form

$$Nu = \frac{(f/8)RePr}{1 + 8.7(f/8)^{0.5}(Pr - 1)} \quad \dots (3.10)$$

A number of modifications of equation (3.10) are to be found in the literature and may be summarized by the equation

$$Nu = \frac{(f/8)RePr}{k_1 + k_2(f/8)^{0.5}(Pr^n - 1)} \quad \dots (3.11)$$

For it, **Petukhov and Popov [44]** had suggested that  $k_1 = 1$ ,  $k_2 = 12.7$  and  $n = 2/3$ , where data were correlated best in the region of fully developed turbulent flow by this expression. Since equation (3.11) is based on a model for fully developed turbulent flow ( $Re > 10000$ ), it does not account for entrance effects and it is not applicable in the transition range between laminar and fully developed turbulent flow where the Reynolds numbers are between 2300 and  $10^4$ . To overcome these disadvantages of Eq. (3.11),

Gnielinski modified it by replacing  $\text{Re}$  by  $(\text{Re} - 1000)$  and by multiplying with the entrance correction factor derived by **Hausen** [45]. The equation becomes

$$Nu = \frac{(f/8)(\text{Re}-1000)\text{Pr}}{1+12.7(f/8)^{0.5}(\text{Pr}^{2/3}-1)} \left[ 1 + \left( \frac{d_i}{L} \right)^{2/3} \right] \quad \dots (3.12)$$

For estimation purposes, Gnielinski suggested the following simplified forms for equation (3.12);

$$Nu = 0.0214 (\text{Re}^{0.8} - 100) \text{Pr}^{0.4} \left[ 1 + \left( \frac{d_i}{L} \right)^{2/3} \right] \quad \dots (3.13)$$

for  $0.5 < \text{Pr} < 1.5$ ; and  $10^4 < \text{Re} < 5 \times 10^6$  and

$$Nu = 0.012 (\text{Re}^{0.87} - 280) \text{Pr}^{0.4} \left[ 1 + \left( \frac{d_i}{L} \right)^{2/3} \right] \quad \dots (3.14)$$

for  $1.5 < \text{Pr} < 500$ ; and  $3000 < \text{Re} < 5 \times 10^6$

Nowadays equation (3.12) is known as Gnielinski equation where  $f$  is Darcy friction factor for turbulent flow in smooth tubes obtained using equation (3.3). The viscosity correction, equation (3.9) also can be used to correct for the difference between the temperature of the wall of tube and the bulk temperature of the fluid.

Equation (3.3) in connection with equation (3.12) has been shown to represent the majority of the experimental data within 20%. This equation is valid for developing or fully developed turbulent flow  $2300 < \text{Re} < 5 \times 10^6$ ,  $0.5 < \text{Pr} < 2000$  and  $d_i/L < 1$  [43].

### 3.2.2 Fluid Flow and Heat Transfer in the Annulus of Concentric Tubes.

When a fluid flows in a conduit having a non-circular cross section, such as an annulus, it is convenient to express heat transfer coefficients and friction

factors by the same types of equations and curves used for pipes and tubes. To permit this type of representation for annulus heat transfer, it has been found advantageous to employ an equivalent diameter  $D_e$ . The equivalent diameter is four times the hydraulic radius, and the hydraulic radius is, in turn, the radius of a pipe equivalent to the annulus cross section.

The hydraulic radius is obtained as the ratio of the flow area to the wetted perimeter. For a fluid flowing in an annulus the flow area is  $(\pi/4)(D_o^2 - D_i^2)$  but the wetted perimeters for heat transfer and pressure drop are different. For heat transfer the wetted perimeter is the outer circumference of the inner tube

$$D'_e = 4r_h = \frac{4 \times (\text{flow area})}{(\text{heat transfer wetted perimeter})} = \frac{4\pi(D_o^2 - D_i^2)}{4\pi D_i} = \frac{D_o^2 - D_i^2}{D_i}$$

... (3.15)

In pressure drop calculations the friction not only results from the resistance of the outer tube but it is also affected by the outer surface of the inner tube. The total wetted perimeter is  $\pi(D_o + D_i)$  and the equivalent diameter for pressure drop calculations in the annulus is:

$$D_e = 4r_h = \frac{4 \times (\text{flow area})}{(\text{frictional wetted perimeter})} = \frac{4\pi(D_o^2 - D_i^2)}{4\pi(D_o + D_i)} = D_o - D_i$$

... (3.16)

This leads to the anomalous result that the Reynolds numbers for the same flow conditions are different for heat transfer and pressure drop. Since Reynolds number evaluated using  $D'_e$  might be above 2100 while that using  $D_e$  is below 2100. Actually, both Reynolds numbers should be considered only approximations, since the sharp distinction between streamline and turbulent flow at the Reynolds number of 2100 is not completely valid in annuli [46].

The details above are very decisive, if equations like that of Dittus and Boelter, equation (3.8), are used in calculating the Nusselt number, where two values for Reynolds number must be estimated, one for friction factor calculations and another for heat transfer calculations [4, 46, 47, 48, 49]. As an effort in the field, **Davis** [50] has proposed the equation;

$$\frac{hD_i}{k} = 0.031 \left( \frac{D_i G}{\mu} \right)^{0.8} \text{Pr}^{0.33} \left( \frac{\mu}{\mu_w} \right)^{0.14} \left( \frac{D_o}{D_i} \right)^{0.15} \quad \dots (3.17)$$

to be used to estimate the Nusselt number in the annulus of  $D_i$  and  $D_o$  as the inner and outer diameter of the annulus respectively, using the outer diameter of the inner tube as the characteristic dimension, which is the surface through which heat transfer occurs.

Heat transfer in turbulent flow of gases and liquids in concentric annuli may be obtained using a modified form of equation (3.12) in tubes using the hydraulic or equivalent diameter  $D_e = D_o - D_i$  to evaluate  $Nu$ ,  $Re$  and  $D/L$  in equation (3.12). According to **Petukhov and Roizen** [51], the Nusselt number in case of heat transfer at the inner wall, and the outer wall insulated, might be calculated using

$$\frac{Nu_i}{Nu_{tube}} = 0.86 \left( \frac{D_i}{D_o} \right)^{-0.16} \quad \dots (3.18)$$

for cases, the heat transfer at the outer wall, and the inner wall insulated

$$\frac{Nu_o}{Nu_{tube}} = 1 - 0.14 \left( \frac{D_i}{D_o} \right)^{0.6} \quad \dots (3.19)$$

The third case is when heat transfer on both walls of the passage, and equal temperatures on both walls, Nusselt number is calculated using

$$\frac{Nu_b}{Nu_{tube}} = \frac{0.86 \left( \frac{D_i}{D_o} \right)^{0.84} + \left[ 1 - 0.14 \left( \frac{D_i}{D_o} \right)^{0.6} \right]}{1 + \frac{D_i}{D_o}} \quad \dots (3.20)$$

Nowadays numerous studies [42, 52, 53, 54, and 55] do ignore the physical fact of what surface in the annulus is concerned with heat transfer and use the Reynolds number value, based on the equivalent diameter  $D_e = D_o - D_i$  in both heat transfer and pressure drop calculations regardless of what correlation is used.

Since all calculations of the present work are based on equation (3.12), then no need for obtaining two values for Reynolds number, i.e. friction factor as well as Nusselt number calculations in the annulus will include the same Reynolds number with the hydraulic diameter defined by  $D_e = D_o - D_i$ . By equation (3.18), the use of equation (3.12) for the annulus is acceptably accurate. Furthermore, for the two sides, equation (3.12) includes the entrance effect term as well as working in larger range of Reynolds number.

### 3.2.3 Empirical Correlations of Turbulent Fluid Flow and Heat Transfer in Tubes Inserted with Wire Coils

Many correlations had been set for predicting the heat transfer and pressure drop. **Ravigururajan and Bergles in (1985)** [56] proposed what might be considered to be the most general and accurate method for predicting heat transfer and pressure drop inside internally ribbed tubes (and plain tubes with coiled wire inserts). Figure 3-1 depicts the rib geometries and profiles (and wire geometry) that were included in their study. The  $n_{corners}$  here is the number of sharp corners of the rib facing the flow (two for triangular or rectangular cross-section ribs and infinity for smoother profiles). The profile

contact angle for a circular sector and circular profiles is taken as  $90^\circ$ . Their method is applicable to the following range of parameters:  $0.01 < e/d_i < 0.02$ ,  $0.1 < p/d_i < 7.0$ ,  $0.3 < \beta/90 < 1.0$ ,  $5000 < Re < 250000$  and  $0.66 < Pr < 37.6$ .

Their ribbed tube heat transfer correlation is:

$$\frac{Nu_a}{Nu_s} = \left\{ 1 + \left[ 2.64 \text{Re}^{0.036} \left( \frac{e}{d_i} \right)^{0.212} \left( \frac{p}{d_i} \right)^{-0.21} \left( \frac{\beta}{90} \right)^{0.29} \text{Pr}^{-0.024} \right]^7 \right\}^{1/7} \dots (3.21)$$

The friction factor is correlated as a ratio to the value for a smooth tube of the same internal diameter as:

$$\frac{f_a}{f_s} = \left\{ 1 + \left[ 29.1 \text{Re}^{a1} \left( \frac{e}{d_i} \right)^{a2} \left( \frac{p}{d_i} \right)^{a3} \left( \frac{\beta}{90} \right)^{a4} \left( 1 + \frac{2.94}{n_{corners}} \right) \sin \theta \right]^{15/16} \right\}^{16/15} \dots (3.22a)$$

$$a1 = 0.67 - 0.06 \left( \frac{p}{d_i} \right) - 0.49 \left( \frac{\beta}{90} \right) \quad a2 = 1.37 - 0.157 \left( \frac{p}{d_i} \right) \\ a3 = -1.66 \times 10^{-6} \text{Re} - 0.33 \left( \frac{\beta}{90} \right) \quad a4 = 4.59 + 4.11 \times 10^{-6} \text{Re} - 0.15 \left( \frac{p}{d_i} \right) \dots (3.22b)$$

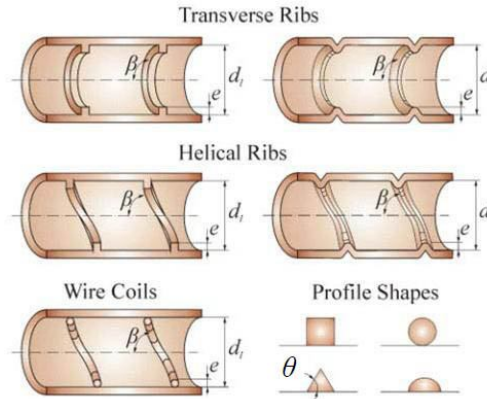


**Figure 3-1:** Internal enhancement geometries and profile shapes considered by Ravigururajan and Bergles (1985) [57].

In equations (3.21) and (3.22), equations (3.3) and (3.11) are used to determine the friction factor and Nusselt number of the reference tube (smooth, plain surface tube) [1, 2, 57, 35, and 58]. But because the friction factor correlation above reported to predict 96% of the data within  $\pm 50\%$ , and the heat transfer correlation to predict the 99% of the data within  $\pm 50\%$ , these correlations are not recommended for general use [35].

### 3.3 Mechanisms of Heat Transfer Augmentation by Turbulence Promoters

One of the most important mechanisms of augmenting heat transfer is the displacement of the turbulent boundary layer. Figure 3-2 depicts a diagram that **Arman and Rabas** [59, 60] used to illustrate this process, showing the separation of the flow as it passes over a transverse rib (creating a small recirculation zone in front of the rib), the formation of a recirculation zone behind the rib, flow reattachment on the base wall, and then flow up and over the next rib. Recirculation eddies are formed above these flow regions. They commented as follows on a rib's effect on the heat transfer process:

1. There are six distinct heat transfer regions, although some are more important than others (the upstream recirculation zone, the rib's upstream, top and downstream faces, the downstream recirculation zone, and finally the boundary layer reattachment zone);
2. Two peaks in local heat transfer occur, one at the top of the rib and the other in the downstream recirculation zone just before the reattachment point;
3. Heat transfer enhancement increases substantially with increasing Prandtl number, so that for large Prandtl number, fluids heat transfer is dominated by flow around the rib surfaces;

4. The surface-averaged heat transfer performance is directly proportional to the maximum enhancement at the rib;
5. The point of the local maximum in the heat transfer coefficient on the base wall between ribs moves upstream towards the back of the rib with increasing Reynolds and Prandtl numbers, and is located on the base wall between the reattachment point and the point of maximum wall shear stress;
6. The Prandtl number has the same influence on thermal performance in the downstream recirculation region as at the rib;
7. The high heat transfer augmentation in the downstream recirculation region is due to the high turbulence levels near the surface;
8. Two more local maximums in heat transfer occur at large Reynolds numbers in the front recirculation zone before the rib and on the rear face of the rib [59, 60].

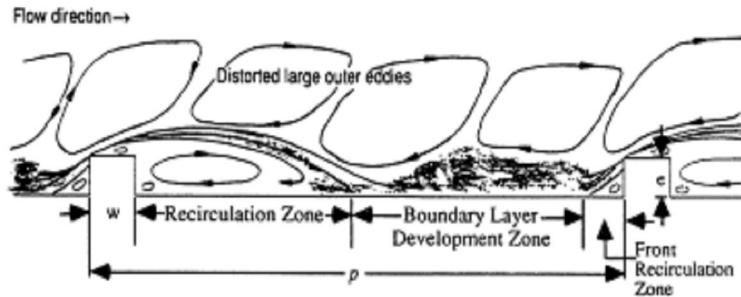


**Figure 3-2:** An enhanced tube with the separation and reattachment mechanism [59].

**Webb, Eckert and Goldstein in 1971 [61]** have presented an interesting composite diagram of the recirculation and reattachment zones as a function of rib spacing for ribs oriented normal to the flow. Figure 3-3 shows this diagram where the flows are characterized by the axial rib pitch to rib height ( $p/e$ ) ratio. For closely spaced ribs (at bottom of diagram), one large recirculation eddy is trapped between two successive ribs with two small

eddies in the corners. As the  $(p/e)$  ratio increases, the large recirculation eddy elongates until it is broken and a reattachment zone is formed, such that two dominant eddies exist at larger ratios. The separation occurs at the ribs, which leads to the formation of a shear layer and finally reattaches at about 6-8 times the rib height, downstream of the rib. The reverse flow boundary was found to originate from the reattachment point and had grown in thickness. The wall shear stress is zero at the reattachment point and was found to increase in the reverse flow region. Webb had shown that reattachment does not take place below a particular  $(p/e)$  ratio [61].

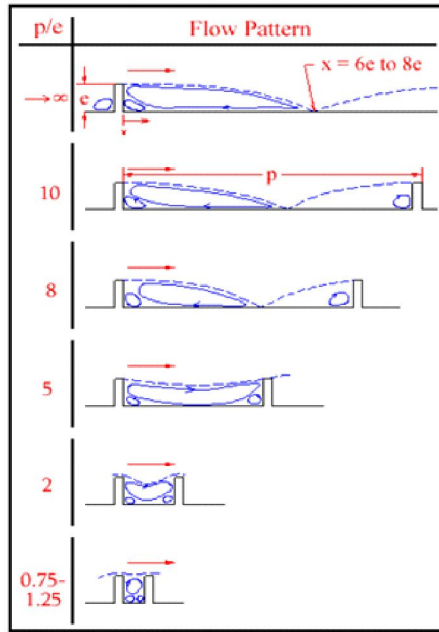


**Figure 3-3:** Recirculation flow patterns over transverse ribs as a function of rib spacing [61].

Similarly, but using an advanced technique, **Acharya et al.**, [62, 63] adopted a laser-Doppler measurement system to investigate the effect of the rib on local heat transfer. They reported a peak in stream-wise turbulence intensity that occurred directly above the rib. Cross-stream turbulence intensity profiles were found to reach a maximum downstream of the rib as well as a peak in heat transfer upstream of the point of flow reattachment.

### 3.4 Performance Evaluation Criteria (PEC)

It is impossible to establish an absolute applicable selection criterion for the use of enhancement techniques, because numerous factors influence the designer's decision. In addition to the relative thermal-hydraulic performance improvements brought about by the enhancement devices, there are many factors that must be considered. They include economic (capital, installation, maintenance, etc.), manufacturability (machining, forming, etc.), reliability (material compatibility, and long-time performance), and finally safety.

Common thermal-hydraulic goals include reducing the size of a heat exchanger required for a specified heat duty, increasing the heat duty of an existing heat exchanger, reducing the approach temperature difference for the process streams, or reducing the pumping power. The presence of system and design constraints leads to a number of performance evaluation criteria (PECs). The geometric variables for tube-side flow in a shell-and-tube heat exchanger are tube diameter, tube length, and number of tubes per pass. The heat exchanger performance is represented by two dependent variables: heat transfer rate ( $q$ ) and pressure drop ( $\Delta p$ ) or pumping power ( $P$ ), as

$$q = (UA)\Delta T_m \quad \dots (3.23)$$

$$\Delta p = f \frac{L}{d_i} \frac{G^2}{2\rho} \quad \dots (3.24)$$

$$P = \Delta p \frac{GA_c}{\rho} \quad \dots (3.25)$$

The primary independent operating variables are the approach temperature difference and the mass flow rate ( $\dot{m}$ ), and in the case of the tubular geometry, the design variables (heat transfer surface area ( $A$ ) or exchanger size) are the diameter ( $d_i$ ) and length ( $L$ ) of tubes and number of

tubes ( $N$ ) per pass. PECs are established for the process stream of interest by selecting one of the operational variables for the performance objective and applying the design constraints on the remaining variables [1, 2, 35, 58].

### 3.4.1 Objective Functions and Constraints

For single-phase flow heat transfer inside enhanced and smooth tubes of the same diameter, PECs for 12 different cases outlined by Webb and Bergles are listed in table 3-1. They represent criteria for comparing the enhanced performance on the basis of three broad geometry constraints [35, 58].

**Table 3-1:** Performance Evaluation Criteria for Single-Phase Forced Convection in Enhanced Tubes Diameter ( $d_i$ ) as the Smooth Tube [58].

Case	Geom.	Fixed				Objective	Consequences						
		$\dot{m}$	P	q	$\Delta T_i$		$\frac{Nu_a}{Nu_s}$	$\frac{L_a}{L_s}$	$\frac{\dot{m}_a}{\dot{m}_s}$	$\frac{Re_a}{Re_s}$	$\frac{P_a}{P_s}$	$\frac{q_a}{q_s}$	$\frac{\Delta T_{ta}}{\Delta T_B}$
FG-1a	$N, L$	X	—	—	X	$\uparrow q$	1	1	1	1	>1	>1	1
FG-1b	$N, L$	X	—	X	—	$\downarrow \Delta T_i$	1	1	1	1	1	1	<1
FG-2a	$N, L$	—	X	—	X	$\uparrow q$	1	1	<1	<1	1	>1	1
FG-2b	$N, L$	—	X	X	—	$\downarrow \Delta T_i$	1	1	<1	<1	1	1	<1
FG-3	$N, L$	—	—	X	X	$\downarrow P$	1	1	<1	<1	<1	1	1
FN-1	$N$	—	X	X	X	$\downarrow L$	1	<1	<1	<1	1	1	1
FN-2	$N$	X	—	X	X	$\downarrow L$	1	<1	1	1	<1	1	1
FN-3	$N$	X	—	X	X	$\downarrow P$	1	<1	1	1	<1	1	1
VG-1	—	X	X	X	X	$\downarrow NL$	>1	<1	1	<1	1	1	1
VG-2a	$NL$	X	X	—	X	$\uparrow q$	>1	<1	1	<1	1	>1	1
VG-2b	$NL$	X	X	X	—	$\downarrow \Delta T_i$	>1	<1	1	<1	1	1	<1
VG-3	$NL$	X	—	X	X	$\downarrow P$	<1	<1	1	<1	<1	1	1

**1. FG criteria.** The cross-sectional envelope area ( $N$  and  $d_i$ ) and tube length ( $L$ ) are held constant. This would typically be applicable for retrofitting the smooth tubes of an existing exchanger with enhanced tubes. That means maintaining the same basic geometry and size ( $N$ ,  $d_i$ , and  $L$ ). The objectives then could be to increase the heat load capacity ( $q$ ) for the same approach temperature ( $\Delta T_i$ ) and mass flow rate ( $\dot{m}$ ) or pumping power (P); that is (FG-1a) and (FG-2a) respectively; or decrease ( $\Delta T_i$ ) or (P) for fixed ( $q$ ) and ( $\dot{m}$ ), i.e. (FG-1b) or (P), i.e. (FG-2b); or reduce (P) for fixed ( $q$ ), i.e. (FG-3).

**2. FN criteria.** These criteria maintain fixed cross-sectional area ( $N$  and  $d_i$ ) and allowing the heat exchanger length to vary. Here the objectives are to seek a reduction in either the heat transfer surface area ( $A \rightarrow L$ ), i.e. (FN-1) and (FN-2); or the pumping power ( $P$ ), i.e. (FN-3) for a fixed heat load.

**3. VG criteria.** In many cases, a heat exchanger is sized for a required thermal duty with specified flow rate. In these situations the FG and FN criteria are not applicable. Because the tube-side velocity must be reduced to accommodate the higher friction characteristics of the enhanced surface, it is necessary to increase the flow area to maintain constant flow rate. This is accomplished by using a greater number of parallel flow circuits. Maintaining a constant exchanger flow rate eliminates the penalty of operating at higher thermal effectiveness encountered in the previous FG and FN cases [58].

### 3.4.2 Algebraic Formulation of the PEC

Calculation of the performance evaluation criteria for any of the 12 cases in Table 3-1 requires algebraic relations that quantify the objective function and constraints. It is convenient to develop the algebraic relations relative to a smooth surface operating at the same fluid temperature. This allows cancellation of the fluid properties from the equations.

The different cases listed in table 3-1 are derived for flow inside enhanced and smooth tubes of the same inside diameter. Considering a shell and tube heat exchanger of length  $L$ , having  $N$  tubes in each pass, and  $N_p$  passes. The total tube-side surface area in the heat exchanger is

$$A = \pi d_i L N N_p \quad \dots (3.26)$$

The basic heat transfer and friction performance characteristics of the enhanced and smooth tubes are normally presented as Colburn factor ( $j$ )

defined as  $j = St \Pr^{2/3} = Nu/\text{Re} \Pr^{1/3}$  and  $f$  vs.  $\text{Re} = d_i G/\mu$ . Because the tube inside diameter is held constant, one may write

$$h = \frac{C_p j G}{\Pr^{2/3}} \quad \dots (3.27)$$

The value of  $(hA)$  of the enhanced surface, as in equation (3.1), relative to that of the smooth surface is the aim of interest. Writing equation (3.27) as the ratio, relative to a smooth surface gives

$$\frac{hA}{h_s A_s} = \frac{j}{j_s} \frac{A}{A_s} \frac{G}{G_s} \quad \dots (3.28)$$

Substituting equation (3.24) in (3.25) and replacing  $A_c$  by  $[(\pi/4)d_i^2]$  gives equation (3.29) for pumping power

$$P = \frac{fAG^3}{8\rho^2} \quad \dots (3.29)$$

Writing equation (3.29) as the ratio, relative to the smooth surface, gives

$$\frac{P}{P_s} = \frac{f}{f_s} \frac{A}{A_s} \left( \frac{G}{G_s} \right)^3 \quad \dots (3.30)$$

Elimination of the term  $G/G_s$  from equations (3.28) and (3.30) gives

$$\frac{hA/h_s A_s}{(P/P_s)^{1/3} (A/A_s)^{2/3}} = \frac{j/j_s}{(f/f_s)^{1/3}} \quad \dots (3.31)$$

To apply one of the PECs, one of the variables on the left side of equation (3.31) is set as the objective function, and the remaining two are set as operating constraints (equal to unity). It is necessary to determine the  $G/G_s$  ratio that satisfies Equation (3.31). The equations of the  $j_s$  and  $f_s$  as a function of  $\text{Re}_s$  and the  $j$  and  $f$  as a function of  $\text{Re}$  must be known [35]. Accordingly, in the present work, these equations would be created from the experimental data to accommodate the requirements of these PECs either for the tube-side or annulus-side heat transfer enhancement.

### 3.5 Thermal Design of the Double Pipe Heat Exchangers

Only two important relationships constitute the entire thermal design procedure of a heat exchanger. These are:

1. Heat transfer rate for a non-adiabatic single-phase flow:

$$q = \dot{m}\Delta H = \dot{m}Cp(T_o - T_i) \quad \dots (3.32)$$

2. Heat transfer rate equation:

$$q = UA \Delta T_m \quad \dots (3.33)$$

Equation (3.33) reflects a convection–conduction heat transfer phenomenon in a two-fluid heat exchanger. Heat transfer rate is proportional to the heat transfer area ( $A$ ) and mean temperature difference ( $T_m$ ) between the fluids. This mean temperature difference is a log-mean temperature difference (LMTD), for counterflow and parallelflow exchangers, it is

$$\Delta T_m = LMTD = \frac{(T_{h2} - T_{c2}) - (T_{h1} - T_{c1})}{\ln[(T_{h2} - T_{c2})/(T_{h1} - T_{c1})]} \quad \dots (3.34)$$

If a wall of a hollow cylinder (like a double pipe heat exchanger) is considered, the overall heat transfer coefficient ( $U$ ) in equation (3.33) may be based on either the inside or outside area of the tube. Accordingly,

$$U_i = \frac{1}{\frac{1}{h_i} + \frac{A_i \ln(r_o/r_i)}{2\pi k L} + \frac{A_i}{A_o} \frac{1}{h_o}} \quad \dots (3.35)$$

$$U_o = \frac{1}{\frac{A_o}{h_i} \frac{1}{h_i} + \frac{A_o \ln(r_o/r_i)}{2\pi k L} + \frac{1}{h_o}} \quad \dots (3.36)$$

Equations (3.35) and (3.36) include three thermal resistances, heat is transferred through. Two are concerned with convection heat transfer in the two sides of the exchanger and the other is caused by the wall itself [4, 64].

## **CHAPTER FOUR**

### **Experimental Work**

#### **4.1 Experimental Rig Design and Assembly.**

An experimental rig was designed and assembled to carry out the experiments that require particular fluid temperatures, particular fluid flow rates, and for each run, temperatures of four points and pressure drop in specific sections, which represent the heart of the present work, must be measured in acceptable accuracy.

Simply, the concerned rig is an assembly of several parts when operated, the result is two streams of fluids having particular temperatures that the study needs, flowing separately and sometimes mixed for specific tasks. In addition, two specialized streams were used in the isothermal pressure drop experiments, which might stop the working as a heat exchange system and mixing the two streams to work under constant temperature conditions. No automatic temperature control devices are available, so manual control is widely adopted to regulate temperatures of fluid streams. Figure 4-1 shows a photograph of the rig whose parts are detailed in the schematic flow diagram depicted in fig. 4-2.

Water was used as the working hot fluid and cold fluid streams for its availability; high heat capacity, which enables easy control of temperature; and conventionality of using it as the cold fluid in many actual heat exchange processes.



Figure 4-1: A photograph of the experimental rig.

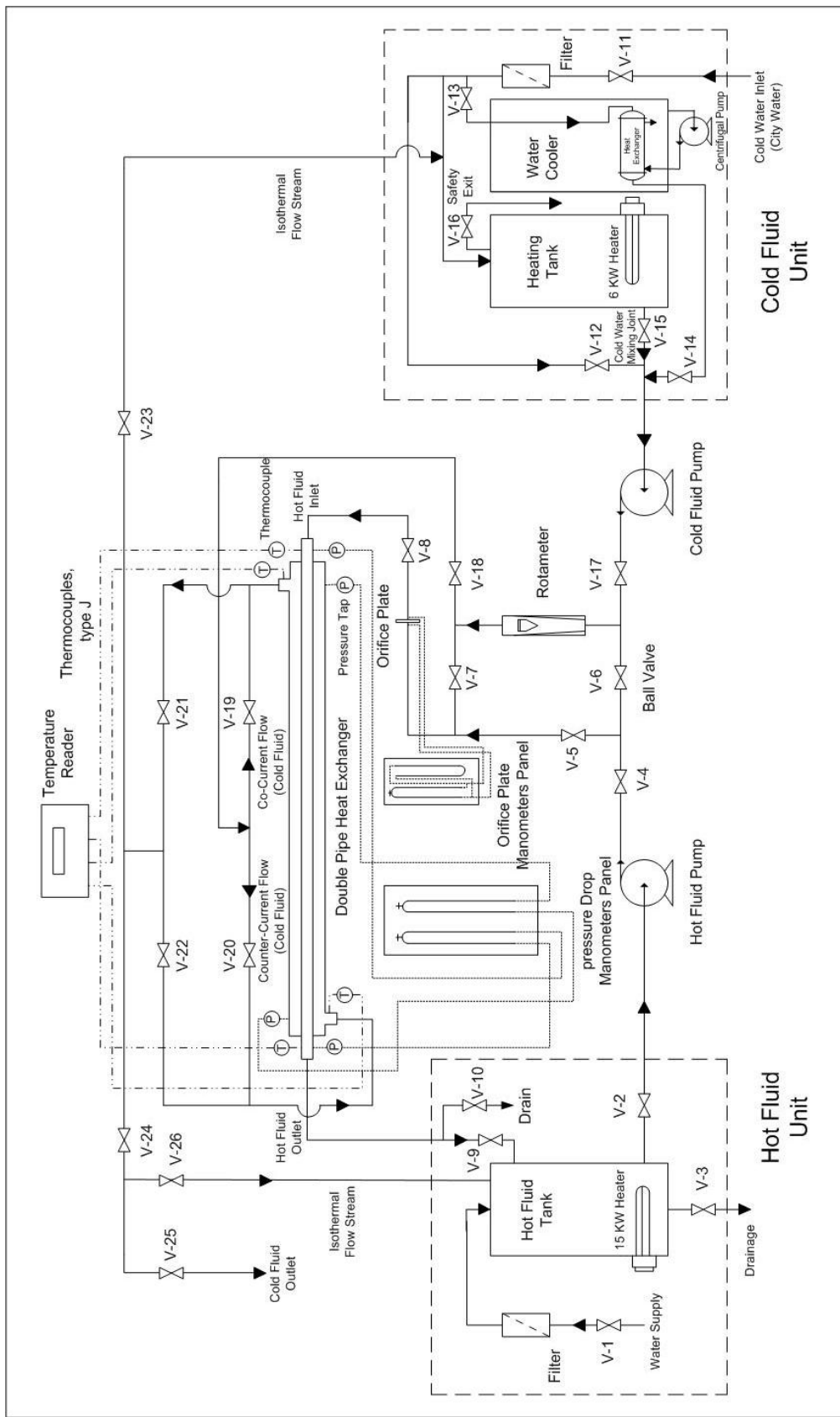


Figure 4-2. A schematic flow diagram of the experimental rig.

#### **4.1.1 Components of the Experimental Rig.**

##### **4.1.1.1 Hot Fluid Unit.**

As depicted in fig. 4-2 the hot fluid unit consists mainly of the following:

**( i ) Insulated Tank:** A tank of ( $50 \times 50 \times 100$  cm) dimensions well-insulated using 5 cm thick of mineral wool insulation to forbid loss of heating energy.

**( ii ) Electric heaters:** 4 electric heaters with 3 kW power for each in addition to a 3.5 kW power supplied by 1500, 1000, and 500 W heaters and 500 W heater controlled by a variac are used to supply thermal energy needed for heat transfer. The partitioned 3.5 kW power is exploited to control temperature of the hot stream to the required value, where the heat transferred from the hot to cold stream through the heat exchanger at any time, is guessed by calculations as shown later.

Hot fluid unit is supplied with water (as the working fluid) after passing through a filter assembled at the inlet of the system. Hot water is circulated throughout the system and returned to the hot fluid tank. Water is replaced periodically so as to keep it free from salts which may be concentrated as a result of continuous heating.

##### **4.1.1.2 Cold Fluid Unit**

The cold fluid unit consists of the following:

**( i ) Main Stream of Tap Water:** The cold fluid used throughout the system is filtered tap water used for one pass without circulating, but since it may come in different temperatures during the different seasons of the year, its temperature must be maintained to the required temperature which is  $20^{\circ}\text{C}$ .

**( ii ) Heating Tank:** To maintain tap water at  $20^{\circ}\text{C}$  which may arrive in temperature less than this degree (during winter), a heating tank provided with

a 6 kW electric heater is used for the task. In most cases, tap water is divided into two streams before entering the unit; one is passed through the heating tank. The two streams are mixed in a joint point before entering the system. The flowrates of the two streams are maintained manually till the temperature of the “mixture” is being settled at the required value.

**( iii ) Water Cooler:** In summer, the task may be different where the tap water is arriving in temperature more than 20 °C, so it is necessary to lower to this temperature. The task is carried out in a manner similar to that used in the preceding case but instead of passing one of the two streams, the water have been divided into the heating tank, it is now passed through a water cooler. The concerned stream is passed through a shell-and-tube heat exchanger immersed inside the pool of the water cooler and exchanging heat with cold water (its temperature is below 5 °C, pumped by a centrifugal pump) without mixing. This exit stream is mixed with the other stream and again controlled manually to produce water at the required temperature. Depending on the techniques discussed above and enough experience, temperature of cold water was controlled to  $20 \pm 0.5$ .

#### **4.1.1.3 Flow Measurement Instrumentation**

Two flow measurement devices have been used, one for each stream:

##### **( i ) Rotameter:**

A rotameter type (FLOWTECH, Lzs-25) with flowrate range between 0.16 and  $1.5\text{m}^3/\text{hr}$ , were used to measure the flowrate of cold water (20 °C). But in case of isothermal pressure drop experiments, which would be explained later, the rotameter was used to measure the flowrate of hotter water, reaches 70 °C, so an accurate calibration was required in order to ensure obtaining results as

acceptable as possible. Calibration of rotameter was performed to produce calibration curves for flowrate of water, at four temperatures (20, 40, 60, and 70 °C). Details of calibration of the rotameter and calibration curves, produced are fixed in appendix B.

### ( ii ) Orifice plate.

An orifice plate was designed and manually fabricated to be used in measuring hot water flowrate. This device is supplied with two manometers, an inverted manometer filled with mercury to be used in measuring relatively high flowrates (between 0.3 and 0.9 m<sup>3</sup>/hr), and the other is an ordinary water manometer to be used in measuring low flowrates (0.3 m<sup>3</sup>/hr and lower). Design and calibration of the orifice plate for the two temperatures (60 and 70 °C) is detailed in appendix B. The mercury manometer graduation is directly fixed on the orifice manometer panel, while the water manometer must be treated differently. That is by using a computer program written for the purpose because the water manometer readings cannot be adjusted directly.

#### **4.1.1.4 Pressure Measurement Instrumentation**

One of the most important data to be obtained in the present work is the pressure drop inside the test section (double-pipe heat exchanger), so four pressure taps were fixed in the inlet and exit of the hot and cold fluid streams to measure pressure drop inside the inner tube and the annulus. Three manometers were used. Two of the manometers—that use water—are employed to measure low pressure drops and the third that uses mercury is employed to measure high pressure drops. The latter is connected to each of the others if needed. When working together, the water manometer must be closed, when measuring high flowrates, or else it might overflow.

#### **4.1.1.5 Temperature Measurement Instrumentation**

Four thermocouples type (J) fixed at the inlet and outlet of the hot and cold fluid streams to measure temperature of the intended fluids at specific points. The ends of thermocouples are screwed to be tightly fixed in the external tubes near the inlet and outlet points. The thermocouples are connected to a temperature reader device type (DORIC) with five buttons.

Since these temperature values play a decisive role in calculating the Nusselt number, and to ensure that the temperatures obtained are as accurate as possible, an accurate calibration for the four thermocouples and the temperature reader device were carried out using a mercury thermometer. The latter was calibrated using boiling distilled water and a mixture of distilled water and ice [65]. The result of the calibration process was converted to four calibration curves to be used to predict the actual values of temperature. Details of calibration are fixed in appendix B.

#### **4.1.1.6 Pipes, Pumps, and Valves**

All pipes used in the construction of the rig are made of galvanized iron pipes of ID=16mm, well-insulated to save energy. Three centrifugal pumps, with maximum volumetric flowrate of  $4 \text{ m}^3/\text{hr}$ , are included, one for the cold fluid unit and the others are employed to pump the hot and cold fluids in concerned streams. 26 ball valves are used in the rig. This type of valve had been used because it could be easily and rapidly opened and sealed and easily used in controlling the volumetric flowrates of the two streams.

#### **4.1.1.7 Test Section (Double-Pipe Heat Exchanger)**

The most important part of the experimental rig is the test section which is a double pipe heat exchanger. Figure 4-3 illustrates its main parts:

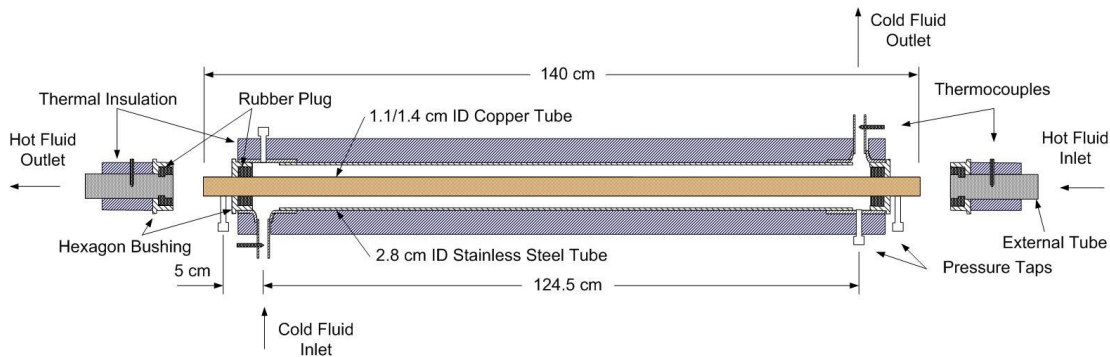


**Figure 4-3:** Sketch of the double-pipe heat exchanger used in the present work.

**( i ) The outer tube:** It is made of stainless steel to avoid corrosion during operation. It is 1.2 m length, ID=2.8 cm and OD=3.0 cm.

**( ii ) The inner tube:** It is made of pure copper (South African Origin) for its low thermal resistance with two sizes used. The first is 1.4 m length, ID=1.1 cm and OD=1.25 cm. The second has the same length but with ID=1.4 cm and OD=1.55 cm.

**( iii ) Pipe fittings:** Two 1-½ inch reducing tee lateral fits are connected to the two ends of the stainless steel tube with making their branches in opposite directions. In addition, four hexagon bushings with their hollows filled with rubber plugs, were used. These were perforated in a way can hold the inner tube without leakage. Two were used to conjoin the inner with the outer tube in a manner enables the operator to disassemble the two tubes in order to change the inner tube easily after each experiment. The other two were used to connect the two ends of the inner tube to the external pipes of the rig [66].

**( iv ) Pressure taps:** Four pressure taps are installed in four points around the double-pipe heat exchanger, and connected to the manometer panel detailed above. Two pressure taps concerning the pressure drop in the inner tube are fixed directly in that tube by perforating it carefully near the two ends keeping

a distance of 134.5 cm between the two perforations. This distance was larger than the effective heat transfer length (124.5 cm) which equals to the distance between the inlet and outlet of cold water or the two centers of the tee fittings, so all pressure drop values registered for the tube side would be multiplied by the ration of (124.5/134.5) to obtain the real value of pressure drop. To avoid leakage in these points, an adhesive material was used, taking into consideration that no protrusion was left inside the tube which may cause an error in reading the actual pressure drop. The annulus side pressure taps were fixed in the centre of the tee lateral body. That was in order to calculate the actual pressure drop in the annulus without that caused by the entrance. The registered value in that case was adopted directly without correction. These taps not like those of the inner tube, they were not removable because the outer tube connected to the reducing tee laterals were left without disassembling all the experimental work. Fig. 4-4 shows the pressure taps.

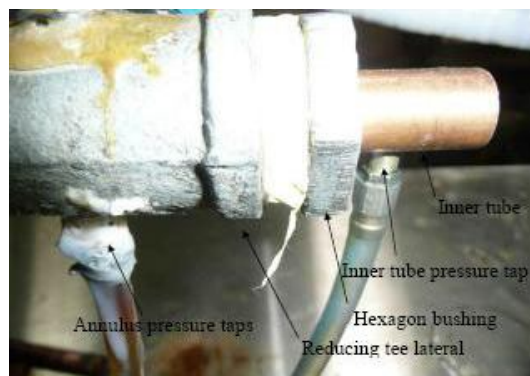


**Figure 4-4:** Pressure taps.

The temperature thermocouples installation was easier because they were fixed in the external tubes belonging to the rig itself and left without removing all the experimental work.

The whole body of the heat exchanger was insulated with a layer of mineral wool insulation to avoid heat loss.

#### 4.1.2 Turbulence Promoter Selection and Fabrication

Three types of inserts with different pitch length and wire diameter, (defined in fig. 4-5a), was used in the present work:

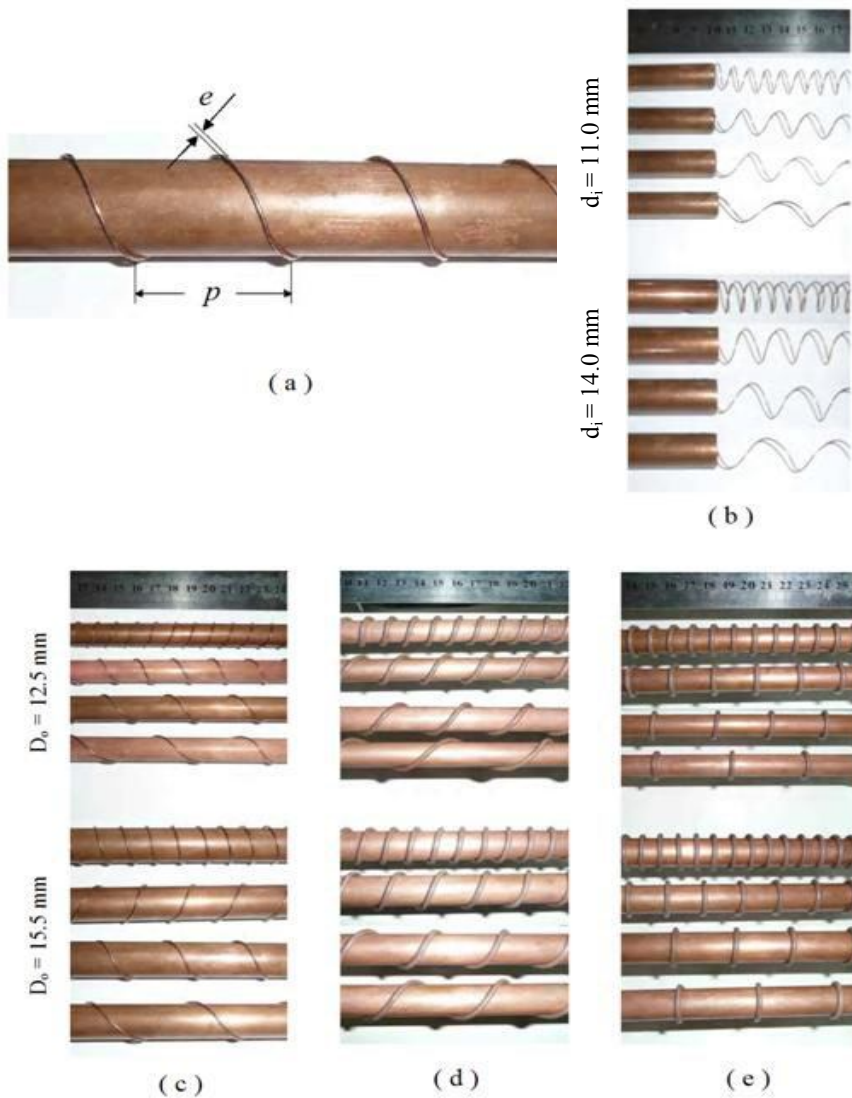


**Figure 4-5:** Turbulence promoters used in the present work, (a) Definition of pitch length  $p$  and wire diameter  $e$ , (b) Inner coiled wire inserts, (c) Coiled wire on the outer surface of the inner tube  $e = 1 \text{ mm}$ , (d) Coiled wire on the outer surface of the inner tube  $e = 2.2 \text{ mm}$ , (e) Circular rib on the outer surface of the inner tube  $e = 2.2 \text{ mm}$ .

**( i ) Wire coil insert inside the inner tube:** 1 mm diameter copper wire was coiled around a steel bar of about 8.5 and 12 mm diameter to produce wire coils with outside coiling diameters of 11 and 14 mm. Four coiling pitches had been studied (10, 20, 30, and 40 mm), as in fig.4-5b.

**( ii ) Wire coil insert on the outer surface of the inner tube:** Two copper wire sizes were used (1 and 2.2 mm diameter). That was by coiling the interested wires around the copper tubes directly with keeping four coiling pitches to be used (10, 20, 30, and 40 mm), fig. 4-5c, and d.

**( iii ) Circular ribs on the outer surface of the inner tube:** A copper wire with diameter of 2.2 mm was used in fabricating circular ribs to be used as turbulence promoters on the outer surface of the inner tube with four pitch lengths (10, 20, 30, and 40 mm).

## 4.2 Operation of the System

In the present work, experiments were divided into two kinds, isothermal pressure drop experiments and heat exchange experiments:

### 4.2.1 Isothermal Pressure Drop Experiments

The aim of the isothermal pressure drop experiments is to obtain the friction factor or pressure drop, in mm H<sub>2</sub>O, for the range of Reynolds numbers of working fluid flowing through the tube or annulus side of the heat exchanger at constant temperature (no heat exchange). In the present work experiments were performed at four temperatures 20, 40, 60, and 70 °C, which give a satisfactory variety of physical properties, with 8 values for Reynolds number, from 5000 through 40000 for the tube-side enhancement experiments and from 3000 through 10000 based on the equivalent diameter for annulus-side enhancement experiments. The operation of isothermal pressure drop, in case,

if the tube side is intended to study the pressure drop inside, can be summarized in the following steps (referring to fig. 4-2):

- The first step was filling the hot water tank with water at one of the temperatures above. Then temperature is changed to the next.
- The isothermal pressure drop operation was a closed-loop process. That was by sealing valves V-17, V-23, and V-25.
- The interested loop of water was being determined according to its temperature. For 20 and 40 °C water circulated the loop was started from the hot water tank passing through V-2, pumped by the hot water centrifugal pump through V-4, V-6, passing through the rotameter and then V-7 entering the inner tube of the heat exchanger and returning to the tank. V-5 and V-18 was tightly sealed. That loop was decided because the orifice plate was designed and calibrated to work at 60 and 70 °C, while that was accessible in the rotameter. For 60 and 70 °C, the loop was different, starting from the hot water tank, through V-2, V-5 pumped through the orifice plate to the inner tube of the heat exchanger and finally returned to the tank. V-6 and V-7 was tightly sealed.
- Flowrate measured by the rotameter was the wanted one in case of 20 and 40 °C temperatures while that measured by the orifice plate for 60 and 70 °C. For each case, the pressure drop was registered. Then the flowrate was raised for the next using valve V-4.
- Valves V-18, V-20, V-21, V-24, and V-26 were left open, while V-19 and V-22 there was no problem if were being forgotten open.

If the annulus side was intended to study the pressure drop inside, with the aid of fig. 4.2, the main steps are summarized by the following points:

- Filling the hot water tank with water at a specific temperature.
- Sealing valves V-17, V-23, and V-25.

- Valve V-7 should be tightly sealed.
- Valves V-19 and V-22 were left sealed.
- In the present case the path of water was: the hot water tank, V-2, the hot water pump, V-7, the rotameter, V-18, V-20, V-21, V-24, V-26, and returning to the tank. The flowrate measured by the rotameter was the intended flowrate. Then, pressure drop was registered.
- V-5 was left slightly open and V-8 and V-9 were being left open to permit some of water to pass through the inner tube to ensure that no heat exchange was happening.

#### **4.2.2 Heat Exchange Experiments**

The second part of the present work was the heat transfer experiments. Cold water was flowing in open cycle, through the annulus of the double pipe heat exchanger, counter-currently with hot water stream which was flowing in closed cycle through the inner tube. The implementation of a heat transfer experiment can be summarized in the following steps:

- Valves V-23 and V-26 were kept sealed during all the work.
- Valves V-6 and V-7 should be tightly sealed to keep the two streams separated.
- V-11 was the inlet of the water, so it should be opened.
- The cold fluid unit work was depending on whether the water was coming with temperature less or greater than 20 °C (working temperature of cold water for all heat transfer experiments). If less than 20 °C, V-13 and V-14 were both sealed, i.e., the water cooler and its accessories were shut down, while the heating tank was being used (V-15 opened). If the water temperature was greater than 20 °C, then the

water cooler and its accessories were being operated (V-13 and V-14 open), while the heating tank was shut down (V-15 sealed).

- In the mixing point, two streams were mixed, the fresh stream of water and either that coming from the cooling or the heating tank, manually controlled to obtain a water stream at  $20 \pm 0.5$  °C to be used as the cold fluid.
- V-19 and V-22 were always left sealed.
- The cold water path was: the mixing point, pumped by the cold water pump through V-17, the rotameter, V-18, V-20, counter-currently through the annulus of the heat exchanger, V-21, V-24, and through V-25 water was drained outside the system.
- The volumetric flowrate assigned by the rotameter is the flowrate of cold water under study.
- Valves V-1, V-3, and V-10 were left sealed.
- In the present work, all experiments were performed with two temperatures for the hot water stream, 60 and 70 °C. These temperatures were controlled manually. Heat transferred in the exchanger was always known due to the computer program employed, so, by using the variety of heaters, provided to the hot water tank especially those controlled by the variac, temperature of the produced water would be controlled to  $60$  or  $70 \pm 0.5$  °C. The large volume of the hot water tank was widely helping in forbidding the fluctuations in these temperatures.
- The path of hot water was: the hot water tank, V-2, pumped by the hot water pump through V-4 and V-5, and then through the orifice plate and V-8 entering into the inner tube of the double pipe heat exchanger, and finally through V-9 returning to the hot water tank.

- Two divisions of heat exchange experiments were performed, the first was carried out for the case of enhancement of heat transfer inside the inner tube. In that kind, the cold water mass flowrate was kept constant at two values (0.1 and 0.15 kg/s) and hot water was changed for 8 values of Reynolds number in the inner tube starting from 5000 through 40000. The second kind was performed when the annulus as the enhanced side, where constant mass flowrates for the hot water stream (0.1125 and 0.2 kg/s), while the cold water was changed for 8 values of Reynolds number starting from 3000 through 10000.
- Valves V-4 and V-17 were used as control valves of the hot and cold flowrates respectively.
- All steps stated above were in need to wait for few minutes until the steady state conditions were reached for each change in the hot or cold flowrate. When the approval value of volumetric flowrate (determined by using the computer program) was reached, four temperatures of the inlet and outlet points, as well as the pressure drop in the two sides, read on the manometers panel, were being registered.

### **4.3 Calculation Procedure**

#### **4.3.1 Prediction of Physical Properties**

The use of a computer program (fig. 4-6) to perform calculation of the system which includes widely the properties of water like density, dynamic viscosity, conductivity, and heat capacity, needs to deduce equations for these properties to be used in the computer program. Appendix A includes tabulated properties of water which have been converted by curve fitting to polynomial equations. Equations (A.1), (A.2) and (A.3) would be used in the computer program to predict the physical properties of water instead of direct use of table A-1.

### **4.3.2 Isothermal Pressure Drop Calculations**

This class of calculations includes the calculation of Darcy-Weisbach friction factor for all cases studied using the values of isothermal pressure drop obtained during the experiments of isothermal pressure drop, discussed previously, using the equation (3.4). Thus, a large number of points would be available to be used in predicting an isothermal friction factor correlation.

### **4.3.3 Heat Transfer Calculations**

The more complicated calculations are that of heat transfer which includes:

**( i ) Calculation of Reynolds number:** It is an implicit problem where Reynolds number was intended to be calculated with unknown physical properties and mass flowrate in order to appear in the form of an integer (5000, 10000, 15000, etc.) in addition to the great physical meaning might be included if all readings had been taken for particular Reynolds numbers instead of volumetric or mass flowrates. In other words, a specified Reynolds number at particular temperature (particular physical properties) might mean a mass flowrate, different from that at another temperature. A trial and error procedure is adopted for the purpose which may be explained as: an initial volumetric flowrate  $Q$  is assumed as the required value for the Reynolds number under study, using the temperatures of the inlet and outlet streams of the double pipe heat exchanger resulted to predict physical properties which would lead to a new value for  $Q$  for the interested stream, repeating the process until convergence would be reached as illustrated in fig. 4-6 which represents an algorithm for a computer program. Figure 4-6 was written for tube-side enhancement, similar one for annulus enhancement, easily could be imitated by excluding the part of the orifice plate operation which was unnecessary in that case, with some changes in the equations used for calculations to be suitable for the annulus instead of the inner tube.

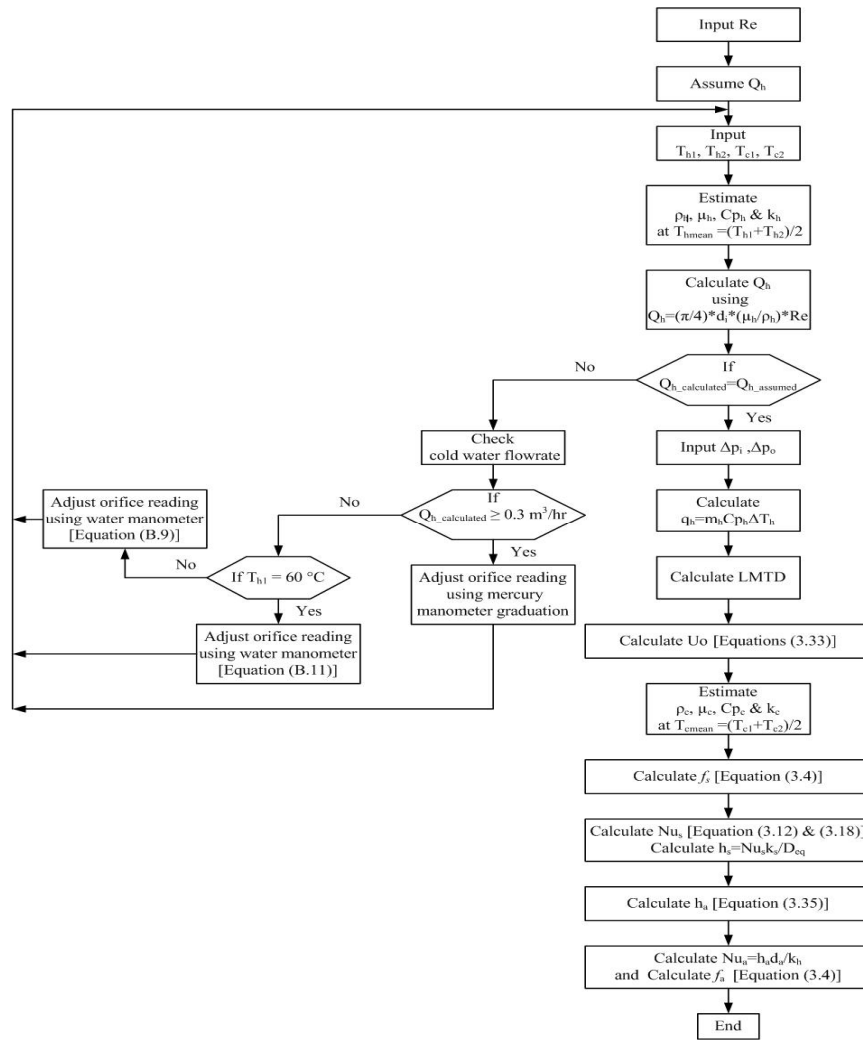


**Figure 4-6:** An algorithm for calculations of tube-side heat transfer enhancement.

**( ii ) Friction factor calculations:** For both enhanced or unenhanced sides of the heat exchanger, friction factor was calculated directly by using equation (3.4) adopting the pressure drop measured by the manometer,

**( iii ) Nusselt number calculations:** The procedure of calculating Nusselt number might be summarized as:

1. Heat Transfer rate is calculated by equation (3.32) for the two sides and the average value is considered.
2. The overall heat transfer coeff.  $U_o$  was calculated by eq. (3.33).

3. Friction factor for the unenhanced side is predicted by equation (3.4).
4. Nusselt number (and then the heat transfer coefficient) for the unenhanced side is calculated by equation (3.12), alone, if it is the tube side or with equation (3.18), if it is the annulus side.
5. By equation (3.36), the heat transfer coefficient is obtained for the enhanced side, and then Nusselt number for that side.

#### 4.4 Error Sources and Uncertainty

In the present work, some of the error sources which may be fixed as the sources of uncertainty in predicting volumetric flowrates, temperatures and pressure drops which might lead to errors in the predicted values:

- 1- Electric power instability.
- 2- Uncertainty in temperature reading resulted from manufacturing defects in the thermocouples and temperature reader device.
- 3- Errors in flow measurements.
- 4- Temperature control difficulties.

The first three might lead to that the heat transfer calculated by  $q = \dot{m}C_p\Delta T$  be not equal, so the average value was used in all calculations with an acceptable deviation ratio defined as:

$$\text{Deviation ratio} = \frac{|q_h - q_c|}{q_{avg.}} \times 100 \leq 5\%. \quad \dots (4.1)$$

The fourth source was constrained to  $\pm 0.5$  °C for the inlet temperatures with keeping the inlet temperature approach as close to 40 or 50 °C as possible.

# **CHAPTER FIVE**

## **Experimental Results**

### **5.1 Introduction**

Experiments on thirty six cases of smooth and augmented tubes and annuli were carried out in order to study the effect of different types of inserts on heat transfer and pressure drop in a double pipe heat exchanger. The primary experimental data taken are temperatures of the four inlets and outlets, pressure drop in the two sides and heat transfer rate at different experimental conditions. Tables C-1 through C-18 includes the experimental results for the smooth, as well as augmented tubes and annuli. In addition, experiments on isothermal pressure drop for all cases have been performed. Their results are displayed in tables C-37 through C-40.

### **5.2 Test of Authenticity of Using the Present Heat Exchanger.**

First of all calculations and comparisons among the heat transfer and pressure drop or friction factor for augmented and smooth tubes annuli, these smooth tubes and annuli must be tested for authenticity to be used in the experimental work. For heat transfer authenticity test, a comparison between Nusselt number calculated empirically by Gnielinski equation (equation 3.12) and that calculated by using the experimental data obtained, has been performed. For the pressure drop authenticity test a comparison between the friction factor calculated theoretically by Petukhov equation (equation 3.3) and that obtained by experimental work (equation (3.4)). Theoretical and experimental Nusselt number and friction factor (for heat exchange and isothermal conditions) are presented in tables C-19, C-24, C-37 and C-38 and plotted in figs. 5-1 through 5-4.

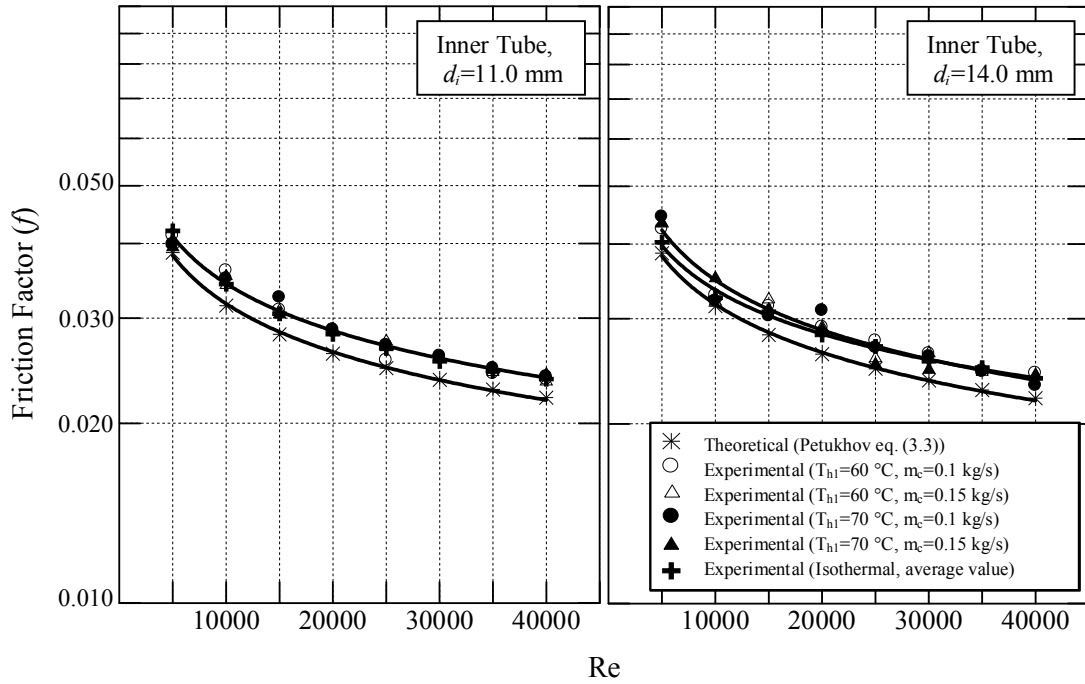


**Figure 5-1:** Comparison of empirical (eq. (3.3)) and experimental friction factor of smooth tubes used in tube-side heat transfer enhancement experiments for two tube sizes.

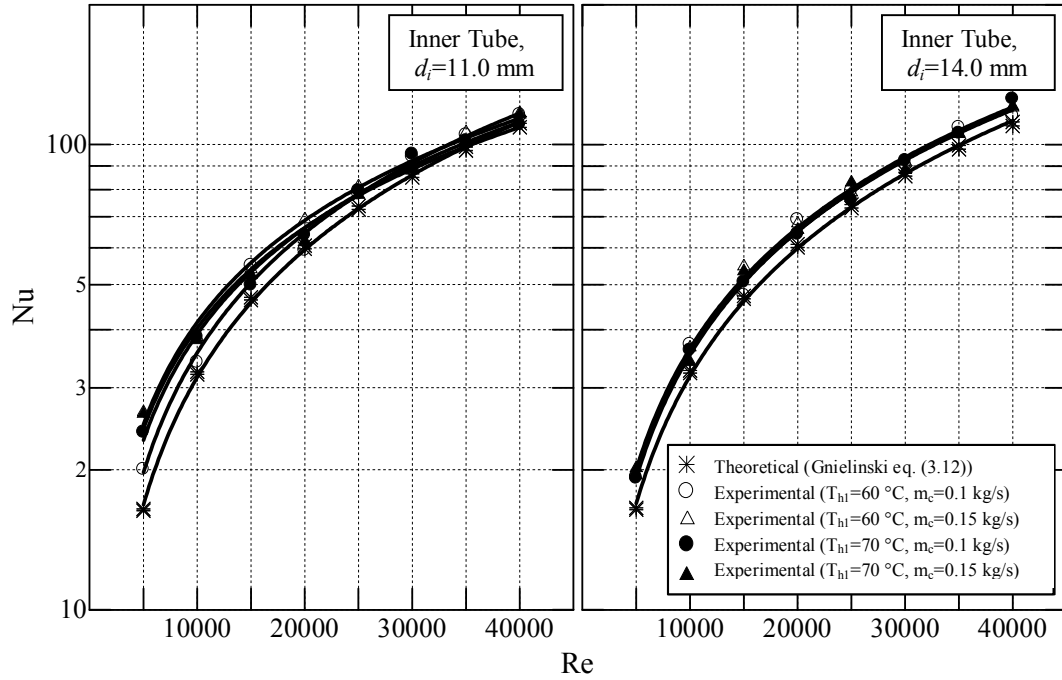


**Figure 5-2:** Comparison of empirical (eq. (3.12)) and experimental Nusselt number inside the smooth tubes used in tube-side heat transfer enhancement experiments.

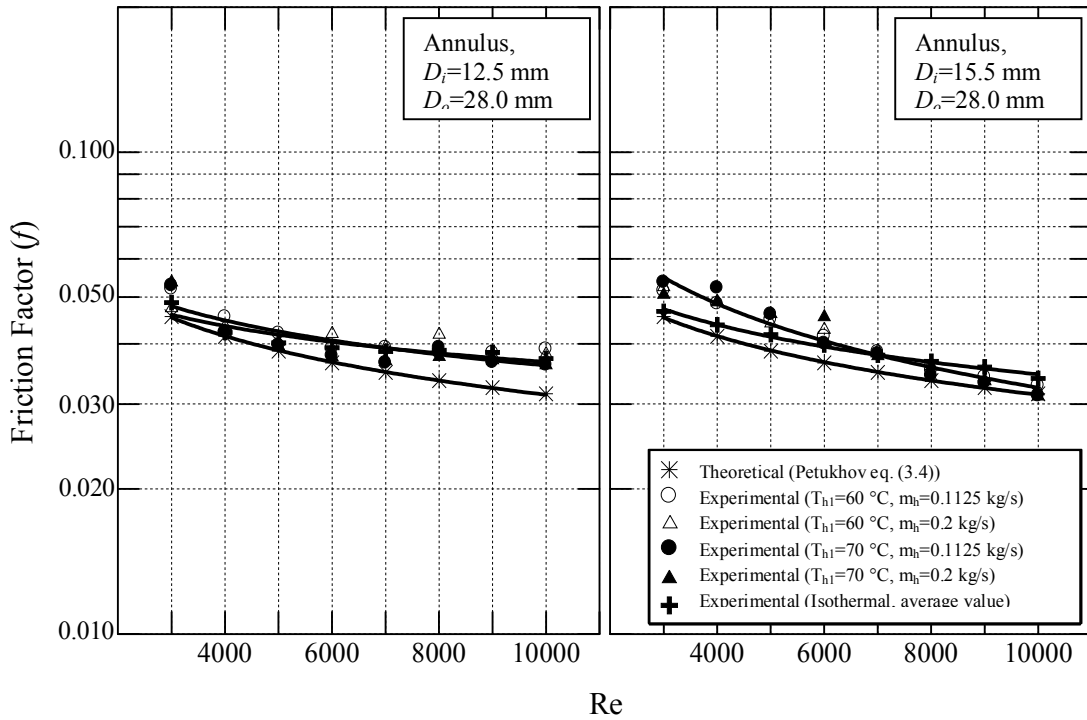


**Figure 5-3:** Comparison of theoretical and experimental friction factor of smooth annuli used in annulus-side heat transfer enhancement experiments.

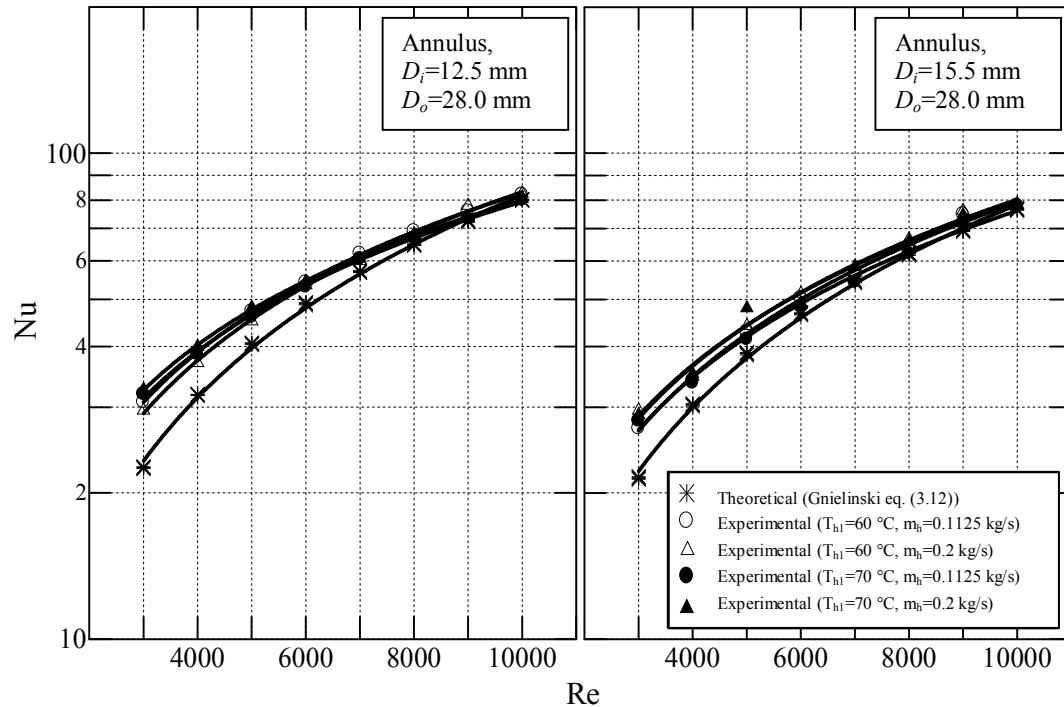


**Figure 5-4:** Comparison of theoretical and experimental Nusselt number of smooth annuli used in annulus-side heat transfer enhancement exnements

Deviations from theoretical values are fixed in table 5-1. These values were obtained by dividing the absolute difference of the experimental and theoretical value by the theoretical value for all values of the friction factor and Nusselt number and then the average value is considered.

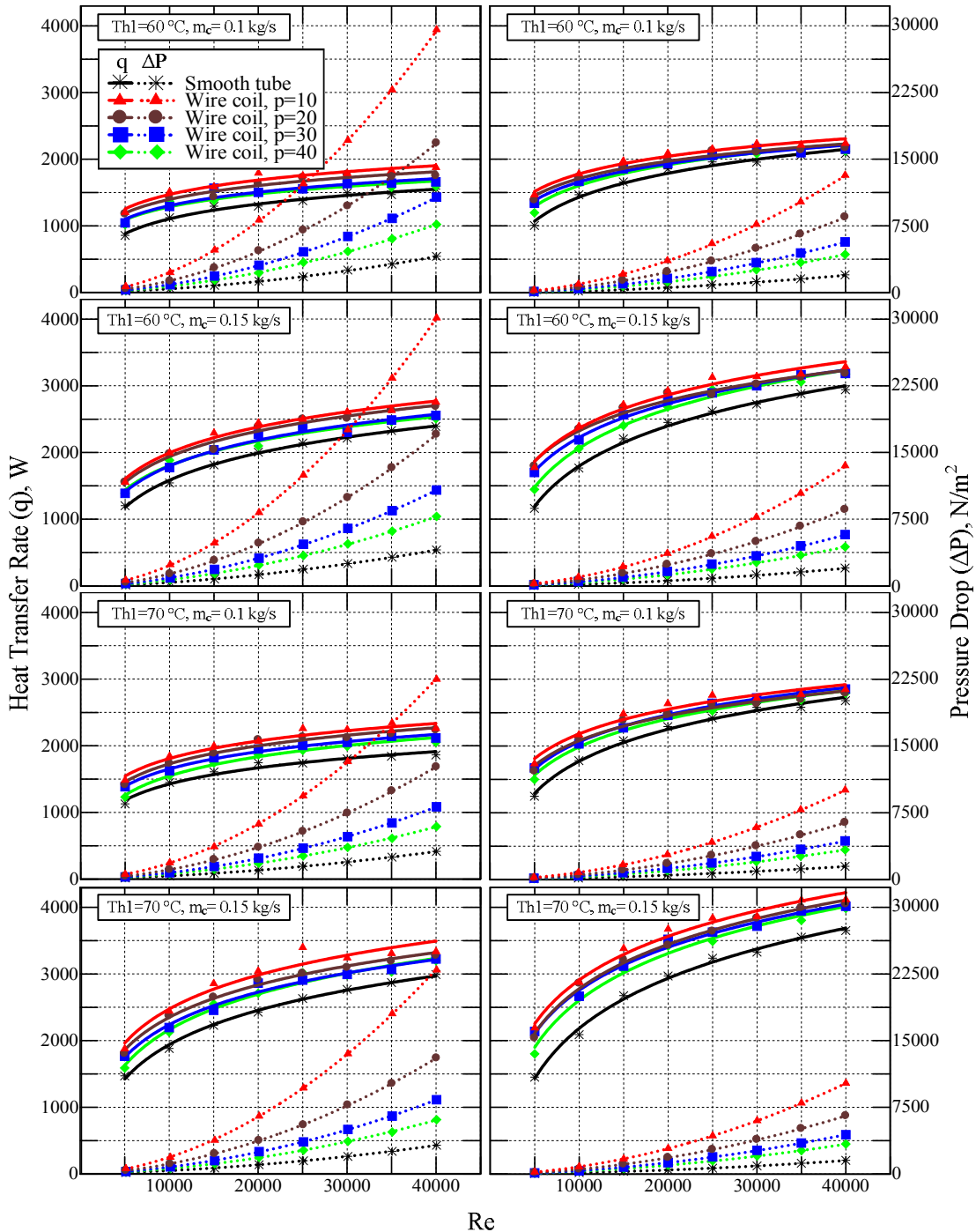
**Table 5-1:** Deviations of Experimental Nusselt and Friction Factor from Values obtained from empirical equations for Smooth Inner Tubes and Annuli.

Type of experiment	Inner tube				Annulus			
	$d_i = 11$		$d_i = 14$		$D_i = 12.5$ $D_o = 28.0$		$D_i = 15.5$ $D_o = 28.0$	
	% dev. in Nu	% dev. in $f$	% dev. in Nu	% dev. in $f$	% dev. in Nu	% dev. in $f$	% dev. in Nu	% dev. in $f$
Dev. in heat exch. exp.	+ 8.66	+ 8.36	+ 8.55	+ 9.18	+ 8.88	+ 10.79	+ 7.77	+ 11.35
Dev. in isothermal pressure drop exp.	—	+ 8.12	—	+ 6.96	—	+ 9.79	—	+ 7.46
Average deviation	+ 8.66	+ 8.24	+ 8.55	+ 8.07	+ 8.88	+ 10.29	+ 7.77	+ 9.41

### 5.3 The Effect of Turbulence Promoters on Heat Transfer Rate and Pressure Drop.

To have a general view of the effect of turbulence promoters, used in the present work, on heat transfer rate and pressure drop in the inner tube and annulus, values of heat transfer rate and pressure drop (tables C-1 through C-18) are plotted versus Reynolds number in figs. 5-5 through 5-8 for all cases.

Figures 5-5 through 5-8 reveals an expected increase of pressure drop with decreasing the coiling or ribbing pitches either in tube-side or annulus-side heat transfer enhancement. On the other hand, the heat transfer rate does not behave in a similar manner except in case of tube-side heat transfer enhancement (fig. 5-5) where the above description becomes valid only for the wire coil of  $e = 1$  mm used on the outer surface of the inner tube (fig. 5-6) for the two annulus sizes, while this fact becomes invalid for the  $e = 2.2$  mm wire coil or circular rib where decreasing the coiling or ribbing pitch for that wire or rib diameter means decreasing heat transfer rate (fig. 5-7 and 5-8).



Inner tube,  
 $d_i=11.0 \text{ mm}$

Inner tube,  
 $d_i=14.0 \text{ mm}$

**Figure 5-5:** Heat transfer rate ( $\text{W}$ ) and pressure drop ( $\text{N}/\text{m}^2$ ) vs. Reynolds number for tube-side heat transfer enhancement using a wire coil of  $e = 1 \text{ mm}$  for two inner tube sizes and four experimental conditions (Notation above belongs to all cases).

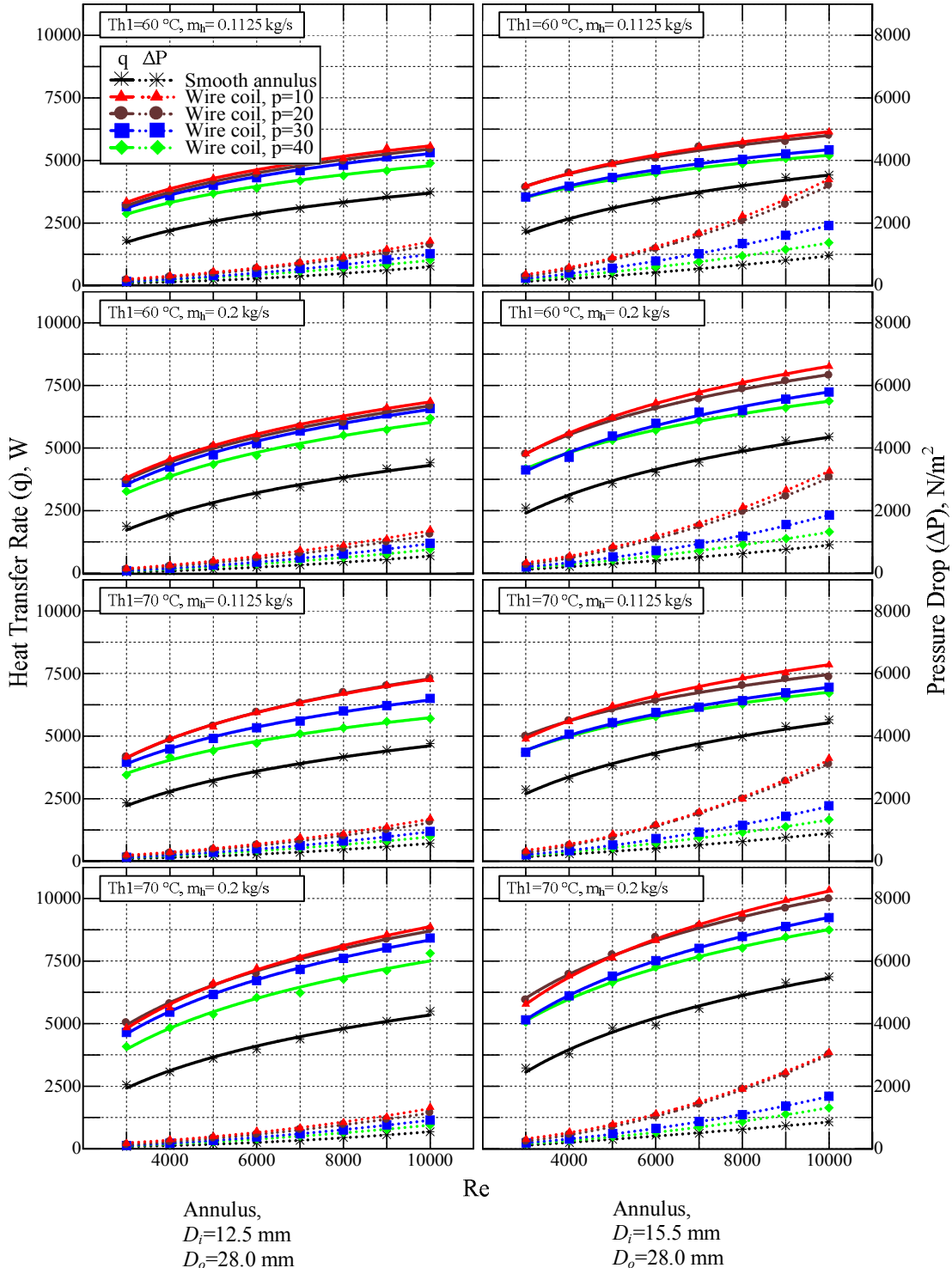


**Figure 5-6:** Heat transfer rate (W) and pressure drop ( $N/m^2$ ) vs. Reynolds number for annulus-side heat transfer enhancement by wire coils of  $e = 1$  mm for two annulus sizes and four experimental conditions (Notation above belongs to all cases).

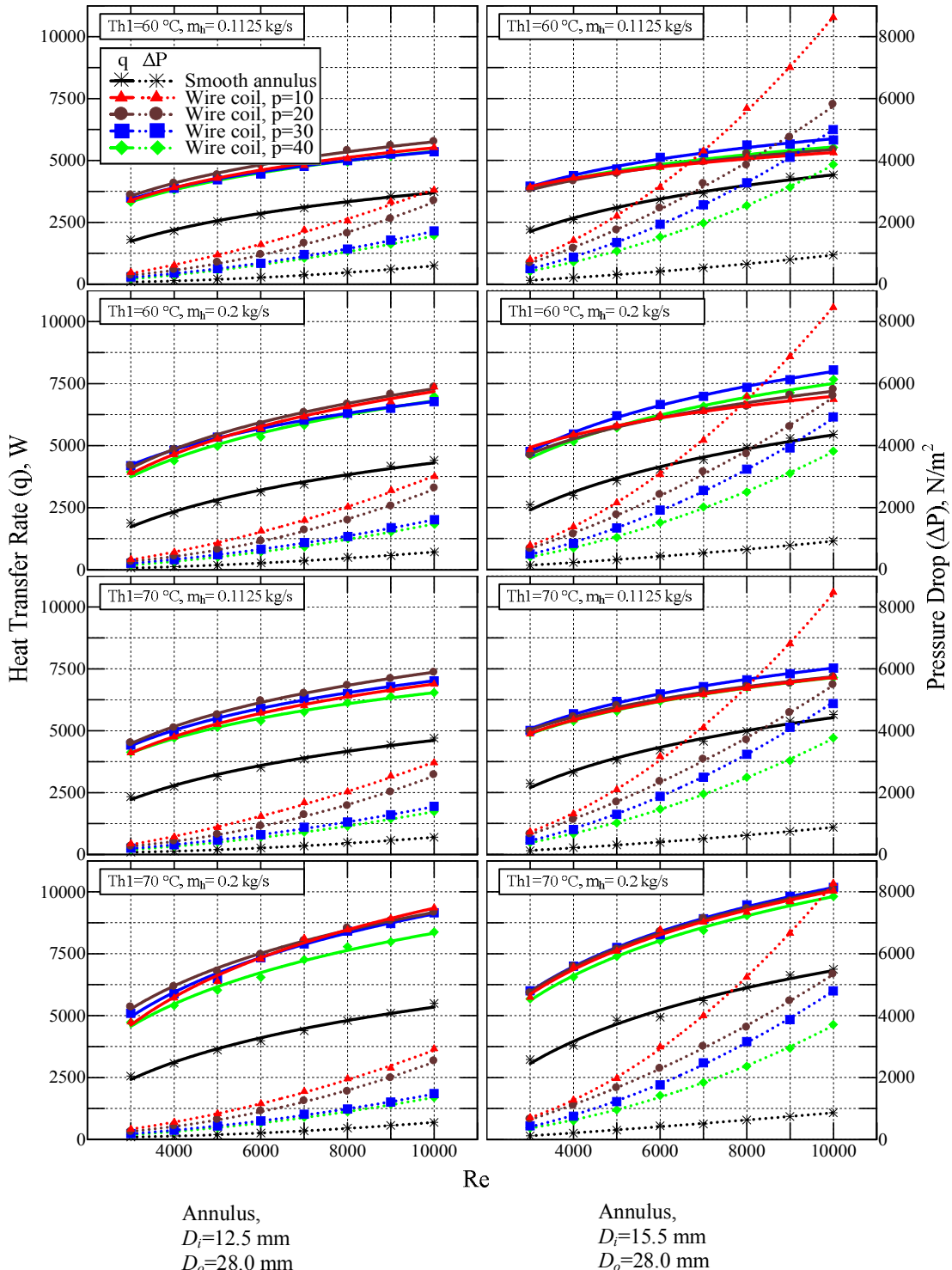


**Figure 5-7:** Heat transfer rate (W) and pressure drop ( $N/m^2$ ) vs. Reynolds number for annulus-side heat transfer enhancement by wire coils of  $e = 2.2\text{ mm}$  for two annulus sizes and four experimental conditions (Notation above belongs to all cases).

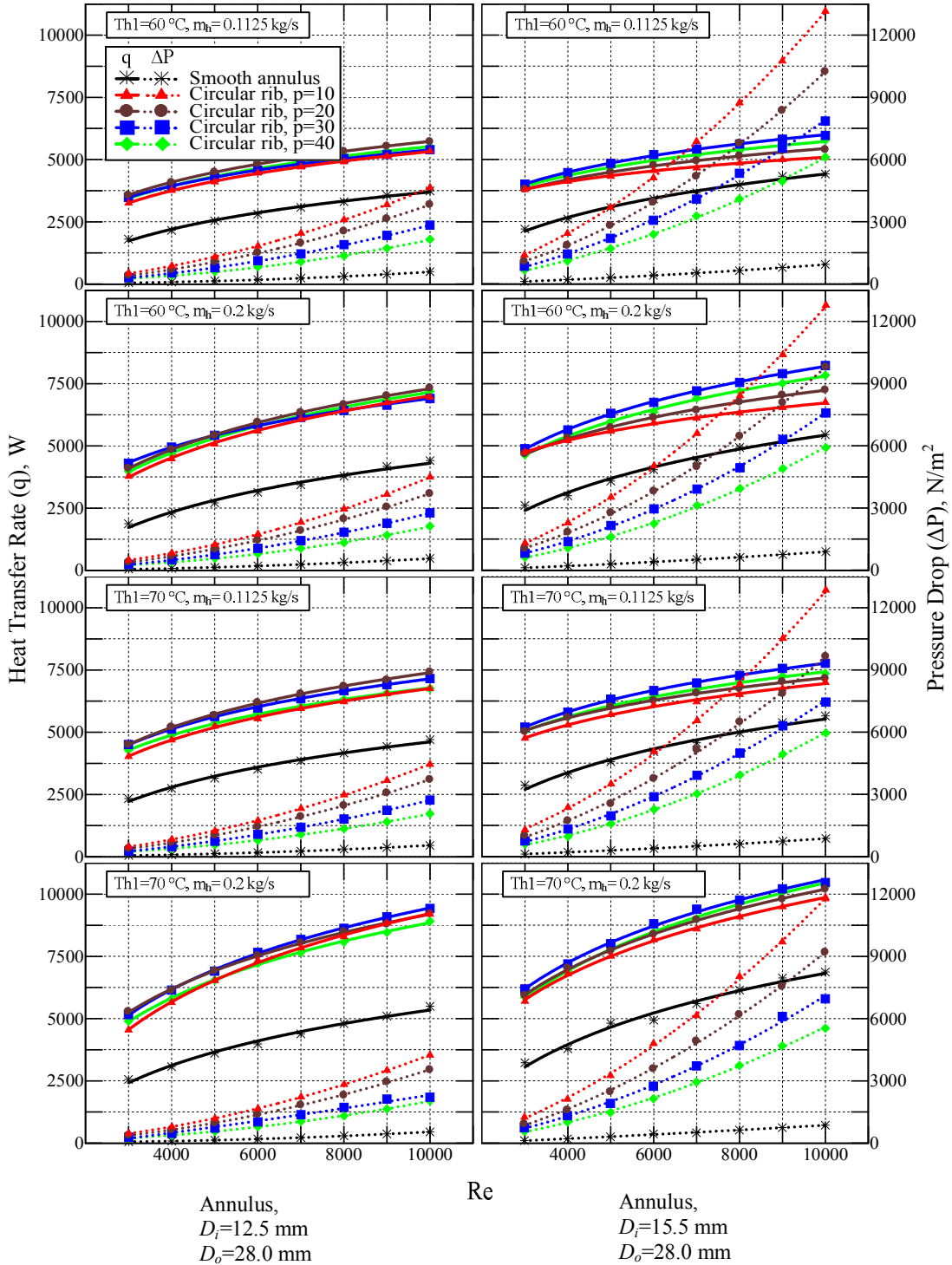


**Figure 5-8:** Heat transfer rate (W) and pressure drop ( $N/m^2$ ) vs. Reynolds number for annulus-side heat transfer enhancement by circular ribs of  $e = 2.2\text{ mm}$  for two annulus sizes and four experimental conditions (Notation above belongs to all cases).

## 5.4 Effect of Turbulence Promoters on Friction Factor

Two collections of friction factor were obtained for each promoter used to augment heat transfer. The first is that for real heat exchange process. These values of friction factor, graphically or in correlation form, would be used for comparisons and PECs to study the effect and usefulness of each insert. The second is that for isothermal operation conditions. The latter might be converted to correlations to be used in design of heat exchangers.

### 5.4.1 Friction Factor in Heat Exchange Process

Friction factor inside the inner tube and annulus either smooth or with wire coil inserts (for all wire diameters adopted), have been calculated using the experimental values of pressure drop using equation (3.4), as tabulated in tables C-19 through C-36 and plotted in fig. 5-9 through 5-12 versus Reynolds number.

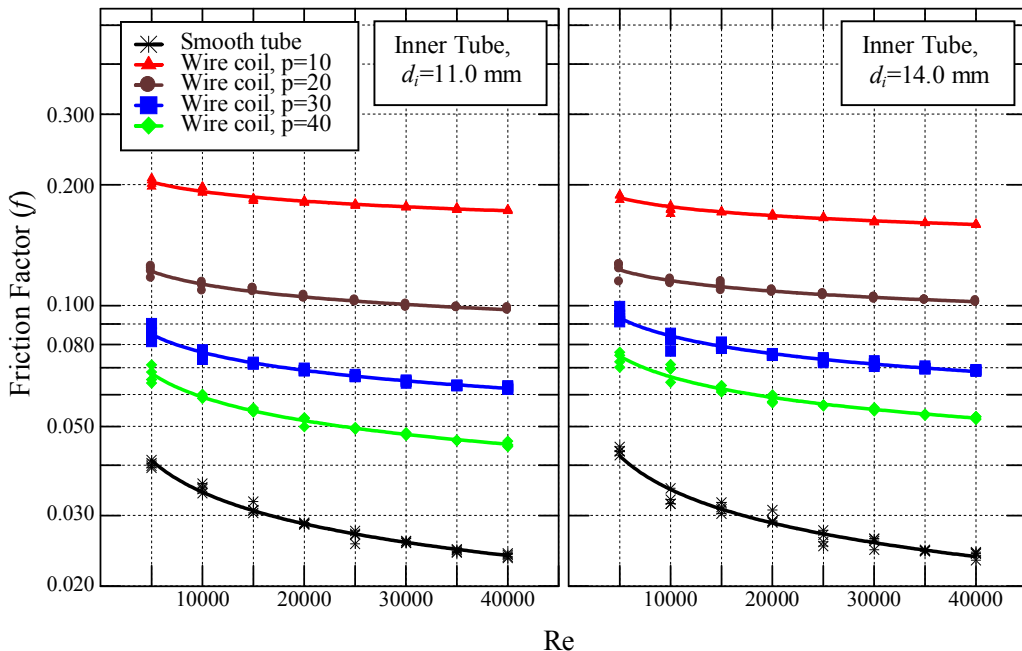


**Figure 5-9:** Friction factor vs. Reynolds number for heat exchange process inside the inner tube inserted with a wire coil of  $e = 1$  mm for two inner tube sizes.

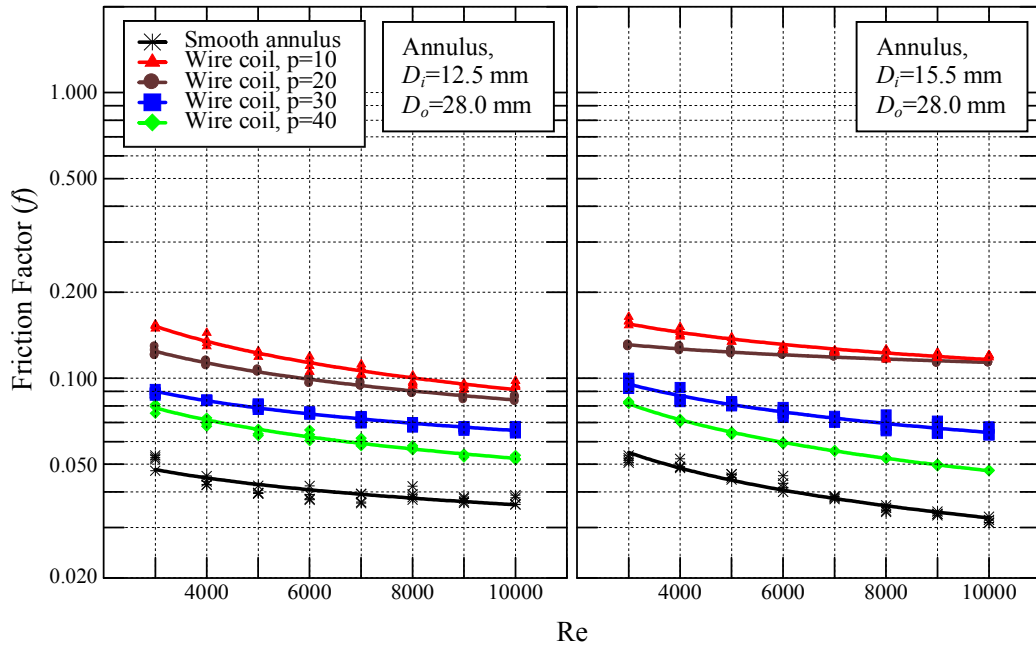


**Figure 5-10:** Friction factor vs. Reynolds number for annulus-side heat transfer enhancement by wire coils of  $e = 1 \text{ mm}$  (heat exchange process) for two annulus sizes.

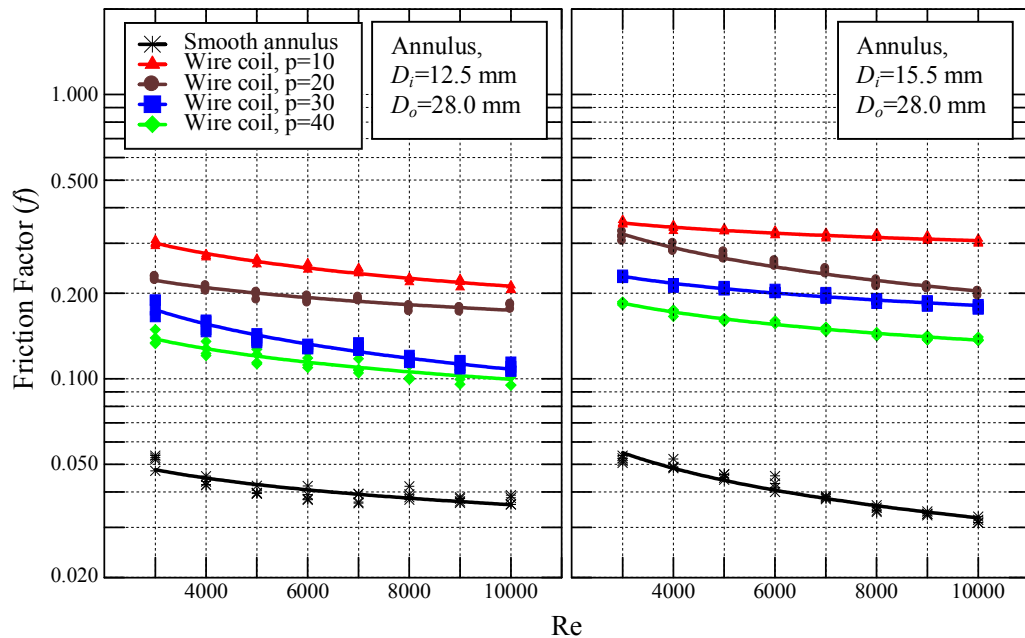


**Figure 5-11:** Friction factor vs. Reynolds number for annulus-side heat transfer enhancement by wire coils of  $e = 2.2 \text{ mm}$  (heat exchange process) for two annulus sizes.

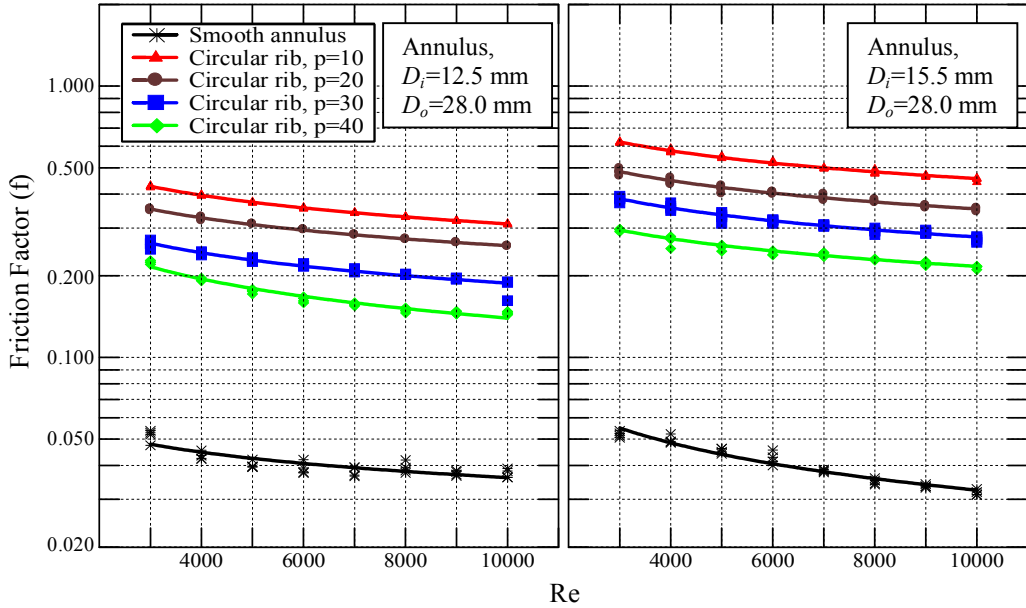


**Figure 5-12:** Friction factor vs. Reynolds number for annulus-side heat transfer enhancement by circular ribs of  $e = 2.2$  mm (heat exchange process) for two annulus sizes.

In figs. 5-9 through 5-12, no sign for the operational conditions have been included and the curve fit represented the average value of friction factor for the four operation conditions for each case considered, because only the geometrical parameters, in addition to Reynolds number, would be included in the proposed correlations produced in the present work. That would be in a similar manner to those appearing in Petukhov equation for smooth tubes or the previous works [1, 2, 8, 9, 10, 11, 35, 51, and 52] for augmented tubes.

#### 5.4.2 Friction Factor in Isothermal Process.

That was performed by using similar calculations to that adopted in heat exchange process but with using the isothermal pressure drop values. Isothermal pressure drop and friction factor obtained are tabulated in tables C-37 through C-40) and plotted in figs. 5-13 through 5-16 versus Reynolds number.

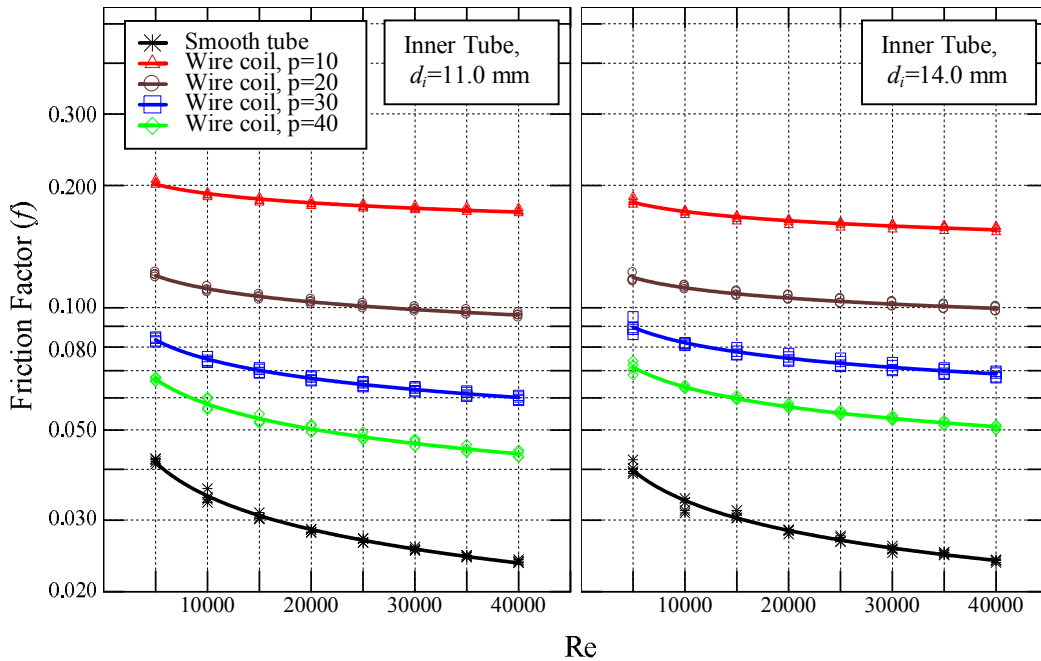


**Figure 5-13:** Friction factor vs. Reynolds number for smooth tube and roughened by a wire coil of  $e = 1 \text{ mm}$  in isothermal conditions for two inner tube sizes.

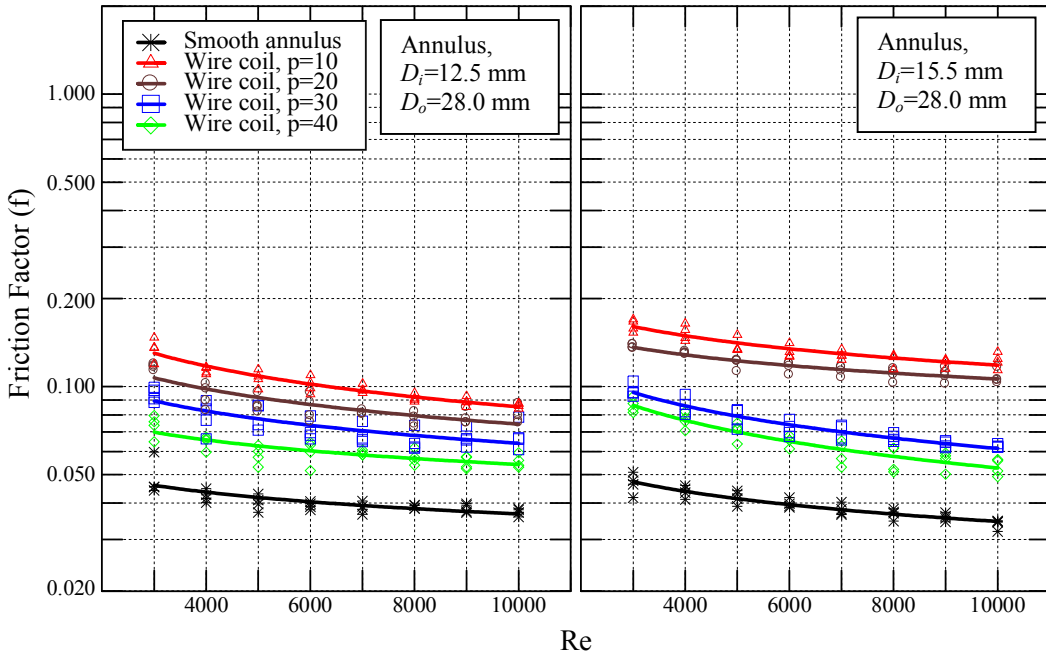


**Figure 5-14:** Friction factor vs. Reynolds number for smooth annulus and with a wire coil of  $e = 1 \text{ mm}$  in isothermal conditions for two annulus sizes.

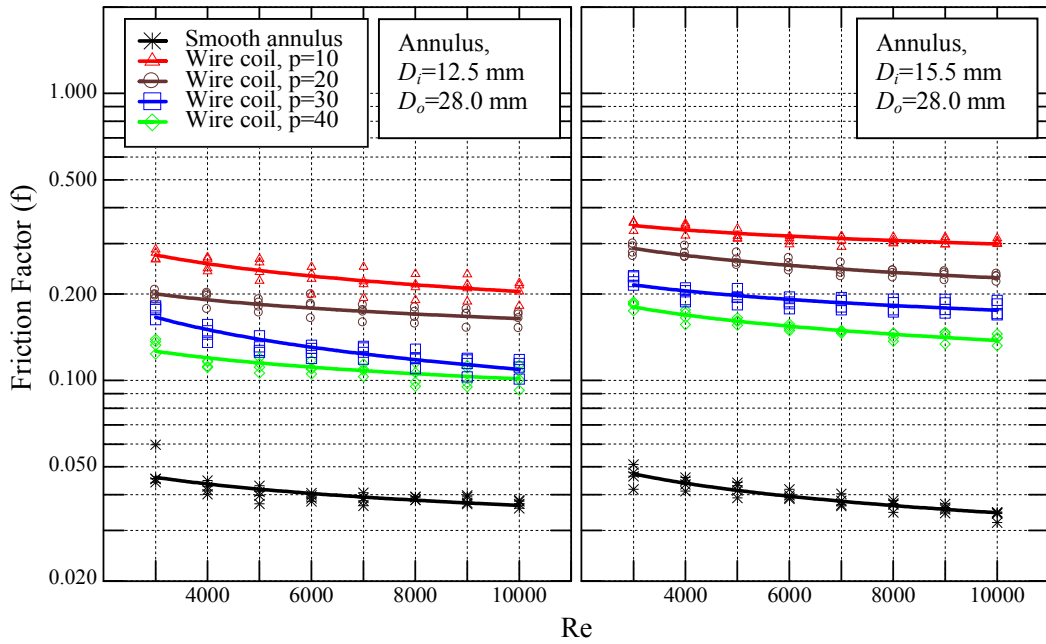


**Figure 5-15:** Friction factor vs. Reynolds number for smooth annulus and with a wire coil of  $e = 2.2 \text{ mm}$  in isothermal conditions for two annulus sizes.

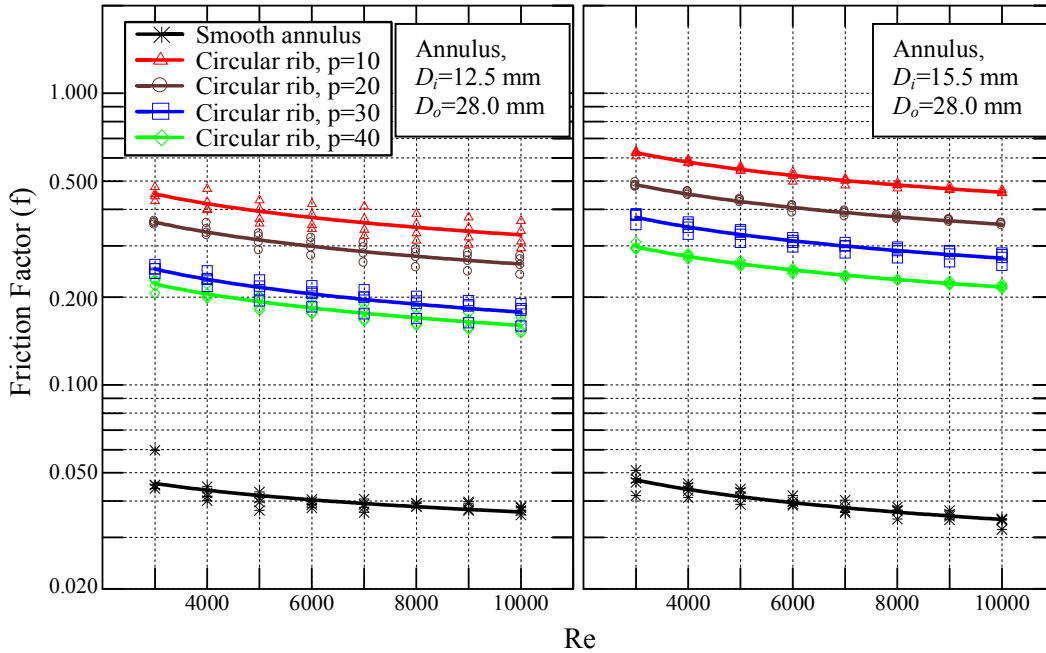


**Figure 5-16:** Friction factor vs. Reynolds number for smooth annulus and with circular ribs of  $e = 2.2 \text{ mm}$  in isothermal conditions for two annulus sizes.

## **5.5 Effect of Turbulence Promoters on Heat Transfer**

In addition to friction factor, heat transfer represented by Nusselt number is the most important factor might be studied in a heat transfer enhancement study, because it might be considered as the real indication to the variations in heat transfer in smooth tubes or those obtained by using turbulence promoters, rather than heat transfer rate plotted in figs. 5-5 through 5-8. Nusselt number values for different types of inserts, different positions, different tube or annulus sizes, and operational conditions are tabulated in tables C-19 through C-36 and plotted in figs. 5-17 through 5-20.

In these plots, the adopted operation conditions are strictly considered because they are the only way to indicate to the Prandtl number which is importantly included in all Nusselt number relationships either for smooth or roughened tubes and annuli.

Similar to relationships of heat transfer rate, the Nusselt number versus Reynolds number curve fits behave, where Nusselt number, for different conditions, increases with Reynolds number and coiling pitch in case of tube-side heat transfer enhancement while that does not occur in the other two cases and the same statement can be said for the variation in wire diameter.

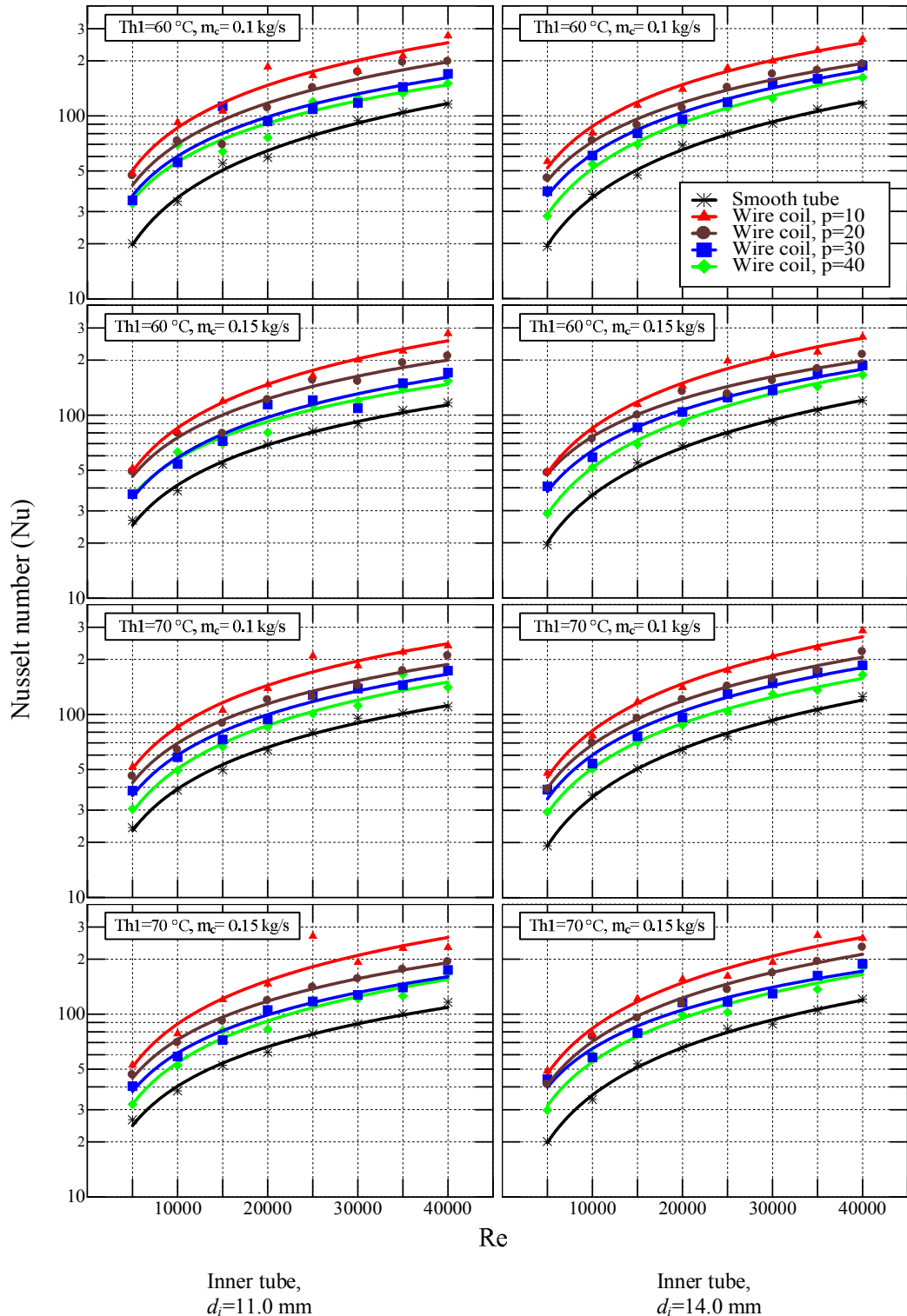


**Figure 5-17:** Nusselt number vs. Reynolds number for tube-side heat transfer enhancement using a wire coil of  $e = 1 \text{ mm}$  for two inner tube sizes and four experimental conditions (Notation above belongs to all cases).

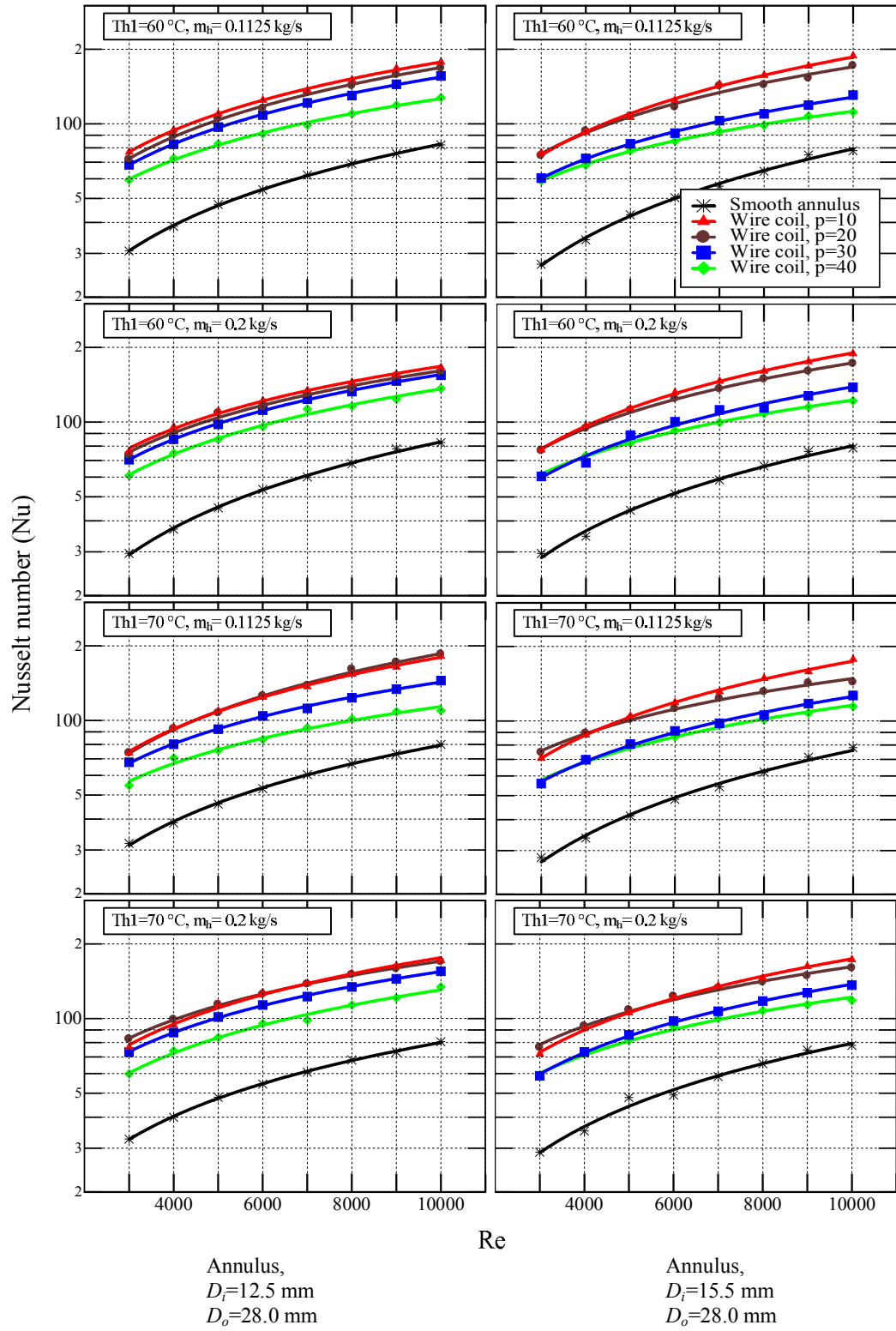


**Figure 5-18:** Nusselt number vs. Reynolds number for annulus-side heat transfer enhancement using a wire coil of  $e = 1 \text{ mm}$  for two annulus sizes and four experimental conditions (Notation above belongs to all cases).

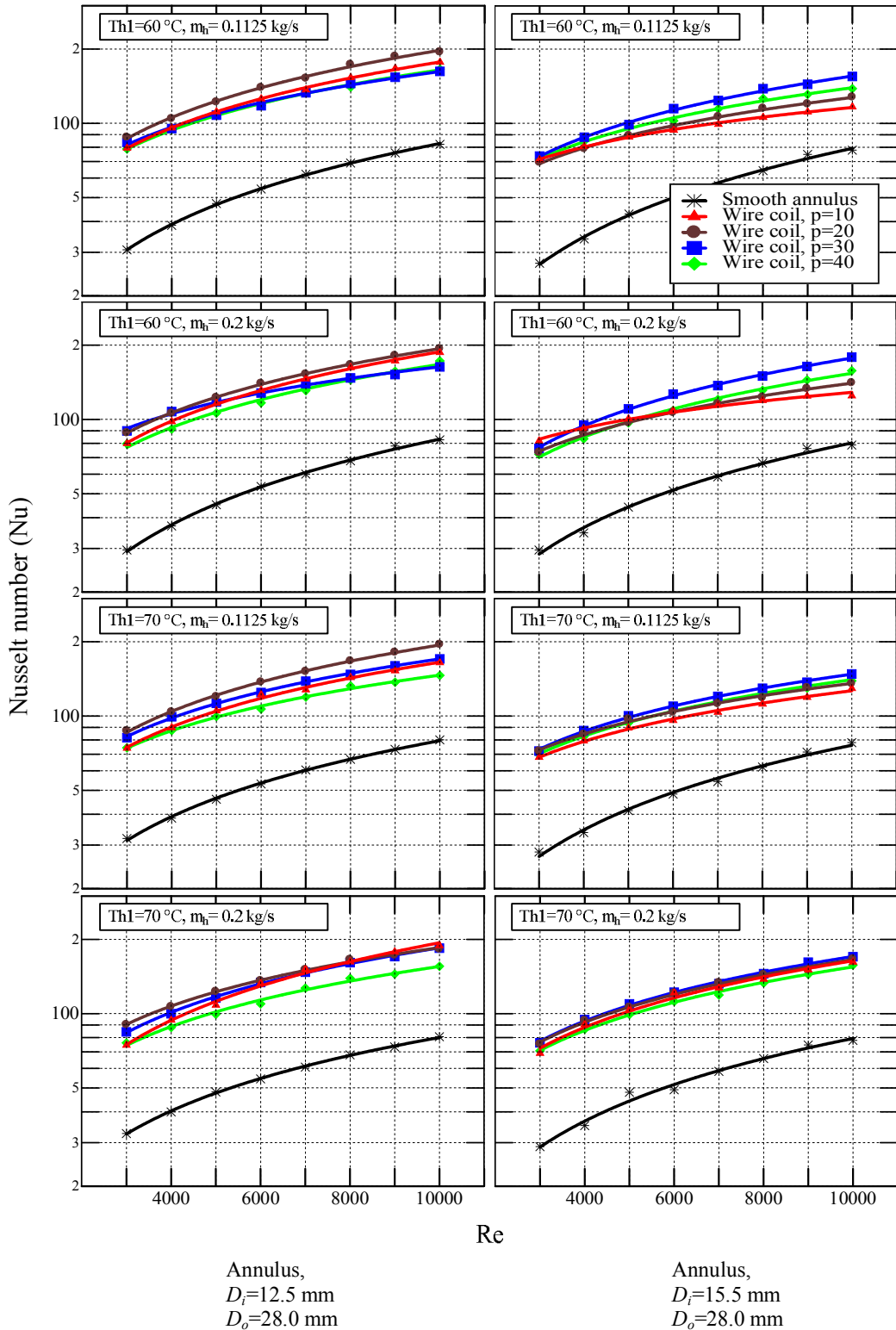


**Figure 5-19:** Nusselt number vs. Reynolds number for annulus-side heat transfer enhancement using a wire coil of  $e = 2.2$  mm for two annulus sizes and four experimental conditions.

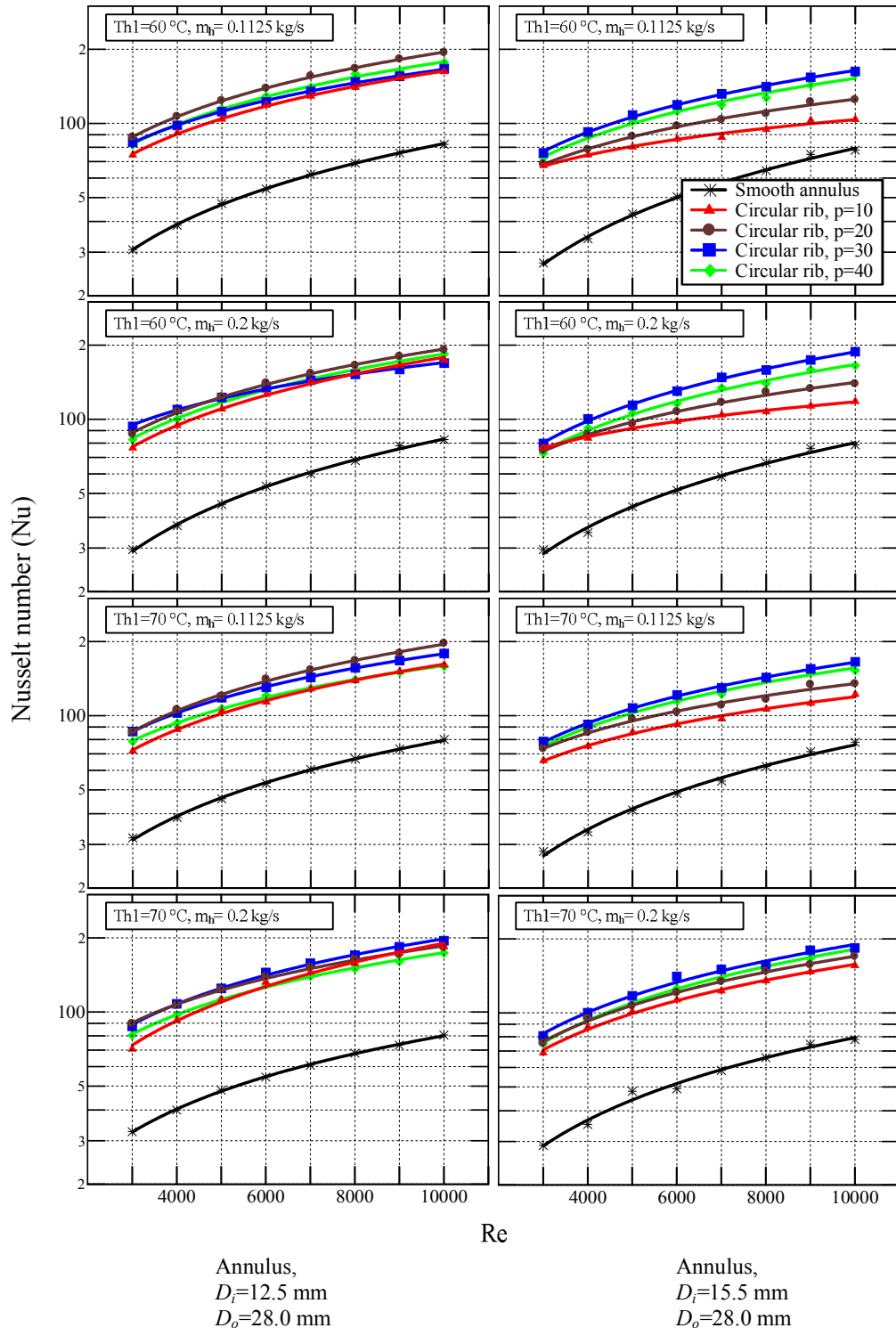


**Figure 5-20:** Nusselt number vs. Reynolds number for annulus-side heat transfer enhancement using circular ribs of  $e = 2.2$  mm for two annulus sizes and four experimental conditions.

## **5.6 Proposed Correlations of Friction Factor and Nusselt Number.**

Comprehensive correlations of friction factor and Nusselt number can be proposed for the three heat transfer enhancement methods. Like these correlations must include all geometrical parameters and operation conditions which are thought to influence the friction factor and Nusselt number. The first step is describing the studied inserts concisely in terms of the most effective geometrical parameters.

### **5.6.1 Concise Description of Inserts.**

A concise description of inserts used in the present work has been accommodated in terms of the most effective geometrical parameters which can be summarized as:

$\left(\frac{e}{d_i}\right)$  or  $\left(\frac{e}{D_e}\right)$ : This parameter represents the effect of the wire or circular rib diameter related to the inner diameter of the tube or the equivalent diameter of the annulus.

$\left(\frac{p}{d_i}\right)$  or  $\left(\frac{p}{D_e}\right)$ : This parameter represents the effect of the coiling or ribbing pitch related to the inner diameter of the tube or the equivalent diameter of the annulus.

The values of these parameters are set in table C-41.

### **5.6.2 Proposed Correlations of Friction Factor**

Curve fits in figures 5-9 through 5-16 each apart represents a correlation for friction factor versus Reynolds number for the intended inner tube or annulus with particular insert type, position of installation, size of tube or annulus or operation conditions. To have more useful correlations of friction factor to be

used in comparing the efficiency of different turbulence promoters in augmenting heat transfer or to be used in heat transfer equipment design, 256 points of friction factor versus Reynolds number for four heat exchange conditions inside the inner tube of the double pipe heat exchanger which have been used in plotting the mentioned figures were admitted together into the STATISTICA software package (a computer software concerned with statistical calculations) to produce a comprehensive empirical correlation of friction factor as a function of Reynolds number, and the two parameters ( $e/d_i$ ) and ( $p/d_i$ ) whose values are calculated for tube-side in table C-41. The correlation proposed is:

$$f_a = 3.6346 \text{Re}^{-0.0964} \left( \frac{e}{d_i} \right)^{0.8912} \left( \frac{p}{d_i} \right)^{-0.7856} \dots (5.1)$$

Equation (5.1) has a coefficient of determination of 0.9915. The latter may be defined as the criterion often used to judge the adequacy of a regression model [67].

Using the 256 friction factor points obtained for isothermal pressure drop experiments (plotted in fig. 5-13 except those for smooth tube), a similar correlation with a coefficient of determination equal to 0.9912 was obtained for isothermal operation conditions. That is:

$$f_a = 4.1497 \text{Re}^{-0.0945} \left( \frac{e}{d_i} \right)^{0.9576} \left( \frac{p}{d_i} \right)^{-0.7963} \dots (5.2)$$

The validity of equations (5.1) and (5.2) is in the range of Reynolds number of 5000 to 40000,  $e/d_i = 0.0714$  to  $0.0909$  and  $p/d_i = 0.7143$  to  $3.6364$ . Of course, equation (5.2) is more authenticable than equation (5.1), because the latter has been created using points fixed in isothermal conditions which

mean real physical properties to be used in calculating the Reynolds number, while Reynolds number calculated using physical properties at arithmetic mean temperature.

For the case of annulus-side heat transfer enhancement using a wire coil set up on the outer surface of the inner tube, 512 friction factor versus Reynolds number points (used in fig. 5-10 and 5-11 except those for smooth tube) are available to be used in correlating an empirical equation for the friction factor as a function of Reynolds number and  $(e/D_e)$  and  $(p/D_e)$ . That is

$$f_a = 16.0619 \text{Re}^{-0.2491} \left( \frac{e}{D_e} \right)^{1.0872} \left( \frac{p}{D_e} \right)^{-0.4652} \quad \dots (5.3)$$

Equation (5.3) has a coefficient of determination of 0.9709. An attempt to improve the value of that criterion (or enhancing the accuracy of equation (5.3)), may be by enforcing a new parameter which may be thought to be an influence in the friction factor in the annulus. That is the ratio of the inner to outer diameter of the annulus or  $(D_i/D_o)$ , which has the value of 0.4464 and 0.5536 for the annulus of  $D_i= 12.5$  mm and  $D_o=28.0$  mm and  $D_i= 15.5$  mm and  $D_o=28.0$  mm respectively. The resulting correlation is

$$f_a = 21.8417 \text{Re}^{-0.2467} \left( \frac{e}{D_e} \right)^{1.0126} \left( \frac{p}{D_e} \right)^{-0.4870} \left( \frac{D_i}{D_o} \right)^{0.6875} \quad \dots (5.4)$$

with a coefficient of determination something larger than that of equation (5.3) to be equal to 0.9820. For the isothermal operation conditions, also the 512 points (used in fig. 5-14 and 5-15 except those for smooth tube) are available to be used to obtain an equation similar to equation (5.3). That is:

$$f_a = 11.5288 \text{Re}^{-0.2088} \left( \frac{e}{D_e} \right)^{1.1142} \left( \frac{p}{D_e} \right)^{-0.4479} \dots (5.5)$$

which has a coefficient of determination of 0.9636, but inserting the parameter ( $D_i/D_o$ ) enables having an equation with larger coefficient of determination of 0.9829 with producing the following equation

$$f_a = 17.4238 \text{Re}^{-0.2069} \left( \frac{e}{D_e} \right)^{1.0108} \left( \frac{p}{D_e} \right)^{-0.4774} \left( \frac{D_i}{D_o} \right)^{0.9179} \dots (5.6)$$

Equations (5.4) and (5.6) are valid for the range of Reynolds number of 3000 to 10000,  $D_i/D_o=0.4464$  to  $0.5536$ ,  $e/D_e= 0.0645$  to  $0.176$  and  $p/D_e= 0.6452$  to  $3.2$ .

The third part of the present work was using circular ribs set up on the outer surface of the inner tube. Using the 256 points of friction factor versus Reynolds number plotted in fig. 5-12 except those of smooth tube gives the equation:

$$f_a = 204.7049 \text{Re}^{-0.2666} \left( \frac{e}{D_e} \right)^{2.1579} \left( \frac{p}{D_e} \right)^{-0.4821} \left( \frac{D_i}{D_o} \right)^{0.0001} \dots (5.7)$$

with a coefficient of determination of 0.9833 while the empirical correlation for friction factor under isothermal conditions is obtained by adopting the 256 points plotted in fig. 5-16 (except those for smooth annulus) to obtain equation (5.8) with a coefficient of determination of 0.9803

$$f_a = 169.1513 \text{Re}^{-0.2657} \left( \frac{e}{D_e} \right)^{2.0482} \left( \frac{p}{D_e} \right)^{-0.4967} \left( \frac{D_i}{D_o} \right)^{0.0001} \dots (5.8)$$

Equations (5.7) and (5.8) look not greatly dependent on the parameter ( $D_i/D_o$ ) as its power seems. They are valid for the range of Reynolds number

of 3000 to 10000,  $D_i/D_o = 0.4464$  to  $0.5536$ ,  $e/D_e = 0.1419$  to  $0.1760$  and  $p/D_e = 0.6452$  to  $3.2$ .

In the subsequent calculations, correlations of friction factor for smooth tube and annulus under heat exchange conditions are needed. For the smooth tube, friction factor as a function of Reynolds number could be obtained using data depicted in table C-1. The best fit is

$$f_s = 0.4185 \text{ Re}^{-0.2708} \quad \dots (5.9)$$

having a coefficient of determination of 0.9847 and validity for water with the range of Reynolds number of 5000 to 40000. For smooth annulus, the friction factor correlation using the data in table C-5 is

$$f_s = 0.8168 \text{ Re}^{-0.3395} \left( \frac{D_i}{D_o} \right)^{0.0672} \quad \dots (5.10)$$

with a coefficient of determination of 0.9123. Equation (5.10) is valid for water flowing in an annulus of  $(D_i/D_o)$  of 0.4464 to 0.5536 for the range of Reynolds number of 3000 to 10000.

### 5.6.3 Proposed Correlations of Nusselt Number

Making use of the STATISTICA software, empirical equations for the Nusselt number as a function of Reynolds number, geometrical characteristics of inserts (table C-41) and the inner tube and annuli, and Prandtl number which plays a vital role in heat transfer can be obtained for the three cases studied in the present work. In case of the tube-side heat transfer enhancement, it is expected that the affecting factors in the final correlation of Nusselt number are the Reynolds number, Prandtl number, and the geometrical parameters ( $e/d_i$ ) and ( $p/d_i$ ). Using the 256 points of Nusselt

number plotted in fig. 5-17 give equation (5.11) which has a coefficient of determination of 0.9796.

$$\bar{N}u_a = 0.0668 \text{Re}^{0.7938} \text{Pr}^{0.2741} \left( \frac{e}{d_i} \right)^{0.2049} \left( \frac{p}{d_i} \right)^{-0.3532} \quad \dots (5.11)$$

Equation (5.11) is valid for the range of Reynolds number of 5000 to 40000,  $e/d_i = 0.0714$  to  $0.0909$  and  $p/d_i = 0.7143$  to  $3.6364$ . In addition, this equation is valid for water only in the range of temperatures employed in the hot fluid stream of the present work which is about 50 to 70 °C.

For the case of annulus-side heat transfer enhancement using wire coil set up on the outer surface of the inner tube, the form of the correlation of Nusselt number is expected to be more complicated than that of tube-side heat transfer enhancement. The best curve fit of the 512 points of Nusselt number plotted in figs. 5-18 and 5-19 that might be suggested is the equation

$$\begin{aligned} \bar{N}u_a = & 0.002 \text{Re}^{1.1462} \left( \frac{e}{D_e} \right)^{0.2464} \left( \frac{p}{D_e} \right)^{0.1475} \text{Pr}^{0.3} \\ & \times \left[ \frac{\left( \frac{e}{D_e} \right)^{-0.8156}}{\left( \frac{e}{D_e} \right)^{2.5892} + 0.01} \right] \left[ \frac{\left( \frac{p}{D_e} \right)^{-0.5503}}{\left( \frac{p}{D_e} \right)^{1.515} + 3.8717} \right] \left( \frac{D_i}{D_o} \right)^{-0.3823} \end{aligned} \quad \dots (5.12)$$

which has a coefficient of determination of 0.9563. This correlation is considered to be valid for the range of Reynolds number of 3000 to 10000,  $D_i/D_o = 0.4464$  to  $0.5536$ ,  $e/D_e = 0.0645$  to  $0.176$  and  $p/D_e = 0.6452$  to  $3.2$ .

For the case of annulus-side heat transfer enhancement using circular ribs set up on the outer surface of the inner tube the best curve fit of the 256 points plotted in fig. 5-20 is the following equation:

$$\overline{Nu}_a = 0.1006 \text{Re}^{0.3298} \left( \frac{e}{D_e} \right)^{-0.4696} \left( \frac{p}{D_e} \right)^{-0.0645} \text{Pr}^{0.29} \\ \times \left[ \frac{\left( \frac{e}{D_e} \right)^{0.0527}}{\left( \frac{e}{D_e} \right)^{-2.3452} + 0.5044} \right] \left[ \frac{\left( \frac{p}{D_e} \right)^{0.51}}{\left( \frac{p}{D_e} \right)^{0.001} - 0.983} \right] \left( \frac{D_i}{D_o} \right)^{-0.12} \dots (5.13)$$

which has a coefficient of determination of 0.9503 and valid for the range of Reynolds number of 3000 to 10000,  $D_i/D_o=0.4464$  to  $0.5536$ ,  $e/D_e=0.1419$  to  $0.1760$  and  $p/D_e = 0.6452$  to  $3.2$ . Equations (5.12) and (5.13) are valid to be used for water in the range of temperature of about  $20$  to  $35$  °C.

For smooth tube, the empirical correlations of Nusselt number corresponding to equation (3.12) is

$$\overline{Nu}_s = 0.013 \text{Re}^{0.833} \text{Pr}^{0.265} \dots (5.14)$$

with a coefficient of determination of 0.9952, and for the smooth annulus, it is

$$\overline{Nu}_s = 0.0124 \text{Re}^{0.843} \text{Pr}^{0.45} \left( \frac{D_i}{D_o} \right)^{-0.2392} \dots (5.15)$$

having a coefficient of determination of 0.9947 and valid for  $D_i/D_o=0.4464$  to  $0.5536$ . The last two correlations are valid for water with the ranges of Prandtl and Reynolds number adopted in the present work.

It is important to mention that equations (5.9) and (5.10) and equations (5.14) and (5.15) are assumed to be more accurate than Petukhov and Gnielinski equation respectively, for the double pipe heat exchanger used in the present work including the deviation values depicted in table 5-1.

# **CHAPTER SIX**

## **Discussion**

### **6.1 Introduction**

The study of heat transfer enhancement in heat exchangers by mechanical methods, like those adopted in the present work, consists of two principal results; the first is the gain of the enhancement process represented by augmentation of heat transfer (Nusselt number), and the second is the penalty paid for this gain; it is the growth of friction factor which is axiomatically followed by increasing pumping power. In general, implementation of the aim for which, one suggests to enhance or design an enhanced heat exchanger, is based on the judgment whether the followed method is beneficial or not.

### **6.2 The Influence of the Experimental Conditions**

In the present work, the variation of the operational conditions, represented by the mass flow rate of the unenhanced side and the inlet temperature of the hot fluid stream (60 or 70 °C) have given the chance to have a large quantity of experimental data to correlate as accurate relationships as possible, either for friction factor or Nusselt number. These variations are the only way available to have a variety in the physical properties especially in the calculations of Nusselt number. These properties are briefly expressed by Prandtl number which has a vital role in heat transfer since it relates the convective and conductive heat transfer in the fluid as being a function of temperature [64]. Prandtl number in the present work has been varied from 2.6 to 3.4 in hot fluid stream in tube-side heat transfer enhancement experiments and from 5.5 to 6.5 in cold fluid stream in annulus-

side heat transfer enhancement experiments. So these ranges do not represent wide scopes to consider that the experimental results, obtained assess the proper influence of Prandtl number. Hence, using different liquids as the working fluid or by adding different quantities of a particular substance like propylene glycol to water may produce an enough variation of Prandtl number [8].

The change of the experimental conditions represented by changing the mass flow rate of cold fluid stream in case of tube-side enhancement or by changing the mass flow rate of hot fluid stream in case of annulus-side enhancement, both at a given inlet temperature of hot fluid stream, have given an observable change in heat transfer rate as shown in figs. 5-5 through 5-8. That is axiomatic since that any change in the mass flow rate of the unenhanced side would affect the heat transfer coefficient in that side and then affect the heat transfer coefficient leading to influence heat transfer rate in the enhanced side through equation (3.35) or (3.36). Accidentally that change is leading to a slight change in Prandtl number which could not be considered as an effective influence on heat transfer.

On the other hand, changing the hot fluid temperature, for both enhancement cases, affects directly Prandtl number which leads to affect the heat transfer not only in the hot fluid stream but also in the other side. In another word, raising the hot fluid inlet temperature (in case of tube-side enhancement) leads to lower Prandtl number which leads to lower heat transfer, represented by Nusselt number and not the heat transfer rate which axiomatically increases due to the increase in temperature difference. This is obvious in fig. 5-17, where for the two tube sizes, values of Nusselt number in case of hot fluid temperature is 70 °C, are lower than those when it is 60 °C.

The same behavior happens, but with lesser magnitude, when the case is the annulus-side enhancement, where raising the hot fluid inlet temperature means making the other side working at higher temperature which leads to lower the Prandtl number and then lowering the Nusselt number as shown in figs. 5-18 through 5-20, i.e., relatively lowering heat transfer. The whole situation is agreeing with the information concerning heat transfer in smooth tubes or annuli as in equations (3.8) and (3.12) or with that of Arman and Rabas [59, 60] for ribbed surfaces to enhance heat transfer as discussed in chapter three but to a lesser degree that cannot be considered as picturing the relationship between the heat transfer and Prandtl number.

What happens for the pressure drop or friction factor, either in heat exchange or isothermal conditions, starting with the tube-side enhancement (fig. 5-5), is that raising the mass flowrate of the unenhanced side (in heat exchange conditions) means raising heat transfer and then lowering the mean temperature of the other side. That means that the enhanced side fluid density will be increased, but with larger manner the viscosity will do (that is obvious in the density or viscosity versus temperature relationships as shown in appendix A). That means that the Reynolds number at which the reading is taken needs larger mass flowrate which means larger velocity, and then larger pressure drop according to equation (3.4).

The reverse occurs for the annulus-side enhancement case (figs. 5-6 through 5-8), where increasing the hot stream mass flowrate leads to increase the mean temperature of the annulus side fluid which means lowering the mass flowrate required for a particular Reynolds number and lowering the pressure drop in that stream. On the other hand, raising the inlet temperature of hot fluid, in both enhancement cases, means lowering the mass flowrate required for a particular Reynolds number leading to lower the pressure drop.

The friction factor, in both heat exchange and isothermal processes, has been intended to be calculated as a function of geometrical parameters in addition to Reynolds number without granting an importance to the physical properties outside the Reynolds number. As a result, the curves in figs. 5-9 through 5-16 represent the average value for each case. To reduce complexity in the coming calculations, the experimental conditions would be reduced to only two conditions that concern the working at a particular hot stream inlet temperature (60 or 70 °C), considering the average values for the two groups working at a specified mass flowrate of unenhanced side.

## 6.3 Friction Factor in Enhanced Tubes and Annuli

It is important to point out that the heat transfer enhancement by turbulence promoters is simply an action to disturb the laminar sublayer which prevents or decreases heat transfer. Such enhancement always is accompanied by pressure drop or drag due to the obstruction created by adding these turbulence promoters. So, looking for a suitable promoter, one must take into consideration reducing the pressure drop might be reached by investigating an affluent passage through which the fluid could pass with keeping the promoter to work as efficient heat transfer enhancer as possible.

### 6.3.1 The Effect of the Wire or Rib Diameter and Coiling or Ribbing Pitch on Friction Factor.

In the tube-side heat transfer enhancement, fast propagation of pressure drop or friction factor with increasing the intensity of coils or decreasing the coiling pitches of the wire coil is observed. A glance at figs. 5-9 and 5-13 shows that the friction factor in the inner tube inserted with a wire coil is developing non-linearly; for example, increasing the wire coiling from  $p=20$  to  $p=10$  leads to increase the friction factor about three times that when

increasing the wire coiling from  $p=40$  to  $p=30$  with slightly greater propagation at large Reynolds numbers than that at lower ones. This fact emphasizes an attention to avoid the exaggeration in increasing the intensity of coils inside the tube even when that leads to increase heat transfer.

The friction factor recorded in case of the annulus-side enhancement using wire coil set up on the outer surface of the inner tube (figs. 5-10, 5-11, 5-14, and 5-15) is affected by the wire diameter or ( $e/D_e$ ) as well as coiling pitches or ( $p/D_e$ ) giving friction factor values in case of wire coil of  $e= 2.2$  mm twice that of  $e=1$  mm with the same coiling pitch and at the same Reynolds number. That is for the annulus of  $D_i=12.5$  mm and with greater magnitude in case of the  $D_i=15.5$  mm annulus which has a narrower annular gap. Here, the wire coil works as roughness installed on the outer surface of the inner tube helping the friction factor to increase, especially in case of  $e=1$  mm. This action might be one of two causes of increasing the friction factor in case of using the  $e=2.2$  mm wire, which might be considered as swirl generator around the inner tube lengthening the path of fluid flow in a similar manner to the method of enhancing heat transfer in the annulus by using a spiraling tape to induce swirl leading to more friction [34]. Also, the wire of this size might work as a series of obstacles standing in that path increasing the friction factor, especially in case of the 10 mm coiling pitch, where fluid crosses over “ribs” that the close coils might formulate [68].

The obstruction encountered in the case of using the  $e=2.2$  mm wire coil becomes larger in case of using circular ribs with the same diameter giving a huge friction factor values especially in case of the annulus of  $D_i=15.5$  mm where the passage of flowing becomes relatively very narrow with consecutive obstacles (circular ribs) blocking the way of fluid flow without permitting to the fluid to flow spirally around the inner tube producing, as a

result, greater friction factor, reaching to one fold as compared to that of the wire coil of 2.2 mm at the same Reynolds number, as shown in figs. 5-11 and 5-12. The last observation gives an urgent fact that the spiral coil permits the fluid to flow more easily than the ribs which work as obstacles, granting no chance to the fluid to flow in ease fluency [68].

In fact, each of the two sides of figs. 5-9 or 5-13 represents an  $(e/d_i)$  ratio, so comparing the act of the coiling pitch in case of the tube-side heat transfer enhancement, is simply by seeing the curve fits of the same colors in the two sides of each of these figures, while comparing the effect of the coil pitch ratio  $(p/d_i)$  at a particular  $(e/d_i)$  is accessible by comparing the curve fits in the same figure side. The same description might be said for the annulus-side heat transfer enhancement methods.

### 6.3.2 The Effect of the Annulus Diameter Ratio ( $D_i/D_o$ )

In addition to the geometrical parameters of inserts, another parameter,  $(D_i/D_o)$ , had appeared in the friction factor correlations in the annulus-side heat transfer enhancement, to distinguish between the two annuli used giving an importance to the extent of the annular gap. This parameter might be simply considered as a correction factor concerned with the double pipe heat exchanger, used in the present work. But, since it had appeared in values greater than the deviation values fixed in table 5-1 for the two annuli used in the present work (that can be proved easily by predicting the values of  $(D_i/D_o)$  with the exponents appearing in the concerned correlations). In addition, that factor had appeared in both friction factor and Nusselt number correlation, so it is apt to consider it in fluid flow and heat transfer in annulus.

In order to use this factor safely the whole boundary conditions concerning the present heat exchanger must be mentioned to give a perfect

image about the authenticity of using this parameter. The boundary condition that might be absent in describing the annuli in chapter five is the effective length of the present heat exchanger which is 1.245 m, so a boundary condition including this length might be  $(L/D_e)$  having a value of between 80.32 and 99.60. Indeed, the parameter  $(D_i/D_o)$  had appeared in all correlations of friction factor belonging to the annulus either smooth or enhanced but with dissimilar exponents, so ignoring that parameter in case of the friction factor correlation for the annulus-side enhancement by circular ribs, where its exponent is close to zero, might be considered as a good approximation. Also, appearing in slight power in equation (5.10) for smooth annulus might lead to consider it as a correction factor for the present annuli.

### **6.3.3 The Effect of Disruption Shape of Insert on Friction Factor**

In the three methods of heat transfer enhancement, adopted in the present work, a circular section of the enhancement devices (circular wires and ribs), have been used. This shape produces smaller friction factor than that given by a rectangular one or a shape with sharp corners but, unfortunately, produces smaller Nusselt number. This is due to the disruption effect of the owned corners [69].

### **6.3.4 The Dependency of Friction Factor on Reynolds Number**

In general, dependency of friction factor on Reynolds number in the tube-side heat transfer enhancement using wire coil, as revealed in the present work, is low as compared to the dependency on the geometrical characteristics of the wire coil itself as shown in figs. 5-9 and 5-13 which are typified in equations (5.1) and (5.2). The relationship between friction factor and Reynolds number is slightly different in case of the two types of the annulus-side enhancement where the friction factor is more dependent on Reynolds number as obviously

seen in figs 5-10 through 5-12 and 5-14 through 5-16 and presented in equations (5.3) through (5.8). Such observations might be considered as an agreement with the well-known Moody diagram, where the wire coil or the circular ribs might be considered as roughness on the inner or outer surface of the tube. It is to be admitted that the Reynolds number range adopted in the tube-side enhancement is larger than that adopted in the annulus-side enhancement where the dependency on Reynolds number decreases with increasing the relative roughness [38].

### **6.3.5 Friction Factor Augmentation**

The friction factor augmentation is one of the most important purposes of heat transfer enhancement study, because it represents the magnitude of penalty, one might pay if he followed a specified enhancement method. It is defined by the ratio between the friction factors of enhanced (augmented) tube or annulus and that of smooth ones at the same Reynolds numbers [8,35].

#### **6.3.5.1 Friction Factor Augmentation for Tube-Side Heat Transfer Enhancement**

For the tube-side heat transfer enhancement, the equation of friction factor augmentation is obtained by dividing equation (5.1) by equation (5.9). The latter represents the actual friction factor relationship of smooth tube in the present work. The produced equation is:

$$\frac{f_a}{f_s} = 8.6848 \text{Re}^{0.1744} \left( \frac{e}{d_i} \right)^{0.8912} \left( \frac{p}{d_i} \right)^{-0.7856} \quad \dots (6.1)$$

Inserting values of the dimensionless parameters into equation (6.1) gives values of friction factor augmentation as listed in tables C-20 through C-23 and plotted in fig. 6-1 which shows the friction factor augmentation of tube-side heat transfer enhancement by wire coil in the adopted ranges.

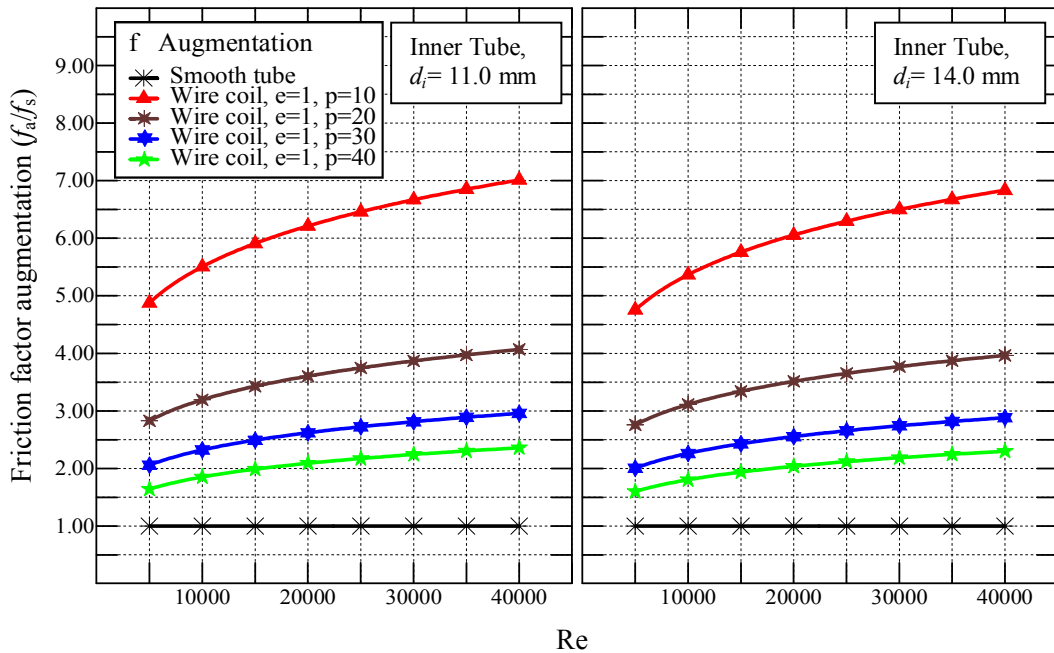


**Figure 6-1:** Friction factor augmentation vs. Reynolds number for tube-side heat transfer enhancement using a wire coil of  $e = 1$  mm for two inner tube sizes.

The maximum value recorded for friction factor augmentation is 7 times that for smooth tube. That value is for friction factor in the tube of  $d_i=11$  mm inserted with a wire coil of  $e=1$  mm and  $p=10$  mm at Reynolds number of 40000, as compared to that of smooth tube, i.e.,  $e/d_i=0.0909$  and  $p/d_i=0.9091$ , and something less for the same values of  $e$  and  $p$  for the other tube size. It is obvious that the friction factor augmentation, like the friction factor itself, greatly affected by the coiling pitch or  $(p/d_i)$  depending largely upon Reynolds number at high  $(p/d_i)$  values and slightly at lower ones.

The values of friction factor augmentation calculated using equation (6.1) is agreeing with the experimental values of friction factor plotted in fig. 5-9. To have an idea about the agreement of the values obtained for the friction factor of the tube inserted with a wire coil, studied in the present

work, a comparison with previous works at least for specified values of dimensionless parameters and physical properties can be performed.

As a one of the most well-known studies in the field of heat transfer enhancement by wire coils was that of Ravigururajan and Bergles in (1985) [56] which led to equation (3.22), for friction factor, and (3.21), for Nusselt number, in (1996). The friction correlation predicted 96% of the data within  $\pm 50\%$ , and the heat transfer correlation predicted 99% of the data within  $\pm 50\%$ . Because of the high deviation, recently, these correlations are not recommended for general use [35]. Moreover, these equations cover ranges outside those adopted in the present work.

Viedma et al., in (2005) [8] showed a comparison between their results and correlations proposed by Sethumadhavan and Rao (1982), Zhang et al., (1991), and Inaba et al., (1994) for a wire coil of  $e/d_i = 0.1$  and  $p/d_i = 1.2$  for turbulent flow regime. The ranges adopted by that comparison fall in the ranges adopted in the present work for  $(p/d_i)$ , ( $p/d_i = 0.7143$  to  $3.6364$ ) and slightly larger for  $(e/d_i)$ , ( $e/d_i = 0.0714$  to  $0.0909$ ), but for comparison, these considered values can be inserted in the proposed equation (5.1), to give fig. 6-2. It reveals good agreement of the present work results with that of Sethumadhavan and Rao and good agreement in being not largely dependent on Reynolds number with that of Zhang et al. Also the present results disagree with the results of Viedma et al. Generally, the results of Zhang et al. and Viedma et al. overpredict the results of the present work while those of Sethumadhavan and Rao, and Inaba et al. underpredict [8].

The large contradiction in the friction factor results obtained by the mentioned works and other works might be, as an interpretation suggested by Rabas [8], resulting from the vibrations of the coil and the tube and the clearance that sometimes exists between the coil and the tube wall, enforcing

many authors not to correlate their experimental friction factor results [8]. In the present work, considerable care has been given to the registration of the pressure drop especially at high Reynolds numbers which increase these vibrations and always the average of many readings is considered.

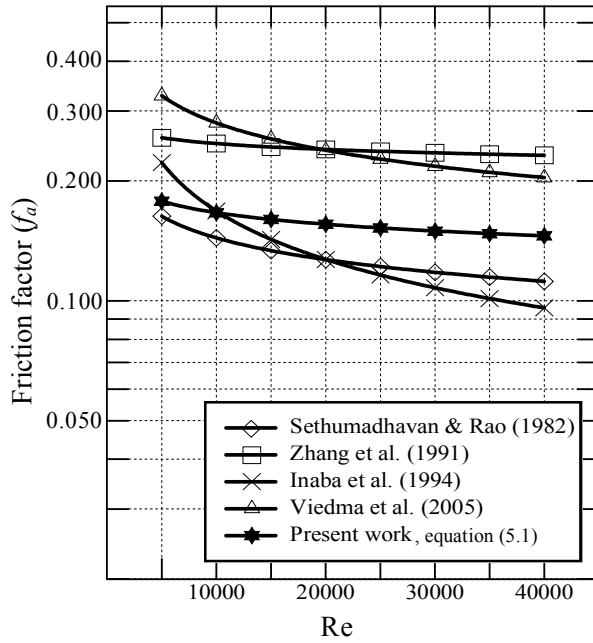


**Figure 6-2:** Comparison of present work friction factor (equation (5.1)) with that of previous works for tube-side heat transfer enhancement by wire coil of  $e/d_i = 0.1$  and  $p/d_i = 1.2$ .

### 6.3.5.2 Friction Factor Augmentation for Annulus-Side Heat Transfer Enhancement by Wire Coil

In case of the annulus-side heat transfer enhancement using wire coil set up on the outer surface of the inner tube, the experimental results collected in the present work are more numerous than those of the first case giving a more comprehensive relationship. Here the friction factor augmentation relationship can be obtained by dividing equation (5.4) by (5.10)

$$\frac{f_a}{f_s} = 26.7406 \text{ Re}^{0.0928} \left( \frac{e}{D_e} \right)^{1.0126} \left( \frac{p}{D_e} \right)^{-0.4870} \left( \frac{D_i}{D_o} \right)^{0.6203} \quad \dots (6.2)$$

Using equation (6.2) directly with substituting values of the geometrical parameters to obtain the values of friction factor augmentation as listed in tables C-25 through C-32 which are plotted versus Reynolds number in fig. 6-3 which indicates a huge jump in friction factor augmentation registered for the wire of  $e=2.2$  mm and of greater value in case of the annulus of the smallest gap (annulus of  $D_i=15.5$  mm), reaching the greatest magnitude of 8.5 as compared to smooth annulus, registered for the wire coil of  $e=2.2$  wound around the inner tube of 15.5 mm outer diameter with  $p=10$  mm ( $e/D_e=0.176$  and  $p/D_e=0.8$ ) at Reynolds number of 10000.

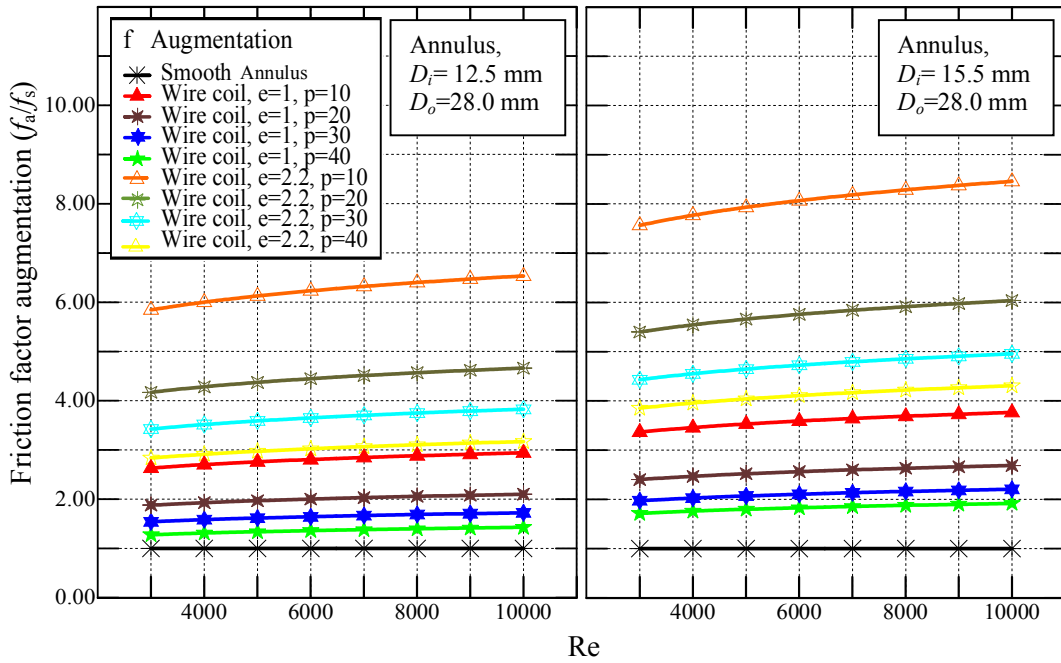


**Figure 6-3:** Friction factor augmentation vs. Reynolds number for annulus-side heat transfer enhancement using two wire coils of 1 and  $e=2.2$  mm for two annulus sizes.

That magnitude, when compared to the friction factor augmentation registered for the case of using 1 mm diameter wire with the same coiling pitch ( $e/D_e=0.08$  and  $p/D_e=0.80$ ) at the same Reynolds number, reveals a great dependency of friction factor augmentation on wire diameter, as clearly observed by equation (6.2). The wire coil here progressively formulates

obstacle not only increases friction factor but also decreases heat transfer as will be seen later giving an imagination that increasing the wire diameter as well as decreasing the coiling pitch might lead to unwanted result at least in the dimensions adopted in the present work. Here, the least friction factor augmentation registered is 1.275 at Reynolds number of 3000 in case of largest annulus with  $e=1$  mm wire and  $p=40$  mm.

### **6.3.5.3 Friction Factor Augmentation for Annulus-Side Heat Transfer Enhancement by Circular Ribs**

There is no doubt that the results of the friction factor augmentation of annulus-side enhancement by wire coil foretells the magnification of that by circular ribs in similar manner to that in discussing the effect of the type of augmentation device on friction factor, but just to show the effect of changing to circular ribs instead of wire coil, the study continues. Friction factor augmentation of annulus-side heat transfer enhancement by circular ribs is obtained by dividing equation (5.7) by (5.10) as:

$$\frac{f_a}{f_s} = 250.6181 \text{Re}^{0.0729} \left( \frac{e}{D_e} \right)^{2.1579} \left( \frac{p}{D_e} \right)^{-0.4821} \left( \frac{D_i}{D_o} \right)^{-0.0671} \quad \dots (6-3)$$

Equation (6.3), after inserting the required parameters gives the values of friction factor augmentation as listed in tables C-33 through C-36 which are plotted in fig. 6-4. Figure 6-4 reveals a friction factor augmentation of more than one and a half times that for the same dimensions in case of the annulus-side enhancement by wire coil. This supports the previous interpretation of the effect of the swirl in reducing the friction factor. Friction factor augmentation ratio in equation (6-3) is Reynolds number-independent with greatest friction factor augmentation is in case of the least ribbing pitch with the least annular gap.

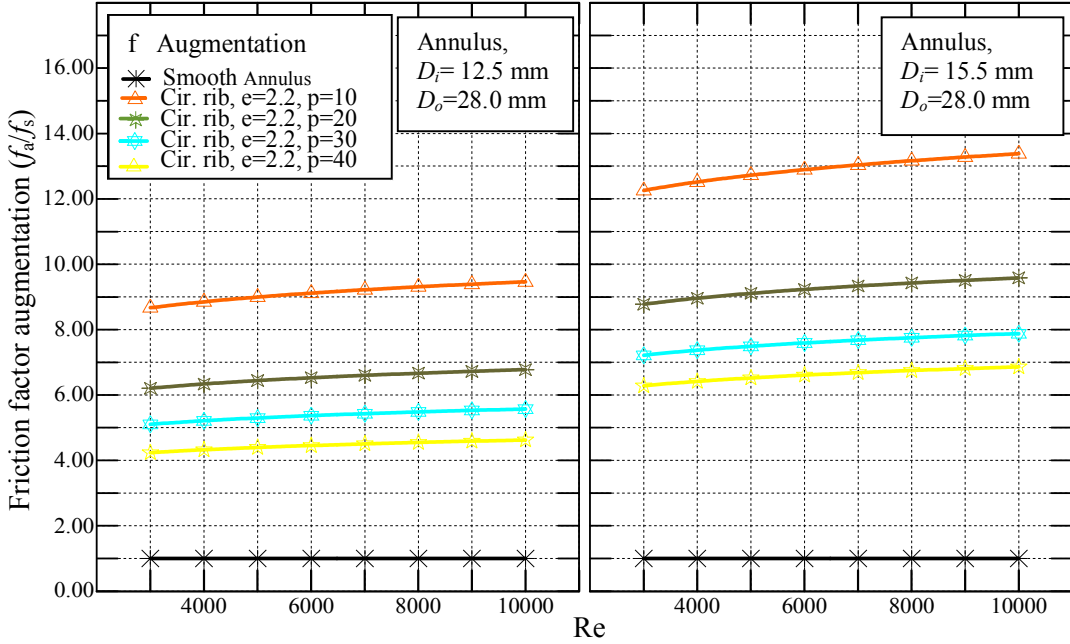


**Figure 6-4:** Friction factor augmentation vs. Reynolds number for annulus-side heat transfer enhancement using circular ribs of  $e = 2.2$  mm for two annulus sizes.

It is important to state that the methods of heat transfer enhancement in the annulus of double pipe heat exchanger (by wire coils, as well as circular ribs), adopted in the present work are completely new, with no similar works to be compared with, for friction factor or Nusselt number, like those for tube-side heat transfer enhancement by wire coils.

## 6.4 Heat Transfer in Enhanced Tubes and Annuli

The enhancement of heat transfer by turbulence promoters has more difficult mechanisms than the manner by which the friction factor increases as a result of adding these turbulators, differing according to their types, their geometrical characteristics and, the position where they are attached to or in the vicinity of installment. In addition, Prandtl number plays an important role in the mechanism of heat transfer when using roughened tubes.

### **6.4.1 The Effect of the Wire or Rib Diameter and Coiling or Ribbing Pitch on Nusselt Number.**

The geometrical characteristics of inserts either wire coils or circular ribs affect heat transfer differently as compared to magnifying the friction factor, where the latter increases with increasing the intensity of roughness either by decreasing the coiling or ribbing pitches or by increasing the diameter of wire coils or ribs, while that doesn't occur always in case of heat transfer. In case of tube-side heat transfer enhancement by wire coils, Nusselt number increases with decreasing the coiling pitches or  $(p/d_i)$  for the same tube size, as shown in fig. 5-17. In addition, the ratio  $(e/d_i)$  influences Nusselt number, in spite of using one wire size here, but with varying the tube diameter that is possible. The behavior discussed here cannot be generalized for geometrical dimensions outside the range adopted in the present work.

Enhancement of heat transfer by wire coils, inserted inside the inner tube, might be considered to act in two ways, one might overcome the other. The first is as a swirl flow generator, generating a helical flow at the periphery of the flow. This rotating flow is superimposed upon the axially directed central core flow and promotes centrifugal forces that aid convection. The second is as a turbulence promoter increasing the flow turbulence level by a separation and reattachment mechanism. Moreover, when wire coils are in contact with the tube wall, they act as roughness elements disturbing the existing laminar sublayer. Wire coils increase heat transfer rate through one or two of the mechanisms mentioned above, depending on flow conditions and wire geometry. However, it is expected that wire coils will act as random roughness at high Reynolds numbers [8].

When the coiling pitches approach one another reaching a limit which prevents the formation of these reattachment points, as obviously seen in fig. 3-3 where heat transfer will decrease [61]. This does not occur in case of tube-side heat transfer enhancement because the coiling pitch range, adopted in the present work, does not reach this limit. But in case of the annulus-side heat transfer, this is obvious, especially in case of 2.2 mm wire coil. In the annulus-side heat transfer like in tube-side, heat transfer is imposed upon the mechanism of separation and reattachment mechanism, as well as the enhancement of heat transfer by swirl generation. In case of using the wire coil of  $e=1$  mm, for the two annulus sizes, Nusselt number was kept increasing with decreasing the coiling pitch as clearly presented in fig. 5-18. Very close values of Nusselt number are observed in case  $p=20$  and 10, giving an idea that the coiling pitch plays no more role in enhancing heat transfer.

The last observation might be considered as a critical value to start a reverse relationship as in case of the  $e= 2.2$  mm wire as clear in fig. 5-19, where heat transfer keeps increasing with decreasing coiling pitch to a specified value and then the relationship goes reversely when the coils become close to each other preventing the formation of the reattachment regions which increase the local heat transfer coefficient. In fig. 5-19, the maximum Nusselt number values are obtained for  $p=20$  mm using the annulus of  $D_i= 12.5$  mm, while for the annulus having the smallest annular gap, it is when  $p=30$  mm. The last observation confirms the great role of the mechanism of separation and reattachment which needs enough space to form as in fig. 3-2 [59].

Considering the case of 2.2 mm wire coil, the role of swirl appears clearly as a heat transfer inducer in a manner similar to that of Coetzee [34],

who used a spiraling tape around the inner tube of the double pipe heat exchanger. The enhanced heat transfer is by swirls tending to increase the effective flow path of the fluid through the tube or annulus. This would increase heat transfer, as well as pressure drop, but this effect decreases or disappears altogether at higher helix angles since fluid flow simply passes axially over coils [57, 68].

What happens in case of annulus-side heat transfer enhancement by circular ribs supports the opinion of giving the swirl flow an importance in heat transfer. In this case, the effect of the swirl flow completely disappears, keeping the only means for enhancing heat transfer being the mechanism of separation and reattachment leading to lower Nusselt number values in addition to increase the friction factor as seen previously. In the last case the majority of experiments have given close values of Nusselt number especially in case of close ribs (the least values of  $(p/D_e)$ ).

The complex situation encountered in case of annulus-side heat transfer enhancement has led to the complex correlations of Nusselt number (equation (5.12) and (5.13)). These correlations have been desired to express all points or curves included in figs. 5-18 through 5-20, but revealing an accurate description as these correlations do not express all these points or curves giving as reasonably accurate relationships as possible to express the majority of them and to surpass the irregular points or curves, as will be seen in the Nusselt number augmentation curves, depicted later.

#### **6.4.2 The Effect of the Annulus Diameter Ratio ( $D_i/D_o$ )**

The  $(D_i/D_o)$  parameter has appeared in Nusselt number correlations for the annulus-side heat transfer enhancement, giving significance to the annular gap size in enhanced annuli as well as smooth ones as in equations (5.12) and

(5.13) and (5.15) respectively. Since the exponent of that parameter in equation (5.15) makes it giving values close to those fixed as deviation values of Nusselt number in smooth annuli used in the present work (table 5-1), it might be valuable to consider it as a correction factor concerned with the smooth annuli used presently.

On the other hand, such parameter seems more effective in equations (5.12) and (5.13) to suppose reasonably that this factor is more than a correction factor in case of the annulus-side heat transfer either by wire coils or circular ribs. No clear explanation is available for such case in the literature, where most valuable description of fluid flow and heat transfer around ribs is cited for a flat plate or circular tube, as in fig. 3-2. The present situation might be different where the local circulation eddies are formed over the ribs and the separation and reattachment zones, undergoing an impedance caused by the outer wall of the annulus, meaning that the impedance is greatly affected by the annular gap size which is represented by the ratio ( $D_i/D_o$ ) [59].

#### **6.4.3 The Dependency of Nusselt Number on Reynolds Number**

It seems clearly that the dependency of Nusselt number on Reynolds number in case of tube-side enhancement by wire coils as obviously seen in fig. 5-17 and equation (5.11), is very close to that for smooth tubes. On the other hand, the relation for the case of the annulus-side enhancement is different where the dependency is related to the geometrical characteristics of inserts themselves as obvious in equations (5.12) and (5.13). Indeed, the complex exponents of Reynolds number in these equations have come as a result of the complex physics of fluid flow and heat transfer in the annulus. Clearer picture would be formed later in the study of Nusselt number augmentation.

#### **6.4.4 The Effect of Prandtl Number on Heat Transfer**

Many studies refer to the great role, Prandtl number plays in the enhancement of heat transfer by wire coils or by other disruption shapes. Mathematically, the effect of Prandtl number appears significantly in the exponent of Prandtl number in Nusselt number correlations (e.g., equations (5.11), (5.12) and (5.13)). As a conclusion Webb et al., [61] attained that Prandtl number exponent doesn't differ greatly from the value of about 0.33 depending on Prandtl number itself. The value of this exponent decreases with Prandtl number.

In the present work, Prandtl number exponents are 0.27 for tube-side heat transfer enhancement and 0.3 and 0.29 for annulus-side enhancement by wire coils and circular ribs respectively. No doubt that the narrow range of Prandtl number adopted in the present work (using water as the only working fluid), doesn't anyway permit to have more accurate idea about the dependency of heat transfer in enhanced tubes and annuli.

#### **6.4.5 Nusselt Number Augmentation**

It is defined by the ratio between the Nusselt numbers of enhanced (augmented) tube or annulus and that of smooth ones at the same Prandtl and Reynolds numbers [8, 35].

##### **6.4.5.1 Nusselt Number Augmentation for Tube-Side Heat Transfer Enhancement**

The equation of Nusselt number augmentation for the tube-side heat transfer enhancement is obtained by dividing equation (5.11) by equation (5.14), which represents the actual Nusselt number correlation of smooth tube in the present work, to give the equation

$$\frac{\bar{N}u_a}{\bar{N}u_s} = 5.1385 \text{ Re}^{-0.0392} \text{ Pr}^{0.0091} \left( \frac{e}{d_i} \right)^{0.2049} \left( \frac{p}{d_i} \right)^{-0.3532} \quad \dots (6.4)$$

Inserting the required values of dimensionless parameters from table C-41 into equation (6.4) gives the values of Nusselt number augmentation for tube-side heat transfer enhancement by wire coils for the two tube sizes and all values of the adopted geometrical characteristics as listed in tables C-20 through 23 and plotted in fig. 6-5. The latter reveals good agreement with fig. 5-17 that shows the Nusselt number-Reynolds number relationship for different conditions. The four experimental conditions have been summarized into two cases only (concerned with the change of the hot fluid inlet temperature), because Prandtl number has insignificant variation for the other two conditions. Also the variation of the inlet temperature of hot fluid with fixing that of cold one leads to variation of the approach temperature difference which would be adopted in the PEC calculations discussed later.

For all values of the characteristic variables in fig. 6-5, the Nusselt number augmentation decreases with Reynolds number leading to suggest that the heat transfer enhancement inside the inner tube by wire coils at low Reynolds numbers is more efficient than that at high Reynolds number especially when knowing that these low values of Reynolds number have given the lowest friction factor augmentation values as stated previously. But in general, Nusselt number augmentation is weakly dependent on Reynolds number especially at high values.

The maximum value of Nusselt number augmentation obtained is 2.43 for the 14 mm diameter tube and 2.34 for the other size, both at Reynolds number of 5000,  $e = 10$  and  $p = 10$ , corresponding to maxima in friction factor augmentation of 4.75 and 4.88. For the same geometries, for high

Reynolds number (40000), the maxima registered, are 2.24 and 2.16 with corresponding friction factor augmentation values of 6.83 and 7.01 respectively. That means that the maximum heat transfer augmentation is 2.43 for the wire geometries of ( $e/d_i = 0.0714$  and  $p/d_i = 0.7143$ ). Close values for the two experimental conditions have been registered.

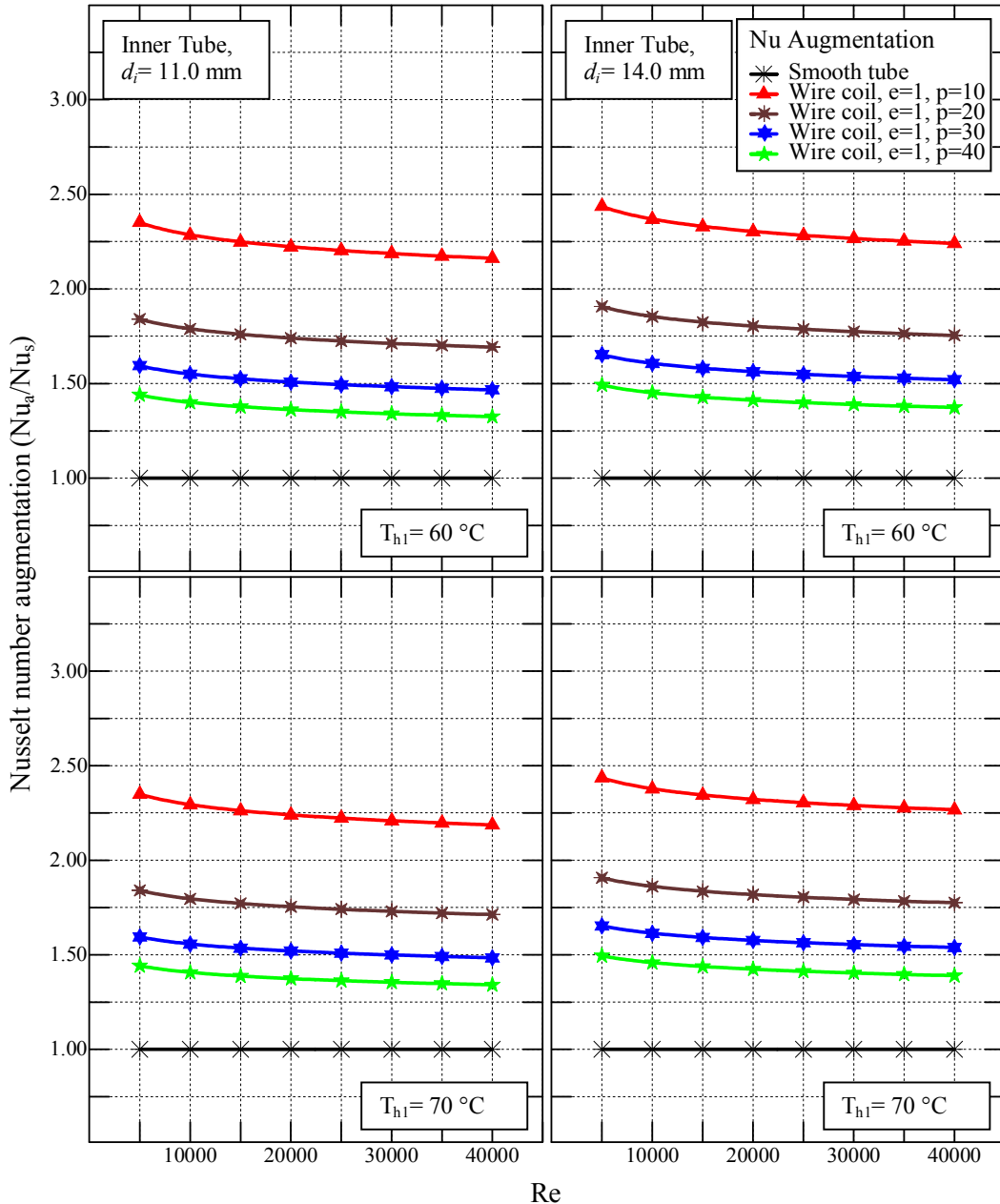


**Figure 6-5:** Nusselt number augmentation vs. Reynolds number for inner tube-side heat transfer enhancement using a wire coil of  $e = 1$  mm for two inner tube sizes.

Similar to the comparison performed for friction factor correlation (equation (5.1)), another comparison must be performed for Nusselt number (equation (5.11)), with results or correlations proposed by other works which were carried out in similar ranges of Reynolds and Prandtl number as well as geometrical characteristics. The work of Sethumadhavan and Rao and Viedma [8], Kumar and Judd [9] and Klaczak [70], are chosen for the comparison. The comparison is for a specified Prandtl number equaling to 3,  $e/d_i=0.1$  and  $p/d_i=1.2$ , as depicted in fig. 6-6. It reveals that the results of the present work are very close to those of Kumar and Judd and in good agreement with the results of Klaczak, and in general, lower than the results of Sethumadhavan and Rao and Viedma. Indeed, the latter has also high friction factor compared to the present work (fig. 6-2). At the same time the work of Klaczak is very appropriate to be compared with, because water was used as the only flowing fluid with similar geometrical characteristics [70].

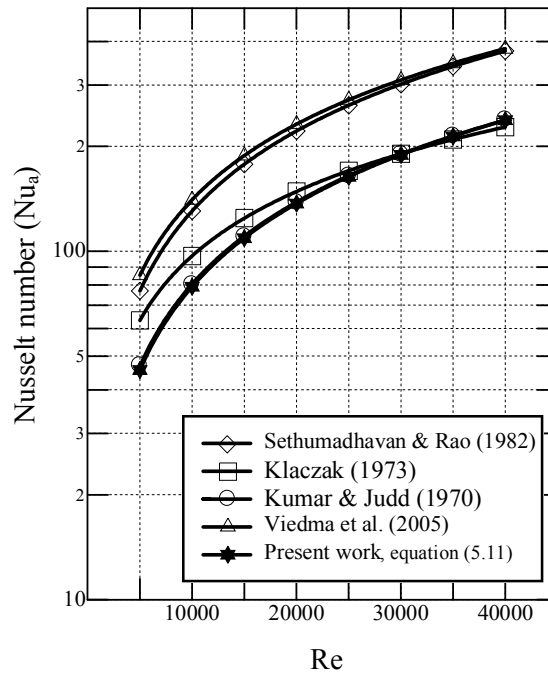


**Figure 6-6:** Comparison of Nusselt number resulted in the present work (equation (5.11)) with that of previous works for tube-side heat transfer enhancement with wire coil of  $e/d_i=0.1$  and  $p/d_i=1.2$  and  $\text{Pr}=3.0$ .

#### 6.4.5.2 Nusselt Number Augmentation for Annulus-Side Heat Transfer Enhancement by Wire Coil

The Nusselt number augmentation relationship of annulus-side heat transfer enhancement by wire coil is obtained by dividing equation (5.12) by (5.15)

$$\frac{\bar{N}u_a}{\bar{N}u_s} = 0.1613 \text{ Re}^{-0.843+1.1462\left(\frac{e}{D_e}\right)^{0.2464}\left(\frac{p}{D_e}\right)^{0.1475}} \text{ Pr}^{-0.15} \\ \times \left[ \frac{\left(\frac{e}{D_e}\right)^{-0.8156}}{\left(\frac{e}{D_e}\right)^{2.5892} + 0.01} \right] \left[ \frac{\left(\frac{p}{D_e}\right)^{-0.5503}}{\left(\frac{p}{D_e}\right)^{1.515} + 3.8717} \right] \left( \frac{D_i}{D_o} \right)^{-0.1431} \quad \dots (6.5)$$

Substituting the required values of geometrical parameters from table C-41 for the two wire sizes produces the values of Nusselt number augmentation as listed in tables C-25 through C-32 and plotted in fig. 6-7 which shows a complex situation for Nusselt number augmentation specified in the range of the geometrical characteristics adopted in the present work. A great role is observed for the ratios ( $e/D_e$ ) and ( $p/D_e$ ) to determine the relationship of the augmentation ratio with Reynolds number. Unlike the tube-side heat transfer enhancement a great dependency of Nusselt number augmentation upon Reynolds number is observed specially for low values of ( $e/D_e$ ). The case of the group of greater ( $e/D_e$ ) ratio ( $e=2.2$  mm) reveals low Reynolds number dependency giving close augmentation ratio for the four ( $p/D_e$ ) ratios with reflection in the relationship at the values of  $p= 20$  and  $30$  mm ( $e=2.2$  mm) have given values of Nusselt number augmentation larger than  $p= 10$  and  $40$  mm. The maximum value of Nusselt number augmentation for annulus-side enhancement by wire coils is registered at Reynolds number of 3000 for  $e=1$  mm and  $p=10$  mm for the annulus of  $D_i=12.5$  mm ( $e/D_e=0.0645$  and  $p/D_e=0.6452$ ) having a value of 3.25. For the other annulus, it is 3.15. These

values are corresponding to friction factor augmentation of 2.63 and 3.37 respectively. The largest value for high Reynolds number (10000) is for  $e=2.2$  mm and  $p=20$  mm having a value of 2.49 and 2.3 with friction factor augmentation of 4.66 and 6.03 for the two annuli respectively. Then, the maximum for 10000 Reynolds number is 2.49 for ( $e/D_e=0.176$  and  $p/D_e=1.6$ ).

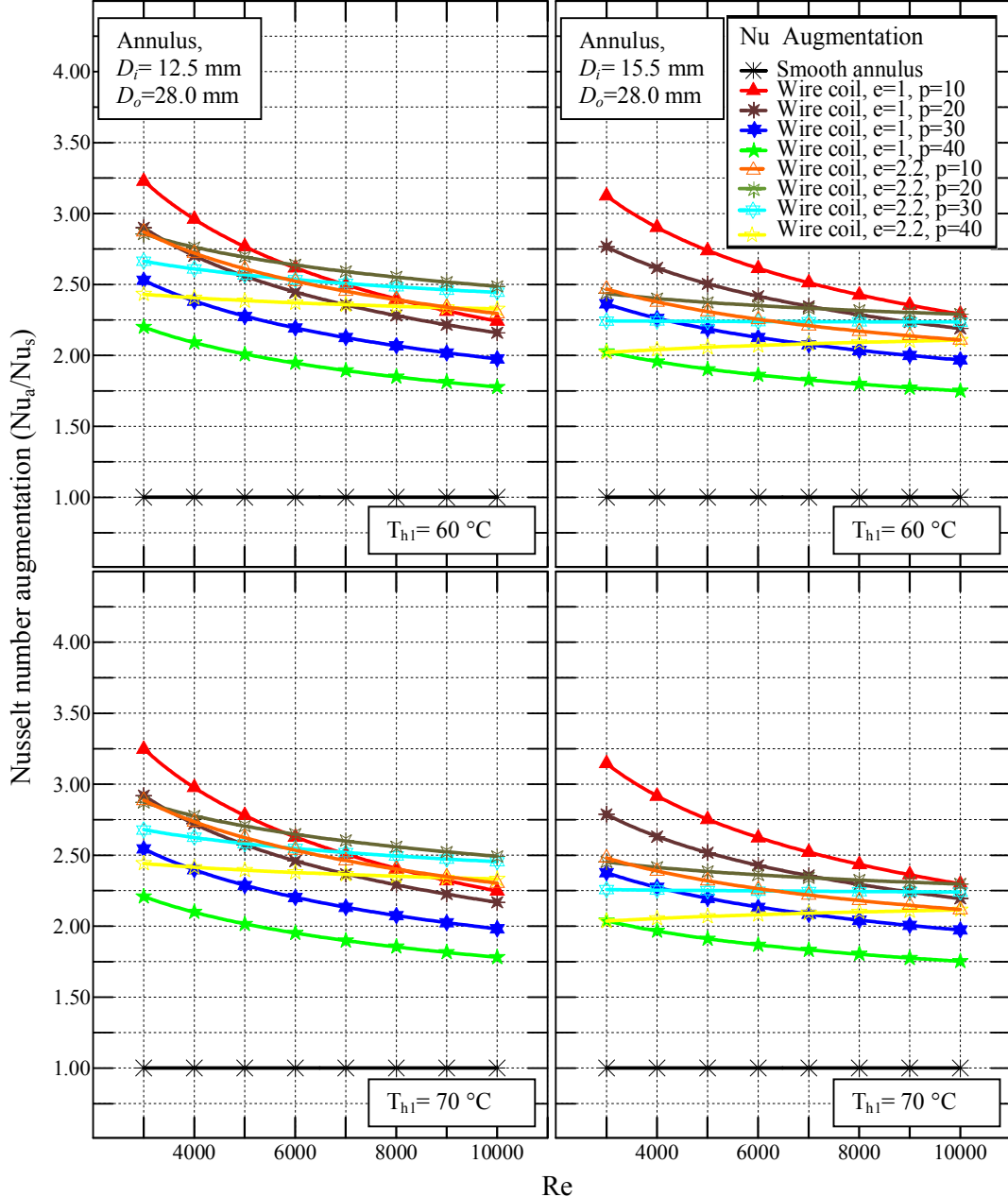


**Figure 6-7:** Nusselt number augmentation vs. Reynolds number for annulus-side heat transfer enhancement using two wire coils of  $e=1$  and  $2.2$  mm for two annulus sizes.

### 6.4.5.3 Nusselt Number Augmentation for Annulus-Side Heat Transfer Enhancement by Circular Ribs

Nusselt number augmentation relationship of the annulus-side heat transfer enhancement by circular ribs can be obtained by dividing equation (5.13) by (5.15) to be

$$\frac{\bar{N}u_a}{\bar{N}u_s} = 8.1129 \text{Re}^{-0.843+0.3298} \left( \frac{e}{D_e} \right)^{-0.4696} \left( \frac{p}{D_e} \right)^{-0.0645} \text{Pr}^{-0.16} \\ \times \left[ \frac{\left( \frac{e}{D_e} \right)^{0.0527}}{\left( \frac{e}{D_e} \right)^{-2.3452} + 0.5044} \right] \left[ \frac{\left( \frac{p}{D_e} \right)^{0.51}}{\left( \frac{p}{D_e} \right)^{0.001} - 0.983} \right] \left( \frac{D_i}{D_o} \right)^{0.1192} \dots (6.6)$$

Substituting values of the geometrical parameters from table C-41 gives fig. 6-8 (values are listed in tables C-33 through C-36) which shows close Nusselt number augmentation regardless of the values of the geometrical parameters of inserts with simple superiority for the coils with the largest coiling pitches especially in case of the annulus of  $D_i=15.5$  mm which has the least annular gap. In general all Nusselt number augmentation ratios in case of using circular ribs are less than the corresponding values in case of using wire coils. The high friction factor augmentation ratios registered for this case, as explained previously, gives an impression that the use of circular ribs has less efficiency than the wire coil regardless of the geometrical dimensions.

A comparison between the proposed methods of annulus-side heat transfer enhancement with the method of Coetzee [34] shows that the proposed method has higher efficiency than Coetzee's which had a maximum value of Nusselt number augmentation of 2.06 with friction factor augmentation of 2.03. These are less than the values obtained in the present

work that equal to 3.25 with friction factor augmentation of 2.63 in case of wire coil insert as discussed previously.

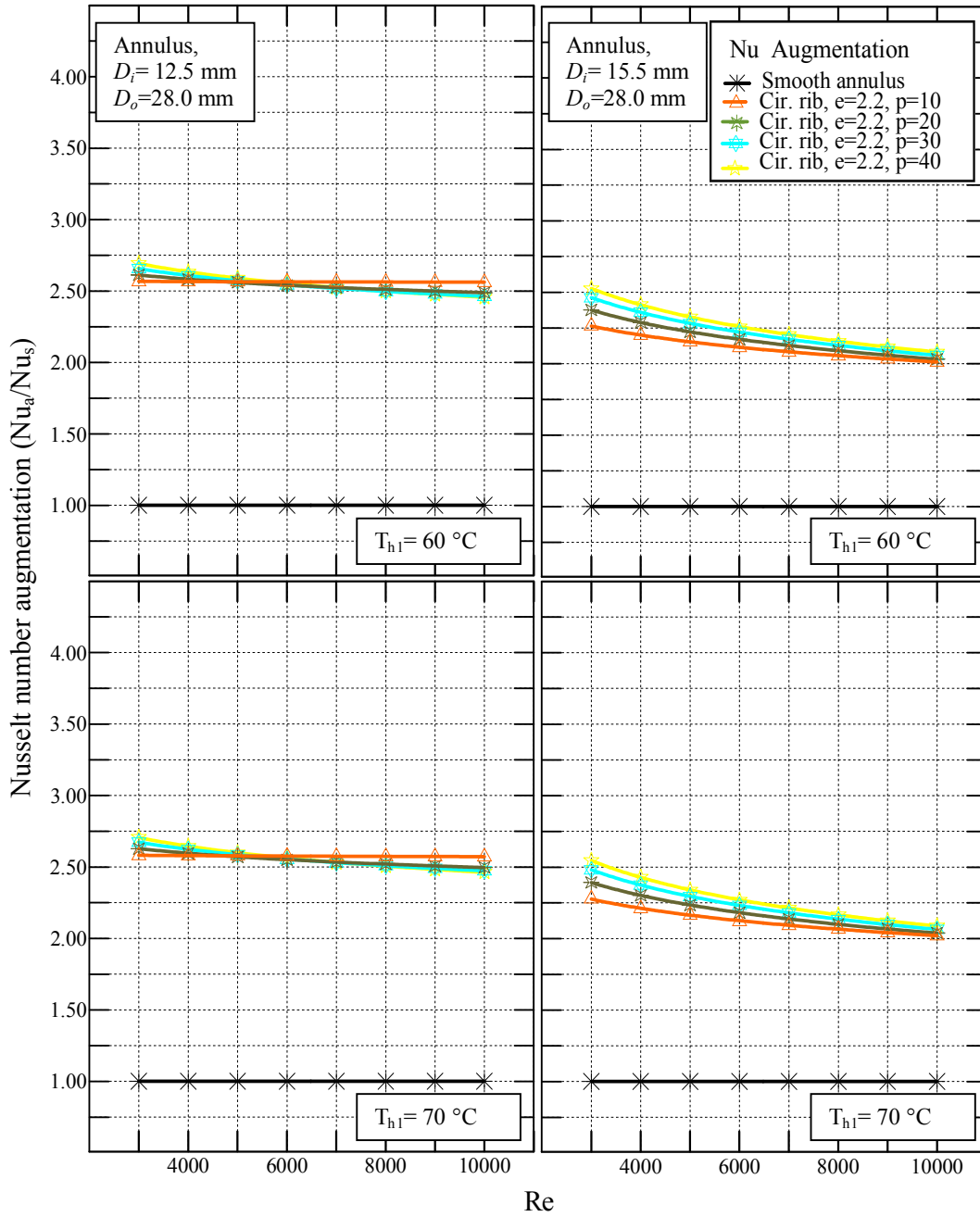


**Figure 6-8:** Nusselt number augmentation vs. Reynolds number for annulus-side heat transfer enhancement using circular ribs of  $e = 2.2$  mm for two annulus sizes (the axis scales, in spite of unclarity, have been taken the same as in fig. 6-7 to enable comparison between the two methods of annulus-side heat transfer enhancement).

## 6.5 Performance Evaluation Criteria (PEC)

One possibility to quantify the performance improvement is to calculate Nusselt number and friction factor augmentation ratios as detailed previously. That has led to the fact that the friction factor of an enhanced surface in single-phase flow is higher than that of the smooth surface, when operated at the same velocity (or Reynolds number). However, this method is not sufficient to describe the most effective enhancement method because it does not define the actual performance improvement, subject to specific operating constraints. If one simply calculated the Nusselt number augmentation ratio, at equal velocities, an unfair comparison may result. This is because the enhanced surface would be allowed to operate at a higher pressure drop. The plain surface would give a higher  $h$  value if it were allowed to operate at a higher velocity, giving the same pressure drop as the enhanced surface. Thus, the pressure drop constraint is a very important consideration for calculating the performance benefits of an enhanced surface in single-phase flow [35]. Twelve performance evaluation criteria (PECs) had been set to accommodate different cases that might be encountered in the industrial application as listed in table 3-1.

To apply these criteria to the results of the present work, starting from equation (3.31) derived previously. One of the groupings on the left side becomes the objective function, with the other two set as 1.0 for the corresponding operating constraints, which also provide the mass flux ratio ( $G_a/G_s$ ) that satisfies equation (3.31). This ratio, equaling to the corresponding Reynolds number ratio ( $Re_a/Re_s$ ), is usually for most cases larger than unity. To avoid confusion in defining the “smooth tube” term in equation (3.31) with that used in the previous calculations, a new notation is used “o” to

distinguish the smooth tube case at the same Reynolds number from that required to satisfy equation (3.31), leading to write it in the form

$$\frac{h_a A_a / h_o A_o}{(P_a / P_o)^{1/3} (A_a / A_o)^{2/3}} = \frac{j_a / j_o}{(f_a / f_o)^{1/3}} \quad \dots (6.7)$$

The application of PECs requires to have fixed tube diameter, so each of the two tubes, used in the present work, would be considered separately. In addition, constant physical properties must be assumed, to qualify the requirements set by Webb and Bergles [35, 58]. Three cases of performance evaluation criteria will be applied to the results of the present work.

### 6.5.1 PEC Application for Tube-Side Heat Transfer Enhancement

In the tube-side heat transfer enhancement case, the four experimental conditions would be briefed into two only, concerning the inlet approach temperature difference ( $\Delta T_i$ ). The two approach temperature differences are 40 and 50 °C. Indeed, this classification is applied due to a difference in the average Prandtl number for each ( $\Delta T_i$ ). Prandtl number values would be fixed to the values of 3.14 and 2.72 and 3.14 and 2.71 for tubes of 11 and 14 mm inner diameter, respectively, as presented in figs. 6-9, 6-10 and 6-11.

**(i) FG-2a criterion:** the area of flow cross section ( $N$  and  $d_i$ ) and tube length  $L$  are kept constant. This would typically be applicable for retrofitting the smooth tube of an existing exchanger with enhanced tubes, thereby maintaining the same basic geometry and size ( $N$ ,  $d_i$  and  $L$ ). The objective then could be to increase the heat load capacity ( $q$ ) for the same approach temperature ( $\Delta T_i$ ) and pumping power ( $P$ ) [1, 35, 58].

To apply this criterion, the ratios ( $P_a/P_o$ ) and ( $A_a/A_o$ ) in equation (6.7) are set to unity. Then equation (6.7) becomes

$$h_a A_a / h_o A_o = \frac{j_a / j_o}{(f_a / f_o)^{1/3}} \quad \dots (6.8)$$

Returning to the definition of Colburn factor, at fixed physical properties, equation (6.8) becomes

$$h_a A_a / h_o A_o = \frac{(Nu_a / Nu_o)}{(f_a / f_o)^{1/3} (Re_a / Re_o)} \quad \dots (6.9)$$

where  $Nu_o$  is the Nusselt number for smooth tube calculated at constant pumping power and heat exchange surface area. To satisfy the constrain of constant pumping power,  $Nu_o$  is evaluated at  $Re_o$  which is obtained by using the ( $P_a/P_o$ ) that has been set to unity. Using equation (3.30) with changing the notation of smooth tube and replacing the mass flux by the Reynolds number (physical properties are constant), then

$$(f_o Re_o^3) = (f_a Re_a^3) \quad \dots (6.10)$$

For the tube-side heat transfer enhancement, equations (6.10) and (5.9) for the value of  $Re_o$  which would be used to calculate  $Nu_o$ . In addition, equation (6.10) can be substituted in equation (6.9) to simplify it to be

$$\frac{h_a A_a}{h_o A_o} = \frac{Nu_a}{Nu_o} \quad \dots (6.11)$$

Then the (FG-2a) criterion can be expressed as:

$$\frac{q_a}{q_o} = \left( \frac{Nu_a}{Nu_o} \right)_{L, d_i, \Delta T_i, P} \quad \dots (6.12)$$

Equation (5.11) is used to calculate the values of  $\text{Nu}_a$ , for the range of Reynolds number (5000 to 40000), and with equation (6.12), to obtain the heat transfer ratios (FG-2a) for the tube-side heat transfer enhancement as listed in table C-42, and plotted in fig. 6-10.

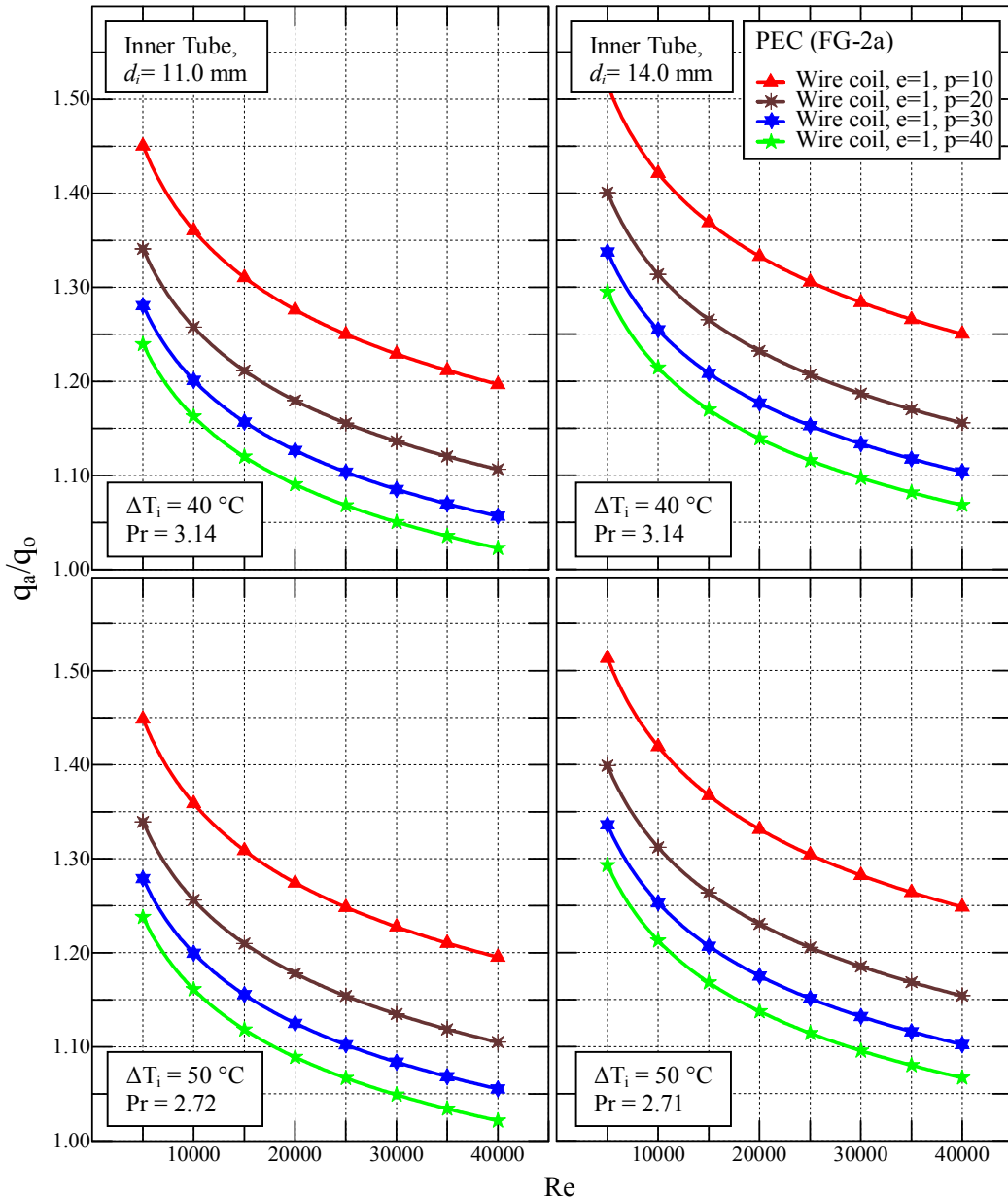


**Figure 6-9:** Application of the performance evaluation criterion (FG-2a) to the tube-side heat transfer enhancement by wire coils for two tube sizes and two experimental conditions.

Indeed the (FG-2a) criterion represents the actual enhancement ratio ( $E_h$ ) defined by equation (3.1) which refers to the most effective method of heat transfer enhancement [35].

In fig. 6-9, the wire coil of 10 mm coiling pitch has the best performance in case of the two tube sizes, having a value of 1.45 for the 11 mm diameter tube and 1.52 for the other size, both at Reynolds number of 5000. The best performance at 40000 Reynolds number is registered for the same geometrical dimensions having the values of 1.2 and 1.25 respectively. That means that the best enhancement ratio is 1.52 for the geometries of  $e/d_i = 0.0714$  and  $p/d_i = 0.7143$ . It is obvious that the arrangement of the four geometries in the heat transfer augmentation depicted in fig. 6-5 has been left unchanged here.

**( ii ) FG-3 criterion:** in this criterion the basic geometry and size ( $N, d_i, L$ ) are also kept constant like the (FG-2a), i.e. constant heat exchange surface area. The objective then could be decreasing the pumping power with keeping the inlet temperature approach and the heat duty constant [1, 35, 58]. So, to apply this criterion the ratios ( $A_a/A_o$ ) and ( $h_a A_a/h_o A_o$ ) in equation (6.7) are set to unity. Then equation (6.7), with substituting the definition of ( $j$ ), becomes

$$\frac{P_a}{P_o} = \left( \frac{f_a}{f_o} \right) \left( \frac{Nu_o}{Nu_a} \right) \left( \frac{Re_a}{Re_o} \right)^3 \quad \dots (6.13)$$

To satisfy the constrain of constant heat duty,  $f_o$  and  $Nu_o$  are evaluated at  $Re_o$  which is obtained by using the ratio  $h_a A_a/h_o A_o = 1$  to give

$$(Nu_o) = (Nu_a) \quad \dots (6.14)$$

which enables omitting the Nusselt number ratio from equation (6.13) giving

$$\frac{P_a}{P_o} = \left[ \left( \frac{f_a}{f_o} \right) \left( \frac{Re_a}{Re_o} \right)^3 \right]_{L,d_i,\Delta T_i,q} \quad \dots (6.15)$$

By calculating the values of  $Nu_a$  (by using equation (5.11)) for equation (6.14), this equation and equation (5.14) are solved directly for  $Re_o$ . The values of the pumping power ratio ( $P_a/P_o$ ) are fixed in table C-43 and plotted in fig. 6-10.

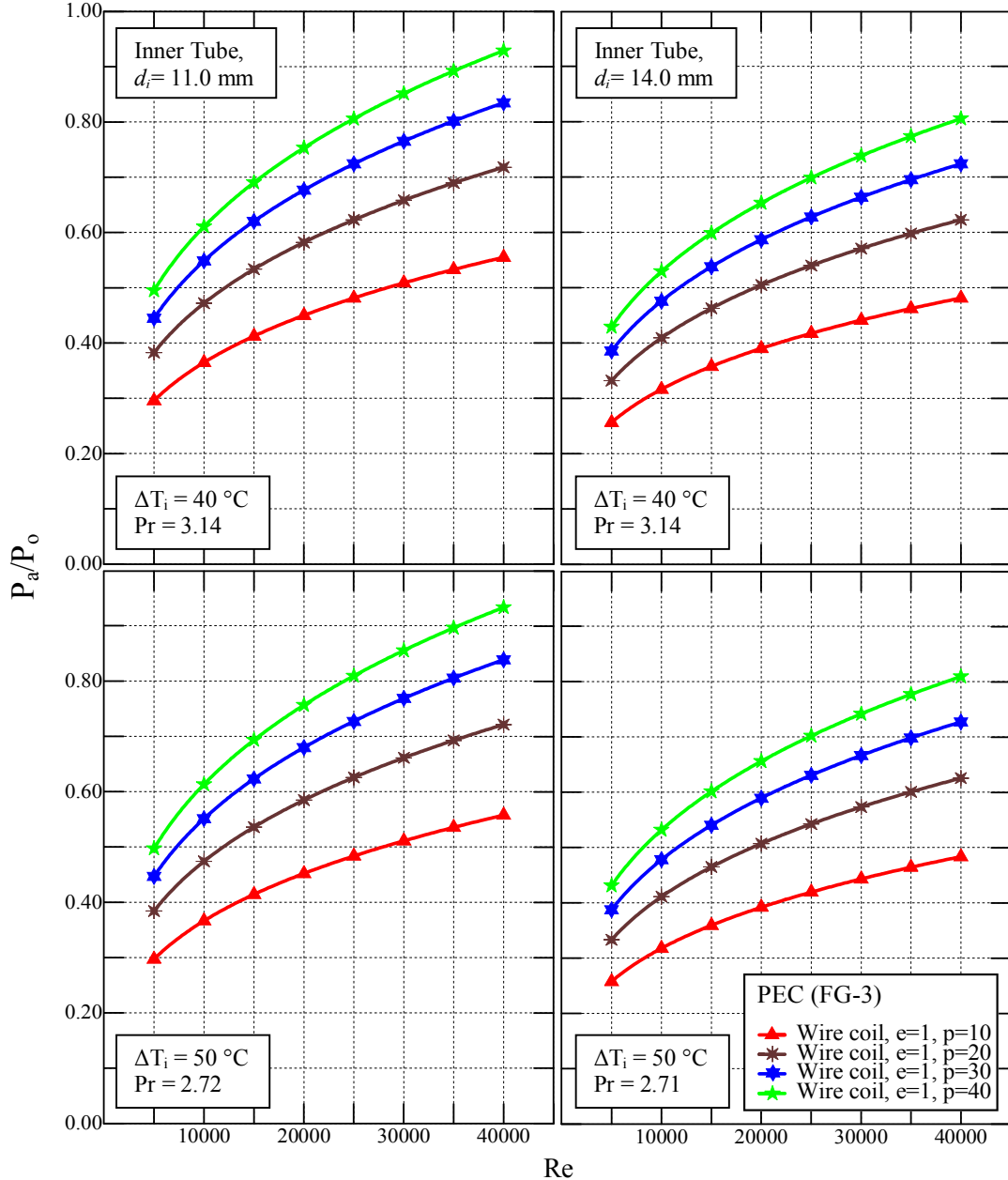


**Figure 6-10:** Application of the performance evaluation criterion (FG-3) to the tube-side heat transfer enhancement by wire coils for two tube sizes and two experimental conditions.

Figure 6-10 reveals that the pumping power, needed with adopting the wire coil of 10 mm coiling pitch is about 30% and 55% that for smooth tube for  $Re = 5000$  and  $40000$ , respectively for the 11 mm diameter tube and for the other tube size the values are 25% and 45% for  $Re = 5000$  and  $40000$ , respectively. The other three geometries have lesser pumping power with the conventional arrangement.

**( iii ) FN-1 criterion:** the flow cross section ( $N$  and  $d_i$ ) is kept constant, and the heat exchanger length is allowed to vary. Here, the objective is to seek a reduction in heat transfer surface area ( $A \rightarrow L$ ) for a fixed heat load and pumping power [1, 35, 58]. To apply this criterion, the ratios ( $h_a A_a/h_o A_o$ ) and ( $P_a/P_o$ ) in equation (6.7) are set to unity. Then, equation (6.7), with substituting the definition of ( $j$ ), becomes

$$\frac{A_a}{A_o} = \left( \frac{f_a}{f_o} \right)^{1/2} \left( \frac{Nu_o}{Nu_a} \right)^{3/2} \left( \frac{Re_a}{Re_o} \right)^{3/2} \quad \dots (6.16)$$

To satisfy the constrain of constant heat duty and pumping power,  $f_o$  and  $Nu_o$  are evaluated at  $Re_o$ . The latter is obtained by setting both ( $h_a A_a/h_o A_o$ ) and ( $P_a/P_o$ ) to unity as follows:

$$\frac{h_a A_a}{h_o A_o} = 1 \quad \dots (6.17)$$

$$\left( \frac{Nu_a}{Nu_o} \right) \left( \frac{A_a}{A_o} \right) = 1 \quad \dots (6.18)$$

and

$$\frac{P_a}{P_o} = 1 \quad \dots (6.19)$$

Substituting equation (3.30) in equation (6.19) with replacing the mass flux ratio by the Reynolds number ratio

$$\frac{f_a}{f_o} \frac{A_a}{A_o} \left( \frac{\text{Re}_a}{\text{Re}_o} \right)^3 = 1 \quad \dots (6.20)$$

Dividing equation (6.20) by equation (6.18) leads to the relationship

$$\left( f_o \text{Re}_o^3 / N u_o \right) = \left( f_a \text{Re}_a^3 / N u_a \right) \quad \dots (6.21)$$

Equations (6.21), (5.9) and (5.14) could be solved iteratively for  $\text{Re}_o$  until convergence occurs to find the values of  $\text{Re}_o$  corresponding to those of  $\text{Re}_a$ . Furthermore, equation (6.21) can be substituted in equation (6.16) to give the final form of the heat exchange surface area reduction relationship as:

$$\frac{A_a}{A_o} = \left[ \left( \frac{f_o}{f_a} \right) \left( \frac{\text{Re}_o}{\text{Re}_a} \right)^3 \right]_{d_i, \Delta T_i, q, P} \quad \dots (6.22)$$

Values of heat exchange surface area reduction ratio ( $A_a/A_o$ ) are fixed in table C-44 and plotted in fig. 6-11. It reveals that the best heat exchange surface area reduction is obtained by using the wire coil with the coiling pitch of 10 mm, where the enhanced surface area is about 0.58 and 0.77 of that for smooth tube for  $\text{Re} = 5000$  and 40000 respectively using the tube of  $d_i = 11$  mm. For the other tube, the ratios are 0.55 and 0.73 for the two Reynolds numbers respectively. Indeed these values, for a constant diameter, represent the reduction of tube lengths. Also, the conventional arrangement of the four geometries for the two tube sizes is kept the same.

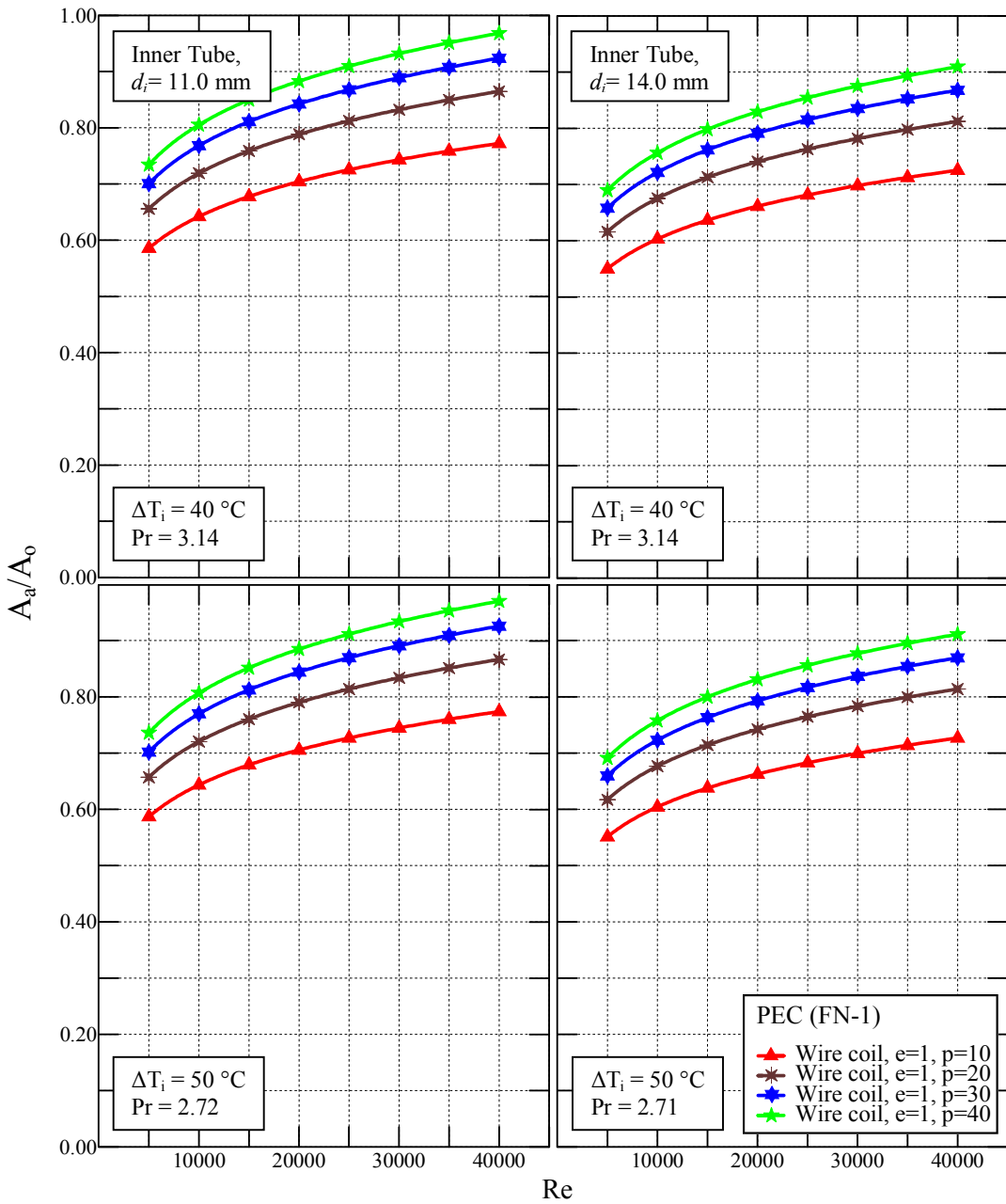


**Figure 6-11:** Application of the performance evaluation criterion (FN-1) to the tube-side heat transfer enhancement by wire coils for two tube sizes and two experimental conditions.

In figs. 6-9 through 6-11, plots have been set to show the ratios ( $q_a/q_o$ ), ( $P_a/P_o$ ) and ( $A_a/A_o$ ) for two concise experimental conditions represented by working with two approach temperature differences. A very slight effect is

noticed in the three ratios to the extent that it cannot be read directly in the plots, but by observing the concerned tables (tables C-42 through C-44). Generally, the three ratios are slightly larger in case of working with the 40 °C approach temperature difference. This confirms the exergetic fact that working at lower approach temperature differences is the most efficient. Indeed, the only representation which can be fixed for the approach temperature difference in the mathematics of heat transfer is the changes in physical properties.

### 6.5.2 PEC Application for Annulus-Side Heat Transfer Enhancement

The performance evaluation criteria of Webb and Bergles [35, 58] had been set to accommodate the heat transfer enhancement inside tubes or ducts. To make these criteria suitable for annulus-side heat transfer enhancement, the general equation (6.7) must be checked to suit that use. First, (3.24) is substituted in equation (3.25) with changing the notations for annulus

$$P = f \frac{L}{D_e} \frac{G^3 A_c}{2\rho^2} \quad \dots (6.23)$$

Substituting the cross sectional area and the equivalent diameter of annulus in equation (6.23) leads to:

$$P = fL \frac{G^3}{8\rho^2} \pi(D_o + D_i) \quad \dots (6.24)$$

Writing equation (6.24) as the ratio, relative to a smooth surface with omitting the property parameters gives:

$$\frac{P_a}{P_o} = \frac{f_a}{f_o} \frac{L_a}{L_o} \left( \frac{G_a}{G_o} \right)^3 \left[ \frac{(D_o + D_i)_a}{(D_o + D_i)_o} \right] \quad \dots (6.25)$$

Since the evaluation performance criteria had been set for equal diameter tubes, then equation (6.25) can be simplified for annuli having the same inner and outer diameters. The parenthesis of diameters in equation (6.25) can be omitted safely to give the equation:

$$\frac{P_a}{P_o} = \frac{f_a}{f_o} \frac{L_a}{L_o} \left( \frac{G_a}{G_o} \right)^3 \quad \dots (6.26)$$

But the length ratio is equal to the ratio of the outer surface of the inner tube of the annulus, leading to:

$$\frac{P_a}{P_o} = \frac{f_a}{f_o} \frac{A_a}{A_o} \left( \frac{G_a}{G_o} \right)^3 \quad \dots (6.27)$$

Equation (6.27) is the same as equation (3.30) having the area abbreviation referring to the area of the outer surface of the inner tube of the annulus. On the other hand, equation (3.28) can be used without any change because the area ratio stated there is the heat transfer surface area (outer surface of the inner tube in case of the annulus). Then, equations (3.28) and (6.27) can be used to produce the general equation of the performance evaluation criteria for annulus which is the same as equation (6.7) provided that both the inner and outer diameters of the annulus must be constant, i.e.

$$\left[ \frac{h_a A_a / h_o A_o}{(P_a / P_o)^{1/3} (A_a / A_o)^{2/3}} = \frac{j_a / j_o}{(f_a / f_o)^{1/3}} \right]_{D_i, D_o} \quad \dots (6.28)$$

This means that equations of the three ratios, derived for the tube-side enhancement, can be used for the annulus-side enhancement but with considering the specificity of the annulus, as shown later.

It is important to state that the area ratios in both equations (6.7) and (6.28) are the same as the effective length ratio for the double pipe heat exchanger because the only way to change the surface area, with keeping the diameters constant, is by changing the effective length of the exchanger.

In the present work, the PECs are applied for the annulus-side heat transfer enhancement by wire coils and circular ribs together, with using the concerned equations for each type, to make a direct comparison for the two cases. Moreover, the four experimental conditions have been briefed in one only because the differences caused by changing these conditions are very slight and cannot be recognized for comparison. The average values for physical properties of the four conditions have been considered. The application of the three criteria is as follows:

**( i ) FG-2a criterion:** using the modified conditions, the area of flow cross section is constant with keeping the  $D_i$  and  $D_o$  constant, as well as the tube length  $L$  is kept constant. This would typically be applicable for retrofitting the smooth annulus of an existing exchanger with an enhanced one. The objective then could be to increase the heat load capacity ( $q$ ) for the same approach temperature ( $\Delta T_i$ ) and pumping power ( $P$ ). The corresponding equation for the annulus-side heat enhancement is:

$$\frac{q_a}{q_o} = \left( \frac{Nu_a}{Nu_o} \right)_{L, D_i, D_o, \Delta T_i, P} \dots (6.29)$$

Likely, equation (6.10) also can be used safely to predict the corresponding Reynolds number  $Re_o$  by direct solution with equation (5.10)

for smooth annulus.  $Nu_a$  is obtained by using equation (5.12) for annulus-side heat transfer enhancement by wire coil and by using equation (5.13) for the enhancement by circular ribs. Results obtained for the  $(q_a/q_o)$  are fixed in table C-45. The plot of these results is in fig. 6-12.

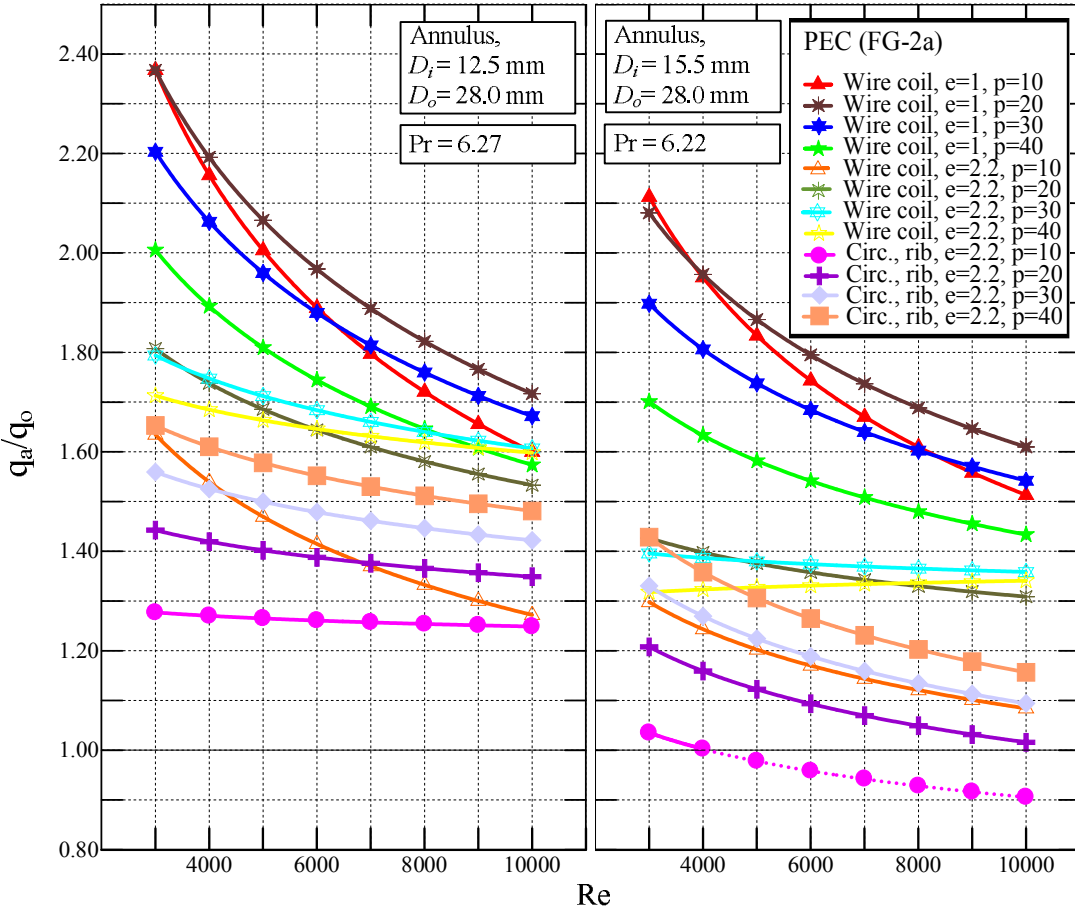


**Figure 6-12:** Application of the performance evaluation criterion (FG-2a) to the annulus-side heat transfer enhancement by wire coils and circular ribs for two annulus sizes and one experimental condition.

Figure 6-12 gives a very important conclusion for the annulus-side heat transfer enhancement study performed in the present work, where the most effective annulus-side insert geometries have become known which is the wire coil insert of geometries  $e=1$  mm and  $p=20$  mm (i.e.  $e/D_e=0.0645$  and

$p/D_e = 1.2903$ ) for the whole Reynolds number range adopted in the present work. The value of the enhancement ratio is 2.367 for  $Re = 3000$  and 1.717 for  $Re = 10000$ . These results are for the annulus of  $D_i=12.5$  mm, for the  $D_i=15.5$  mm annulus the result is something different, where the superiority is registered for the insert of  $e=1$  mm and  $p= 20$  mm (i.e.  $e/D_e = 0.08$  and  $p/D_e = 1.6$ ) for Reynolds number range larger than 4000, but for lower Reynolds numbers, the best is the insert of  $e= 1$  mm and  $p= 10$  mm ( $e/D_e = 0.08$  and  $p/D_e = 0.8$ ).

A general view of fig. 6-12 gives an imagination that the wire of 1 mm diameter has given the best thermal performance for all coiling pitches adopted, to the extent that even that of  $p = 40$  has a thermal performance better than that of the insert of  $e = 2.2$  mm for all coiling pitches. Moreover the circular ribs give the least performance to the extent that the circular ribs of 10 mm coiling pitches, in case of the annulus of  $D_i=15.5$  mm, have a performance lower than smooth annulus.

( ii ) **FG-3 criterion:** to apply this criterion the basic geometry and size ( $D_i$ ,  $D_o$  and  $L$ ) kept constant, i.e. constant heat exchange surface area. The objective then could be decreasing the pumping power with keeping the inlet temperature approach and the heat duty constant. Corresponding to equation (6.15), the equation of pumping power ratio for the annulus-side heat transfer enhancement is:

$$\frac{P_a}{P_o} = \left[ \left( \frac{f_a}{f_o} \right) \left( \frac{Re_a}{Re_o} \right)^3 \right]_{L, D_i, D_o, \Delta T_i, q} \dots (6.30)$$

Equation (6.14) can be used for the annulus-side enhancement to evaluate the  $Re_o$  required for calculating  $f_o$  by equation (5.10) in a manner

similar to that used for the tube-side heat transfer enhancement but with using the concerned equations of friction factor and heat transfer for the annulus-side heat transfer by wire coil and circular ribs which are equations (5.4) and (5.6) and (5.12) and (5.13) respectively. The predicted results of the ( $P_a/P_o$ ) are listed in table C-46. Figure 6-13 shows these results.

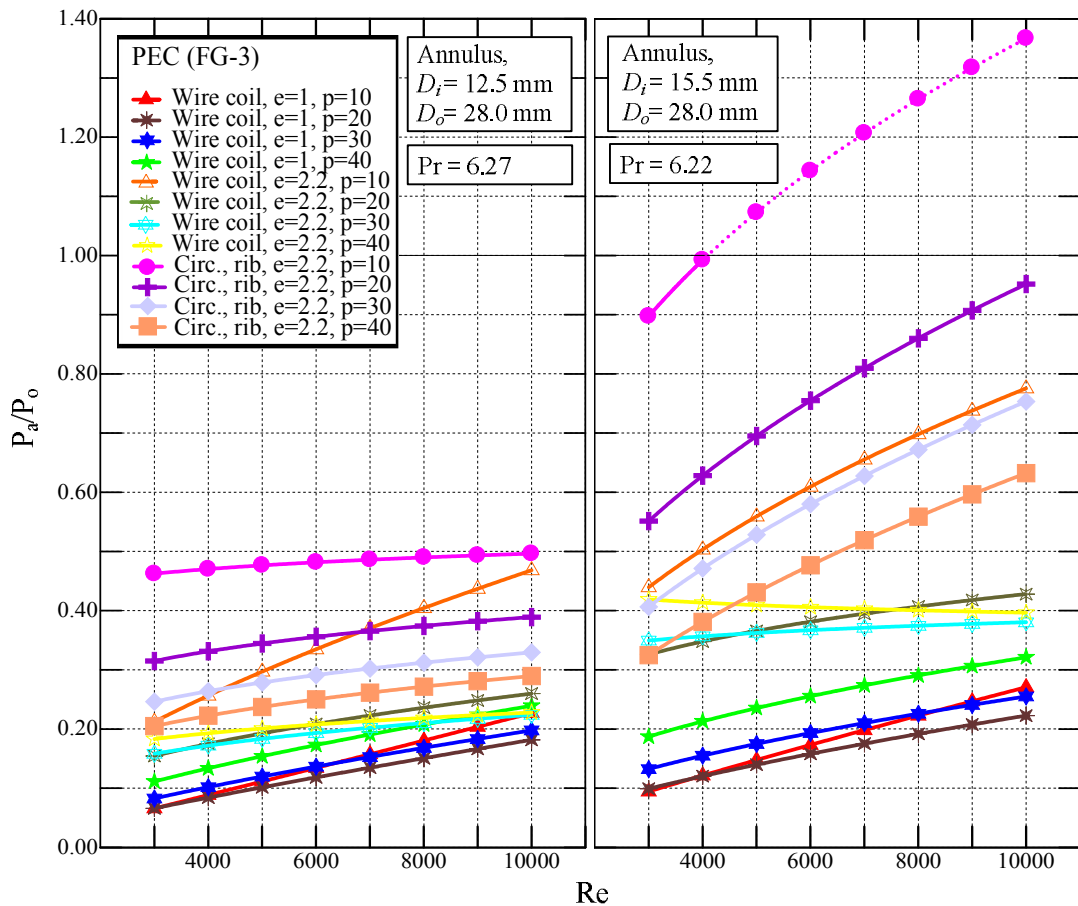


**Figure 6-13:** Application of the performance evaluation criterion (FG-3) to the annulus-side heat transfer enhancement by wire coils and circular ribs for two annulus sizes and one experimental condition.

In fig. 6-13 the best pumping power ratio, performed, is by the wire coil insert of geometries  $e=1$  mm and  $p=20$  mm ( $e/D_e=0.0645$  and  $p/D_e=1.2903$ ) for the annulus of  $D_i=12.5$  mm having the value of 0.066 at  $Re = 3000$  and

0.094 performed by the wire coil of  $e=1$  mm and  $p= 10$  mm for the annulus of  $D_i=15.5$  mm. And the best values for  $\text{Re} = 10000$  is 0.182 and 0.223 for the two annuli respectively, both for the wire coil having  $e=1$  mm and  $p= 20$  mm. Close results for the inserts of  $e= 1$  mm are observed. Furthermore, the circular ribs have the worst pumping power ratio in an arrangement similar to that observed in case of  $(q_a/q_o)$  ratio.

**( iii ) FN-1 criterion:** in this criterion the flow cross section is kept constant ( $D_i$  and  $D_o$  must be constant), and the heat exchanger length is allowed to vary. Here the objective is to seek a reduction in heat transfer surface area for a fixed heat load and pumping power. The equation corresponding to equation (6.22) for the heat exchange area or length reduction of annulus-side heat transfer enhancement is:

$$\frac{A_a}{A_o} = \left[ \left( \frac{f_o}{f_a} \right) \left( \frac{\text{Re}_o}{\text{Re}_a} \right)^3 \right]_{D_i, D_o, \Delta T_i, q, P} \dots (6.31)$$

The iterative solution of equation (6.21), (5.15) and (5.12) or (5.13) (the latter is for wire coil and circular ribs respectively) is followed to predict the requirements of equation (6.31) as explained previously. The predicted results are fixed in table C-47. These results are plotted in fig. 6-14 which shows that the best value of heat exchange surface area or length reduction in the double pipe heat exchanger is that performed by the wire coil of  $e=1$  mm and  $p= 20$  mm equaling 0.283 for the annulus of  $D_i=12.5$  mm at  $\text{Re} = 3000$ . For the other annulus size the best value is 0.335 for the wire coil of  $e=1$  mm and  $p=10$  at  $\text{Re} = 3000$ , and the best values for  $\text{Re} = 10000$  are 0.453 and 0.498 for the two annuli respectively, both performed by the wire coil of  $e=1$  mm

and  $p = 20$  mm. The circular ribs also give the worst surface area reduction and the wire coil of 2.2 mm is in between.

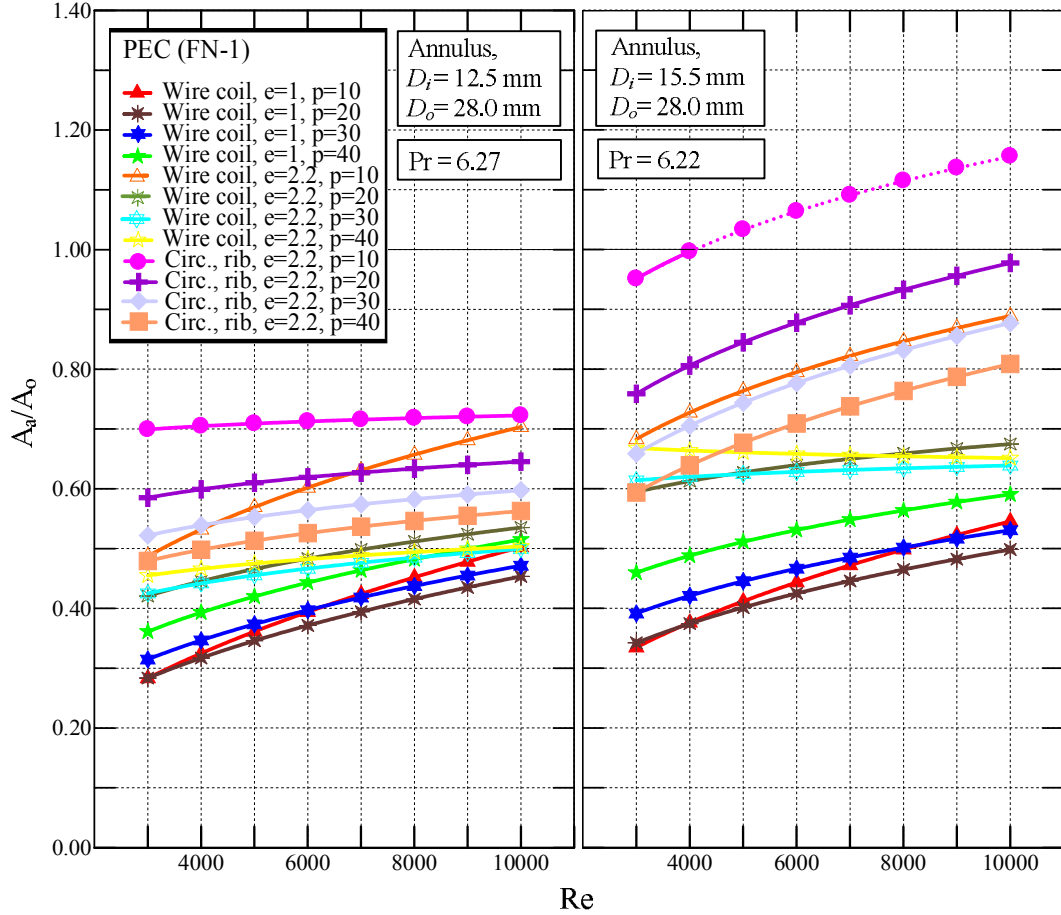


**Figure 6-14:** Application of the performance evaluation criterion (FN-1) to the annulus-side heat transfer enhancement by wire coils and circular ribs for two annulus sizes and one experimental condition.

In general, the wire coil of geometries  $e = 1$  mm and  $p = 20$  can be considered as the best heat transfer enhancer in the annulus for the three PECs studied in the present work for the ranges of geometries and sizes and Reynolds number adopted.

## CHAPTER SEVEN

### Conclusions and Recommendations

#### 7.1 Conclusions

In the present work, the following can be concluded:

- 1- According to high performance results, the proposed method of annulus-side heat transfer enhancement by wire coils can be considered as a promising method of promoting heat transfer in the annulus of the double pipe heat exchanger.
- 2- For both tube and annulus side heat transfer enhancement, Nusselt number and friction factor are more dependent on Reynolds number at low values than high ones.
- 3- In the annulus-side enhancement, swirl flow is greatly important for enhancing heat transfer especially when the mechanism of separation and reattachment becomes weak when coils become relatively close with relatively low pressure drop as compared to inserts that forbid the generation of swirls (like circular ribs).
- 4- Friction factor and heat transfer in enhanced annuli are affected by the annular gap size.
- 5- In annulus-side enhancement, the performance of wire coils is better than circular ribs in all calculations and PECs.
- 6- Heat transfer, as well as friction factor increases with decreasing the coiling pitch in the tube-side heat transfer enhancement by wire coils giving a maximum heat transfer augmentation ratio of 2.43 compared to smooth tube at  $Re = 5000$  with 4.75 augmentation of friction factor. That is obtained with wire coil of  $e/d_i = 0.0714$  and  $p/d_i = 0.7143$ . The

maximum values at  $Re = 40000$  is given by the same wire coil. They are 2.24 and 6.83 respectively.

- 7- Heat transfer as well as friction factor increases with decreasing the coiling pitch in the annulus-side heat transfer enhancement by wire coil to a specified limit, then the relationship reflects giving a maximum heat transfer augmentation ratio of 3.25 compared to smooth annulus at  $Re = 3000$  with 2.63 friction factor augmentation. That is obtained with wire coil of ( $e/D_e=0.0645$  and  $p/D_e=0.6452$ ). The maximum value at  $Re = 10000$  is given by the wire coil of ( $e/D_e=0.176$  and  $p/D_e=1.6$ ). It is 2.49 with 4.66 friction factor augmentation.
- 8- The PEC calculations have determined that the best wire coil insert used in the tube-side enhancement in the ranges adopted is that having  $e/d_i= 0.0909$  and  $p/d_i= 0.9091$ . In the annulus-side enhancement, the best insert is the wire coil of  $e/D_e= 0.0645$  and  $p/D_e= 1.2903$ .

## 7.2 Recommendations

- 1- Using chemical additives with water or using other fluids, in addition to water, enables attaining a wider range of Prandtl number, either in tube-side or annulus-side heat transfer enhancement.
- 2- Using additional tube sizes for the tube-side heat transfer enhancement in order to increase the number of points to make correlations obtained more comprehensive.
- 3- In case of the annulus-side heat transfer enhancement by wire coil, using a wire coil of diameter in between 1 and 2.2 mm might lead to a better maximum of heat transfer enhancement.
- 4- Using circular ribs of diameter less than 2.2 to check if the circular ribs carry out a better performance.

## References

- [1]. Manglik, R. M., "Heat Transfer Enhancement", in "Heat Transfer Handbook", Chap. 14, A. Bejan, and A. D. Kraus (editors), John Wiley & Sons Inc., New Jersey, (2003).
- [2]. Bergles, A. E., "Heat Transfer Enhancement", in "The CRC Handbook of Thermal Engineering", F. Kreith (editor), CRC Press, NY (2000).
- [3]. Zimparov, V. D, Penchev, P. J., and Meyer, J., "Performance Evaluation of Tube-in-Tube Heat Exchangers with Heat Transfer Enhancement in the Annulus", Thermal Science, Vol. 10, (2006), pp. 45-56.
- [4]. Shah, R. K., and Sekulic, D. P., "Fundamentals of Heat Exchanger Design", John Wiley & Sons, Inc., New Jersey, (2003).
- [5]. Ecke, R., "The Turbulence Problem, An Experimentalist's Perspective", Los Alamos Science, Number 29 2005, pp. 124-125.
- [6]. McComb, W. D, "The Physics of Fluid Turbulence", Clarendon Press, Oxford, (1992), pp. 4-5.
- [7]. Oertel, H., "Prandtl's Essentials of Fluid Mechanics", 2<sup>nd</sup> edition, Springer-Verlag New York, Inc., (2004) pp. 126-127.
- [8]. Viedma, A., Garcia, A and Vicente, P. G., "Experimental Investigation on Heat Transfer and Frictional Characteristics of Wire Coils Inserts in Transition Flows at Different Prandtl Numbers", International Journal of Heat and Mass Transfer, Volume 48, Issues 21-22, October 2005, pp 4640-4651.
- [9]. Kumar, P., and Judd, R. L., "Heat Transfer with Coiled Wire Turbulence Promoters", The Canadian Journal of Chemical Engineering, Vol. 48, pp. 378-383, (1970).
- [10]. Zhang, Y. F., Yue Li, F., and Liang, Z. M., "Heat transfer in spiral coil inserted tubes and its application", Advances in Heat Transfer Augmentation and Mixed Convection, ASME, pp. 31-36, (1991).

- [11]. Eiamsa-ard, S., Nivesrangsan, P., Chokphoemphun, P., and Promvonge, P., “Influence of Combined Non-Uniform Wire Coil and Twisted Tape Inserts on Thermal Performance Characteristics”, International Communications in Heat and Mass Transfer 37 (2010) pp. 850–856.
- [12]. Manglik, R. M., and Bergles, A. E., “Heat Transfer and Pressure Drop Correlations for Twisted-Tape Inserts in Isothermal Tubes: Part II – Transition and Turbulent Flows”, Enhanced Heat Transfer, HTD Vol. 202, ASME, (1992), pp. 99-106, cited in “Engineering Data book III”, Chap. 5, J. R. Thome, Wolverine Tube Inc., (2009).
- [13]. Promvonge, P., Eiamsa-ard, S., “Enhancement of heat transfer in a tube with regularly-spaced helical tape swirl generators”, Elsevier Ltd., (2004).
- [14]. Ahmed, S. M., Deju, L., Sarkar M. A., and Nazrul Islam, S. M., “Heat Transfer in Turbulent Flow through a Circular Tube with Twisted Tape Inserts”, The International Conference on Mechanical Engineering, December 2005, Dhaka, Bangladesh.
- [15]. Promvonge, P., Eiamsa-ard, S., and Noothong1, W., “Effect of Twisted-tape Inserts on Heat Transfer in a Tube”, International Conference on Sustainable Energy and Environment, Bangkok, Thailand, (2006).
- [16]. Eiamsa-ard, S., and Promvonge, P., “Enhancement of heat transfer in a circular wavy-surfaced tube with a helical-tape insert”, International Conference on Sustainable Energy and Environment, Bangkok, Thailand, (2006).
- [17]. Kumar, A., and Prasad, B. N., “Enhancement in Solar Water Heater Performance using Twisted Tape Inserts”, IE (I) Journal, Volume 90 (2009).
- [18]. Gouta, R., and Das, A. B., “Some Experimental Studies on Heat Transfer Augmentation for Flow of Liquid through Circular Tubes Using Twisted

Angles and Tapes”, B.Tech. thesis, National Institute of Technology, Rourkela, India, (2008)

- [19]. Yadav, A. S., “Effect of Half Length Twisted-Tape Turbulators on Heat Transfer and Pressure Drop Characteristics inside a Double Pipe U-Bend Heat Exchanger”, Jordan Journal of Mechanical and Industrial Engineering, Volume 3, (2009), pp. 17-22.
- [20]. Thianpong, C., Eiamsa-ard P, Wongcharee, K., “Compound heat transfer enhancement of a dimpled tube with a twisted tape swirl generator”, International Communications in Heat and Mass Transfer 36 (2009) pp. 698–704.
- [21]. Nazrul Islam, S. M., Chowdhuri, M. A., Hossain, R. A, and Sarkar, M. A., “Heat Transfer in Turbulent Flow through Tube with Rod-pin Inserts”, The International Conference on Mechanical Engineering, December 2007, Dhaka, Bangladesh.
- [22]. Promvonge, P., Eiamsa-ard, S., Pethkool, S., and Thianpong, C., “Turbulent Flow Heat Transfer and Pressure Loss in a Double Pipe Heat Exchanger with Louvered Strip Inserts”, Elsevier Ltd., (2007).
- [23]. Alemrajabi, A. A., and Karamipour, H., “Effect of Disks’ Geometry on Heat Transfer in a Tube”, International Conference on Energy and Environment, Iran (2006).
- [24]. Raju, a. V., Sarda, N., and Radha, K. K., “Experimental Investigations in a Circular Tube to Enhance Turbulent Heat Transfer Using Mesh Inserts”, ARPN Journal of Engineering and Applied Sciences, Vol.4, (2009), pp. 53-60.
- [25]. Promvonge, P., Eiamsa-ard, S., “Heat Transfer Enhancement in a Tube with Combined Conical-Nozzle Inserts and Swirl Generator”, [www.thaiscience.info](http://www.thaiscience.info), (2009).

- [26]. Morgan, R. D., "Twisted Tube Heat Exchanger Technology", Brown Finetube Company, Texas, USA.
- [27]. Rainieri, S., Farina, A., and Pagliarini, G., "Experimental Investigation of Heat Transfer and Pressure Drop Augmentation for Laminar Flow in Spirally Enhanced Tubes", Università di Parma, Parma, Spain.
- [28]. Zimparov, V., and Penchev, P., "Performance Evaluation of Deep Spirally Corrugated Tubes for Shell-and-Tube Heat Exchangers", 3<sup>rd</sup> International Symposium on Heat Transfer Enhancement and Energy Conservation, Guangzhou, China.
- [29]. Kotcioglu, I., Ayhan, T., Olgun, H., and Ayhan, B., "Heat Transfer and Flow Structure in a Rectangular Channel with Wing-Type Vortex Generator", Tr. J. of Engineering and Environmental Science, 22, (1998), pp. 185-195.
- [30]. Layek, A., Saini, J. S., and Solanki, S. C., "Heat Transfer and Friction Characteristics of Solar Air Heater Having Compound Turbulator on Absorber Plate", Advances in Energy Research (2006).
- [31]. Naphon, P., "Heat Transfer Characteristics and Pressure Drop in Channel with V-Corrugated Upper and Lower Plates", Elsevier Ltd., (2006).
- [32]. Park, D., Silva, C., Marotta, E., and Fletcher, L., "Study of Laminar Forced Convection Heat Transfer for Dimpled Heat Sinks", Journal of Thermophysics and Heat Transfer, Vol. 22, No. 2, (2008).
- [33]. Agrawal, A. K., and Sengupta, S., "Laminar Fluid Flow and Heat Transfer in an Annulus with an Externally Enhanced Inner Tube", Int. J. Heat and Fluid Flow, Vol. 14, No. 1, (1993), pp. 54-63.
- [34]. Coetzee, H., "Heat Transfer and Pressure Drop Characteristics of Angled Spiraling Tape Inserts in a Heat Exchanger Annulus", M. Sc. thesis, Rand Afrikaans University, Johannesburg, South Africa, (2001).

- [35]. Webb, R. L., and Kim, N., “Principles of Enhanced Heat Transfer”, 2<sup>nd</sup> edition, Taylor & Francis Routledge, New York, (2005).
- [36]. Petukhov, B. S., “Heat Transfer and Friction in Turbulent Pipe Flow with Variable Physical Properties”, in “Advances in Heat Transfer”, Vol.6, J. B. Hartnett, and T. F. Irvine, (editors) Academic Press Inc., (1970), pp. 503-564.
- [37]. Streeter, V. L., “Fluid Mechanics”, 9<sup>th</sup> edition McGraw-Hill Inc., New York, (1998).
- [38]. Munson, B. R., and Young, D. F., “Fundamentals of Fluid Mechanics”, 4<sup>th</sup> Edition, John Wiley & Sons, Inc., (2002).
- [39]. Colburn, A. P., Transactions of the AIChE 26 (1933). pp 174, cited in “Heat Transfer, a Practical Approach”, McGraw-Hill, New York, (2002).
- [40]. Dittus, F. W., and Boelter, L. M., University of California Publications on Engineering 2 (1930), p. 433, cited in “Heat Transfer, a Practical Approach”, McGraw-Hill, New York, (2002).
- [41]. Sieder, E. N., and Tate, G. E., “Heat Transfer and Pressure Drop of Liquids in Tubes”, Ind. Eng. Chem., vol. 8, pp. 1429-1435, 1936, cited in “Heat Exchanger Design Handbook”, D. B. Spalding (editor), Hemisphere Publishing Corporation, New York, (1983).
- [42]. Çengel, Y. A., “Heat Transfer, a Practical Approach”, McGraw-Hill, New York, (2002).
- [43]. Gnielinski, V., “Forced Convection in Ducts”, in “Heat Exchanger Design Handbook”, D. B. Spalding (editor), Hemisphere Publishing Corporation, New York, (1983).
- [44]. Petukhov, B. S., and Popov, V. N., “Theoretical Calculation of Heat Exchange and Frictional Resistance in Turbulent Flow in Tubes of an Incompressible Fluid with Variable Physical Properties”, High Temp. (USSR), vol. 1, pp. 69-83, 1963, cited in “Heat Exchanger Design

Handbook”, D. B. Spalding (editor), Hemisphere Publishing Corporation, New York, (1983).

- [45]. Hausen H., “Darstellung des Wärmeüberganges in Rohren durch verallgemeinerte Potenzbeziehungen”, Z. Ver. Dtsch. Ing., Beiheft Verfahrenstech., no. 4, pp. 91-134, 1943, cited in “Heat Exchanger Design Handbook”, D. B. Spalding (editor), Hemisphere Publishing Corporation, New York, (1983).
- [46]. Kern, D. Q., “Process Heat Transfer”, McGraw-Hill, New York, (1965).
- [47]. Kakaç, S., and Liu, N, “Heat Exchangers, Selection, Rating, and Thermal Design”, 2<sup>nd</sup> edition, CRC Press, Florida, (2002).
- [48]. McKetta, J. J., “Heat Transfer Design Methods”, Marcel Dekker Inc., New York, (1992)
- [49]. Coa, E., “Heat Transfer in Process Engineering”, McGraw-Hill, New York, (2010).
- [50]. Davis, E. S., “Heat transfer and pressure drop in annuli”, Trans. Am. Soc. Mech. Eng. 65 (1943), cited in “Chemical Engineering”, Vol. 1, 6<sup>th</sup> edition, J. M. Coulson, and J. F. Richardson, Butterworth-Heinemann, Oxford, (1999).
- [51]. Petukhov, B. S., and Roizen L. I., “Generalized Relationship for Heat Transfer in a Turbulent Flow of Gas in Tubes of Annular Section, High Temp. (USSR), vol. 2, pp. 65-68, (1964), cited in: “Heat Exchanger Design Handbook”, D. B. Spalding (editor), Hemisphere Publishing Corporation, New York, (1983).
- [52]. Kaviany, M., “Principles of Heat Transfer”, John Wiley & Sons Inc., New York, (2002).
- [53]. Incropera, F. P., and DeWitt, D. P., “Fundamentals of Heat and mass Transfer”, 6<sup>th</sup> edition, John Wiley & Sons Inc., New York, (2006).

- [54].Jiji, L. M., “Heat Convection”, 2<sup>nd</sup> edition, Springer-Verlag Berlin Heidelberg, (2009).
- [55].Sinnott, R. K., “Chemical Engineering Design”, 4<sup>th</sup> edition, Elsevier Butterworth-Heinemann, Oxford, (2005).
- [56].Ravigururajan, T.S. and Bergles, A.E., “General Correlations for Pressure Drop and Heat Transfer for Single-Phase Turbulent Flow in Internally Ribbed Tubes”, Augmentation of Heat Transfer in Energy Systems, ASME Symp. Vol. HTD, 52, 9–20 (1985), cited in “Engineering Data Book III”, Thome, J. R., Wolverine Tube Inc., Switzerland, (2009).
- [57].Thome, J. R., “Engineering Data Book III”, Wolverine Tube Inc., Switzerland, (2009).
- [58].Bergles, A. E., “Techniques to Enhance Heat Transfer”, in “Handbook of Heat Transfer”, chap. 11, 3<sup>rd</sup> edition, W. M. Rohsenow, J. R. Hartnett, and Y. I. Cho, (editors), McGraw-Hill, New York, (1998).
- [59].Arman, B. and Rabas, T. J., “Disruption Shape Effects on the Performance of Enhanced Tubes with the Separation and Reattachment Mechanism”, Enhanced Heat Transfer, HTD Vol. 202, ASME, (1992), pp. 67-76.
- [60].Arman, B. and Rabas, T. J., “The Influence of the Prandtl Number on the Thermal Performance of Tubes with the Separation and Reattachment Mechanism”, Energy Systems Division, Argonne National Laboratory, (1992).
- [61].Webb, R.L., Eckert, E.R.G. and Goldstein, R.J., “Heat Transfer and Friction in Tubes with Repeated-Rib Roughness”, Int. J. Heat Mass Transfer, Vol. 14, (1971), pp. 601-617.

- [62]. Acharya, S., Myrum, T., and Baker, R., "Turbulent Flow and Heat Transfer Past a Surface Mounted Two Dimensional Rib", ASME HTD Vol. 239, (1993), pp. 27-34.
- [63]. Acharya, S., Dutta, S., Myrum, T., and Baker, R., "Turbulent flow past a surface mounted rib", Journal of fluid Engineering, Vol. 116, No.2, (1994), pp. 238-246.
- [64]. Holman, J. P., "Heat Transfer", 9<sup>th</sup> edition, McGraw-Hill, New York, (2007).
- [65]. Eckert, E. R., and Goldstein, R. J., "Measurement Techniques in Heat Transfer", Technivision Services, Slough, England, (1970)
- [66]. Sherwood, D. R., and Wistance, D. J., "The Piping Handbook", (1973).
- [67]. Montgomery, D. C., and Runger, G. C., "Applied Statistics and Probability for Engineers", 3<sup>rd</sup> edition, John Wiley & Sons, Inc., (2003).
- [68]. Henry, F. S., and Collins, M. W., "Prediction of Flow over Helically Ribbed Surfaces", International Journal for Numerical Methods in Fluids, Volume 13, Issue 3, pp. 321–340, 20 July 1991.
- [69]. Nunner, W., "Heat Transfer and Pressure Drop in Rough Tubes", United Kingdom Atomic Energy Authority, Harwell, (1956).
- [70]. Klaczak, A., "Heat transfer in tubes with spiral and helical turbulators", Journal of Heat Transfer, (1973), pp. 557-559.
- [71]. Perry, R. H., "Perry's Chemical Engineers' Handbook", 7<sup>th</sup> edit., McGraw-Hill Inc., New York, (1997).
- [72]. Wagner, W., "International Steam Tables", 2<sup>nd</sup> Springer-Verlag Berlin Heidelberg, (2008).

## Appendix A: Physical Properties of Liquid Water

Physical properties of water needed in the calculations of the present work are listed in table A-1 and plotted versus temperature in fig. A-1.

**Table A-1:** Physical Properties of Liquid Water [71, 72].

T °C	$\rho$ (kg/m <sup>3</sup> )	$\mu \times 10^{-3}$ (Pa.s)	k (W/m.°C)
12	999.5	1.2341	0.5856
14	999.2	1.1684	0.5892
16	998.9	1.1081	0.5927
18	998.6	1.0527	0.5961
20	998.2	1.0016	0.5995
22	997.8	0.9544	0.6027
24	997.3	0.9107	0.6059
26	996.8	0.8701	0.6090
28	996.2	0.8324	0.6120
30	995.6	0.7972	0.6150
32	995.0	0.7644	0.6178
34	994.4	0.7337	0.6206
36	993.7	0.7050	0.6233
38	993.0	0.6780	0.6260
40	992.2	0.6527	0.6286
42	991.4	0.6289	0.6311
44	990.6	0.6065	0.6335
46	989.8	0.5853	0.6359
48	988.9	0.5654	0.6382
50	988.0	0.5465	0.6405
52	987.1	0.5286	0.6426
54	986.2	0.5117	0.6448
56	985.2	0.4957	0.6468
58	984.2	0.4805	0.6488
60	983.2	0.4660	0.6508
62	982.2	0.4523	0.6526
64	981.1	0.4392	0.6545
66	980.0	0.4267	0.6562
68	978.9	0.4149	0.6579
70	977.8	0.4035	0.6596
72	976.6	0.3927	0.6612
74	975.4	0.3824	0.6627

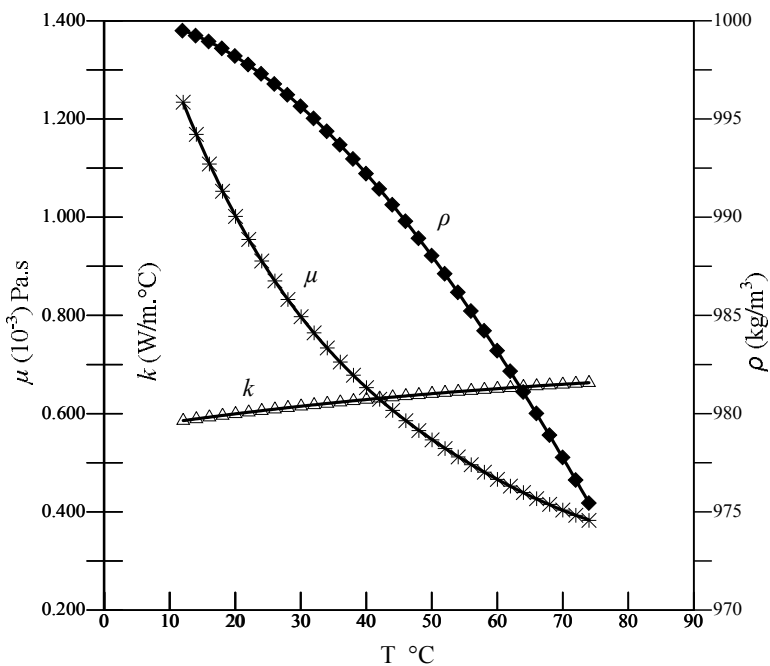


**Figure A-1:** Physical properties of liquid water.

These properties are correlated in three polynomials (as functions of temperature) to make them easy to be used in computer programs as below:

$$\rho = 1000.1 + 0.02215T - 0.00627T^2 + 0.00002T^3 \quad \dots (\text{A-1})$$

$$\mu = (1777.2 - 58.616T + 1.3358T^2 - 0.02068T^3 + 0.00019T^4) \times 10^{-6} \quad \dots (\text{A-2})$$

$$k = 0.56837 + 0.00211T - 1.11452 \times 10^{-5}T^2 + 1.9724 \times 10^{-8}T^3 \quad \dots (\text{A-3})$$

where T in degree centigrade. In addition, the heat capacity, Cp is fixed at a value of 4.184 kJ/kg.K and 4.182 kJ/kg.K for hot and cold water, respectively, because the change in the heat capacity values is very slight through the range of temperatures, adopted.

## Appendix B: Calibration of Measurement Instrumentations

### B.1 Calibration of Thermocouples and Temperature Reader

The four thermocouples together with the temperature reader device are calibrated by using a mercury thermometer. Calibration results are fixed in table B-1

**Table B-1:** Calibration of Thermocouples.

T <sub>real</sub> °C	T <sub>h1</sub> °C	T <sub>h2</sub> °C	T <sub>c1</sub> °C	T <sub>c2</sub> °C
17.5	16.77	16.85	16.70	16.63
19.0	18.23	18.39	18.52	18.44
21.0	20.36	20.65	20.57	20.45
22.5	21.80	21.99	22.08	21.56
24.0	23.45	23.53	23.64	23.47
25.0	24.40	24.25	24.66	24.48
27.0	26.49	26.61	26.50	26.79
29.5	29.04	29.17	29.47	29.01
31.0	30.50	30.91	30.97	30.52
33.0	32.69	32.77	32.85	32.53
34.5	34.10	34.31	34.38	34.15
35.5	35.23	35.04	35.01	35.05
37.0	36.70	36.88	36.94	36.56
39.0	38.82	38.93	38.99	38.58
41.0	40.80	40.78	41.33	40.59
43.0	42.91	43.04	43.08	42.44
45.0	44.80	45.49	45.20	44.62
47.5	47.59	47.66	47.68	47.14
49.0	49.23	49.21	49.22	48.65
51.0	51.09	51.05	51.06	50.21
53.0	53.14	53.30	53.31	52.67
55.0	55.19	55.36	55.36	54.69
57.5	57.71	58.00	57.41	57.21
59.0	59.51	59.46	59.45	58.70
60.5	60.90	61.01	60.98	60.23
63.0	63.46	63.30	63.52	62.75
65.0	65.31	65.63	65.59	65.00
66.5	66.99	67.17	67.32	66.27
68.0	68.53	69.11	68.89	67.78
70.0	70.70	70.76	70.70	69.49
72.0	72.60	72.52	72.35	71.81
75.0	75.71	75.89	75.60	74.83

Values of the four thermocouples are so close that they cannot be distinguished if plotted. Correlating the values above gives calibration curves (straight lines)

$$T_{h1} = 0.9744T_{h1,real} + 1.2018 \quad \dots (B.1)$$

$$T_{h2} = 0.9740T_{h2,real} + 1.0910 \quad \dots (B.2)$$

$$T_{c1} = 0.9779T_{c1,real} + 0.9035 \quad \dots (B.3)$$

$$T_{c2} = 0.9924T_{c2,real} + 0.7511 \quad \dots (B.4)$$

## B.2 Calibration of Rotameter

The rotameter is calibrated manually by using a graduated container of 100 liter volume and a stop watch at four temperatures (20, 40, 60 and 70 °C). The results of the calibration process are fixed in table B-2 and plotted in fig. B-1.

**Table B-2:** Calibration of the Rotameter at 20, 40, 60 and 70 °C.

$Q_{\text{meas.}}$ (m <sup>3</sup> /hr)	$Q_{\text{obs.}}$ (m <sup>3</sup> /hr)			
	20 °C	40 °C	60 °C	70 °C
0.20	0.169	0.196	0.209	0.211
0.30	0.264	0.291	0.307	0.308
0.40	0.359	0.394	0.413	0.411
0.50	0.451	0.489	0.513	0.511
0.60	0.551	0.593	0.608	0.617
0.70	0.642	0.691	0.725	0.724
0.80	0.762	0.802	0.837	0.842
0.90	0.846	0.884	0.932	0.936
1.00	0.944	0.991	1.039	1.041
1.10	1.046	1.095	1.146	1.146
1.20	1.139	1.185	1.240	1.255
1.30	1.231	1.291	1.347	1.350

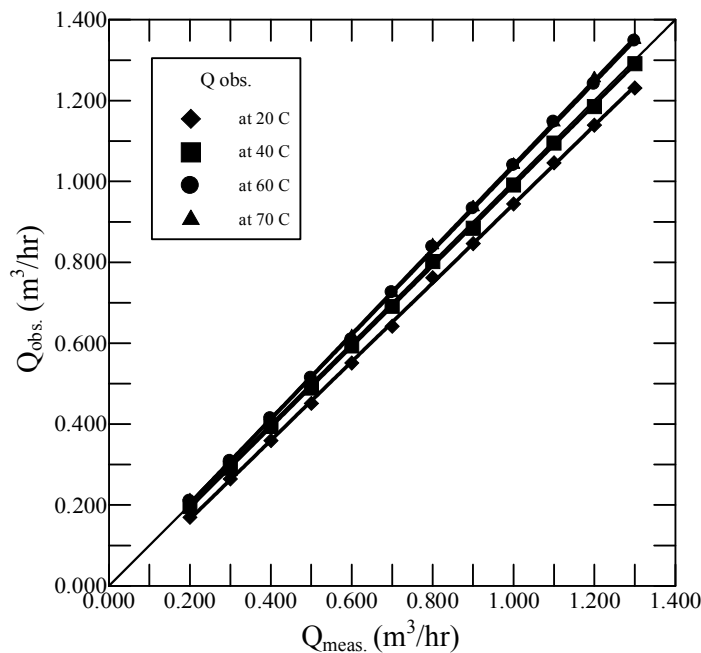


**Figure B-1:** Calibration of the rotameter at 20, 40, 60 and 70 °C.

The calibration curves of the rotameter at the four temperatures which are plotted above are

$$Q_{obs.,20C} = 0.9739Q_{meas.} - 0.0301 \quad \dots (B.5)$$

$$Q_{obs.,40C} = 0.9960Q_{meas.} - 0.0053 \quad \dots (B.6)$$

$$Q_{obs.,60C} = 1.0411Q_{meas.} - 0.0045 \quad \dots (B.7)$$

$$Q_{obs.,70C} = 1.0468Q_{meas.} - 0.0057 \quad \dots (B.8)$$

where Q is in m<sup>3</sup>/hr. Equations above are used to correct the values of the volumetric flowrates taken from the rotameter.

### B.3 Design and Calibration of the Orifice Plate

An orifice plate is designed as in fig. B-2. The inner diameter of the connecting pipe ( $D_1$ ) is 16 mm and the plate perforation ( $D_0$ ) is 6 mm diameter. To avoid manufacture defaults, actual values of volumetric flowrates are intended to be considered in graduating the mercury manometer and finding an equation for the water manometer to be used in the computer program, so values of an actual calibration are used to produce these equations (volumetric flowrate as a function of pressure drop in mmHg and mmH<sub>2</sub>O respectively). The calibration values at 60 and 70 °C are listed in table B-3 and plotted in fig. B-3. The equations produced via curve fitting are

$$Q_{obs.,60C} = 0.0233 / (\Delta p_{H_2O})^{0.4801} \quad \dots (B.9)$$

$$Q_{obs.,60C} = 0.0764 / (\Delta p_{Hg})^{0.4996} \quad \dots (B.10)$$

$$Q_{obs.,70C} = 0.0206 / (\Delta p_{H_2O})^{0.5062} \quad \dots (B.11)$$

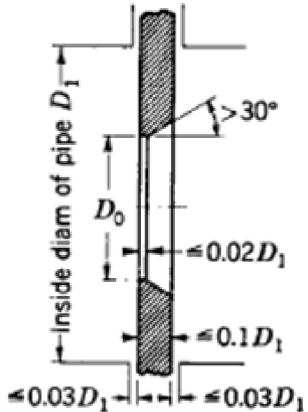


**Figure B-2:** An orifice plate design [37].

$$Q_{obs,70C} = 0.0720 / (\Delta p_{Hg})^{0.5093} \quad \dots (B.12)$$

Equations (B.10) and (B.12) are used to graduate the mercury manometer, while equations (B.9) and (B.11) are used to determine the flowrate by using the computer program.

**Table B-3:** Calibration of the Orifice Plate at 60 and 70 °C.

60 °C			70 °C		
$Q_{obs.}$ ( $\text{m}^3/\text{hr}$ )	$\Delta p$ (mmH <sub>2</sub> O)	$\Delta p$ (mmHg)	$Q_{obs.}$ ( $\text{m}^3/\text{hr}$ )	$\Delta p$ (mmH <sub>2</sub> O)	$\Delta p$ (mmHg)
0.11	26	1.9	0.0833	16	1.25
0.14	37	3	0.1134	29	2.50
0.165	63	5	0.1325	39	3.25
0.186	83	6.3	0.1600	57	5.00
0.226	120	10	0.2037	92	8.25
0.272	163	13.5	0.3084	210	17.5
0.308	203	16.5	0.4130	375	31.0
0.412	---	28.5	0.5177	---	46.5
0.516	---	44	0.6224	---	67.5
0.62	---	62	0.7270	---	93.0
0.724	---	87.5	0.8318	---	123.5
0.828	---	119	---	---	---

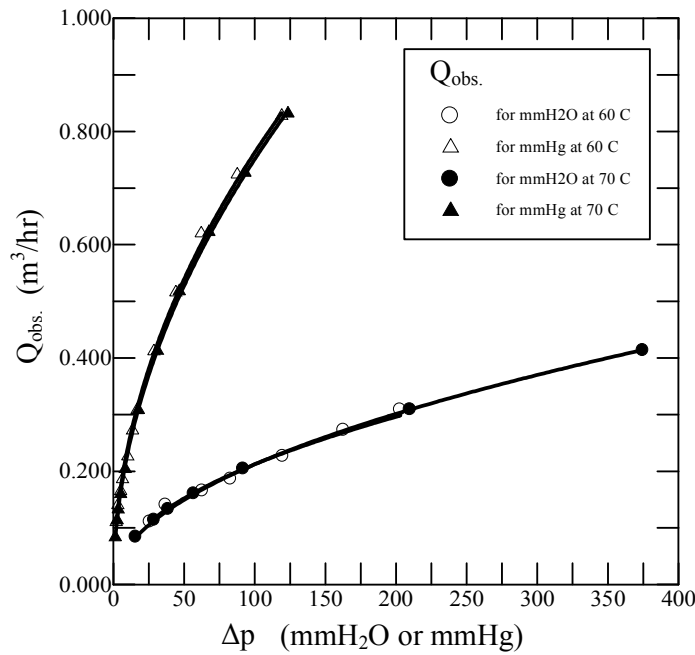


**Figure B-3:** Calibration of the orifice at 60 and 70 °C.

## **Appendix C: Experimental and Predicted Results.**

This part includes the experimental and predicted results, either plotted or used to complete calculations. To recognize the plotted values, they are written in *Italic*.

For place saving, only some of the tables (C-1, C-2, C-19, C-20, C-37, C-41 and C-42) are presented in printed matter. The others are included in a CD-ROM on the back cover of the thesis.

**Table C-1:** Experimental Results of Tube-Side Heat Transfer Enhancement for Two Sizes of Inner Tube (Enhancement Status: Smooth Tube).

Re Inner tube	Q <sub>h</sub> 10 <sup>-4</sup> (m <sup>3</sup> /s)	Temperatures and Temperature Difference (°C)					Pressure Drop					Heat Transfer Rate (W)							
		T <sub>h1</sub>	T <sub>h2</sub>	T <sub>c1</sub>	T <sub>c2</sub>	LMTD	Inner tube		Annulus		q <sub>h</sub>	q <sub>c</sub>	q <sub>avg.</sub>	Dev. %					
Inner Tube Dimensions: L=1.245 m d= 0.011 m																			
<b>Experimental Conditions:</b> Hot Water Inlet Temperature: 60 ± 0.5 °C Cold Water Mass Flowrate: 0.1 kg/s																			
5000	0.2192	60.23	50.76	22.17	20.12	34.22	12.5	122.2	8	78.34	855.732	857.31	856.521	0.18					
10000	0.4286	60.18	53.76	22.70	20.04	35.57	41.7	407.9	8	78.34	1133.75	1112.41	1123.08	1.90					
15000	0.6356	60.24	55.23	22.95	19.90	36.30	78.7	770.5	7.5	73.44	1311.47	1275.51	1293.49	2.78					
20000	0.8383	60.36	56.57	23.47	20.40	36.53	126	1233	7	68.55	1308.02	1283.87	1295.95	1.86					
25000	1.0476	60.07	56.90	23.27	19.95	36.87	176	1722	7	68.55	1367.13	1388.42	1377.78	1.55					
30000	1.2477	60.48	57.50	23.79	20.30	36.94	254	2484	7.5	73.44	1530.33	1459.52	1494.92	4.74					
35000	1.4536	60.31	57.86	23.66	20.14	37.18	322	3154	7	68.55	1465.72	1472.06	1468.89	0.43					
40000	1.6594	60.32	58.00	23.81	20.18	37.16	410	4015	7.5	73.44	1584.41	1518.07	1551.24	4.28					
<b>Experimental Conditions:</b> Hot Water Inlet Temperature: 60 ± 0.5 °C Cold Water Mass Flowrate: 0.15 kg/s																			
5000	0.2252	60.32	47.14	22.05	20.17	32.29	13	126.9	17.5	171.40	1224.92	1179.32	1202.12	3.79					
10000	0.4355	60.23	51.60	22.55	20.10	34.5	40.7	398.8	17	166.50	1549.37	1536.89	1543.13	0.81					
15000	0.6437	60.35	53.43	23.30	20.44	34.98	80.5	788.6	17	166.50	1835.35	1794.08	1814.72	2.27					
20000	0.8526	60.25	54.41	23.49	20.37	35.38	131	1278	17	166.50	2051.14	1957.18	2004.16	4.69					
25000	1.0585	60.25	55.32	23.40	20.00	36.08	193	1894	17	166.50	2149.22	2132.82	2141.02	0.77					
30000	1.2610	60.43	56.12	24.00	20.50	36.02	256	2511	17	166.50	2237.75	2195.55	2216.65	1.90					
35000	1.4663	60.42	56.58	24.13	20.40	36.23	330	3227	17	166.50	2317.98	2339.83	2328.91	0.94					
40000	1.6710	60.40	56.98	24.35	20.48	36.27	413	4043	17	166.50	2352.5	2427.65	2390.08	3.14					
<b>Experimental Conditions:</b> Hot Water Inlet Temperature: 70 ± 0.5 °C Cold Water Mass Flowrate: 0.1 kg/s																			
5000	0.1971	69.80	55.52	22.77	20.14	40.93	9.72	95.18	8	78.34	1156.07	1099.87	1127.97	4.98					
10000	0.3793	69.85	60.76	23.85	20.3	43.17	31.5	308.2	8	78.34	1414.22	1484.61	1449.42	4.86					
15000	0.5603	69.78	62.92	24.03	20.1	44.27	63.9	625.4	8	78.34	1575.67	1643.53	1609.6	4.22					
20000	0.7392	69.96	64.17	24.47	20.32	44.66	98.1	960.8	8	78.34	1753.86	1735.53	1744.7	1.05					
25000	0.9125	70.20	65.60	24.21	20.00	45.79	141	1378	7	68.55	1719.39	1760.62	1740	2.37					
30000	1.0910	70.12	66.17	24.41	20.00	45.94	193	1885	7	68.55	1764.96	1844.26	1804.61	4.39					
35000	1.2645	70.32	66.84	24.88	20.38	45.95	247	2420	7	68.55	1801.78	1881.9	1841.84	4.35					
40000	1.4454	70.16	66.98	24.71	20.30	46.06	313	3064	7	68.55	1881.96	1844.26	1863.11	2.02					
<b>Experimental Conditions:</b> Hot Water Inlet Temperature: 70 ± 0.5 °C Cold Water Mass Flowrate: 0.15 kg/s																			
5000	0.2027	69.77	51.70	22.19	19.90	39.16	10.2	99.71	18	176.3	1506.05	1436.52	1471.28	4.73					
10000	0.3881	69.77	57.68	22.95	20.02	42.07	33.3	326.3	17	166.5	1926.39	1837.99	1882.19	4.70					
15000	0.5701	70.00	60.32	23.50	20.00	43.34	62	607.3	17	166.5	2263.99	2195.55	2229.77	3.07					
20000	0.7480	70.30	62.22	23.91	20.12	44.21	101	988	17	166.5	2477.92	2377.47	2427.69	4.14					
25000	0.9299	70.14	63.12	24.45	20.33	44.22	145	1423	17	166.5	2675.87	2584.48	2630.17	3.47					
30000	1.1057	70.30	64.20	24.42	20.00	45.03	196	1922	17	166.5	2763.76	2772.67	2768.21	0.32					
35000	1.2858	70.14	64.80	24.86	20.19	44.94	255	2493	17	166.5	2813.08	2929.49	2871.29	4.05					
40000	1.4621	70.34	65.27	24.85	20.15	45.30	323	3163	17	166.5	3036.59	2948.31	2992.45	2.95					
Inner Tube Dimensions: L=1.245 m d= 0.014 m																			
<b>Experimental Conditions:</b> Hot Water Inlet Temperature: 60 ± 0.5 °C Cold Water Mass Flowrate: 0.1 kg/s																			
5000	0.2788	59.87	51.20	22.55	20.12	34.10	6.2	60.870	16	156.68	996.479	1016.23	1006.35	1.96					
10000	0.5470	59.97	53.62	23.66	20.07	34.91	18.5	181.29	16	156.68	1431.11	1501.34	1466.23	4.79					
15000	0.8098	60.10	55.23	24.22	20.17	35.47	38.9	380.70	16	156.68	1624.26	1693.71	1658.98	4.19					
20000	1.0723	60.22	56.03	24.81	20.37	35.53	62.9	616.37	15	146.89	1850.10	1856.81	1853.45	0.36					
25000	1.3295	60.50	56.85	25.00	20.41	35.97	91.6	897.37	15	146.89	1997.62	1919.54	1958.58	3.99					
30000	1.5968	60.13	57.10	25.04	20.45	35.86	126	1232.7	14	137.09	1991.79	1919.54	1955.66	3.69					
35000	1.8507	60.42	57.70	25.22	20.32	36.28	158	1550.0	14	137.09	2071.83	2049.18	2060.51	1.10					
40000	2.1142	60.30	57.88	25.32	20.38	36.23	205	2003.2	14	137.09	2105.69	2065.91	2085.80	1.91					
<b>Experimental Conditions:</b> Hot Water Inlet Temperature: 60 ± 0.5 °C Cold Water Mass Flowrate: 0.15 kg/s																			
5000	0.2816	59.86	49.91	21.64	19.78	34.01	6.48	63.450	29	283.98	1155.42	1166.78	1161.10	0.98					
10000	0.5534	59.84	52.20	22.82	19.97	34.57	18.5	181.29	29	283.98	1742.84	1787.81	1765.32	2.55					
15000	0.8177	60.37	53.66	23.65	20.22	35.05	40.7	398.83	29	283.98	2260.62	2151.64	2206.13	4.94					
20000	1.0806	60.42	54.80	24.12	20.30	35.39	63.9	625.44	29	283.98	2501.33	2396.29	2448.81	4.29					
25000	1.3461	60.26	55.42	24.10	20.02	35.78	87.9	861.11	29	283.98	2683.16	2559.38	2621.27	4.72					
30000	1.6125	60.06	55.86	24.40	20.16	35.68	129	1259.9	28	274.19	2788.86	2659.75	2724.31	4.74					
35000	1.8653	60.40	56.66	24.88	20.27	35.95	160	1568.1	28	274.19	2872.01	2891.85	2881.93	0.69					
40000	2.1300	60.30	56.87	24.95	20.37	35.92	206	2021.3	27	264.39	3007.69	2873.03	2940.36	4.58					
<b>Experimental Conditions:</b> Hot Water Inlet Temperature: 70 ± 0.5 °C Cold Water Mass Flowrate: 0.1 kg/s																			
5000	0.2469	69.95	57.53	22.93	19.97	42.11	5.09	49.854	16	156.68	1259.06	1237.87	1248.47	1.70					
10000	0.4801	70.14	61.22	24.32	20.00	43.48	13.9	135.96	15	146.89	1756.23	1806.62	1781.43	2.83					
15000	0.7107	70.21	62.95	25.00	20.11	44.01	28.7	280.99	15	146.89	2114.87	2045.00	2079.94	3.36					
20000	0.9369	70.34	64.34	25.67	20.22	44.39	50.9	498.54	15	146.89	2303.37	2279.19	2291.28	1.06					
25000	1.1673	70.14	64.98	26.00	20.33	44.39	68.5	670.76	15	146.89	2467.71	2371.19	2419.45	3.99					
30000	1.3875	70.43	65.96	26.53	20.26	44.79	93.5	915.5	15	146.89	2540.05	2622.11	2581.08	3.18					
35000	1.6149	70.35	66.36	26.14	20.11	45.22	119	1169.3	14	137.09	2638.55	2521.75	2580.15	4.53					
40000	1.8403	70.35	66.74	26.48	20.17	45.21	147	1441.2	14	137.09	2720.17	2638.84	2679.51	3.04					
<b>Experimental Conditions:</b> Hot Water Inlet Temperature: 70 ± 0.5 °C Cold Water Mass Flowrate: 0.15 kg/s																			
5000	0.2498	69.85	56.04	22.51	20.14	41.36	5.09	49.854	28	274.19	1416.84	1486.7	1451.77	4.81					
10000	0.4889	69.77	59.10																

**Table C-2:** Experimental Results of Tube-Side Heat Transfer Enhancement for Two Sizes of Inner Tube (Enhancement Status: Wire coil, e= 1 mm, p= 10 mm).

Re Inner tube	Q <sub>h</sub> 10 <sup>-4</sup> (m <sup>3</sup> /s)	Temperatures and Temperature Difference (°C)					Pressure Drop				Heat Transfer Rate (W)													
		T <sub>h1</sub>	T <sub>h2</sub>	T <sub>c1</sub>	T <sub>c2</sub>	LMTD	Inner tube		Annulus		q <sub>h</sub>	q <sub>c</sub>	q <sub>avg.</sub>	Dev. %										
							mmH <sub>2</sub> O	N/m <sup>2</sup>	mmH <sub>2</sub> O	N/m <sup>2</sup>														
Inner Tube Dimensions: L=1.245 m d= 0.011 m																								
Experimental Conditions: Hot Water Inlet Temperature: 60 ± 0.5 °C Cold Water Mass Flowrate: 0.1 kg/s																								
5000	0.2265	59.87	46.87	23.20	20.34	31.33	65.11	637.58	9.5	93.03	1215.22	1196.05	1205.64	1.59										
10000	0.4336	60.50	51.92	23.90	20.34	34.03	226.4	2216.9	9	88.13	1533.28	1488.79	1511.04	2.94										
15000	0.6432	60.05	53.84	23.99	20.34	34.76	483.1	4730.5	9	88.13	1645.63	1526.43	1586.03	7.52										
20000	0.8503	60.13	54.90	24.37	20.18	35.24	826	8088.5	9.5	93.03	1831.64	1752.26	1791.95	4.43										
25000	1.0512	60.32	56.18	24.29	20.19	36.01	1241	12156	9	88.13	1791.93	1714.62	1753.27	4.41										
30000	1.2526	60.50	56.95	24.33	20.16	36.48	1738	17023	9	88.13	1830.46	1743.89	1787.18	4.84										
35000	1.4580	60.43	57.33	24.65	20.35	36.38	2315	22670	9	88.13	1860.41	1798.26	1829.34	3.4										
40000	1.6619	60.46	57.66	24.54	20.14	36.71	3004	29414	9	88.13	1915.14	1840.08	1877.61	4.00										
Experimental Conditions: Hot Water Inlet Temperature: 60 ± 0.5 °C Cold Water Mass Flowrate: 0.15 kg/s																								
5000	0.2310	60.23	44.00	22.60	20.11	30.24	66.65	652.63	18	176.3	1548.41	1561.98	1555.19	0.87										
10000	0.4437	60.27	49.12	23.30	20.19	32.79	245.3	2402	18	176.3	2040.79	1950.90	1995.84	4.50										
15000	0.6526	60.25	51.72	23.80	20.15	33.95	493.4	4831.3	18	176.3	2294.61	2289.65	2292.13	0.22										
20000	0.8599	60.18	53.35	24.15	20.21	34.56	840.5	8230.4	18	176.3	2420.02	2471.56	2445.79	2.11										
25000	1.0655	60.25	54.45	24.20	20.29	35.10	1267	12409	17.5	171.4	2545.58	2452.74	2499.16	3.71										
30000	1.2705	60.24	55.31	24.40	20.19	35.48	1786	17485	17.5	171.4	2577.45	2640.93	2609.19	2.43										
35000	1.4736	60.33	56.00	24.70	20.50	35.56	2374	23250	17	166.5	2627.27	2634.66	2630.96	0.28										
40000	1.6820	60.25	56.25	24.60	20.23	35.83	3063	29994	17.5	171.4	2769.75	2741.30	2755.52	1.03										
Experimental Conditions: Hot Water Inlet Temperature: 70 ± 0.5 °C Cold Water Mass Flowrate: 0.1 kg/s																								
5000	0.2022	70.00	51.79	23.80	20.32	38.36	52.76	516.67	9	88.13	1514.04	1455.34	1484.69	3.95										
10000	0.3845	70.13	58.61	24.97	20.50	41.54	183.3	1794.7	9	88.13	1817.80	1869.35	1843.58	2.80										
15000	0.5637	70.42	61.45	25.00	20.41	43.19	367.5	3598.5	9	88.13	2073.39	1919.54	1996.46	7.71										
20000	0.7401	70.44	63.53	25.26	20.38	44.16	626.7	6136.5	8.5	83.24	2095.70	2040.82	2068.26	2.65										
25000	0.9190	70.50	64.35	25.50	20.23	44.56	948.8	9290.9	9	88.13	2315.75	2203.91	2259.83	4.95										
30000	1.0989	70.18	65.15	25.69	20.37	44.64	1340	13125	9	88.13	2264.39	2225.66	2245.02	1.73										
35000	1.2744	70.23	65.90	25.65	20.40	45.04	1782	17449	8.5	83.24	2260.04	2195.55	2227.79	2.89										
40000	1.4488	70.33	66.50	25.75	20.37	45.35	2283	22353	8.5	83.24	2272.16	2248.84	2260.50	1.03										
Experimental Conditions: Hot Water Inlet Temperature: 70 ± 0.5 °C Cold Water Mass Flowrate: 0.15 kg/s																								
5000	0.2079	70.23	47.81	22.88	19.95	36.75	56.46	552.92	17	166.5	1918.02	1837.99	1878.01	4.26										
10000	0.3943	70.33	54.95	24.05	20.23	40.22	187.9	1840.1	18	176.3	2491.00	2396.29	2443.64	3.88										
15000	0.5775	70.30	58.25	24.55	20.00	41.89	381.4	3734.5	18	176.3	2856.24	2854.22	2855.23	0.07										
20000	0.7597	70.16	60.25	24.75	19.97	42.79	659.1	6453.8	18	176.3	3088.27	2998.49	3043.38	2.95										
25000	0.9384	70.41	61.62	25.48	20.24	43.13	982.1	9617.2	17.5	171.4	3382.18	3287.05	3334.62	2.85										
30000	1.1163	70.10	63.11	25.14	19.90	44.08	1375	13461	17.5	171.4	3198.55	3287.05	3242.80	2.73										
35000	1.2919	70.30	64.00	25.45	20.22	44.31	1834	17956	17	166.5	3335.24	3280.78	3308.01	1.65										
40000	1.4693	70.24	64.72	25.65	20.31	44.50	2337	22887	17	166.5	3322.81	3349.78	3336.30	0.81										
Inner Tube Dimensions: L=1.245 m d= 0.014 m																								
Experimental Conditions: Hot Water Inlet Temperature: 60 ± 0.5 °C Cold Water Mass Flowrate: 0.1 kg/s																								
5000	0.2881	59.70	47.11	23.34	19.90	31.56	29.6	289.9	14	137.1	1497.02	1438.61	1467.81	3.98										
10000	0.5519	60.14	52.26	23.96	19.73	34.32	97.2	951.8	14	137.1	1792.52	1768.99	1780.75	1.32										
15000	0.8170	60.00	54.14	24.45	19.73	34.98	215	2103	14	137.1	1972.56	1973.9	1973.23	0.07										
20000	1.0765	60.25	55.48	24.94	20.00	35.39	367	3589	14	137.1	2114.66	2065.91	2090.29	2.33										
25000	1.3382	60.21	56.26	24.92	19.82	35.86	562	5502	13.5	132.2	2176.47	2132.82	2154.65	2.03										
30000	1.6005	60.17	56.75	25.61	20.32	35.49	782	7659	14	137.1	2253.51	2212.28	2232.9	1.85										
35000	1.8509	60.5	57.61	25.61	20.3	36.09	1038	10161	13	127.3	2201.49	2220.64	2211.07	0.87										
40000	2.1171	60.27	57.72	25.63	20.24	36.04	1342	13143	13	127.3	2222.03	2254.1	2238.06	1.43										
Experimental Conditions: Hot Water Inlet Temperature: 60 ± 0.5 °C Cold Water Mass Flowrate: 0.15 kg/s																								
5000	0.2923	59.85	45.10	22.77	19.95	30.73	29.6	290.1	27	264.4	1780.50	1768.99	1774.74	0.65										
10000	0.5608	60.21	50.10	23.80	19.90	33.21	103	1006	27	264.4	2337.97	2446.47	2392.22	4.54										
15000	0.8282	60.12	52.22	24.32	19.95	34.00	222	2175	27	264.4	2696.88	2741.3	2719.09	1.63										
20000	1.0901	60.25	53.81	24.67	19.95	34.71	373	3653	26.5	259.5	2892.19	2960.86	2926.53	2.35										
25000	1.3528	60.25	54.77	25.10	20.00	34.96	569	5575	26	254.6	3053.50	3199.23	3126.36	4.66										
30000	1.6091	60.45	55.75	25.42	20.37	35.20	787	7705	25	244.8	3114.14	3167.87	3141.00	1.71										
35000	1.8717	60.31	56.29	25.64	20.45	35.25	1060	10379	25	244.8	3097.96	3255.69	3176.82	4.96										
40000	2.1345	60.34	56.55	25.41	20.24	35.62	1375	13461	25	244.8	3330.52	3243.14	3286.83	2.66										
Experimental Conditions: Hot Water Inlet Temperature: 70 ± 0.5 °C Cold Water Mass Flowrate: 0.1 kg/s																								
5000	0.2555	69.85	52.95	23.96	19.90	39.12	23.1	226.6	14	137.1	1774.74	1697.89	1736.31	4.43										
10000	0.4903	69.75	58.73	24.95	19.87	41.76	78.7	770.5	14	137.1	2217.50	2124.46	2170.98	4.29										
15000	0.7192	69.98	61.55	25.80	19.87	42.92	167	1632	14	137.1	2486.42	2479.93	2483.17	0.26										
20000	0.9429	70.32	63.51	26.43	20.12	43.64	282	2765	14	137.1	2631.49	2638.84	2635.17	0.28										
25000	1.1673	70.50	64.62	26.45	19.96	44.35	424	4151	14	137.1	2812.04	2714.12	2763.08	3.54										
30000	1.3962	70.21	65.35	26.27	19.90	44.69	592	5801	13	127.3	2779.58	2663.93	2721.76	4.25										
35000	1.6219	70.13	66.00	26.84	20.13	44.57	794	7777	13	127.3	2743.55	2806.12	2774.84	2.26										
40000	1.8474	70.13	66.45	27.15	20.19	44.60	10																	

**Table C-3:** Experimental Results of Tube-Side Heat Transfer Enhancement for Two Sizes of Inner Tube (Enhancement Status: Wire Coil,  $e=1$  mm,  $p=20$  mm).

Re Inner tube	$Q_h \cdot 10^{-4}$ ( $\text{m}^3/\text{s}$ )	Temperatures and Temperature Difference ( $^\circ\text{C}$ )					Pressure Drop				Heat Transfer Rate (W)													
		T <sub>h1</sub>	T <sub>h2</sub>	T <sub>c1</sub>	T <sub>c2</sub>	LMTD	Inner tube		Annulus		q <sub>h</sub>	q <sub>c</sub>	q <sub>avg.</sub>	Err. %										
							mmH <sub>2</sub> O	N/m <sup>2</sup>	mmH <sub>2</sub> O	N/m <sup>2</sup>														
Inner Tube Dimensions: L=1.245 m d= 0.011 m																								
Experimental Conditions: Hot Water Inlet Temperature: $60 \pm 0.5^\circ\text{C}$ Cold Water Mass Flowrate: 0.1 kg/s																								
5000	0.2258	60.00	47.11	22.74	19.97	31.93	39.09	382.78	9	88.13	1201.35	1158.41	1179.88	3.64										
10000	0.4349	60.06	51.97	23.70	20.32	33.95	129.6	1269	9	88.13	1450.15	1413.52	1431.83	2.56										
15000	0.6394	60.11	54.56	23.69	20.33	35.31	278.6	2728.4	8.5	83.24	1461.85	1405.15	1433.50	3.96										
20000	0.8480	60.07	55.31	24.05	20.22	35.55	473.9	4640.9	9	88.13	1662.53	1601.71	1632.12	3.73										
25000	1.0500	60.28	56.38	24.12	19.90	36.32	710.9	6961.4	9	88.13	1685.97	1764.80	1725.39	4.57										
30000	1.2577	60.16	56.74	24.29	20.05	36.28	985.8	9653.5	9	88.13	1770.89	1773.17	1772.03	0.13										
35000	1.4576	60.39	57.41	24.44	20.31	36.52	1321	12935	8.5	83.24	1787.85	1727.17	1757.51	3.45										
40000	1.6689	60.08	57.47	24.21	20.11	36.61	1707	16715	8.5	83.24	1792.99	1714.62	1753.81	4.47										
Experimental Conditions: Hot Water Inlet Temperature: $60 \pm 0.5^\circ\text{C}$ Cold Water Mass Flowrate: 0.15 kg/s																								
5000	0.2296	60.50	44.51	22.54	20.00	30.75	41.65	407.89	18	176.3	1515.83	1593.34	1554.59	4.99										
10000	0.4420	60.34	49.55	23.22	20.05	33.16	138.8	1359.6	17.5	171.4	1967.07	1988.54	1977.80	1.09										
15000	0.6476	60.24	52.75	23.47	20.14	34.65	291.6	2855.3	17	166.5	1998.81	2088.91	2043.86	4.41										
20000	0.8553	60.42	53.82	23.85	19.96	35.20	488.7	4786	18	176.3	2325.64	2440.20	2382.92	4.81										
25000	1.0610	60.43	54.83	24.10	20.03	35.56	732.2	7169.9	17.5	171.4	2447.16	2553.11	2500.14	4.24										
30000	1.2698	60.20	55.42	23.87	19.85	35.95	1009	9880.1	17.5	171.4	2499.63	2521.75	2510.69	0.88										
35000	1.4708	60.47	56.11	24.20	20.00	36.19	1351	13234	17.5	171.4	2640.39	2634.66	2637.52	0.22										
40000	1.6735	60.50	56.68	24.29	19.90	36.49	1732	16959	17.5	171.4	2631.68	2753.85	2692.77	4.54										
Experimental Conditions: Hot Water Inlet Temperature: $70 \pm 0.5^\circ\text{C}$ Cold Water Mass Flowrate: 0.1 kg/s																								
5000	0.2006	70.22	52.64	23.72	20.41	38.93	29.62	290.06	8.5	83.24	1449.89	1384.24	1417.06	4.63										
10000	0.3838	70.07	58.92	24.31	20.20	42.14	103.7	1015.2	9	88.13	1756.10	1718.80	1737.45	2.15										
15000	0.5620	70.30	61.98	24.51	20.05	43.83	218.5	2139.2	8.5	83.24	1917.15	1865.17	1891.16	2.75										
20000	0.7398	70.40	63.62	25.04	19.95	44.51	359.2	3517	9	88.13	2055.49	2128.64	2092.06	3.50										
25000	0.9173	70.38	64.72	25.33	20.23	44.77	539.7	5284.5	9	88.13	2127.12	2132.82	2129.97	0.27										
30000	1.0959	70.19	65.51	25.42	20.31	44.98	749.8	7342.1	8.5	83.24	2100.78	2137.00	2118.89	1.71										
35000	1.2737	70.20	66.00	25.51	20.33	45.18	1004	9834.8	8.5	83.24	2190.99	2166.28	2178.63	1.13										
40000	1.4472	70.31	66.66	25.63	20.10	45.61	1279	12527	8.5	83.24	2163.00	2312.65	2237.82	6.69										
Experimental Conditions: Hot Water Inlet Temperature: $70 \pm 0.5^\circ\text{C}$ Cold Water Mass Flowrate: 0.15 kg/s																								
5000	0.2069	70.23	48.46	22.81	20.00	37.14	33.32	326.32	17	166.5	1853.19	1762.71	1807.95	5.00										
10000	0.3932	70.22	55.44	23.89	20.13	40.57	111.1	1087.7	18	176.3	2386.98	2358.65	2372.82	1.19										
15000	0.5755	70.23	58.81	24.21	20.05	42.29	226.8	2220.8	17.5	171.4	2696.92	2609.57	2653.24	3.29										
20000	0.7587	70.10	60.49	24.61	20.07	42.91	376.7	3689.2	18	176.3	2990.70	2847.94	2919.32	4.89										
25000	0.9333	70.23	62.54	25.02	20.11	43.81	557.2	5456.7	17	166.5	2942.27	3080.04	3011.16	4.58										
30000	1.1141	70.15	63.33	24.95	20.04	44.24	785	7686.5	17	166.5	3114.31	3080.04	3097.18	1.11										
35000	1.2900	70.20	64.30	25.32	20.11	44.53	1032	10107	17	166.5	3118.67	3268.23	3193.45	4.68										
40000	1.4621	70.50	65.11	25.50	20.19	44.96	1324	12962	17	166.5	3228.24	3330.96	3279.60	3.13										
Inner Tube Dimensions: L=1.245 m d= 0.014 m																								
Experimental Conditions: Hot Water Inlet Temperature: $60 \pm 0.5^\circ\text{C}$ Cold Water Mass Flowrate: 0.1 kg/s																								
5000	0.2859	59.87	47.93	23.10	19.83	32.24	19.55	191.45	14	137.1	1408.47	1367.51	1387.99	2.95										
10000	0.5529	59.87	52.30	23.90	19.75	34.23	65.72	643.57	14	137.1	1725.11	1735.53	1730.32	0.60										
15000	0.8151	60.13	54.32	24.50	20.05	34.95	141.6	1386.8	14.5	142	1951.03	1860.99	1906.01	4.72										
20000	1.0760	60.21	55.58	24.81	20.14	35.42	238.8	2338.6	14	137.1	2051.65	1952.99	2002.32	4.93										
25000	1.3359	60.31	56.39	25.22	20.22	35.63	360.1	3526	14	137.1	2156.12	2091.00	2123.56	3.07										
30000	1.5981	60.14	56.98	25.31	20.22	35.79	505.4	4949.1	13	127.3	2079.00	2128.64	2103.82	2.36										
35000	1.8537	60.35	57.55	25.55	20.43	35.95	669.2	6553.5	13	127.3	2136.36	2141.18	2138.77	0.23										
40000	2.1136	60.36	57.86	25.56	20.38	36.12	865.5	8475.1	13	127.3	2174.63	2166.28	2170.45	0.38										
Experimental Conditions: Hot Water Inlet Temperature: $60 \pm 0.5^\circ\text{C}$ Cold Water Mass Flowrate: 0.15 kg/s																								
5000	0.2922	59.75	45.25	22.60	19.67	31.01	20.36	199.42	28	274.2	1749.61	1837.99	1793.80	4.93										
10000	0.5581	60.50	50.44	23.91	20.12	33.36	68.5	670.76	28	274.2	2314.85	2377.47	2346.16	2.67										
15000	0.8265	60.24	52.38	24.21	19.97	34.19	148.1	1450.3	28	274.2	2677.34	2659.75	2668.55	0.66										
20000	1.0921	60.15	53.66	24.60	20.03	34.58	245.3	2402	27	264.4	2920.32	2866.76	2893.54	1.85										
25000	1.3515	60.20	54.95	24.86	20.38	34.95	367.5	3598.5	26	254.6	2922.40	2810.30	2866.35	3.91										
30000	1.6090	60.34	55.87	25.12	20.20	35.44	506.3	4958.2	26	254.6	2961.52	3086.32	3023.92	4.13										
35000	1.8720	60.27	56.31	25.51	20.41	35.33	682.2	6680.4	26	254.6	3052.19	3199.23	3125.71	4.70										
40000	2.1334	60.29	56.67	25.22	20.13	35.80	873.8	8556.7	25	244.8	3179.42	3192.96	3186.19	0.42										
Experimental Conditions: Hot Water Inlet Temperature: $70 \pm 0.5^\circ\text{C}$ Cold Water Mass Flowrate: 0.1 kg/s																								
5000	0.2538	69.71	53.98	23.97	20.13	39.50	13.88	135.96	14	137.1	1640.81	1605.89	1623.35	2.15										
10000	0.4889	69.85	59.00	25.18	20.22	41.66	50.91	498.54	14	137.1	2177.20	2074.27	2125.74	4.84										
15000	0.7181	70.00	61.74	25.53	19.95	43.12	105.5	1033.3	14	137.1	2432.39	2333.56	2382.97	4.15										
20000	0.9422	70.24	63.69	26.10	20.34	43.74	179.6	1758.5	13	127.3	2529.08	2408.83	2468.96	4.87										
25000	1.1682	70.31	64.71	26.41	20.26	44.17	272.1	2664.9	13.5	132.2	2680.21	2571.93	2626.07	4.12										
30000	1.3935	70.20	65.62	26.65	20.31	44.42	381.4	3734.5	13	127.3	2614.15	2651.39	2632.77	1.41										
35000	1.6155	70.34	66.32																					

**Table C-4:** Experimental Results of Tube-Side Heat Transfer Enhancement for Two Sizes of Inner Tube (Enhancement Status: Wire Coil, e= 1 mm, p= 30 mm).

Re Inner tube	Q <sub>h</sub> 10 <sup>-4</sup> (m <sup>3</sup> /s)	Temperatures and Temperature Difference (°C)					Pressure Drop				Heat Transfer Rate (W)													
		T <sub>h1</sub>	T <sub>h2</sub>	T <sub>c1</sub>	T <sub>c2</sub>	LMTD	Inner tube		Annulus		q <sub>h</sub>	q <sub>c</sub>	q <sub>avg.</sub>	Dev. %										
							mmH <sub>2</sub> O	N/m <sup>2</sup>	mmH <sub>2</sub> O	N/m <sup>2</sup>														
Inner Tube Dimensions: L=1.245 m d= 0.011 m																								
Experimental Conditions: Hot Water Inlet Temperature: 60 ± 0.5 °C Cold Water Mass Flowrate: 0.1 kg/s																								
5000	0.2229	60.10	48.70	22.31	19.82	33.14	26.8	262.4	8	78.34	1048.19	1041.32	1044.75	0.66										
10000	0.4313	60.11	53.00	23.11	19.95	34.99	86.09	842.98	8	78.34	1263.75	1321.51	1292.63	4.47										
15000	0.6416	60.00	54.22	23.58	19.75	35.44	186.1	1821.9	8.5	83.24	1527.76	1601.71	1564.73	4.73										
20000	0.8446	60.12	55.80	23.50	19.90	36.26	309.2	3027.5	8	78.34	1502.57	1505.52	1504.04	0.20										
25000	1.0499	60.17	56.50	23.80	20.15	36.36	461.9	4523.1	8	78.34	1586.42	1526.43	1556.43	3.85										
30000	1.2572	60.05	56.91	24.05	20.12	36.39	637.8	6245.3	8.5	83.24	1625.16	1643.53	1634.34	1.12										
35000	1.4582	60.21	57.53	24.21	20.21	36.66	845.1	8275.7	8	78.34	1608.60	1672.80	1640.70	3.91										
40000	1.6724	59.84	57.43	24.02	20.04	36.60	1089	10660	8	78.34	1659.16	1664.44	1661.80	0.32										
Experimental Conditions: Hot Water Inlet Temperature: 60 ± 0.5 °C Cold Water Mass Flowrate: 0.15 kg/s																								
5000	0.2281	60.41	45.40	22.49	20.32	31.06	29.62	290.06	18	176.3	1413.71	1361.24	1387.47	3.78										
10000	0.4396	60.32	50.30	23.01	20.25	33.55	94.42	924.56	18	176.3	1816.16	1731.35	1773.75	4.78										
15000	0.6473	60.31	52.74	23.45	20.17	34.67	190.7	1867.3	18	176.3	2019.21	2057.54	2038.38	1.88										
20000	0.8567	60.31	53.71	23.76	20.22	35.00	319.3	3127.2	17	166.5	2329.62	2220.64	2275.13	4.79										
25000	1.0600	60.43	54.96	24.00	20.21	35.58	476.7	4668.1	17.5	171.4	2387.95	2377.47	2382.71	0.44										
30000	1.2708	59.90	55.61	23.86	20.10	35.77	659.1	6453.8	17	166.5	2245.30	2358.65	2301.97	4.92										
35000	1.4699	60.34	56.33	24.42	20.36	35.94	860.9	8429.8	17	166.5	2426.75	2546.84	2486.79	4.83										
40000	1.6761	60.30	56.67	24.39	20.23	36.17	1096	10732	17	166.5	2504.83	2609.57	2557.20	4.10										
Experimental Conditions: Hot Water Inlet Temperature: 70 ± 0.5 °C Cold Water Mass Flowrate: 0.1 kg/s																								
5000	0.1997	70.10	53.42	23.13	19.77	39.94	20.36	199.42	9	88.13	1368.82	1405.15	1386.99	2.62										
10000	0.3809	70.34	59.68	24.06	20.27	42.75	68.5	670.76	8	78.34	1665.91	1584.98	1625.44	4.98										
15000	0.5605	70.38	62.26	24.38	20.13	44.04	140.7	1377.8	8.5	83.24	1865.93	1777.35	1821.64	4.86										
20000	0.7390	70.24	63.93	24.95	20.19	44.51	235.1	2302.3	8.5	83.24	1910.79	1990.63	1950.71	4.09										
25000	0.9157	70.34	65.00	24.76	19.95	45.31	349.9	3426.3	8	78.34	2003.13	2011.54	2007.34	0.42										
30000	1.0907	70.50	65.83	25.21	20.38	45.37	482.3	4722.5	8	78.34	2086.02	2019.91	2052.97	3.22										
35000	1.2694	70.34	66.31	25.43	20.19	45.51	638.7	6254.4	8.5	83.24	2094.92	2191.37	2143.14	4.50										
40000	1.4489	70.22	66.60	25.12	20.13	45.78	823.8	8067.2	8	78.34	2147.75	2086.82	2117.28	2.88										
Experimental Conditions: Hot Water Inlet Temperature: 70 ± 0.5 °C Cold Water Mass Flowrate: 0.15 kg/s																								
5000	0.2058	69.95	49.44	22.52	19.66	37.92	22.22	217.54	18	176.3	1736.63	1794.08	1765.36	3.25										
10000	0.3925	69.90	56.00	23.47	20.04	40.97	74.98	734.21	17	166.5	2240.81	2151.64	2196.22	4.06										
15000	0.5744	69.98	59.31	23.86	20.04	42.60	148.1	1450.3	17	166.5	2515.05	2396.29	2455.67	4.84										
20000	0.7552	70.23	60.98	24.48	19.92	43.36	249.9	2447.4	18	176.3	2865.15	2860.49	2862.82	0.16										
25000	0.9321	70.22	62.73	24.96	20.25	43.86	361.9	3544.2	17	166.5	2861.81	2954.58	2908.20	3.19										
30000	1.1116	70.12	63.66	24.73	19.88	44.58	505.4	4949.1	17	166.5	2943.13	3042.41	2992.77	3.32										
35000	1.2904	70.12	64.34	25.10	20.19	44.58	659.1	6453.8	17	166.5	3056.18	3080.04	3068.11	0.78										
40000	1.4631	70.42	65.10	25.54	20.34	44.82	846	8284.8	17	166.5	3188.55	3261.96	3225.25	2.28										
Inner Tube Dimensions: L=1.245 m d= 0.014 m																								
Experimental Conditions: Hot Water Inlet Temperature: 60 ± 0.5 °C Cold Water Mass Flowrate: 0.1 kg/s																								
5000	0.2855	59.78	48.19	23.00	19.86	32.37	14.02	137.3	15	146.9	1365.32	1313.15	1339.24	3.90										
10000	0.5519	59.95	52.44	23.82	19.93	34.29	47.21	462.3	14.5	142	1708.49	1626.8	1667.64	4.90										
15000	0.8158	59.93	54.41	24.40	19.95	34.99	101.8	97.1	14.5	142	1855.23	1860.99	1858.11	0.31										
20000	1.0785	59.87	55.61	24.83	20.1	35.27	164.8	1613	14	137.1	1892.22	1978.09	1935.15	4.44										
25000	1.3363	60.22	56.44	25.00	20.14	35.76	242.5	2375	14	137.1	2079.76	2032.45	2056.11	2.30										
30000	1.6000	60.10	56.86	24.40	19.18	36.68	344.3	3372	14	137.1	2134.25	2183.00	2158.63	2.26										
35000	1.8588	60.11	57.42	25.42	20.31	35.89	454.5	4451	13	127.3	2058.26	2137.00	2097.63	3.75										
40000	2.1200	60.11	57.70	25.42	20.15	36.10	580.4	5683	13	127.3	2102.93	2203.91	2153.42	4.69										
Experimental Conditions: Hot Water Inlet Temperature: 60 ± 0.5 °C Cold Water Mass Flowrate: 0.15 kg/s																								
5000	0.2903	59.96	45.88	22.53	19.80	31.41	14.81	145	29.5	288.9	1687.37	1712.53	1699.95	1.48										
10000	0.5571	60.31	50.85	23.34	19.82	33.91	49.99	489.5	29	284	2173.01	2208.10	2190.55	1.60										
15000	0.8230	60.38	52.80	24.00	19.92	34.60	99.97	978.9	28	274.2	2570.69	2559.38	2565.04	0.44										
20000	1.0860	60.36	54.20	24.31	19.83	35.20	167.5	1641	28	274.2	2755.73	2810.30	2783.01	1.96										
25000	1.3508	60.24	54.98	24.78	20.22	35.11	250.9	2456	27	264.4	2926.38	2860.49	2893.43	2.28										
30000	1.6089	60.32	55.90	25.00	20.10	35.56	344.3	3372	27	264.4	2928.16	3073.77	3000.97	4.85										
35000	1.8686	60.45	56.37	25.42	20.33	35.53	458.2	4487	27	264.4	3138.88	3192.96	3165.92	1.71										
40000	2.1283	60.50	56.78	25.38	20.42	35.74	586.9	5747	26	254.6	3259.23	3111.41	3185.32	4.64										
Experimental Conditions: Hot Water Inlet Temperature: 70 ± 0.5 °C Cold Water Mass Flowrate: 0.1 kg/s																								
5000	0.2536	69.80	54.03	23.81	19.74	39.85	12.03	117.8	15	146.9	1643.24	1702.07	1672.66	3.52										
10000	0.4874	69.82	59.46	24.73	19.96	42.23	37.03	362.6	15	146.9	2072.14	1994.81	2033.48	3.80										
15000	0.7147	70.12	62.26	25.32	19.96	43.54	75.9	743.3	14	137.1	2303.34	2241.55	2272.45	2.72										
20000	0.9400	70.31	63.93	26.12	20.23	43.94	125.9	1233	14	137.1	2457.57	2463.20	2460.38	0.23										
25000	1.1665	70.36	64.86	26.45	20.11	44.33	187.9	1840	14	137.1	2628.27	2651.39	2639.83	0.88										
30000	1.3933	70.26	65.58	26.73	20.11	44.49	261	2556	14	137.1	2670.81	2768.48	2719.65	3.59										
35000	1.6184	70.30	66.12	26.93	20.19	44.64	341.6	3345	14	137.1	2770.48	2818.67	2794.58	1.72										
40000	1.8394																							

**Table C-5:** Experimental Results of Tube-Side Heat Transfer Enhancement for Two Sizes of Inner Tube (Enhancement Status: Wire Coil,  $e=1$  mm,  $p=40$  mm).

Re Inner tube	$Q_h \cdot 10^{-4}$ ( $\text{m}^3/\text{s}$ )	Temperatures and Temperature Difference ( $^\circ\text{C}$ )					Pressure Drop				Heat Transfer Rate (W)													
		T <sub>h1</sub>	T <sub>h2</sub>	T <sub>c1</sub>	T <sub>c2</sub>	LMTD	Inner tube		Annulus		q <sub>h</sub>	q <sub>c</sub>	q <sub>avg.</sub>	Dev. %										
							mmH <sub>2</sub> O	N/m <sup>2</sup>	mmH <sub>2</sub> O	N/m <sup>2</sup>														
Inner Tube Dimensions: L=1.245 m    d= 0.011 m																								
Experimental Conditions: Hot Water Inlet Temperature: $60 \pm 0.5^\circ\text{C}$ Cold Water Mass Flowrate: 0.1 kg/s																								
5000	0.2234	59.72	48.76	22.58	20.12	32.71	21.48	210.31	8	78.34	1010.31	1028.77	1019.54	1.81										
10000	0.4307	60.50	52.80	22.93	19.65	35.31	69.42	679.82	8	78.34	1366.59	1371.70	1369.14	0.37										
15000	0.6355	60.42	55.08	23.41	20.14	35.97	139.8	1368.7	8	78.34	1397.53	1367.51	1382.52	2.17										
20000	0.8409	60.47	56.04	23.62	20.10	36.39	222.2	2175.4	8.5	83.24	1533.84	1472.06	1502.95	4.11										
25000	1.0503	60.10	56.52	23.70	19.85	36.53	342.5	3353.8	8	78.34	1548.11	1610.07	1579.09	3.92										
30000	1.2491	60.50	57.33	24.32	20.24	36.63	467.5	4577.5	8.5	83.24	1629.77	1706.26	1668.01	4.59										
35000	1.4524	60.43	57.85	24.00	20.14	37.07	611.9	5991.5	7.5	73.44	1542.19	1614.25	1578.22	4.57										
40000	1.6643	60.10	57.82	24.02	20.13	36.88	775.7	7595.9	7.5	73.44	1561.86	1626.80	1594.33	4.07										
Experimental Conditions: Hot Water Inlet Temperature: $60 \pm 0.5^\circ\text{C}$ Cold Water Mass Flowrate: 0.15 kg/s																								
5000	0.2272	60.43	45.91	22.33	20.08	31.57	21.29	208.48	17.5	171.4	1361.70	1411.43	1386.56	3.59										
10000	0.4389	60.50	50.32	23.11	20.04	33.71	71.28	697.95	18	176.3	1842.25	1925.81	1884.03	4.44										
15000	0.6454	60.50	52.94	23.43	20.17	34.88	142.6	1395.9	18	176.3	2010.42	2045.00	2027.71	1.71										
20000	0.8529	60.35	54.26	23.56	20.28	35.37	240.7	2356.7	17	166.5	2139.78	2057.54	2098.66	3.92										
25000	1.0591	60.50	55.00	23.95	20.17	35.68	348	3408.2	18	176.3	2399.01	2371.19	2385.10	1.17										
30000	1.2694	60.13	55.53	24.00	20.34	35.66	481.3	4713.4	17	166.5	2404.76	2295.92	2350.34	4.63										
35000	1.4693	60.42	56.30	24.06	20.18	36.24	626.7	6136.5	17	166.5	2492.36	2433.92	2463.14	2.37										
40000	1.6800	60.14	56.52	24.10	20.10	36.23	794.2	7777.2	17	166.5	2503.88	2509.2	2506.54	0.21										
Experimental Conditions: Hot Water Inlet Temperature: $70 \pm 0.5^\circ\text{C}$ Cold Water Mass Flowrate: 0.1 kg/s																								
5000	0.1984	69.86	54.54	22.90	20.00	40.43	17.59	172.22	8	78.34	1248.90	1212.78	1230.84	2.93										
10000	0.3808	70.12	59.94	24.00	20.37	42.76	54.61	534.8	8	78.34	1590.41	1518.07	1554.24	4.65										
15000	0.5580	70.41	62.85	24.21	20.00	44.50	108.3	1060.5	8	78.34	1729.03	1760.62	1744.82	1.81										
20000	0.7369	70.39	64.15	24.45	20.04	45.02	177.7	1740.4	8	78.34	1884.21	1844.26	1864.24	2.14										
25000	0.9177	70.14	64.90	24.98	20.45	44.80	262	2565.2	8	78.34	1970.19	1894.45	1932.32	3.92										
30000	1.0911	70.33	65.95	25.20	20.36	45.36	359.2	3517	8	78.34	1957.25	2024.09	1990.67	3.36										
35000	1.2659	70.50	66.52	25.42	20.25	45.67	461.9	4523.1	8	78.34	2062.93	2162.09	2112.51	4.69										
40000	1.4565	69.82	66.30	25.00	20.21	45.45	597	5846.5	8	78.34	2099.89	2003.18	2051.53	4.71										
Experimental Conditions: Hot Water Inlet Temperature: $70 \pm 0.5^\circ\text{C}$ Cold Water Mass Flowrate: 0.15 kg/s																								
5000	0.2034	69.80	51.22	22.52	19.93	38.74	16.66	163.16	17	166.5	1553.85	1624.71	1589.28	4.46										
10000	0.3903	69.85	56.82	23.56	20.11	41.32	57.39	561.99	17	166.5	2088.41	2164.19	2126.30	3.56										
15000	0.5730	70.33	59.30	24.15	20.15	42.57	112	1096.8	17	166.5	2593.23	2509.20	2551.22	3.29										
20000	0.7496	70.44	61.80	24.72	20.31	43.57	184.2	1803.8	18	176.3	2655.32	2766.39	2710.86	4.10										
25000	0.9295	70.41	62.92	24.94	19.87	44.25	266.6	2610.5	18	176.3	2853.50	3180.41	3016.95	10.8										
30000	1.1063	70.48	63.95	24.91	20.12	44.69	368.4	3607.6	17	166.5	2960.18	3004.77	2982.47	1.49										
35000	1.2820	70.48	64.85	25.34	20.39	44.80	474.9	4650	17	166.5	2956.91	3105.14	3031.02	4.89										
40000	1.4645	70.34	65.05	25.59	20.45	44.67	616.5	6036.8	17	166.5	3173.77	3224.32	3199.05	1.58										
Inner Tube Dimensions: L=1.245 m    d= 0.014 m																								
Experimental Conditions: Hot Water Inlet Temperature: $60 \pm 0.5^\circ\text{C}$ Cold Water Mass Flowrate: 0.1 kg/s																								
5000	0.2808	60.14	50.00	23.14	20.23	33.25	11.18	109.46	15	146.9	1174.03	1216.96	1195.50	3.59										
10000	0.5507	60.06	52.62	24.31	20.33	33.99	39.8	389.77	16	156.7	1688.73	1644.44	1676.58	1.45										
15000	0.8130	60.16	54.64	24.43	20.12	35.12	75.9	743.27	15	146.9	1848.62	1802.44	1825.53	2.53										
20000	1.0763	60.12	55.64	25.03	20.31	35.21	125	1223.7	15	146.9	1985.64	1973.9	1977.77	0.59										
25000	1.3317	60.41	56.72	25.14	20.22	35.88	188.8	1849.1	14	137.1	2022.92	2057.54	2040.23	1.70										
30000	1.5987	60.11	56.96	25.43	20.43	35.60	262.9	2574.3	14	137.1	2073.22	2091.00	2082.11	0.85										
35000	1.8576	60.21	57.41	25.63	20.36	35.80	346.2	3390.1	14	137.1	2140.95	2203.91	2172.43	2.90										
40000	2.1139	60.32	57.88	25.52	20.45	36.10	437.8	4287.4	13	127.3	2122.76	2120.27	2121.52	0.12										
Experimental Conditions: Hot Water Inlet Temperature: $60 \pm 0.5^\circ\text{C}$ Cold Water Mass Flowrate: 0.15 kg/s																								
5000	0.2850	60.22	47.96	22.42	20.11	32.57	11.11	108.77	29	284	1441.82	1449.06	1445.44	0.50										
10000	0.5565	60.10	51.20	23.52	20.21	33.71	41.65	407.89	29	284	2042.12	2076.36	2059.24	1.66										
15000	0.8229	60.17	53.02	23.85	20.05	34.62	78.68	770.47	29	284	2424.67	2383.74	2404.20	1.70										
20000	1.0881	60.20	54.10	24.52	20.32	34.72	128.7	1259.9	29	284	2734.40	2634.66	2684.53	3.72										
25000	1.3508	60.20	55.02	24.71	19.92	35.29	194.4	1903.5	28	274.2	2881.87	3004.77	2943.32	4.18										
30000	1.6162	60.06	55.55	24.93	20.12	35.28	270.3	2646.8	28	274.2	3001.88	3017.31	3009.60	0.51										
35000	1.8679	60.41	56.46	25.13	20.22	35.76	352.7	3453.5	27	264.4	3037.70	3080.04	3058.87	1.38										
40000	2.1286	60.41	56.85	25.28	20.12	35.92	447.1	4378.1	27	264.4	3119.53	3236.87	3178.20	3.69										
Experimental Conditions: Hot Water Inlet Temperature: $70 \pm 0.5^\circ\text{C}$ Cold Water Mass Flowrate: 0.1 kg/s																								
5000	0.2512	69.75	55.34	23.42	19.81	40.69	8.331	81.579	15	146.9	1487.34	1509.7	1498.52	1.49										
10000	0.4837	70.34	59.98	24.9	20.22	42.54	30.55	299.12	15	146.9	2055.90	1957.18	2006.54	4.92										
15000	0.7153	70.14	62.14	25.57	20.22	43.23	59.24	580.12	15	146.9	2346.16	2237.37	2291.76	4.75										
20000	0.9393	70.46	63.88	26.12	20.27	43.97	99.04	969.88	15	146.9	2532.66	2446.47	2489.56	3.46										
25000	1.1668	70.25	64.93	26.23	20.23	44.36	143.5	1405	14	137.1	2543.04	2509.2	2526.12	1.34										
30000	1.3940	70.17	65.60	26.53	20.07	44.58	202.7	1985.1	14	137.1	2609.46	2701.57	2655.51	3.47										
35000	1.6213	70.11	66.07																					

**Table C-6:** Experimental Results of Annulus-Side Heat Transfer Enhancement for Two Annulus Sizes (Enhancement Status: Smooth Annulus).

**Table C-7:** Experimental Results of Annulus-Side Heat Transfer Enhancement for Two Annulus Sizes (Enhancement Status: Wire Coil,  $e=1$  mm,  $p=10$  mm).

Re	$Q_c \cdot 10^{-4}$	Temperatures and Temperature Difference (°C)					Pressure Drop				Heat Transfer Rate (W)			
		T <sub>h1</sub>	T <sub>h2</sub>	T <sub>c1</sub>	T <sub>c2</sub>	LMTD	Inner tube		Annulus		q <sub>h</sub>	q <sub>c</sub>	q <sub>avg.</sub>	Dev. %
Annul -us	(m <sup>3</sup> /s)						mmH <sub>2</sub> O	N/m <sup>2</sup>	mmH <sub>2</sub> O	N/m <sup>2</sup>				
Annulus Dimensions: L=1.245 m D <sub>o</sub> =0.028 m D <sub>i</sub> =0.0125 m														
Experimental Conditions: Hot Water Inlet Temperature: 60 ± 0.5 °C Hot Water Mass Flowrate: 0.1125 kg/s														
3000	0.8577	60.21	53.22	29.53	19.89	31.99	211	2066.7	19	186.06	3290.19	3447.74	3368.97	4.68
4000	1.1467	60.36	52.31	28.68	20.50	31.74	211	2066.7	30	293.77	3789.14	3911.50	3850.32	3.18
5000	1.4531	60.47	51.57	27.61	20.37	32.02	212.9	2084.8	44	430.86	4189.23	4387.67	4288.45	4.63
6000	1.7597	59.85	50.40	26.75	20.43	31.51	212.9	2084.8	57.5	563.06	4448.12	4638.96	4543.54	4.20
7000	2.0728	60.50	50.27	26.07	20.28	32.16	214.8	2102.9	74	724.64	4815.26	5006.46	4910.86	3.89
8000	2.3772	60.00	49.30	25.6	20.45	31.54	214.8	2102.9	91	891.11	5036.49	5107.13	5071.81	1.39
9000	2.7174	60.50	48.97	24.81	19.87	32.28	215.7	2112	117	1145.7	5427.17	5600.89	5514.03	3.15
10000	3.0096	60.27	48.41	24.70	20.26	31.72	215.7	2112	143	1400.3	5582.50	5580.50	5581.50	0.04
Experimental Conditions: Hot Water Inlet Temperature: 60 ± 0.5 °C Hot Water Mass Flowrate: 0.2 kg/s														
3000	0.8473	59.98	55.44	30.63	19.87	32.36	581.3	5692.4	18	176.26	3799.07	3801.25	3800.16	0.06
4000	1.1402	60.05	54.72	29.73	19.95	32.49	581.3	5692.4	29	283.98	4460.14	4649.92	4555.03	4.17
5000	1.4347	60.28	54.29	28.92	20.18	32.72	583.2	5710.5	43	421.07	5012.43	5228.89	5120.66	4.23
6000	1.7421	60.28	53.74	27.88	20.18	32.98	583.2	5710.5	59	577.75	5472.67	5594.56	5533.62	2.20
7000	2.0376	60.28	53.30	27.42	20.42	32.87	585	5728.7	78	763.81	5840.86	5948.73	5894.80	1.83
8000	2.3393	60.28	52.98	26.96	20.48	32.91	585	5728.7	94	920.48	6108.64	6322.75	6215.69	3.44
9000	2.6595	60.50	52.65	26.27	20.26	33.30	585	5728.7	114	1116.3	6568.88	6667.42	6618.15	1.49
10000	2.9574	60.49	52.44	26.07	20.39	33.22	585.9	5737.7	144	1410.1	6736.24	7007.19	6871.72	3.94
Experimental Conditions: Hot Water Inlet Temperature: 70 ± 0.5 °C Hot Water Mass Flowrate: 0.1125 kg/s														
3000	0.8333	70.26	61.46	32.07	19.92	39.84	210.1	2057.6	18	176.26	4142.16	4220.71	4181.44	1.88
4000	1.1143	70.42	60.19	31.23	20.50	39.44	211.5	2071.2	27	264.39	4815.26	4984.45	4899.86	3.45
5000	1.4160	69.82	58.70	29.78	20.48	39.12	212	2075.7	40	391.7	5234.18	5490.73	5362.46	4.78
6000	1.7292	70.46	58.10	28.56	20.15	39.89	212.9	2084.8	53	519	5817.85	6064.84	5941.34	4.16
7000	2.0357	70.46	57.40	27.76	20.16	39.91	212.9	2084.8	76	744.22	6147.34	6452.65	6300.00	4.85
8000	2.3447	70.47	56.54	27.13	20.11	39.79	212.9	2084.8	87	851.94	6556.85	6865.57	6711.21	4.60
9000	2.6768	70.50	55.94	26.21	19.76	40.10	214.8	2102.9	110	1077.2	6853.39	7202.59	7027.99	4.97
10000	2.9672	70.34	54.91	26.02	20.15	39.34	214.8	2102.9	138	1351.3	7263.57	7260.53	7262.05	0.04
Experimental Conditions: Hot Water Inlet Temperature: 70 ± 0.5 °C Hot Water Mass Flowrate: 0.2 kg/s														
3000	0.8146	70.27	64.62	34.32	19.73	40.25	576.7	5647.1	17	166.47	4727.92	4953.26	4840.59	4.66
4000	1.0941	69.94	63.25	32.91	20.48	39.83	578.5	5665.2	29	283.98	5598.19	5667.94	5633.07	1.24
5000	1.3921	70.46	62.68	31.70	20.08	40.65	578.5	5665.2	40	391.7	6510.30	6743.56	6626.93	3.52
6000	1.6878	70.46	62.00	30.66	20.20	40.79	579.9	5678.8	57	558.17	7079.33	7360.45	7219.89	3.89
7000	1.9790	70.18	61.25	29.92	20.49	40.51	581.3	5692.4	68	665.88	7472.62	7781.20	7626.91	4.05
8000	2.2820	69.77	60.36	29.12	20.50	40.25	581.3	5692.4	85	832.35	7874.29	8202.40	8038.35	4.08
9000	2.5809	70.30	60.32	28.65	20.50	40.73	581.8	5696.9	103	1008.6	8351.26	8771.60	8561.43	4.91
10000	2.9097	70.20	59.59	27.59	20.28	40.93	583.2	5710.5	135	1322	8876.06	8867.70	8871.88	0.09
Annulus Dimensions: L=1.245 m D <sub>o</sub> =0.028 m D <sub>i</sub> =0.0155 m														
Experimental Conditions: Hot Water Inlet Temperature: 60 ± 0.5 °C Hot Water Mass Flowrate: 0.1125 kg/s														
3000	0.9036	60.35	51.95	30.89	20.25	30.57	69	675.29	36	352.53	3953.88	4008.14	3981.01	1.36
4000	1.2218	60.50	51.21	29.43	20.46	30.91	69	675.29	59	577.75	4372.80	4569.75	4471.28	4.40
5000	1.5534	60.47	50.36	27.99	20.40	31.20	69.4	679.82	90	881.31	4758.78	4917.19	4837.98	3.27
6000	1.8799	60.45	49.57	27.18	20.47	31.14	69.4	679.82	123	1204.5	5121.22	5261.28	5191.25	2.70
7000	2.2099	60.50	49.00	26.57	20.42	31.18	69.4	679.82	170	1664.7	5413.05	5669.16	5541.11	4.62
8000	2.5468	60.45	48.25	25.83	20.44	31.09	70.3	688.89	227	2222.9	5744.42	5729.12	5736.77	0.27
9000	2.8798	60.45	47.81	25.39	20.44	31.06	71.3	697.95	283	2771.2	5951.53	5949.96	5950.75	0.03
10000	3.2136	60.45	47.41	25.02	20.44	31.01	71.3	697.95	345	3378.4	6139.81	6143.82	6141.81	0.07
Experimental Conditions: Hot Water Inlet Temperature: 60 ± 0.5 °C Hot Water Mass Flowrate: 0.2 kg/s														
3000	0.8766	60.42	54.86	33.63	20.25	30.53	181	1776.6	35	342.73	4652.61	4888.14	4770.37	4.94
4000	1.1888	60.45	53.85	31.86	20.48	30.92	181	1776.6	57	558.17	5522.88	5639.23	5581.06	2.08
5000	1.5088	60.40	53.16	30.53	20.44	31.27	181	1776.6	88	861.73	6058.43	6347.11	6202.77	4.65
6000	1.8376	60.46	52.42	29.33	20.32	31.61	181	1776.6	120	1175.1	6727.87	6904.07	6815.97	2.59
7000	2.1590	60.47	51.87	28.53	20.50	31.65	181	1776.6	160	1566.8	7196.48	7229.76	7213.12	0.46
8000	2.4935	60.44	51.33	27.71	20.40	31.82	182	1785.7	217	2124.9	7623.25	7604.03	7613.64	0.25
9000	2.8225	60.44	50.95	27.17	20.40	31.89	182	1785.7	272	2663.5	7941.23	7972.42	7956.82	0.39
10000	3.1535	60.44	50.58	26.69	20.40	31.93	183	1794.7	333	3260.9	8250.85	8276.36	8263.60	0.31
Experimental Conditions: Hot Water Inlet Temperature: 70 ± 0.5 °C Hot Water Mass Flowrate: 0.1125 kg/s														
3000	0.8677	70.30	60.17	34.32	20.50	37.79	68.5	670.76	32	313.36	4768.19	4996.73	4882.46	4.68
4000	1.1900	70.12	58.37	31.80	20.45	38.12	69.4	679.82	55	538.58	5530.73	5630.04	5580.38	1.78
5000	1.5141	70.44	57.60	30.39	20.27	38.67	69.4	679.82	88	861.73	6043.79	6388.37	6216.08	5.54
6000	1.8458	70.44	56.67	29.04	20.22	38.87	69.4	679.82	119	1165.3	6481.54	6788.69	6635.11	4.63
7000	2.1666	70.46	55.90	28.27	20.45	38.72	70.3	688.89	160	1566.8	6853.39	7065.79	6959.59	3.05
8000	2.4997	70.45	55.12	27.52	20.37	38.70	70.3	688.89	202	1978.1	7215.83	7454.31	7335.07	3.25
9000	2.8254	70.50	54.82	27.00	20.48	38.74	70.3	688.89	261	2555.8	7380.58	7683.58	7532.08	4.02
10000	3.1665	70.39	53.73	26.34	20.39	38.44	71.3</td							

**Table C-8:** Experimental Results of Annulus-Side Heat Transfer Enhancement for Two Annulus Sizes (Enhancement Status: Wire Coil, e=1 mm, p= 20 mm).

Re	Q <sub>c</sub> 10 <sup>-4</sup> (m <sup>3</sup> /s)	Temperatures and Temperature Difference (°C)					Pressure Drop				Heat Transfer Rate (W)			
		T <sub>h1</sub>	T <sub>h2</sub>	T <sub>c1</sub>	T <sub>c2</sub>	LMTD	Inner tube		Annulus		q <sub>h</sub>	q <sub>c</sub>	q <sub>avg.</sub>	Dev. %
Annul -us							mmH <sub>2</sub> O	N/m <sup>2</sup>	mmH <sub>2</sub> O	N/m <sup>2</sup>				
Annulus Dimensions: L=1.245 m D <sub>o</sub> = 0.028 m D <sub>i</sub> = 0.0125 m														
Experimental Conditions: Hot Water Inlet Temperature: 60 ± 0.5 °C Hot Water Mass Flowrate: 0.1125 kg/s														
3000	0.859	59.91	53.25	29.2	20.08	31.92	212	2075.7	16	156.68	3134.86	3266.99	3200.93	4.13
4000	1.1601	59.98	52.24	28.03	20.13	32.03	211	2066.7	26	254.6	3643.22	3822.17	3732.69	4.79
5000	1.4464	60.12	51.33	27.06	20.23	32.07	212	2075.7	38	372.11	4137.45	4172.42	4154.93	0.84
6000	1.7779	60.23	50.83	26.16	20.13	32.36	212.9	2084.8	53	519	4424.58	4472.27	4448.42	1.07
7000	2.0774	60.15	50.08	25.91	20.25	31.98	215.7	2112	70	685.47	4739.95	4904.95	4822.45	3.42
8000	2.3891	60.23	49.51	25.27	20.35	31.97	212.9	2084.8	85	832.35	5045.9	4903.73	4974.82	2.86
9000	2.7088	60.34	48.96	24.8	20.15	32.06	215.7	2112	106	1038	5356.57	5255.28	5305.92	1.91
10000	3.0105	60.44	48.58	24.58	20.35	31.89	215.7	2112	131	1282.8	5582.5	5313.05	5447.77	4.95
Experimental Conditions: Hot Water Inlet Temperature: 60 ± 0.5 °C Hot Water Mass Flowrate: 0.2 kg/s														
3000	0.8453	60.12	55.62	30.55	20.16	32.43	583.2	5710.5	15	146.89	3765.6	3661.81	3713.71	2.79
4000	1.1392	60.23	54.94	29.53	20.23	32.66	583.2	5710.5	25	244.81	4426.67	4417.67	4422.17	0.2
5000	1.4343	60.33	54.29	28.78	20.34	32.74	581.3	5692.4	37	362.32	5054.27	5048.25	5051.26	0.12
6000	1.7616	60.12	53.73	27.21	19.88	33.38	583.2	5710.5	52	509.2	5347.15	5385.94	5366.55	0.72
7000	2.0512	60.45	53.62	27.13	20.13	33.4	585	5728.7	68	665.88	5715.34	5988.86	5852.1	4.67
8000	2.3528	60.15	53.12	26.6	20.34	33.16	585	5728.7	83	812.77	5882.7	6143.68	6013.19	4.34
9000	2.6659	60.23	52.62	26.15	20.17	33.26	585.9	5737.7	104	1018.4	6368.05	6650.44	6509.24	4.34
10000	2.9763	60.08	52.3	25.71	20.2	33.22	585.9	5737.7	129	1263.2	6510.3	6841.38	6675.84	4.96
Experimental Conditions: Hot Water Inlet Temperature: 70 ± 0.5 °C Hot Water Mass Flowrate: 0.1125 kg/s														
3000	0.8313	70.45	61.41	32	20.21	39.81	208.3	2039.5	14	137.09	4255.13	4085.56	4170.34	4.07
4000	1.1191	70.34	60.28	31.01	20.34	39.63	208.3	2039.5	24	235.02	4735.24	4977.84	4856.54	5
5000	1.4277	70.41	59.07	29.35	20.18	39.97	209.2	2048.5	36	352.53	5337.74	5459.21	5398.47	2.25
6000	1.7269	70.5	58.17	28.65	20.18	39.89	209.2	2048.5	50	489.62	5803.73	6099.69	5951.71	4.97
7000	2.0413	70.49	57.38	27.64	20.04	40.03	209.2	2048.5	66	646.3	6170.88	6470.6	6320.74	4.74
8000	2.3209	70.28	56.3	27.63	20.5	39.13	210.1	2057.6	80	783.39	6580.39	6901.65	6741.02	4.77
9000	2.6302	70.5	55.85	26.99	20.5	39.29	210.1	2057.6	100	979.24	6895.76	7119.94	7007.85	3.2
10000	2.9656	70.5	54.95	26.06	20.16	39.42	211	2066.7	126	1233.8	7319.39	7299.06	7309.22	0.28
Experimental Conditions: Hot Water Inlet Temperature: 70 ± 0.5 °C Hot Water Mass Flowrate: 0.2 kg/s														
3000	0.8029	70.2	64.26	35.3	20.08	39.36	576.7	5647.1	13	127.3	4970.59	5091.97	5031.28	2.41
4000	1.088	69.8	62.96	33.41	20.49	39.35	576.7	5647.1	22	215.43	5723.71	5858.12	5790.92	2.32
5000	1.38	70	62.42	32.11	20.46	39.89	575.8	5665.2	34	332.94	6342.94	6701.34	6522.14	5.5
6000	1.6901	69.6	61.42	30.44	20.3	40.13	578.5	5665.2	46	450.45	6845.02	7144.97	6995	4.29
7000	1.9844	70.07	61.2	29.76	20.41	40.55	580.4	5683.3	62	607.13	7422.42	7736.26	7579.34	4.14
8000	2.2859	69.99	60.44	28.97	20.5	40.48	581.3	5692.4	78	763.81	7991.44	8073.5	8032.47	1.02
9000	2.5915	69.99	60.06	28.29	20.5	40.62	581.3	5692.4	95	930.28	8309.42	8418.85	8364.13	1.31
10000	2.8962	70.13	59.68	27.78	20.5	40.74	581.3	5692.4	117	1145.7	8744.56	8793.32	8768.94	0.56
Annulus Dimensions: L=1.245 m D <sub>o</sub> = 0.028 m D <sub>i</sub> = 0.0155 m														
Experimental Conditions: Hot Water Inlet Temperature: 60 ± 0.5 °C Hot Water Mass Flowrate: 0.1125 kg/s														
3000	0.8989	60.5	52.31	31.13	20.48	30.58	68.5	670.76	29	283.98	3855.03	3990.7	3922.87	3.46
4000	1.2236	60.5	51.14	29.38	20.38	30.94	68.6	675.29	52	509.2	4405.75	4591.84	4498.8	4.14
5000	1.5529	60.5	50.4	28.06	20.36	31.22	69.42	679.82	83	812.77	4754.07	4986.73	4870.4	4.78
6000	1.8829	60.49	49.77	27.01	20.5	31.33	69.42	679.82	119	1165.3	5045.9	5112.75	5079.33	1.32
7000	2.2186	60.4	48.8	26.35	20.3	31.19	70.35	688.89	166	1625.5	5460.12	5599.12	5529.62	2.51
8000	2.5462	60.5	48.9	25.85	20.44	31.45	70.35	688.89	210	2056.4	5460.12	5746.2	5603.16	5.11
9000	2.8771	60.49	48.59	25.41	20.5	31.46	70.35	688.89	264	2585.2	5601.33	5893.19	5747.26	5.08
10000	3.2187	60.48	47.77	24.9	20.42	31.28	71.28	697.95	326	3192.3	5983.94	6012.09	5998.02	0.47
Experimental Conditions: Hot Water Inlet Temperature: 60 ± 0.5 °C Hot Water Mass Flowrate: 0.2 kg/s														
3000	0.8775	60.5	54.84	33.42	20.37	30.63	180.5	1767.5	28	274.19	4736.29	4772.34	4754.31	0.76
4000	1.1913	60.4	53.9	31.67	20.48	31.02	180.5	1767.5	50	489.62	5439.2	5556.9	5498.05	2.14
5000	1.5136	60.49	53.14	30.27	20.42	31.45	181.4	1776.6	80	783.39	6150.48	6215.81	6183.15	1.06
6000	1.8364	60.5	52.72	29.25	20.46	31.75	180.5	1767.5	113	1106.5	6510.5	6730.88	6620.59	3.33
7000	2.1666	60.17	51.98	28.26	20.46	31.71	181.4	1776.6	155	1517.8	6853.39	7047.72	6950.56	2.8
8000	2.4931	60.28	51.66	27.66	20.46	31.9	182.4	1785.7	201	1968.3	7213.22	7486.52	7349.87	3.72
9000	2.8247	60.38	51.34	27.05	20.45	32.09	182.4	1785.7	251	2457.9	7564.67	7776.05	7670.36	2.76
10000	3.1585	60.17	50.81	26.5	20.45	31.99	182.4	1785.7	314	3074.8	7832.45	7970.83	7901.64	1.75
Experimental Conditions: Hot Water Inlet Temperature: 70 ± 0.5 °C Hot Water Mass Flowrate: 0.1125 kg/s														
3000	0.8642	70.13	59.83	34.69	20.5	37.35	68.5	670.76	27	264.39	4848.21	5109.67	4978.94	5.25
4000	1.1888	70.14	58.47	31.95	20.39	38.13	68.5	670.76	50	489.62	5493.07	5728.43	5610.75	4.19
5000	1.5103	70.13	57.61	30.4	20.48	38.42	69.42	679.82	77	754.01	5893.16	6246.53	6069.85	5.82
6000	1.8397	70.13	56.87	29.07	20.48	38.68	69.42	679.82	114	1116.3	6241.48	6589.76	6415.62	5.43
7000	2.1686	70.43	56.34	28.18	20.46	38.98	70.35	688.89	155	1517.8	6632.16	6981.86	6807.01	5.14
8000	2.5048	70.43	55.7	27.25	20.46	39.08	70.35	688.89	203	1987.9	6933.41	7093.75	7013.58	2.29
9000	2.8361	70.5	55.35	26.72	20.43	39.18	70.35	688.89	260	2546	7131.11	7440.99	7286.05	4.25
10000	3.1695	70.43	55.26	26.19	20.46	39.33	70.81	693.42	316	3094.4	7140.52			

**Table C-9:** Experimental Results of Annulus-Side Heat Transfer Enhancement for Two Annulus Sizes (Enhancement Status: Wire Coil  $e=1$  mm,  $p=30$  mm).

Re	$Q_c \cdot 10^{-4}$ (m <sup>3</sup> /s)	Temperatures and Temperature Difference (°C)					Pressure Drop				Heat Transfer Rate (W)			
		T <sub>h1</sub>	T <sub>h2</sub>	T <sub>c1</sub>	T <sub>c2</sub>	LMTD	Inner tube		Annulus		q <sub>h</sub>	q <sub>c</sub>	q <sub>avg.</sub>	Dev. %
Annul -us							mmH <sub>2</sub> O	N/m <sup>2</sup>	mmH <sub>2</sub> O	N/m <sup>2</sup>				
Annulus Dimensions: L=1.245 m D <sub>o</sub> =0.028 m D <sub>i</sub> =0.0125 m														
Experimental Conditions: Hot Water Inlet Temperature: 60 ± 0.5 °C Hot Water Mass Flowrate: 0.1125 kg/s														
3000	0.8657	60.28	53.61	28.68	19.92	32.63	210.1	2057.6	11.5	112.61	3139.57	3162.62	3151.09	0.73
4000	1.1789	59.72	52.18	27.07	19.69	32.57	210.1	2057.6	19.5	190.95	3549.08	3629.04	3589.06	2.23
5000	1.4811	60.05	51.52	26.4	19.92	32.61	211	2066.7	30	293.77	4015.07	4003.61	4009.34	0.29
6000	1.7759	60.39	51.3	26.13	20.26	32.62	211	2066.7	40	391.7	4278.66	4348.51	4313.59	1.62
7000	2.0716	60.51	50.9	25.9	20.5	32.46	210.1	2057.6	53	519	4523.43	4666.51	4594.97	3.11
8000	2.391	60.5	50.45	25.23	20.32	32.63	211	2066.7	66.5	651.19	4730.54	4897.79	4814.16	3.47
9000	2.7241	60.5	49.82	24.55	19.92	32.83	212	2075.7	83	812.77	5027.08	5262.49	5144.78	4.58
10000	3.0119	60.5	49.48	24.61	20.28	32.43	212.9	2084.8	102	998.82	5187.11	5441.22	5314.17	4.78
Experimental Conditions: Hot Water Inlet Temperature: 60 ± 0.5 °C Hot Water Mass Flowrate: 0.2 kg/s														
3000	0.8576	59.89	55.52	29.75	19.68	32.91	580.8	5687.9	11	107.72	3656.82	3601.12	3628.97	1.53
4000	1.1611	59.78	54.66	28.38	19.7	33.15	581.3	5692.4	19	186.06	4284.42	4203.43	4243.92	1.91
5000	1.4631	59.83	54.04	27.47	19.91	33.24	581.3	5692.4	29	283.98	4845.07	4613.55	4729.31	4.9
6000	1.7541	59.94	53.61	27.2	20.26	33.04	581.3	5692.4	39	381.9	5296.94	5077.51	5187.23	4.23
7000	2.0575	60.5	53.56	26.73	20.26	33.53	582.2	5701.5	52	509.2	5807.39	5552.83	5680.11	4.48
8000	2.3517	60.4	53.26	26.48	20.5	33.34	582.2	5701.5	65	636.5	5974.75	5866.15	5920.45	1.83
9000	2.6678	60.47	52.81	25.97	20.29	33.5	583.2	5710.5	81	793.18	6409.89	6321.24	6365.56	1.39
10000	2.9635	60.5	52.58	25.78	20.5	33.38	583.2	5710.5	100	979.24	6627.46	6527.45	6577.45	1.52
Experimental Conditions: Hot Water Inlet Temperature: 70 ± 0.5 °C Hot Water Mass Flowrate: 0.1125 kg/s														
3000	0.8461	70.11	61.55	30.83	19.8	40.5	206.4	2021.3	10.5	102.82	4029.19	3890.9	3960.04	3.49
4000	1.1324	70.46	60.73	29.79	20.5	40.45	208.3	2039.5	18	176.26	4579.91	4386.36	4483.14	4.32
5000	1.4374	70.07	59.44	28.48	20.45	40.28	208.3	2039.5	27	264.39	5003.54	4813.49	4908.51	3.87
6000	1.7387	70.21	58.75	27.75	20.48	40.33	208.3	2039.5	38	372.11	5394.22	5271.79	5333	2.3
7000	2.045	70.33	58.33	27.02	20.5	40.51	208.3	2039.5	49	479.83	5648.4	5561.39	5604.9	1.55
8000	2.3654	70.5	57.66	26.26	20.22	40.75	209.2	2048.5	63.5	621.82	6043.79	5959.66	6001.72	1.4
9000	2.6573	70.32	57.07	26.1	20.5	40.27	209.2	2048.5	78	763.81	6236.78	6207.49	6222.13	0.47
10000	2.9615	70.32	56.69	25.84	20.5	40.19	209.2	2048.5	95	930.28	6415.64	6597	6506.32	2.79
Experimental Conditions: Hot Water Inlet Temperature: 70 ± 0.5 °C Hot Water Mass Flowrate: 0.2 kg/s														
3000	0.8205	69.89	64.23	33.37	20.03	40.24	573	5610.8	10	97.924	4736.29	4561.66	4648.97	3.76
4000	1.1133	70.11	63.58	31.78	20.03	40.88	573	5610.8	17.5	171.37	5464.3	5453.37	5458.84	0.2
5000	1.4225	70.06	62.59	30.05	19.8	41.38	573.9	5619.9	27	264.39	6250.9	6079.92	6165.41	2.77
6000	1.7202	70.11	62.04	29.25	19.92	41.49	575.8	5638	38	372.11	6752.98	6692.87	6722.92	0.89
7000	2.0135	70.5	61.87	28.68	20.2	41.74	577.6	5656.1	48	470.03	7221.58	7120.62	7171.1	1.41
8000	2.3056	70.5	61.33	28.28	20.43	41.56	578.5	5665.2	61	597.34	7673.46	7547.99	7610.72	1.65
9000	2.6101	70.48	60.84	27.75	20.41	41.57	578.5	5665.2	77.5	758.91	8066.75	7990.27	8028.51	0.95
10000	2.9101	70.5	60.52	27.43	20.43	41.56	579.5	5674.3	93	910.69	8351.26	8496.23	8423.75	1.72
Annulus Dimensions: L=1.245 m D <sub>o</sub> =0.028 m D <sub>i</sub> =0.0155 m														
Experimental Conditions: Hot Water Inlet Temperature: 60 ± 0.5 °C Hot Water Mass Flowrate: 0.1125 kg/s														
3000	0.9102	60.29	52.94	30.02	20.47	31.36	68.5	670.76	23	225.22	3459.65	3624.11	3541.88	4.64
4000	1.2371	60.09	51.79	28.3	20.49	31.54	68.5	670.76	39.5	386.8	3906.81	4029.19	3968	3.08
5000	1.5662	60.19	51.15	27.19	20.48	31.82	68.5	670.76	56	548.37	4255.13	4383.39	4319.26	2.97
6000	1.8964	60.5	50.83	26.42	20.47	32.18	69.42	679.82	79	773.6	4551.67	4706.74	4629.2	3.35
7000	2.245	60.3	50	25.47	20.16	32.27	69.42	679.82	103	1008.6	4848.21	4973.33	4910.77	2.55
8000	2.5642	60.38	49.76	25.22	20.46	32.14	69.42	679.82	136	1331.8	4998.83	5092.09	5045.46	1.85
9000	2.9159	60.25	49.36	24.6	20.16	32.32	69.42	679.82	163	1596.2	5125.92	5401.77	5263.85	5.24
10000	3.239	60.29	48.75	24.4	20.38	31.98	69.42	679.82	195	1909.5	5429.86	5426.86	5428.36	0.06
Experimental Conditions: Hot Water Inlet Temperature: 60 ± 0.5 °C Hot Water Mass Flowrate: 0.2 kg/s														
3000	0.8944	60.09	55.17	31.57	20.49	31.5	180.5	1767.5	21	205.64	4117.06	4130.88	4123.97	0.34
4000	1.2225	60.19	54.53	29.36	20.48	32.41	181	1772.1	35	342.73	4736.29	4526.48	4631.39	4.53
5000	1.5308	60.27	53.87	29.23	20.45	32.22	181.4	1776.6	54	528.79	5355.52	5604.61	5480.06	4.55
6000	1.858	60.37	53.4	28.3	20.38	32.54	181.4	1776.6	74	724.64	5832.5	6136.66	5984.58	5.08
7000	2.1892	60.45	52.9	27.49	20.32	32.77	181.4	1776.6	96	940.07	6317.84	6546.82	6432.33	3.56
8000	2.5227	60.18	52.41	26.63	20.46	32.74	182.4	1785.7	121	1184.9	6501.94	6492.56	6497.25	0.14
9000	2.843	60.43	52.23	26.44	20.5	32.85	182.4	1785.7	159	1557	6861.76	7044.13	6952.95	2.62
10000	3.1808	60.28	51.64	25.9	20.44	32.77	182.4	1785.7	190	1860.6	7232.34	7244.89	7238.62	0.17
Experimental Conditions: Hot Water Inlet Temperature: 70 ± 0.5 °C Hot Water Mass Flowrate: 0.1125 kg/s														
3000	0.8846	70.34	61.3	32.56	20.49	39.28	68.04	666.23	20	195.85	4255.13	4450.42	4352.77	4.49
4000	1.2067	70.5	59.99	30.67	20.33	39.74	68.5	670.76	33.5	328.04	4947.06	5201.73	5074.4	5.02
5000	1.5291	70.5	59.07	29.36	20.42	39.88	68.5	670.76	52	509.2	5380.1	5700.23	5540.17	5.78
6000	1.866	70.43	58.06	28.05	20.25	40.05	68.5	670.76	73	714.84	5822.56	6070.18	5946.37	4.16
7000	2.1862	70.38	57.63	27.43	20.5	39.97	68.5	670.76	93.5	915.59	6001.43	6318.91	6160.17	5.15
8000	2.5248	70.4	57.05	26.62	20.4	40.11	68.5	670.76	116	1135.9	6283.85	6550.5	6417.17	4.16
9000	2.8588	70.43	56.18	26.06	20.4	39.92	68.5	670.76	146	1429.7	6705.12	6751.89	6728.51	0.7
10000	3.1924	70.43	55.69	25.63	20.4	39.85	68.5	670.76	180	1762.6	6935.76			

**Table C-10:** Experimental Results of Annulus-Side Heat Transfer Enhancement for Two Annulus Sizes (Enhancement Status: Wire Coil, e=1 mm, p= 40 mm).

Re	$Q_c \cdot 10^{-4}$	Temperatures and Temperature Difference (°C)					Pressure Drop				Heat Transfer Rate (W)			
		T <sub>h1</sub>	T <sub>h2</sub>	T <sub>c1</sub>	T <sub>c2</sub>	LMTD	Inner tube		Annulus		q <sub>h</sub>	q <sub>c</sub>	q <sub>avg.</sub>	Dev. %
Annul -us	(m <sup>3</sup> /s)	mmH <sub>2</sub> O	N/m <sup>2</sup>	mmH <sub>2</sub> O	N/m <sup>2</sup>									
Annulus Dimensions: L=1.245 m D <sub>o</sub> = 0.028 m D <sub>i</sub> = 0.0125 m														
Experimental Conditions: Hot Water Inlet Temperature: 60 ± 0.5 °C Hot Water Mass Flowrate: 0.1125 kg/s														
3000	0.8747	60.05	53.96	27.78	19.91	33.15	208.3	2039.5	11	107.72	2866.56	2871.3	2868.93	0.17
4000	1.1806	59.99	53.03	26.76	19.87	33.19	208.3	2039.5	17	166.47	3276.07	3393.23	3334.65	3.51
5000	1.4982	59.94	52.21	25.65	19.68	33.4	210.1	2057.6	25	244.81	3638.51	3731.62	3685.07	2.53
6000	1.7785	60.27	52.1	25.79	20.47	33.03	211.1	2066.7	35	342.73	3845.62	3947.07	3896.34	2.6
7000	2.1064	60.5	51.76	24.9	20.07	33.61	212	2075.7	45	440.66	4113.92	4244.66	4179.29	3.13
8000	2.3949	60.33	51.19	24.95	20.46	33	211	2066.7	56	548.37	4302.2	4486.22	4394.21	4.19
9000	2.7025	60.25	50.68	24.65	20.5	32.82	212	2075.7	66	646.3	4504.6	4679.14	4591.87	3.8
10000	3.0674	60.48	50.14	23.59	19.75	33.54	212.9	2084.8	82	802.98	4867.04	4915.21	4891.13	0.98
Experimental Conditions: Hot Water Inlet Temperature: 60 ± 0.5 °C Hot Water Mass Flowrate: 0.2 kg/s														
3000	0.8653	59.94	56.03	28.85	19.79	33.6	573.9	5619.9	10	97.924	3271.89	3269.42	3270.65	0.08
4000	1.166	59.83	55.27	27.92	19.79	33.66	576.7	5647.1	16	156.68	3815.81	3953.96	3884.88	3.56
5000	1.469	60.05	54.94	27.12	19.91	33.97	582.3	5710.5	24	235.02	4276.05	4417.89	4346.97	3.26
6000	1.7591	59.94	54.39	26.85	20.36	33.56	582.3	5710.5	33	323.15	4644.24	4762.08	4703.16	2.51
7000	2.0592	59.94	53.96	26.45	20.47	32	582.3	5710.5	44	430.86	5004.06	5136.47	5070.27	2.61
8000	2.3744	60.5	53.94	25.87	20.28	34.14	585	5728.7	54	528.79	5489.41	5536.97	5513.19	0.86
9000	2.6687	60.37	53.63	25.73	20.5	33.88	585	5728.7	65	636.5	5640.03	5822.48	5731.26	3.18
10000	2.9957	60.5	53.11	25.15	20.2	34.12	585	5728.7	81	793.18	6183.95	6186.66	6185.31	0.04
Experimental Conditions: Hot Water Inlet Temperature: 70 ± 0.5 °C Hot Water Mass Flowrate: 0.1125 kg/s														
3000	0.8575	70.17	62.82	29.53	19.91	41.76	203.6	1994.2	10	97.924	3459.65	3439.8	3449.72	0.58
4000	1.1466	70.28	61.65	29.05	20.14	41.37	205.5	2012.3	15	146.89	4062.14	4260.08	4161.11	4.76
5000	1.4736	69.9	60.35	26.91	19.85	41.73	208.3	2039.5	23	225.22	4495.19	4339.6	4417.39	3.52
6000	1.7746	69.8	59.64	26.36	20.09	41.46	208.3	2039.5	32	313.36	4782.31	4641.58	4711.94	2.99
7000	2.0663	70.34	59.34	26.22	20.4	41.48	208.3	2039.5	42	411.28	5177.7	5016.55	5097.13	3.16
8000	2.3703	69.96	58.46	25.8	20.5	40.98	211	2066.7	53	519	5413.05	5240.52	5326.78	3.24
9000	2.6815	70.13	58.2	25.39	20.43	41.16	210.1	2057.6	64	626.71	5615.45	5548.5	5581.97	1.2
10000	2.9839	70.4	58.59	25.19	20.5	41.55	212.9	2084.8	78	763.81	5558.97	5838.31	5698.64	4.9
Experimental Conditions: Hot Water Inlet Temperature: 70 ± 0.5 °C Hot Water Mass Flowrate: 0.2 kg/s														
3000	0.843	69.97	65.1	31.3	19.65	41.97	568.3	5565.5	9	88.131	4075.22	4094.74	4084.98	0.48
4000	1.1353	69.53	63.78	30.15	19.91	41.58	570.2	5583.6	15	146.89	4811.6	4847.58	4829.59	0.75
5000	1.4312	69.74	63.35	29.17	20.14	41.88	570.2	5583.6	22	215.43	5347.15	5389.4	5368.28	0.79
6000	1.7247	70.49	63.44	28.77	20.17	42.49	572.1	5601.8	31	303.56	5899.44	6185.49	6042.47	4.73
7000	2.0509	70.29	62.71	27.21	20.06	42.86	573.9	5619.9	41	401.49	6342.94	6116.49	6229.71	3.64
8000	2.3217	69.92	61.94	27.6	20.5	41.88	573.9	5619.9	52	509.2	6677.66	6874.99	6776.33	2.91
9000	2.6287	69.9	61.56	27.08	20.46	41.95	573.9	5619.9	63	616.92	6978.91	7258.35	7118.63	3.93
10000	2.9642	70.5	61.38	26.36	19.9	42.8	573.9	5619.9	77	754.01	7631.62	7988.11	7809.86	4.56
Annulus Dimensions: L=1.245 m D <sub>o</sub> = 0.028 m D <sub>i</sub> = 0.0155 m														
Experimental Conditions: Hot Water Inlet Temperature: 60 ± 0.5 °C Hot Water Mass Flowrate: 0.1125 kg/s														
3000	0.9145	60.2	52.88	29.74	20.33	31.49	69.42	679.82	19	186.06	3445.52	3588.07	3516.8	4.05
4000	1.2389	60.38	52.24	28.16	20.5	31.98	69.42	679.82	30	293.77	3831.5	3957.71	3894.61	3.24
5000	1.5686	60.49	51.66	27.09	20.45	32.29	69.42	679.82	44	430.86	4156.28	4344.2	4250.24	4.42
6000	1.9017	60.5	51.09	26.19	20.46	32.44	69.42	679.82	60	587.54	4429.29	4545.4	4487.35	2.59
7000	2.2338	60.37	50.59	25.62	20.44	32.4	70.35	688.89	77	754.01	4603.45	4827.15	4715.3	4.74
8000	2.5693	60.27	50.17	25.07	20.44	32.39	70.81	693.42	96	940.07	4754.07	4962.93	4858.5	4.3
9000	2.9016	60.32	49.8	24.74	20.44	32.37	71.28	697.95	117	1145.7	4951.76	5205.55	5078.66	5
10000	3.2395	60.49	49.54	24.32	20.45	32.5	71.28	697.95	139	1361.1	5154.17	5230.82	5192.49	1.48
Experimental Conditions: Hot Water Inlet Temperature: 60 ± 0.5 °C Hot Water Mass Flowrate: 0.2 kg/s														
3000	0.8908	60.32	55.41	31.92	20.5	31.54	180.5	1767.5	18	176.26	4108.69	4240.49	4174.59	3.16
4000	1.211	60.28	54.63	30.18	20.5	32.07	180.5	1767.5	29	283.98	4727.92	4887.38	4807.65	3.32
5000	1.5457	60.37	54.09	28.58	20.25	32.8	181.4	1776.6	43	421.07	5255.1	5369.36	5312.23	2.15
6000	1.8624	60.25	53.54	27.97	20.5	32.66	181.4	1776.6	57	558.17	5614.93	5801.99	5708.46	3.28
7000	2.198	60.49	53.35	27.11	20.35	33.19	182.4	1785.7	75	734.43	5974.75	6197.54	6086.14	3.66
8000	2.5196	60.4	52.95	26.7	20.5	33.07	182.4	1785.7	93	910.69	6234.16	6515.79	6374.97	4.42
9000	2.8575	60.27	52.49	26.06	20.44	33.12	182.4	1785.7	113	1106.5	6510.3	6698.94	6604.62	2.86
10000	3.1912	60.48	52.28	25.62	20.44	33.33	183.3	1794.7	135	1322	6861.76	6895.93	6878.84	0.5
Experimental Conditions: Hot Water Inlet Temperature: 70 ± 0.5 °C Hot Water Mass Flowrate: 0.1125 kg/s														
3000	0.8846	70.45	61.43	32.55	20.5	39.4	66.65	652.63	18	176.26	4245.71	4443.05	4344.38	4.54
4000	1.2049	70.5	60.05	30.7	20.43	39.71	66.65	652.63	29	283.98	4918.82	5158.93	5038.87	4.77
5000	1.5434	70.3	58.93	28.8	20.16	40.12	66.65	652.63	42	411.28	5351.86	5560.87	5456.37	3.83
6000	1.8812	70.2	58.15	27.54	20.05	40.34	67.57	661.7	58	567.96	5671.94	5876.96	5774.45	3.55
7000	2.2199	70.42	57.67	26.71	19.89	40.67	67.57	661.7	76	744.22	6001.43	6315.42	6158.42	5.1
8000	2.5233	70.19	57.14	26.57	20.5	40.03	68.5	670.76	93	910.69	6142.64	6388.82	6265.73	3.93
9000	2.8601	70.46	56.98	26.02	20.4	40.38	68.5	670.76	112	1096.7	6345.04	6705.2	6525.12	5.52
10000	3.1875	70.45	56.54	25.67	20.49	40.26	68.96	675.29	134	1312.2	6547.44	6887.85	6717.64	5.07

**Table C-11:** Experimental Results of Annulus-Side Heat Transfer Enhancement for Two Annulus Sizes (Enhancement Status: Wire Coil,  $e = 2.2$  mm,  $p = 10$  mm).

**Table C-12:** Experimental Results of Annulus-Side Heat Transfer Enhancement for Two Annulus Sizes (Enhancement Status: Wire Coil,  $e=2.2$  mm,  $p=20$  mm).

Re	$Q_c \cdot 10^{-4}$ (m <sup>3</sup> /s)	Temperatures and Temperature Difference (°C)					Pressure Drop				Heat Transfer Rate (W)			
		T <sub>h1</sub>	T <sub>h2</sub>	T <sub>c1</sub>	T <sub>c2</sub>	LMTD	Inner tube		Annulus		q <sub>h</sub>	q <sub>c</sub>	q <sub>avg.</sub>	Dev. %
Annul -us							mmH <sub>2</sub> O	N/m <sup>2</sup>	mmH <sub>2</sub> O	N/m <sup>2</sup>				
Annulus Dimensions: L=1.245 m D <sub>o</sub> =0.028 m D <sub>i</sub> =0.0125 m														
Experimental Conditions: Hot Water Inlet Temperature: 60 ± 0.5 °C Hot Water Mass Flowrate: 0.1125 kg/s														
3000	0.8523	60.26	52.62	30.09	19.89	31.43	206.4	2021.3	28	274.19	3596.15	3624.78	3610.47	0.79
4000	1.1627	60.09	51.42	28.19	19.77	31.77	207.3	2030.4	47	460.24	4080.97	4083.18	4082.07	0.05
5000	1.4473	60.04	50.77	27.87	20.46	31.23	207.3	2030.4	71	695.26	4363.39	4472.6	4417.99	2.47
6000	1.7499	60.31	50.3	27.21	20.46	31.44	208.3	2039.5	97	949.86	4711.71	4926.5	4819.1	4.46
7000	2.0585	60	49.55	26.45	20.5	31.25	208.3	2039.5	134	1312.2	4918.82	5108.92	5013.87	3.79
8000	2.367	60.34	48.97	25.97	20.45	31.35	209.7	2053.1	167	1635.3	5351.86	5450.39	5401.13	1.82
9000	2.6904	60.17	48.34	25.28	20.26	31.37	210.1	2057.6	215	2105.4	5569.95	5640.07	5605.01	1.25
10000	3.002	60.17	47.83	24.81	20.36	31.25	210.1	2057.6	275	2692.9	5810.01	5573.56	5691.78	4.15
Experimental Conditions: Hot Water Inlet Temperature: 60 ± 0.5 °C Hot Water Mass Flowrate: 0.1125 kg/s														
3000	0.8376	60.14	55.13	31.76	19.77	31.74	576.7	5647.1	27	264.39	4192.37	4186.74	4189.55	0.13
4000	1.1336	59.92	54.25	30.31	19.89	31.93	577.6	5656.1	45	440.66	4744.66	4924.94	4834.8	3.73
5000	1.4181	60.03	53.7	29.63	20.5	31.78	577.6	5656.1	67	656.09	5296.94	5398.34	5347.64	1.9
6000	1.7179	59.86	52.96	28.79	20.5	31.76	579.5	5674.3	95	930.28	5773.92	5938.66	5856.29	2.81
7000	2.0227	60.41	52.85	28	20.48	32.39	580.4	5683.3	131	1282.8	6326.21	6343.61	6334.91	0.27
8000	2.3286	60.2	52.19	27.34	20.5	32.27	580.4	5683.3	163	1596.2	6702.77	6643.16	6672.96	0.89
9000	2.6477	60.09	51.61	26.64	20.27	32.38	581.8	5696.9	210	2056.4	7098.85	7031.6	7065.22	0.95
10000	2.9559	60.09	51.29	26.23	20.27	32.42	583.2	5710.5	269	2634.2	7366.63	7344.79	7355.71	0.3
Experimental Conditions: Hot Water Inlet Temperature: 70 ± 0.5 °C Hot Water Mass Flowrate: 0.1125 kg/s														
3000	0.8299	69.61	60.03	32.7	19.66	38.61	203.6	1994.2	26	254.6	4509.31	4511.13	4510.22	0.04
4000	1.1217	69.84	59.05	31.09	20.05	38.87	205.5	2012.3	43	421.07	5078.85	5162.68	5120.77	1.64
5000	1.4295	69.72	57.96	29.53	19.89	39.12	206.4	2021.3	65	636.5	5535.43	5746.24	5640.83	3.74
6000	1.7298	70.5	57.54	28.72	19.96	39.64	206.4	2021.3	93	910.69	6100.27	6319.42	6209.84	3.53
7000	2.0195	70.46	56.86	28.24	20.38	39.28	206.4	2021.3	130	1273	6401.52	6619.75	6510.64	3.35
8000	2.3509	70.06	55.56	26.99	20.02	39.18	206.4	2021.3	160	1566.8	6825.15	6834.92	6830.03	0.14
9000	2.6637	70.03	54.95	26.4	19.99	39.13	206.4	2021.3	205	2007.4	7098.94	7118.83	7108.89	0.28
10000	2.9787	70	54.36	25.88	19.96	39.06	206.4	2021.3	262	2565.6	7361.75	7356.49	7359.12	0.07
Experimental Conditions: Hot Water Inlet Temperature: 70 ± 0.5 °C Hot Water Mass Flowrate: 0.2 kg/s														
3000	0.8025	70.18	63.74	35.66	19.77	39.05	575.8	5638	24	235.02	5388.99	5313.2	5351.1	1.42
4000	1.0962	70.07	62.65	33.32	19.89	39.68	576.2	5642.5	43	421.07	6209.06	6136.21	6172.63	1.18
5000	1.3783	69.85	61.68	32.22	20.46	39.4	576.7	5647.1	64	626.71	6836.66	6756.3	6796.48	1.18
6000	1.6721	70.51	61.7	31.28	20.42	40.25	577.6	5656.1	92	900.9	7372.21	7569.82	7471.01	2.64
7000	1.9667	70.47	61.06	30.47	20.5	40.28	578.5	5665.2	126	1233.8	7874.29	8174.74	8024.51	3.74
8000	2.2697	70.29	60.3	29.65	20.45	40.24	578.5	5665.2	157	1537.4	8359.63	8706.53	8533.08	4.07
9000	2.5957	70.23	59.68	28.4	20.25	40.62	579.9	5678.8	202	1978.1	8826.85	8824.06	8825.45	0.03
10000	2.9035	70.23	59.26	27.81	20.25	40.69	580.4	5683.3	258	2526.4	9178.3	9156.93	9167.62	0.23
Annulus Dimensions: L=1.245 m D <sub>o</sub> =0.028 m D <sub>i</sub> =0.0155 m														
Experimental Conditions: Hot Water Inlet Temperature: 60 ± 0.5 °C Hot Water Mass Flowrate: 0.1125 kg/s														
3000	0.9161	59.85	51.69	29.96	19.95	30.81	71.7	702.49	71	695.26	3840.91	3823.81	3832.36	0.45
4000	1.2357	59.96	50.98	28.42	20.47	31.02	72.2	707.02	119	1165.3	4226.89	4096.71	4161.8	3.13
5000	1.5625	59.78	50.36	27.38	20.5	31.11	72.2	707.02	179	1752.8	4433.99	4483.53	4458.76	1.11
6000	1.8938	60.29	50.15	26.51	20.5	31.67	74.1	725.15	251	2457.9	4772.9	4747.56	4760.23	0.53
7000	2.2427	59.7	49.41	25.54	20.18	31.63	71.3	697.95	332	3251.1	4843.5	5014.85	4929.18	3.48
8000	2.5717	60.3	49.51	25.25	20.18	32.11	73.1	716.08	393	3848.4	5078.85	5439.69	5259.27	6.86
9000	2.8925	59.87	49.05	24.94	20.51	31.63	71.3	697.95	485	4749.3	5092.97	5345.89	5219.43	4.85
10000	3.2397	59.96	48.71	24.44	20.33	31.82	72.2	707.02	593	5806.9	5297.39	5559.27	5428.33	4.82
Experimental Conditions: Hot Water Inlet Temperature: 60 ± 0.5 °C Hot Water Mass Flowrate: 0.2 kg/s														
3000	0.8814	60.23	54.7	32.96	20.42	30.64	181	1776.6	68	665.88	4627.5	4606.76	4617.13	0.45
4000	1.2137	60.12	53.71	30.53	19.95	31.63	181	1776.6	116	1135.9	5363.89	5353.92	5358.9	0.19
5000	1.5395	60	53.04	29	20.18	31.92	181	1776.6	179	1752.8	5824.13	5662.42	5743.28	2.82
6000	1.8592	60.2	52.73	28.2	20.42	32.15	182	1785.7	246	2408.9	6250.9	6032.35	6141.62	3.56
7000	2.1845	59.75	52.11	27.5	20.5	31.93	182	1785.7	321	3143.4	6393.15	6377.57	6385.36	0.24
8000	2.502	59.5	51.66	27.06	20.75	31.67	184	1803.8	380	3721.1	6560.51	6584.65	6572.58	0.37
9000	2.8492	59.97	51.69	26.38	20.37	32.44	183	1794.7	470	4602.4	6925.91	7142.94	7034.43	3.09
10000	3.1823	59.97	51.44	25.93	20.37	32.53	183	1794.7	572	5601.2	7135.11	7381.03	7258.07	3.39
Experimental Conditions: Hot Water Inlet Temperature: 70 ± 0.5 °C Hot Water Mass Flowrate: 0.1125 kg/s														
3000	0.8793	70.02	59.57	33.65	19.95	37.97	69.4	679.82	68	665.88	4918.82	5020.61	4969.71	2.05
4000	1.2042	70.22	58.64	31.23	19.95	38.84	69.4	679.82	115	1126.1	5450.71	5663.09	5556.9	3.82
5000	1.5269	70.22	57.6	29.73	20.18	38.93	69.4	679.82	173	1694.1	5940.23	6080.16	6010.2	2.33
6000	1.866	70.12	56.88	28.23	20.07	39.3	70.3	688.89	241	2360	6232.07	6350.34	6291.21	1.88
7000	2.2003	70.22	56.36	27.3	20.07	39.51	70.3	688.89	315	3084.6	6523.9	6635.35	6579.63	1.69
8000	2.5382	70.32	55.94	26.49	20.07	39.72	70.3	688.89	378	3701.5	6768.67	6797.48	6783.07	0.42
9000	2.8473	69.82	55.23	26.33	20.48	38.96	69.4	679.82	468	4582.8	6867.51	6947.92	6907.72	1.16
10000	3.209	70.13	54.88	25.47	20.11	39.51	70.8	693.42	560					

**Table C-13:** Experimental Results of Annulus-Side Heat Transfer Enhancement for Two Annulus Sizes (Enhancement Status: Wire Coil,  $e = 2.2$  mm,  $p = 30$  mm).

**Table C-14:** Experimental Results of Annulus-Side Heat Transfer Enhancement for Two Annulus Sizes (Enhancement Status: Wire Coil,  $e=2.2$  mm,  $p=40$  mm).

Re	$Q_c \cdot 10^{-4}$ (m <sup>3</sup> /s)	Temperatures and Temperature Difference (°C)					Pressure Drop				Heat Transfer Rate (W)			
		T <sub>h1</sub>	T <sub>h2</sub>	T <sub>c1</sub>	T <sub>c2</sub>	LMTD	Inner tube		Annulus		q <sub>h</sub>	q <sub>c</sub>	q <sub>avg.</sub>	Dev. %
Annul -us							mmH <sub>2</sub> O	N/m <sup>2</sup>	mmH <sub>2</sub> O	N/m <sup>2</sup>				
Annulus Dimensions: L=1.245 m D <sub>o</sub> =0.028 m D <sub>i</sub> =0.0125 m														
Experimental Conditions: Hot Water Inlet Temperature: 60 ± 0.5 °C Hot Water Mass Flowrate: 0.1125 kg/s														
3000	0.848	59.95	53.05	30	20.43	31.27	202.7	1985.1	18	176.26	3247.83	3383.54	3315.69	4.09
4000	1.1482	60.22	52.26	28.56	20.5	31.71	203.6	1994.2	30	293.77	3746.77	3859.42	3803.1	2.96
5000	1.448	60.48	51.68	27.1	19.99	32.53	203.6	1994.2	46	450.45	4142.16	4353.57	4247.87	4.98
6000	1.7652	60.39	50.9	26.45	20.46	32.16	204.6	2003.2	65	636.5	4466.94	4410.57	4438.75	1.27
7000	2.0723	60.5	50.5	26.03	20.34	32.27	205.5	2012.3	85	832.35	4707	4918.84	4812.92	4.4
8000	2.3852	60.49	50.05	25.37	20.39	32.31	205.5	2012.3	108	1057.6	4914.11	4955.37	4934.74	0.84
9000	2.6905	60.25	49.35	25.09	20.44	31.93	207.3	2030.4	131	1282.8	5130.63	5219.47	5175.05	1.72
10000	3.0073	60.35	49.19	24.71	20.31	32.14	207.3	2030.4	160	1566.8	5253.01	5520.7	5386.86	4.97
Experimental Conditions: Hot Water Inlet Temperature: 60 ± 0.5 °C Hot Water Mass Flowrate: 0.2 kg/s														
3000	0.8393	60.49	55.79	31.3	20.05	32.35	573.9	5619.9	16.5	161.57	3932.96	3936.32	3934.64	0.09
4000	1.1411	59.9	54.75	29.49	20.12	32.47	573.9	5619.9	28	274.19	4309.52	4458.54	4384.03	3.4
5000	1.4321	60.42	54.57	28.86	20.4	32.85	574.8	5628.9	42	411.28	4895.28	5052.1	4973.69	3.15
6000	1.7365	60.4	53.96	27.84	20.5	33.01	576.7	5647.1	60	587.54	5388.99	5315.8	5352.4	1.37
7000	2.0453	60.35	53.4	27.17	20.34	33.12	576.7	5647.1	76	744.22	5815.76	5826.49	5821.12	0.18
8000	2.3428	60.5	52.98	26.81	20.5	33.08	576.7	5647.1	103	1008.6	6292.74	6166.17	6229.45	2.03
9000	2.6475	60.38	52.59	26.44	20.48	33.02	577.6	5656.1	126	1233.8	6518.67	6581.95	6550.31	0.97
10000	2.9646	60.44	52.06	25.94	20.31	33.11	577.6	5656.1	150	1468.9	7012.38	6962.59	6987.49	0.71
Experimental Conditions: Hot Water Inlet Temperature: 70 ± 0.5 °C Hot Water Mass Flowrate: 0.1125 kg/s														
3000	0.8331	69.92	61.26	32.03	19.99	39.56	201.8	1976	15.5	151.78	4076.26	4181.09	4128.68	2.54
4000	1.1333	70.35	60.4	30.11	20.11	40.26	202.3	1980.6	26.5	259.5	4683.47	4725.36	4704.41	0.89
5000	1.4347	70.29	59.4	28.85	20.25	40.28	202.7	1985.1	39.5	386.8	5125.92	5145.13	5135.53	0.37
6000	1.7344	70.35	59.01	28	20.45	40.43	203.6	1994.2	56.5	553.27	5337.74	5460.96	5399.35	2.28
7000	2.035	70.2	58.27	27.45	20.5	40.21	203.6	1994.2	73	714.84	5615.45	5898.74	5757.09	4.92
8000	2.3453	70.34	57.23	26.72	20.5	40.08	205.5	2012.3	92	900.9	6170.88	6084.58	6127.73	1.41
9000	2.6959	70.39	57	25.55	19.81	40.9	206.4	2021.3	117	1145.7	6302.67	6455.87	6379.27	2.4
10000	2.9715	70.5	56.68	25.68	20.37	40.42	206.4	2021.3	141	1380.7	6505.07	6582.24	6543.66	1.18
Experimental Conditions: Hot Water Inlet Temperature: 70 ± 0.5 °C Hot Water Mass Flowrate: 0.2 kg/s														
3000	0.8162	69.6	64.04	34	19.87	39.73	567.4	5556.4	15	146.89	4652.61	4806.66	4729.63	3.26
4000	1.1105	69.77	63.45	31.99	20.05	40.53	567.4	5556.4	25	244.81	5288.58	5527.25	5407.91	4.41
5000	1.3979	70.33	63.22	30.94	20.47	41.05	567.4	5556.4	37	362.32	5945.69	6101.54	6025.59	2.52
6000	1.6971	70.48	62.76	29.87	20.5	41.43	569.3	5574.6	53	519	6460.1	6630.18	6545.14	2.6
7000	1.9997	70.32	61.82	29.19	20.3	41.32	569.3	5574.6	72	705.05	7112.8	7412.91	7262.86	4.13
8000	2.3043	70.49	61.36	28.5	20.26	41.54	569.7	5579.1	90	881.31	7639.98	7918.44	7799.21	3.58
9000	2.6212	70.17	60.64	27.55	20.24	41.5	571.1	5592.7	115	1126.1	7970.52	7989.73	7980.13	0.24
10000	2.9275	70.17	60.15	27.1	20.24	41.47	571.1	5592.7	137	1341.6	8380.55	8374.43	8377.49	0.07
Annulus Dimensions: L=1.245 m D <sub>o</sub> =0.028 m D <sub>i</sub> =0.0155 m														
Experimental Conditions: Hot Water Inlet Temperature: 60 ± 0.5 °C Hot Water Mass Flowrate: 0.1125 kg/s														
3000	0.9221	60.05	51.56	29.61	19.72	31.13	69.4	679.82	43	421.07	3996.24	3803.08	3899.66	4.95
4000	1.2343	60.06	50.85	28.57	20.42	30.96	69.4	679.82	74	724.64	4335.15	4194.95	4265.05	3.29
5000	1.5625	59.58	49.85	27.38	20.5	30.75	69.4	679.82	110	1077.2	4579.91	4483.53	4531.72	2.13
6000	1.8962	59.8	49.62	26.43	20.47	31.21	70.3	688.89	156	1527.6	4791.73	4714.1	4752.91	1.63
7000	2.2256	59.99	49.2	25.88	20.5	31.33	70.3	688.89	202	1978.1	5078.85	4994.78	5036.82	1.67
8000	2.5538	60.47	49.08	25.53	20.5	31.65	71.3	697.95	260	2546	5361.27	5358.87	5360.07	0.04
9000	2.8986	60.04	48.19	24.77	20.5	31.33	71.3	697.95	320	3133.6	5577.8	5163.75	5370.77	7.71
10000	3.2297	60	48.09	24.53	20.5	31.36	71.7	702.49	395	3868	5605.36	5430.37	5517.87	3.17
Experimental Conditions: Hot Water Inlet Temperature: 60 ± 0.5 °C Hot Water Mass Flowrate: 0.2 kg/s														
3000	0.8951	59.93	54.41	32.15	19.84	31.05	181	1767.5	41	401.49	4619.14	4593.06	4606.1	0.57
4000	1.2136	59.93	53.85	30.42	20.07	31.6	181	1767.5	70	685.47	5087.74	5236.93	5162.34	2.89
5000	1.5401	59.8	52.94	29	20.15	31.78	181	1776.6	105	1028.2	5740.45	5683.64	5712.04	0.99
6000	1.8748	59.5	52.21	27.91	19.98	31.91	182	1785.7	154	1508	6100.27	6200.63	6150.45	1.63
7000	2.2031	59.81	51.88	27.19	20.07	32.21	182	1785.7	205	2007.4	6635.82	6542.75	6589.29	1.41
8000	2.5417	59.95	51.56	26.49	19.95	32.53	182	1785.7	254	2487.3	7020.75	6934.25	6977.5	1.24
9000	2.8293	59.4	51.05	26.76	20.6	31.53	183	1794.7	316	3094.4	6987.28	7269.45	7128.36	3.96
10000	3.1925	59.97	50.93	25.93	20.09	32.41	183	1794.7	389	3809.2	7564.67	7772.1	7668.39	2.71
Experimental Conditions: Hot Water Inlet Temperature: 70 ± 0.5 °C Hot Water Mass Flowrate: 0.1125 kg/s														
3000	0.8838	70.1	59.64	33.19	19.95	38.28	69	675.29	40	391.7	4932.52	4876.93	4900.22	0.95
4000	1.1963	69.91	58.48	31.29	20.48	38.31	68.5	670.76	69	675.67	5380.1	5391.16	5385.63	0.21
5000	1.5222	69.55	57.37	29.68	20.5	38.35	69	675.29	105	1028.2	5733.13	5826.65	5779.89	1.62
6000	1.8483	69.55	56.58	28.64	20.5	38.44	69.4	679.82	150	1468.9	6104.98	6273.91	6189.45	2.73
7000	2.179	69.49	55.94	27.72	20.5	38.52	69.4	679.82	200	1958.5	6377.99	6561.33	6469.66	2.83
8000	2.51	69.6	55.49	27.03	20.5	38.66	69.9	684.36	255	2497.1	6641.58	6836.36	6738.97	2.89
9000	2.8527	69.7	54.96	26.24	20.41	38.84	71.3	697.95	310	3035.6	6938.12	6943.45	6940.78	0.08
10000	3.1877	69.7	54.46	25.75	20.41	38.79	71.3	697.95	385	3770.1	7173.47	7107.67	7140.57</	

**Table C-15:** Experimental Results of Annulus-Side Heat Transfer Enhancement for Two Annulus Sizes (Enhancement Status: Circular Rib,  $e = 2.2$  mm,  $p = 10$  mm).

**Table C-16:** Experimental Results of Annulus-Side Heat Transfer Enhancement for Two Annulus Sizes (Enhancement Status: Circular Rib,  $e = 2.2$  mm,  $p = 20$  mm).

<b>Re</b>	$Q_c \times 10^{-4}$ ( $\text{m}^3/\text{s}$ )	Temperatures and Temperature Difference ( $^{\circ}\text{C}$ )					Pressure Drop				Heat Transfer Rate (W)								
		$T_{h1}$	$T_{h2}$	$T_{c1}$	$T_{c2}$	LMTD	Inner tube		Annulus		$q_h$	$q_c$	$q_{avg.}$	Dev. %					
Annulus Dimensions: $L=1.245\text{ m}$ $D_o=0.028\text{ m}$ $D_i=0.0125\text{ m}$																			
Experimental Conditions: Hot Water Inlet Temperature: $60 \pm 0.5\text{ }^{\circ}\text{C}$ Hot Water Mass Flowrate: $0.1125\text{ kg/s}$																			
3000	0.8512	59.92	52.36	30.09	20	31.08	206.4	2021.3	43	421.07	3556.99	3581.21	3569.1	0.68					
4000	1.1503	60.07	51.4	28.69	20.21	31.28	207.3	2030.4	71	695.26	4081.7	4067.99	4074.84	0.34					
5000	1.4511	60.3	50.76	27.77	20.33	31.47	208.3	2039.5	110	1077.2	4488.69	4502.63	4495.66	0.31					
6000	1.7652	60.3	50.06	26.75	20.16	31.69	208.3	2039.5	155	1517.8	4821.23	4852.36	4836.8	0.64					
7000	2.0625	60.21	49.37	26.35	20.43	31.34	209.2	2048.5	202	1978.1	5102.39	5093.24	5097.81	0.18					
8000	2.3791	60.32	48.96	25.67	20.31	31.56	209.7	2053.1	260	2546	5345.94	5319.74	5332.84	0.49					
9000	2.6868	60.14	48.33	25.28	20.37	31.28	211	2066.7	321	3143.4	5560.76	5503.54	5532.15	1.03					
10000	3.0049	60.17	47.95	24.81	20.28	31.36	212	2075.7	391	3828.8	5752.93	5679.12	5716.03	1.29					
Experimental Conditions: Hot Water Inlet Temperature: $60 \pm 0.5\text{ }^{\circ}\text{C}$ Hot Water Mass Flowrate: $0.2\text{ kg/s}$																			
3000	0.8339	59.97	55.09	31.89	20.04	31.43	576.7	5647.1	41	401.49	4086.11	4119.27	4102.69	0.81					
4000	1.1314	59.83	54.03	30.31	20.06	31.69	578.5	5665.2	71	695.26	4852	4835.24	4843.62	0.35					
5000	1.4181	60.4	53.89	29.63	20.5	32.06	579.1	5670.6	105	1028.2	5446.07	5398.34	5422.2	0.88					
6000	1.7259	60.2	53.11	28.59	20.29	32.21	579.5	5674.3	148	1449.3	5931.46	5973.83	5952.64	0.71					
7000	2.0283	60.22	52.64	27.87	20.37	32.31	581.3	5692.4	196	1919.3	6341.85	6344.27	6343.06	0.04					
8000	2.345	60	52	27	20.23	32.38	580.4	5683.3	253	2477.5	6697.34	6621.83	6659.59	1.13					
9000	2.6475	60	51.62	26.64	20.28	32.34	581.3	5692.4	312	3055.2	7010.91	7023.69	7017.3	0.18					
10000	2.9557	60.11	51.4	26.24	20.27	32.48	583.2	5710.5	378	3701.5	7291.41	7360.66	7326.03	0.95					
Experimental Conditions: Hot Water Inlet Temperature: $70 \pm 0.5\text{ }^{\circ}\text{C}$ Hot Water Mass Flowrate: $0.1125\text{ kg/s}$																			
3000	0.8284	69.85	60.35	32.82	19.71	38.8	206	2016.8	40	391.7	4473.81	4526.72	4500.27	1.18					
4000	1.1239	69.96	58.99	31.09	19.87	38.99	206.9	2025.9	70	685.47	5164.59	5257.54	5211.07	1.78					
5000	1.4272	70.1	57.99	29.53	20.03	39.25	207.3	2030.4	106	1038	5700.4	5653.73	5677.07	0.82					
6000	1.728	69.92	56.88	28.72	20.05	38.97	207.3	2030.4	148	1449.3	6138.19	6248.02	6193.11	1.77					
7000	2.0322	70.21	56.38	27.91	20.16	39.18	207.3	2030.4	197	1929.1	6508.33	6568.62	6538.47	0.92					
8000	2.3409	70.25	55.74	27.21	20.17	39.19	207.3	2030.4	252	2467.7	6828.97	6873.94	6851.45	0.66					
9000	2.6561	70.23	55.12	26.52	20.12	39.19	207.8	2034.9	314	3074.8	7111.79	7090.97	7101.38	0.29					
10000	2.9721	70.17	54.52	26.03	20	39.14	207.8	2034.9	380	3721.1	7364.78	7476.5	7420.64	1.51					
Experimental Conditions: Hot Water Inlet Temperature: $70 \pm 0.5\text{ }^{\circ}\text{C}$ Hot Water Mass Flowrate: $0.2\text{ kg/s}$																			
3000	0.8004	69.91	63.62	35.79	19.88	38.73	577.8	5658	38	372.11	5264.4	5305.92	5285.16	0.79					
4000	1.0887	70.23	62.82	33.61	20.23	39.53	578.1	5660.7	65	636.5	6197	6070.72	6133.86	2.06					
5000	1.3792	70.39	62.12	32.32	20.3	39.92	578.5	5665.2	99	969.45	6920.38	6910.31	6915.34	0.15					
6000	1.6835	69.95	60.97	30.91	20.18	39.91	578.5	5665.2	141	1380.7	7511.43	7530.82	7521.13	0.26					
7000	1.9826	70.16	60.59	30.01	20.24	40.25	578.5	5665.2	187	1831.2	8011.15	8076.42	8043.79	0.81					
8000	2.2722	70.31	60.22	29.51	20.49	40.26	579.5	5674.3	236	2311	8444.03	8545.91	8494.97	1.2					
9000	2.5941	70.35	59.8	28.4	20.3	40.71	579.9	5678.8	301	2947.5	8825.85	8762.93	8794.39	0.72					
10000	2.8876	70.5	59.54	28.11	20.43	40.73	580.4	5683.3	361	3535	9167.41	9248.73	9208.07	0.88					
Annulus Dimensions: $L=1.245\text{ m}$ $D_o=0.028\text{ m}$ $D_i=0.0155\text{ m}$																			
Experimental Conditions: Hot Water Inlet Temperature: $60 \pm 0.5\text{ }^{\circ}\text{C}$ Hot Water Mass Flowrate: $0.1125\text{ kg/s}$																			
3000	0.9153	59.94	51.86	29.97	20.02	30.89	71.3	697.95	113	1102.9	3804.1	3797.43	3800.76	0.18					
4000	1.2369	60.03	51.12	28.41	20.39	31.17	72.2	707.02	191	1870.3	4193.82	4137.05	4165.44	1.36					
5000	1.565	59.98	50.43	27.29	20.45	31.31	72.7	711.55	288	2820.2	4496.12	4464.69	4480.41	0.7					
6000	1.8945	60.21	50.13	26.51	20.47	31.64	72.2	707.02	402	3936.5	4743.12	4772.93	4758.02	0.63					
7000	2.2424	60.01	49.49	25.5	20.23	31.81	73.1	716.08	530	5190	4951.95	4930.07	4941.01	0.44					
8000	2.5835	60.15	49.25	24.91	20.13	32.08	74.1	725.15	693	6786.1	5132.85	5152.18	5142.51	0.38					
9000	2.9129	59.81	48.57	24.64	20.21	31.64	74.1	725.15	854	8362.7	5292.41	5383.87	5338.14	1.71					
10000	3.2501	60.02	48.47	24.22	20.27	31.85	73.1	716.08	1045	10233	5435.14	5354.66	5394.9	1.49					
Experimental Conditions: Hot Water Inlet Temperature: $60 \pm 0.5\text{ }^{\circ}\text{C}$ Hot Water Mass Flowrate: $0.2\text{ kg/s}$																			
3000	0.8835	60.21	54.64	32.95	20.22	30.7	181	1767.5	108	1057.6	4662.26	4687.5	4674.88	0.54					
4000	1.2137	60.15	53.86	30.51	19.97	31.72	181	1767.5	188	1841	5266.73	5333.68	5300.2	1.26					
5000	1.5401	60.12	53.27	29.02	20.13	32.11	181	1772.1	283	2771.2	5735.59	5709.33	5722.46	0.46					
6000	1.8563	60.06	52.75	28.34	20.42	32.02	181	1776.3	390	3819	6118.67	6131.02	6124.85	0.2					
7000	2.1842	59.86	52.16	27.53	20.48	32	181	1776.6	510	4994.1	6442.57	6422.39	6432.48	0.31					
8000	2.5138	59.6	51.57	26.94	20.46	31.88	181	1776.6	660	6463	6723.14	6794.25	6758.69	1.05					
9000	2.8568	60	51.67	26.24	20.28	32.56	182	1785.7	825	8078.7	6970.62	7102.55	7036.59	1.87					
10000	3.1879	60.11	51.52	25.82	20.33	32.71	182	1785.7	1001	9802.2	7192	7300.91	7246.46	1.5					
Experimental Conditions: Hot Water Inlet Temperature: $70 \pm 0.5\text{ }^{\circ}\text{C}$ Hot Water Mass Flowrate: $0.1125\text{ kg/s}$																			
3000	0.8789	70.11	59.42	33.66	19.98	37.92	69.4	679.82	103	1008.6	5032.39	5011.06	5021.73	0.42					
4000	1.204	70.17	58.39	31.21	19.99	38.68	70.1	686.17	177	1733.3	5544.95	5631.69	5588.32	1.55					
5000	1.5283	70.28	57.66	29.69	20.14	39.03	69.4	679.82	260	2546	5942.51	6085.7	6014.11	2.38					
6000	1.8643	70.11	56.8	28.22	20.16	39.2	70.3	688.89	385	3770.1	6267.35	6266.74	6267.04	0.01					
7000	2.2041	70.24	56.34	27.19	20.03	39.59	71.3	697.95	527	5160.6	6541.99	6582.57	6562.28	0.62					
8000	2.5344	70.29	55.89	26.52	20.17	39.61	71.3	697.95	663	6492.3	6779.9	6713.17	6746.53	0.99					
9000	2.8509	69.87	55.02	26.32	20.38	38.93	70.3	688.89	802	7853.5	6989.75	7063.86	7026.81	1.05					
10000	3.2097	70.15	54.9	25.44	20.12	39.54	70.3	688.89	985	9645.									

**Table C-17:** Experimental Results of Annulus-Side Heat Transfer Enhancement for Two Annulus Sizes (Enhancement Status: Circular Rib,  $e = 2.2$  mm,  $p = 30$  mm).

Re	$Q_c \times 10^{-4}$ (m <sup>3</sup> /s)	Temperatures and Temperature Difference (°C)					Pressure Drop				Heat Transfer Rate (W)			
		T <sub>h1</sub>	T <sub>h2</sub>	T <sub>c1</sub>	T <sub>c2</sub>	LMTD	Inner tube		Annulus		q <sub>h</sub>	q <sub>c</sub>	q <sub>avg.</sub>	Dev. %
Annul -us							mmH <sub>2</sub> O	N/m <sup>2</sup>	mmH <sub>2</sub> O	N/m <sup>2</sup>				
Annulus Dimensions: L=1.245 m D <sub>o</sub> =0.028 m D <sub>i</sub> =0.0125 m														
Experimental Conditions: Hot Water Inlet Temperature: 60 ± 0.5 °C Hot Water Mass Flowrate: 0.1125 kg/s														
3000	0.8462	60.33	52.95	30.26	20.36	31.31	203.6	1994.2	31.6	309.48	3472.92	3492.68	3482.8	0.57
4000	1.1541	60.43	52.07	28.4	20.21	31.95	204.6	2003.2	55	538.58	3933.84	3941.99	3937.91	0.21
5000	1.4592	60.43	51.31	27.31	20.3	32.05	203.6	1994.2	81	793.18	4291.36	4266.51	4278.94	0.58
6000	1.7742	60.41	50.67	26.31	20.16	32.27	207.3	2030.4	115	1126.1	4583.48	4551.68	4567.58	0.7
7000	2.0726	60.45	50.19	25.95	20.41	32.08	207.3	2030.4	149	1459.1	4830.46	4789.73	4810.1	0.85
8000	2.3863	60.32	49.6	25.39	20.33	32.02	207.3	2030.4	194	1899.7	5044.4	5037.34	5040.87	0.14
9000	2.6949	60.48	49.36	25	20.39	32.12	208.3	2039.5	240	2350.2	5233.12	5183.11	5208.11	0.96
10000	3.0133	60.33	48.85	24.57	20.28	32.03	209.2	2048.5	290	2839.8	5401.93	5393.51	5397.72	0.16
Experimental Conditions: Hot Water Inlet Temperature: 60 ± 0.5 °C Hot Water Mass Flowrate: 0.2 kg/s														
3000	0.8244	60.34	55.2	32.75	20.21	31.15	576.7	5647.1	30	293.77	4298.41	4309.16	4303.79	0.25
4000	1.1268	60.3	54.42	30.67	20.06	31.94	575.8	5638	52	509.2	4922.8	4984.67	4953.73	1.25
5000	1.4229	60.4	53.94	29.5	20.33	32.24	576.7	5647.1	78	763.81	5407.12	5440.55	5423.83	0.62
6000	1.7288	60.42	53.49	28.45	20.28	32.58	577.6	5656.1	109	1067.4	5802.83	5890.41	5846.62	1.5
7000	2.0425	60.22	52.89	27.43	20.2	32.74	577.6	5656.1	147	1439.5	6137.4	6159.15	6148.27	0.35
8000	2.352	60.33	52.65	26.76	20.21	33	578.5	5665.2	188	1841	6427.22	6426.05	6426.64	0.02
9000	2.6604	60.33	52.34	26.22	20.28	33.08	579.5	5674.3	232	2271.8	6682.86	6592.07	6637.46	1.37
10000	2.9797	60.21	51.95	25.68	20.13	33.16	580.4	5683.3	283	2771.2	6911.54	6899.14	6905.34	0.18
Experimental Conditions: Hot Water Inlet Temperature: 70 ± 0.5 °C Hot Water Mass Flowrate: 0.1125 kg/s														
3000	0.8161	70.37	60.86	33.62	20.27	38.64	205.5	2012.3	28	274.19	4476.37	4540.32	4508.35	1.42
4000	1.1177	70.33	59.46	31.24	20.22	39.16	205.5	2012.3	50	489.62	5117.03	5134.75	5125.89	0.35
5000	1.4238	70.21	58.28	29.64	20.13	39.35	205.5	2012.3	77	754.01	5613.97	5646.13	5630.05	0.57
6000	1.7421	69.92	57.13	28.11	19.95	39.45	205.5	2012.3	111	1087	6019.99	5928.78	5974.39	1.53
7000	2.0343	70.47	56.95	27.72	20.26	39.64	205.5	2012.3	145	1419.9	6363.28	6329.4	6346.34	0.53
8000	2.3401	70.45	56.3	27.13	20.28	39.56	207.3	2030.4	186	1821.4	6660.65	6686.1	6673.37	0.38
9000	2.6485	70.43	55.72	26.57	20.32	39.48	208.3	2039.5	229	2242.5	6922.95	6904.62	6913.78	0.27
10000	2.9601	70.42	55.21	26.09	20.29	39.44	209.2	2048.5	279	2732.1	7157.58	7161.93	7159.75	0.06
Experimental Conditions: Hot Water Inlet Temperature: 70 ± 0.5 °C Hot Water Mass Flowrate: 0.2 kg/s														
3000	0.798	69.91	63.79	35.81	20.14	38.68	571.1	5592.7	29	283.98	5121.54	5209.9	5165.72	1.71
4000	1.0863	70.03	62.68	33.81	20.23	39.25	570.1	5582.7	48	470.03	6149.5	6147.83	6148.66	0.03
5000	1.3735	70.33	62.03	32.5	20.5	39.65	571.1	5592.7	74	724.64	6946.85	6869.6	6908.22	1.12
6000	1.6776	69.95	60.87	31.22	20.18	39.7	571.1	5592.7	105	1028.2	7598.33	7721.33	7659.83	1.61
7000	1.9786	70.06	60.32	30.19	20.24	39.98	572.1	5601.8	140	1370.9	8149.15	8208.42	8178.78	0.72
8000	2.2697	70.31	60	29.61	20.49	40.1	573.9	5619.9	176	1723.5	8626.29	8630.82	8628.56	0.05
9000	2.5701	70.35	59.54	29.02	20.5	40.17	574.8	5628.9	217	2124.9	9047.16	9131.08	9089.12	0.92
10000	2.882	70.25	58.99	28.28	20.43	40.24	576.7	5647.1	226	2213.1	9423.64	9434.99	9429.31	0.12
Annulus Dimensions: L=1.245 m D <sub>o</sub> =0.028 m D <sub>i</sub> =0.0155 m														
Experimental Conditions: Hot Water Inlet Temperature: 60 ± 0.5 °C Hot Water Mass Flowrate: 0.1125 kg/s														
3000	0.9065	60.17	51.64	30.72	20.13	30.47	72.2	707.02	87.6	858.02	4013.38	4002.41	4007.9	0.27
4000	1.2254	60.13	50.6	29.18	20.45	30.55	72.2	707.02	148	1449.3	4485.57	4460.7	4473.13	0.56
5000	1.5539	59.81	49.5	27.91	20.45	30.45	73.1	716.08	225	2203.3	4851.83	4834.64	4843.24	0.35
6000	1.8834	60.43	49.49	27.08	20.41	31.16	73.1	716.08	314	3074.8	5151.09	5239.63	5195.36	1.7
7000	2.2163	60.27	48.79	26.31	20.43	31.08	73.1	716.08	418	4093.2	5404.1	5436.08	5420.09	0.59
8000	2.555	60.41	48.46	25.63	20.36	31.32	73.1	716.08	545	5336.8	5623.28	5617.2	5620.24	0.11
9000	2.8993	60.28	47.92	25.03	20.22	31.32	73.1	716.08	669	6551.1	5816.6	5818.15	5817.38	0.03
10000	3.243	60.21	47.49	24.54	20.14	31.33	74.1	725.15	802	7853.5	5989.54	5953.53	5971.53	0.6
Experimental Conditions: Hot Water Inlet Temperature: 60 ± 0.5 °C Hot Water Mass Flowrate: 0.2 kg/s														
3000	0.8822	60.33	54.51	33.3	20	30.62	182	1785.7	85	832.35	4873.32	4890.31	4881.81	0.35
4000	1.1909	60.07	53.3	31.74	20.44	30.54	182	1785.7	142	1390.5	5664.96	5609.64	5637.3	0.98
5000	1.5234	60.49	52.99	30.04	20.07	31.67	182	1785.7	221	2164.1	6279	6333.12	6306.06	0.86
6000	1.8433	60.22	52.12	29.06	20.32	31.48	183	1790.2	303	2967.1	6780.71	6717.88	6749.29	0.93
7000	2.1617	60.14	51.53	28.46	20.46	31.37	183	1794.7	400	3917	7204.9	7211.85	7208.37	0.1
8000	2.492	60.32	51.27	27.7	20.46	31.71	183	1794.7	505	4945.2	7572.35	7524.64	7548.49	0.63
9000	2.8231	60.23	50.79	27.13	20.42	31.72	183	1794.7	645	6316.1	7896.46	7901.07	7898.77	0.06
10000	3.1607	60.26	50.47	26.58	20.31	31.89	183	1794.7	775	7589.1	8186.39	8266.45	8226.42	0.97
Experimental Conditions: Hot Water Inlet Temperature: 70 ± 0.5 °C Hot Water Mass Flowrate: 0.1125 kg/s														
3000	0.8701	70.28	59.19	34.43	20.13	37.43	71.3	697.95	78	763.81	5218.95	5185.11	5202.03	0.65
4000	1.1908	70.5	58.13	31.92	20.27	38.22	71.3	697.95	137	1341.6	5824.8	5782.74	5803.77	0.72
5000	1.5241	70.29	56.92	30.04	20.03	38.54	71.3	697.95	201	1968.3	6294.74	6361.42	6328.08	1.05
6000	1.8464	70.11	55.92	28.94	20.29	38.33	71.3	697.95	295	2888.8	6678.7	6660.13	6669.41	0.28
7000	2.1795	70.32	55.44	27.92	20.28	38.67	72.2	707.02	401	3926.7	7003.34	6944.61	6973.98	0.84
8000	2.5051	70.25	54.77	27.33	20.37	38.51	73.1	716.08	510	4994.1	7284.55	7272.2	7278.38	0.17
9000	2.8435	70.42	54.42	26.81	20.39	38.62	73.1	716.08	645	6316.1	7532.6	7590.37	7561.48	0.76
10000	3.1797	70.34	53.87	26.12	20.25	38.68	73.1	716.08						

**Table C-18:** Experimental Results of Annulus-Side Heat Transfer Enhancement for Two Annulus Sizes (Enhancement Status: Circular Rib,  $e=2.2$  mm,  $p=40$  mm).

Re	$Q_c \cdot 10^{-4}$	Temperatures and Temperature Difference (°C)					Pressure Drop				Heat Transfer Rate (W)			
		T <sub>h1</sub>	T <sub>h2</sub>	T <sub>c1</sub>	T <sub>c2</sub>	LMTD	Inner tube		Annulus		q <sub>h</sub>	q <sub>c</sub>	q <sub>avg.</sub>	Dev. %
Annul -us	(m <sup>3</sup> /s)						mmH <sub>2</sub> O	N/m <sup>2</sup>	mmH <sub>2</sub> O	N/m <sup>2</sup>				
Annulus Dimensions: L=1.245 m D <sub>o</sub> =0.028 m D <sub>i</sub> =0.0125 m														
Experimental Conditions: Hot Water Inlet Temperature: 60 ± 0.5 °C Hot Water Mass Flowrate: 0.1125 kg/s														
3000	0.8477	60.33	53.06	30.10	20.36	31.45	203.2	1989.6	27	264.39	3423.56	3442.47	3433.02	0.55
4000	1.1541	60.23	51.89	28.40	20.21	31.76	203.6	1994.2	43	421.07	3925.51	3941.99	3933.75	0.42
5000	1.4514	60.43	51.26	27.60	20.48	31.80	203.6	1994.2	62	607.13	4314.84	4309.97	4312.41	0.11
6000	1.7699	60.20	50.36	26.52	20.16	31.91	207.3	2030.4	85	832.35	4632.96	4695.57	4664.27	1.34
7000	2.0661	60.45	50.04	26.13	20.50	31.87	206.4	2021.3	111	1087	4901.92	4852.22	4877.07	1.02
8000	2.3805	60.12	49.21	25.60	20.33	31.62	207.3	2030.4	139	1361.1	5134.90	5233.49	5184.19	1.90
9000	2.6915	60.48	49.13	25.11	20.39	31.94	208.3	2039.5	176	1723.5	5340.41	5299.91	5320.16	0.76
10000	3.0045	60.33	48.59	24.74	20.36	31.77	208.3	2039.5	220	2154.3	5524.24	5490.42	5507.33	0.61
Experimental Conditions: Hot Water Inlet Temperature: 60 ± 0.5 °C Hot Water Mass Flowrate: 0.2 kg/s														
3000	0.8301	60.34	55.65	32.00	20.34	31.70	575.2	5632.6	26	254.6	3928.22	4034.63	3981.42	2.67
4000	1.1286	60.30	54.69	30.23	20.36	32.15	575.8	5638	42	411.28	4696.68	4644.37	4670.53	1.12
5000	1.4221	60.40	54.08	29.49	20.39	32.28	576.7	5647.1	60	587.54	5292.75	5395.94	5344.34	1.93
6000	1.7296	60.42	53.51	28.41	20.28	32.62	577.6	5656.1	83	812.77	5779.77	5864.26	5822.01	1.45
7000	2.0394	60.22	52.82	27.45	20.31	32.64	577.6	5656.1	109	1067.4	6191.54	6073.33	6132.43	1.93
8000	2.3361	60.43	52.60	27.11	20.45	32.73	577.6	5656.1	137	1341.6	6548.23	6489.34	6518.79	0.90
9000	2.6439	60.33	52.13	26.65	20.39	32.70	578.5	5665.2	173	1694.1	6862.85	6903.60	6883.23	0.59
10000	2.9618	60.21	51.67	26.10	20.23	32.76	578.5	5665.2	218	2134.7	7144.29	7252.60	7198.45	1.50
Experimental Conditions: Hot Water Inlet Temperature: 70 ± 0.5 °C Hot Water Mass Flowrate: 0.1125 kg/s														
3000	0.8243	70.29	61.23	32.73	20.25	39.25	203.6	1994.2	26	254.6	4263.32	4287.59	4275.46	0.57
4000	1.1256	70.33	59.99	30.61	20.22	39.74	203.6	1994.2	41	401.49	4868.95	4875.78	4872.37	0.14
5000	1.4319	70.21	58.87	29.12	20.15	39.89	205.5	2012.3	59	577.75	5338.71	5356.05	5347.38	0.32
6000	1.7423	69.86	57.70	28.00	20.05	39.72	206	2016.8	81	793.18	5722.53	5776.87	5749.70	0.95
7000	2.0441	70.27	57.42	27.30	20.26	40.00	206	2016.8	110	1077.2	6047.05	6002.16	6024.6	0.75
8000	2.3509	70.33	56.89	26.72	20.29	40.00	205.5	2012.3	138	1351.3	6328.15	6305.38	6316.77	0.36
9000	2.6579	70.42	56.45	26.26	20.32	40.01	206.4	2021.3	172	1684.3	6576.11	6585.92	6581.01	0.15
10000	2.9635	70.45	56.01	25.86	20.42	39.92	206.4	2021.3	212	2076	6797.91	6725.25	6761.58	1.07
Experimental Conditions: Hot Water Inlet Temperature: 70 ± 0.5 °C Hot Water Mass Flowrate: 0.2 kg/s														
3000	0.8060	69.83	64.05	34.89	20.14	39.25	568.7	5569.1	24	235.02	4840.03	4953.73	4896.88	2.32
4000	1.1008	70.03	63.11	32.73	20.10	40.09	569.6	5577.3	39	381.9	5793.51	5795.19	5794.35	0.03
5000	1.3906	70.43	62.62	31.60	20.28	40.56	571.1	5592.7	58	567.96	6533.07	6562.08	6547.58	0.44
6000	1.6977	69.95	61.42	30.34	20.00	40.51	571.1	5592.7	81	793.18	7137.35	7319.04	7228.19	2.51
7000	2.0001	70.06	60.92	29.33	20.14	40.76	572.1	5601.8	107	1047.8	7648.25	7664.82	7656.53	0.22
8000	2.2871	70.37	60.70	28.93	20.49	40.82	573.9	5619.9	134	1312.2	8090.82	8049.50	8070.16	0.51
9000	2.5959	70.35	60.21	28.22	20.42	40.95	573.9	5619.9	168	1645.1	8481.19	8444.20	8462.69	0.44
10000	2.9025	70.27	59.72	27.76	20.33	40.93	573.9	5619.9	208	2036.8	8830.39	8994.20	8912.29	1.84
Annulus Dimensions: L=1.245 m D <sub>o</sub> =0.028 m D <sub>i</sub> =0.0155 m														
Experimental Conditions: Hot Water Inlet Temperature: 60 ± 0.5 °C Hot Water Mass Flowrate: 0.1125 kg/s														
3000	0.9148	60.18	51.72	30.12	19.92	30.92	70.8	693.42	68.9	675.07	3979.94	3890.63	3935.28	2.27
4000	1.2277	60.19	50.86	28.97	20.49	30.79	70.3	688.89	114	1116.3	4392.21	4341.38	4366.79	1.16
5000	1.5575	59.74	49.73	27.66	20.50	30.63	71.3	697.95	175	1713.7	4711.98	4650.93	4681.46	1.30
6000	1.8881	59.93	49.36	26.77	20.50	30.96	71.3	697.95	245	2399.1	4973.26	4938	4955.63	0.71
7000	2.2250	60.11	49.08	25.95	20.45	31.31	71.3	697.95	335	3280.4	5194.17	5105	5149.58	1.73
8000	2.5648	60.34	48.90	25.31	20.35	31.68	70.3	688.89	419	4103	5385.53	5307.29	5346.41	1.46
9000	2.8905	60.17	48.37	25.07	20.44	31.38	70.3	688.89	506	4954.9	5554.32	5583.3	5568.81	0.52
10000	3.2237	60.09	47.97	24.77	20.42	31.28	70.3	688.89	625	6120.2	5705.30	5850.51	5777.91	2.51
Experimental Conditions: Hot Water Inlet Temperature: 60 ± 0.5 °C Hot Water Mass Flowrate: 0.2 kg/s														
3000	0.8900	60.13	54.55	32.43	20.07	30.96	181	1776.6	65	636.5	4673.31	4585.43	4629.37	1.90
4000	1.2001	60.16	53.68	31.19	20.30	31.12	181	1776.6	110	1077.2	5420.75	5448.2	5434.48	0.51
5000	1.5233	60.07	52.90	29.74	20.38	31.41	181	1776.6	165	1615.7	6000.51	5944.96	5972.73	0.93
6000	1.8632	59.73	51.99	28.23	20.20	31.65	185	1812.9	230	2252.2	6474.21	6239.82	6357.01	3.69
7000	2.1773	60.02	51.80	27.98	20.31	31.77	183	1794.7	320	3133.6	6874.72	6964.65	6919.68	1.30
8000	2.5216	60.18	51.55	26.96	20.17	32.29	183	1794.7	403	3946.3	7221.65	7141.65	7181.65	1.11
9000	2.8358	59.63	50.63	26.75	20.41	31.53	185	1812.9	501	4906.0	7527.67	7499.27	7513.47	0.38
10000	3.1760	60.21	50.89	26.21	20.26	32.28	184	1803.8	605	5924.4	7801.41	7879.04	7840.22	0.99
Experimental Conditions: Hot Water Inlet Temperature: 70 ± 0.5 °C Hot Water Mass Flowrate: 0.1125 kg/s														
3000	0.874	70.33	59.58	33.97	20.18	37.86	68.5	670.76	63	616.92	5059.26	5022.89	5041.07	0.72
4000	1.1900	70.14	58.19	31.75	20.50	38.04	68.5	670.76	99	969.45	5624.80	5580.44	5602.62	0.79
5000	1.5141	69.78	56.90	30.17	20.49	37.99	69.4	679.82	163	1596.2	6063.46	6110.61	6087.04	0.77
6000	1.8449	69.72	56.08	28.82	20.48	38.19	70.3	688.89	233	2281.6	6421.88	6416.29	6419.09	0.09
7000	2.1795	69.72	55.43	27.71	20.49	38.37	70.3	688.89	310	3035.6	6724.91	6562.84	6643.88	2.44
8000	2.5026	69.83	54.99	27.32	20.47	38.37	70.3	688.89	402	3936.5	6987.42	7149.81	7068.61	2.30
9000	2.8358	70.00	54.66	26.66	20.50	38.57	69.4	679.82	505	4945.2	7218.96	7286.36	7252.66	0.93
10000	3.1783	69.93	54.15	25.96	20.45									

**Table C-19:** Predicted Results ( $\text{Re}_{\text{s,c}}$ ,  $\text{Pr}_c$ ,  $f_{s,o}$ ,  $\text{Nu}_s$  and empirical values of  $f_{s,i}$  and  $\text{Nu}_{s,i}$ ) for Tube-Side Heat Transfer Enhancement for Two Sizes of Inner Tube (Enhancement Status: Smooth Tube).

$\text{Re}$ Inner tube	$U_0$ W/m <sup>2</sup> .C	Annulus (smooth) <sup>†</sup>					Inner Tube (smooth)					
		$\text{Re}_{\text{s,c}}$	$\text{Pr}_c$	$f_{s,o}$	$\text{Nu}_s$	$h_{s,0}$ W/m <sup>2</sup> .C	$\text{Pr}_h$	$f_{s,i}$	$h_{s,i}$ W/m <sup>2</sup> .C	$\text{Nu}_{s,i}$	Empirical	
Inner Tube Dimensions: L=1.245 m    d <sub>i</sub> = 0.011 m										$f_{s,i}$	$\text{Nu}_{s,i}$	
<b>Experimental Conditions: Hot Water Inlet Temperature: <math>60 \pm 0.5^\circ\text{C}</math></b>										<b>Cold Water Mass Flowrate: 0.1 kg/s</b>		
5000	511.81	3226.3	6.7748	0.0474	26.14	1014	3.2351	0.0412	1176.7	20.03	0.0386	16.4
10000	645.6	3243.8	6.7342	0.0474	26.29	1020.5	3.154	0.036	2004	34.03	0.0315	32.4
15000	728.52	3248.1	6.7243	0.0444	25.26	980.48	3.1132	0.0309	3240	54.95	0.0282	46.9
20000	725.35	3287.9	6.6337	0.0414	24.46	950.95	3.0749	0.0285	3496	59.23	0.0262	60.5
25000	763.91	3262.5	6.6912	0.0414	24.26	942.45	3.0739	0.0255	4619.8	78.26	0.0247	73.7
30000	827.31	3296.5	6.6144	0.0444	25.65	997.53	3.0479	0.0259	5563.6	94.18	0.0236	86.4
35000	807.7	3285.2	6.6398	0.0414	24.44	950.03	3.043	0.0242	6193.4	104.8	0.0228	98.8
40000	853.46	3292.6	6.6231	0.0444	25.62	996.15	3.0392	0.0237	6852.9	116	0.0221	111
<b>Experimental Conditions: Hot Water Inlet Temperature: <math>60 \pm 0.5^\circ\text{C}</math></b>										<b>Cold Water Mass Flowrate: 0.15 kg/s</b>		
5000	761.14	4835.3	6.7812	0.046	44.24	1716	3.3368	0.0405	1558.7	26.6	0.0386	16.5
10000	914.55	4860.4	6.7423	0.0447	43.62	1692.9	3.2117	0.0341	2269.5	38.6	0.0315	32.5
15000	1060.7	4924.2	6.6451	0.0447	44.12	1714.7	3.1583	0.0309	3177.8	53.96	0.0282	47
20000	1158.1	4931.3	6.6345	0.0447	44.17	1717.1	3.1347	0.0285	4071.5	69.1	0.0262	60.7
25000	1213.3	4904.3	6.6752	0.0447	43.96	1707.9	3.1105	0.0274	4801.2	81.42	0.0247	73.8
30000	1258.1	4968.9	6.5787	0.0447	44.46	1729.9	3.0848	0.0256	5290.9	89.66	0.0236	86.5
35000	1314.1	4970.7	6.5761	0.0447	44.48	1730.5	3.0731	0.0244	6274.5	106.3	0.0228	99
40000	1347.1	4988.4	6.5501	0.0447	44.61	1736.5	3.0633	0.0235	6910.6	117	0.0221	111
<b>Experimental Conditions: Hot Water Inlet Temperature: <math>70 \pm 0.5^\circ\text{C}</math></b>										<b>Cold Water Mass Flowrate: 0.1 kg/s</b>		
5000	563.46	3250.4	6.7189	0.0474	26.35	1023	2.8678	0.0399	1429	24.06	0.0386	16.3
10000	686.43	3298.9	6.6091	0.0473	26.77	1040.9	2.7457	0.0349	2300.1	38.59	0.0315	32
15000	743.39	3298.1	6.6109	0.0473	26.76	1040.6	2.6987	0.0325	2973.5	49.82	0.0282	46.3
20000	798.64	3324	6.5536	0.0473	26.98	1050.1	2.6668	0.0287	3815.7	63.87	0.0262	59.6
25000	776.84	3301.2	6.6039	0.0414	24.57	955.39	2.6297	0.027	4763.5	79.65	0.0247	72.4
30000	803.14	3309.1	6.5865	0.0414	24.63	958	2.6189	0.0258	5703.1	95.34	0.0236	84.9
35000	819.56	3342.5	6.5132	0.0414	24.88	969.1	2.5997	0.0247	6100.8	101.9	0.0228	96.9
40000	826.97	3327.7	6.5346	0.0414	24.81	965.83	2.6001	0.0239	6612.7	110.5	0.0221	109
<b>Experimental Conditions: Hot Water Inlet Temperature: <math>70 \pm 0.5^\circ\text{C}</math></b>										<b>Cold Water Mass Flowrate: 0.15 kg/s</b>		
5000	768.13	4827.7	6.793	0.0474	44.99	1744.6	2.9604	0.0394	1563.8	26.4	0.0386	16.3
10000	914.63	4879.1	6.7135	0.0447	43.76	1699.3	2.818	0.0353	2259.9	38	0.0315	32.1
15000	1052	4910.1	6.6663	0.0447	44.01	1709.9	2.7523	0.0304	3124	52.43	0.0282	46.3
20000	1122.7	4941.3	6.6196	0.0447	44.25	1720.5	2.7027	0.0288	3696	61.93	0.0262	59.7
25000	1216	4985.4	6.5544	0.0447	44.59	1735.5	2.6862	0.0268	4653.9	77.95	0.0247	72.6
30000	1256.7	4964.2	6.5856	0.0447	44.43	1728.3	2.6586	0.0256	5283.3	88.42	0.0236	85
35000	1306.2	5001.4	6.5312	0.0447	44.71	1740.9	2.6488	0.0246	6007.2	100.5	0.0228	97.1
40000	1350.5	4998.4	6.5355	0.0447	44.69	1739.9	2.634	0.0241	6940.3	116.1	0.0221	109
<b>Inner Tube Dimensions: L=1.245 m    d<sub>i</sub>= 0.014 m</b>												
<b>Experimental Conditions: Hot Water Inlet Temperature: <math>60 \pm 0.5^\circ\text{C}</math></b>										<b>Cold Water Mass Flowrate: 0.1 kg/s</b>		
5000	486.53	3017.5	6.7405	0.0573	25.63	1233.4	3.2329	0.0424	890.99	19.3	0.0386	16.6
10000	692.47	3056.1	6.6446	0.0573	26	1252.9	3.1635	0.0328	1719.2	37.16	0.0315	32.7
15000	771.21	3080.1	6.5882	0.0573	26.23	1265.1	3.1169	0.0315	2195.7	47.4	0.0282	47.2
20000	860.01	3109.1	6.5201	0.0537	25.43	1228.1	3.0927	0.0291	3194.7	68.92	0.0262	61
25000	897.84	3117.5	6.5004	0.0537	25.51	1232.2	3.0641	0.0275	3687.5	79.48	0.0247	74.2
30000	899.09	3120.4	6.4936	0.0501	24.43	1180.2	3.0672	0.0262	4210.6	90.77	0.0236	87.1
35000	936.47	3122.3	6.4894	0.0501	24.45	1181.1	3.0443	0.0245	5051.8	108.8	0.0228	99.5
40000	949.37	3128.1	6.4758	0.0501	24.5	1183.7	3.0428	0.0243	5359.7	115.5	0.0221	112
<b>Experimental Conditions: Hot Water Inlet Temperature: <math>60 \pm 0.5^\circ\text{C}</math></b>										<b>Cold Water Mass Flowrate: 0.15 kg/s</b>		
5000	562.83	4458.5	6.8546	0.0462	38.49	1849.2	3.2697	0.0433	897.2	19.45	0.0386	16.6
10000	841.98	4532.8	6.7297	0.0462	39.07	1880.5	3.2059	0.032	1693.1	36.64	0.0315	32.7
15000	1037.7	4591.7	6.6337	0.0462	39.52	1905.2	3.1516	0.0323	2534.5	54.77	0.0282	47.3
20000	1140.8	4621.8	6.5856	0.0462	39.75	1917.7	3.1198	0.029	3135.3	67.69	0.0262	61.1
25000	1208	4605.4	6.6118	0.0462	39.63	1910.9	3.1076	0.0258	3659.7	78.98	0.0247	74.3
30000	1258.9	4629.5	6.5735	0.0446	38.92	1877.8	3.1013	0.0263	4261.6	91.96	0.0236	87.2
35000	1321.7	4661.9	6.5226	0.0446	39.16	1890.9	3.0716	0.0244	4903.2	105.7	0.0228	99.7
40000	1349.6	4671.3	6.5081	0.043	38.31	1850.5	3.0687	0.0242	5576.2	120.2	0.0221	112
<b>Experimental Conditions: Hot Water Inlet Temperature: <math>70 \pm 0.5^\circ\text{C}</math></b>										<b>Cold Water Mass Flowrate: 0.1 kg/s</b>		
5000	488.8	3025.9	6.7198	0.0573	25.71	1237.6	2.8173	0.0444	895.88	19.17	0.0386	16.4
10000	675.55	3077.6	6.5943	0.0537	25.15	1213	2.7288	0.0321	1693.2	36.14	0.0315	32.3
15000	779.17	3106.5	6.5261	0.0537	25.41	1226.9	2.6884	0.0303	2373.9	50.61	0.0282	46.6
20000	850.99	3135.1	6.4598	0.0537	25.67	1240.7	2.6546	0.0309	3015.9	64.23	0.0262	60
25000	898.59	3151.3	6.4228	0.0537	25.81	1248.4	2.6448	0.0268	3573	76.08	0.0247	73
30000	950.07	3168.3	6.3846	0.0537	25.97	1256.5	2.6167	0.0259	4346.3	92.47	0.0236	85.5
35000	940.73	3148.4	6.4295	0.0501	24.67	1193	2.6096	0.0244	4970	105.7	0.0228	97.7
40000	977.3	3163.1	6.3962	0.0501	24.8	1199.7	2.6012	0.0232	5899.1	125.4	0.0221	110
<b>Experimental Conditions: Hot Water Inlet Temperature: <math>70 \pm 0.5^\circ\text{C}</math></b>										<b>Cold Water Mass Flowrate: 0.15 kg/s</b>		
5000	578.8	4525.2	6.7423	0.0446	38.14	1835.3	2.8544	0.0434	937.56	20.09	0.0386	16.4
10000	809.17	4571	6.6672	0.0446	38.48	1854	2.7853	0.0351	1594.2	34.08	0.0315	32.3
15000	1021.5	4610.3	6.6039	0.0446	38.78	1870	2.745	0.0311	2503.9	53.47	0.0282	46.7
20000	1123.1	4664.7	6.5184	0.0446	39.18	1892	2.7052	0.0288	3076.6	65.62	0.0262	60.1
25000	1211.1	4681.2	6.4928	0.043	38.39	1854.3	2.6777	0.0252	3892.3	82.95	0.0247	73.1
30000	1241.2	4706.6	6.4539	0.043	38.57	1864.3	2.6612	0.0246	4141.8	88.23	0.0236	85.6
35000	1315.7	4723.7	6.4279</td									

**Table C-20:** Predicted Results ( $Re_{s,c}$ ,  $Pr$ ,  $f$ ,  $h$ ,  $Nu$ ,  $f_a/f_s$  and  $Nu_a/Nu_s$ ) for Tube-Side Heat Transfer Enhancement for Two Sizes of Inner Tube (Enhancement Status: : Wire Coil,  $e=1$  mm,  $p=10$  mm).

Re	U <sub>0</sub> W/m <sup>2</sup> .C	Annulus (smooth) <sup>†</sup>				Inner Tube (augmented)					
		Re <sub>s,c</sub>	Pr <sub>c</sub>	f <sub>s,o</sub>	Nu <sub>s</sub>	h <sub>s,o</sub> W/m <sup>2</sup> .C	Pr <sub>h</sub>	f <sub>a</sub>	h <sub>a,i</sub> W/m <sup>2</sup> .C	Nu <sub>a</sub>	
Inner Tube Dimensions: L=1.245 m d <sub>i</sub> = 0.011 m											
Experimental Conditions: Hot Water Inlet Temperature: 60 ± 0.5 °C Cold Water Mass Flowrate: 0.1 kg/s											
5000	786.85	3275	6.6628	0.0562	29.64	1151.9	3.3582	0.2012	2835.7	48.42	
10000	907.89	3302.4	6.6013	0.0533	28.9	1123.9	3.1954	0.1912	5418.4	92.11	
15000	932.77	3305.9	6.5934	0.0533	28.93	1125.4	3.1553	0.1855	6262.5	106.3	
20000	1039.7	3314.6	6.5743	0.0562	30.03	1168.4	3.1248	0.1815	10936	185.5	
25000	995.46	3311.8	6.5804	0.0533	28.99	1127.7	3.0861	0.1785	9813.1	166.3	
30000	1001.7	3312.2	6.5795	0.0533	28.99	1127.9	3.0615	0.1761	10358	175.4	
35000	1028.2	3332.3	6.5355	0.0533	29.18	1135.9	3.0535	0.1731	12596	213.3	
40000	1045.6	3319.7	6.5631	0.0533	29.06	1130.9	3.0443	0.1729	16214	274.4	
Experimental Conditions: Hot Water Inlet Temperature: 60 ± 0.5 °C Cold Water Mass Flowrate: 0.15 kg/s											
5000	1051.4	4863.9	6.7369	0.0474	45.28	1757.6	3.4344	0.1979	2989.5	51.16	
10000	1244.6	4909.6	6.6672	0.0474	45.65	1773.9	3.2806	0.1976	4780.5	81.46	
15000	1380.3	4936.6	6.6266	0.0473	45.87	1783.5	3.2078	0.1839	7024.7	119.5	
20000	1446.7	4960.7	6.5908	0.0473	46.07	1792.1	3.1651	0.1805	8661.7	147.1	
25000	1455.9	4968.3	6.5795	0.046	45.3	1762.4	3.1336	0.1773	9674.6	164.2	
30000	1503.7	4974.2	6.5709	0.046	45.35	1764.5	3.1112	0.1758	11803	200.2	
35000	1512.5	5010.2	6.5184	0.0447	44.78	1743.9	3.0906	0.1738	13256	224.7	
40000	1572.2	4988.4	6.5501	0.046	45.46	1769.4	3.0861	0.1721	16497	279.6	
Experimental Conditions: Hot Water Inlet Temperature: 70 ± 0.5 °C Cold Water Mass Flowrate: 0.1 kg/s											
5000	791.22	3297.7	6.6118	0.0533	28.85	1122.1	2.9526	0.2054	3066	51.76	
10000	907.49	3350.8	6.4953	0.0533	29.35	1143.3	2.7883	0.1977	5044.9	84.75	
15000	945.03	3348.4	6.5004	0.0533	29.33	1142.3	2.7173	0.1846	6286.7	105.4	
20000	957.63	3357.5	6.4809	0.0503	28.35	1104.7	2.6703	0.1827	8295.4	138.9	
25000	1036.9	3361	6.4733	0.0533	29.44	1147.4	2.6508	0.1794	12511	209.3	
30000	1028.3	3374	6.4456	0.0533	29.56	1152.5	2.6402	0.1773	11057	185	
35000	1011.3	3373.7	6.4463	0.0503	28.49	1110.9	2.6224	0.1753	13123	219.4	
40000	1019.1	3376.6	6.4402	0.0503	28.52	1112	2.607	0.1738	14223	237.7	
Experimental Conditions: Hot Water Inlet Temperature: 70 ± 0.5 °C Cold Water Mass Flowrate: 0.15 kg/s											
5000	1044.9	4870.9	6.7261	0.0447	43.7	1696.5	3.0464	0.2078	3108.4	52.62	
10000	1242.1	4956	6.5978	0.0473	46.03	1790.4	2.8687	0.1926	4646.9	78.25	
15000	1393.6	4971.9	6.5743	0.0473	46.16	1796	2.7926	0.1823	7157.9	120.3	
20000	1454	4981.9	6.5596	0.0473	46.24	1799.6	2.7502	0.1822	8738	146.6	
25000	1580.7	5041	6.4741	0.046	45.87	1787.6	2.7137	0.178	15960	267.5	
30000	1504.1	5000.8	6.5321	0.046	45.56	1773.7	2.6873	0.1761	11475	192.2	
35000	1526.3	5038	6.4784	0.0447	44.99	1753.3	2.663	0.1754	13720	229.6	
40000	1532.9	5055.2	6.4539	0.0447	45.13	1759.1	2.6484	0.1729	13876	232.2	
Inner Tube Dimensions: L=1.245 m d <sub>i</sub> = 0.014 m											
Experimental Conditions: Hot Water Inlet Temperature: 60 ± 0.5 °C Cold Water Mass Flowrate: 0.1 kg/s											
5000	766.74	3038.2	6.6894	0.0501	23.72	1142.5	3.3561	0.1888	2593.3	56.36	
10000	855.46	3054.6	6.6495	0.0501	23.86	1150	3.1959	0.1692	3722.4	80.54	
15000	930.19	3072.5	6.6065	0.0501	24.02	1158.2	3.1486	0.1706	5280.1	114.1	
20000	973.73	3100.3	6.5407	0.0501	24.26	1171	3.1063	0.1678	6474.1	139.7	
25000	990.64	3092.9	6.5579	0.0483	23.64	1140.6	3.0869	0.1665	8467	182.6	
30000	1037.5	3136.6	6.4564	0.0501	24.57	1187.6	3.0752	0.1621	9237.1	199.2	
35000	1010.3	3135.9	6.4581	0.0465	23.42	1131.8	3.0446	0.1608	10614	228.6	
40000	1023.9	3134.4	6.4615	0.0465	23.4	1131.2	3.0476	0.159	12213	263.1	
Experimental Conditions: Hot Water Inlet Temperature: 60 ± 0.5 °C Cold Water Mass Flowrate: 0.15 kg/s											
5000	952.24	4529	6.736	0.043	37.28	1794.2	3.4123	0.1834	2255.7	49.1	
10000	1187.8	4582.4	6.6486	0.043	37.67	1815.4	3.2543	0.1731	3829.7	83	
15000	1318.4	4613.6	6.5987	0.043	37.9	1827.7	3.1976	0.1717	5288.2	114.4	
20000	1390.1	4632.8	6.5683	0.0422	37.58	1813.1	3.1508	0.1665	6674.7	144.2	
25000	1474.5	4659.2	6.5269	0.0414	37.3	1800.9	3.1251	0.165	9156.3	197.7	
30000	1471.1	4697.2	6.4682	0.0398	36.61	1769.4	3.094	0.1613	9832.7	212.1	
35000	1485.9	4713.7	6.443	0.0398	36.72	1775.5	3.0835	0.1606	10272	221.5	
40000	1521.6	4689.5	6.4801	0.0398	36.56	1766.5	3.076	0.1601	12425	267.9	
Experimental Conditions: Hot Water Inlet Temperature: 70 ± 0.5 °C Cold Water Mass Flowrate: 0.1 kg/s											
5000	731.83	3060.8	6.6345	0.0501	23.92	1152.9	2.928	0.1885	2227.4	47.82	
10000	857.18	3095.9	6.551	0.0501	24.22	1169	2.7943	0.1743	3580.9	76.58	
15000	953.99	3127	6.4784	0.0501	24.49	1183.2	2.7249	0.1716	5505.4	117.5	
20000	995.64	3159.4	6.4045	0.0501	24.76	1198	2.6735	0.1693	6603.3	140.7	
25000	1027.1	3154.3	6.4162	0.0501	24.72	1195.6	2.6448	0.166	8187.7	174.3	
30000	1004.2	3145.4	6.4362	0.0465	23.49	1135.9	2.6351	0.1621	9752.2	207.6	
35000	1026.6	3175	6.3697	0.0465	23.73	1148.6	2.6224	0.1611	10905	232	
40000	1052.6	3188.6	6.3393	0.0465	23.84	1154.5	2.6125	0.1594	13529	287.8	
Experimental Conditions: Hot Water Inlet Temperature: 70 ± 0.5 °C Cold Water Mass Flowrate: 0.15 kg/s											
5000	963.3	4586.8	6.6416	0.043	37.7	1817.1	2.9973	0.188	2279.1	49.03	
10000	1178.7	4661.9	6.5226	0.043	38.25	1846.8	2.852	0.1779	3630.8	77.78	
15000	1329.4	4658.1	6.5286	0.0414	37.29	1800.4	2.7794	0.1711	5682.5	121.5	
20000	1420.3	4703.2	6.4589	0.0414	37.61	1817.7	2.7324	0.1681	7286.8	155.5	
25000	1468.1	4737.5	6.407	0.043	38.79	1876.4	2.6971	0.1654	7570.5	161.4	
30000	1461.3	4744.7	6.3962	0.0398	36.93	1786.9	2.673	0.1629	9024.8	192.3	
35000	1543.8	4755.8	6.3796	0.0398	37.01	1791	2.6552	0.161	12668	269.8	
40000	1546	4790.7	6.3279	0.0398	37.24	1803.8	2.6413	0.1591	12240	260.6	

†Predicted values of smooth annulus are used to complete calculations only.

††Augmentation values are predicted by using the proposed correlations and not experimental results.

**Table C-21:** Predicted Results ( $Re_{s,c}$ ,  $Pr$ ,  $f$ ,  $h$ ,  $Nu$ ,  $f_a/f_s$  and  $Nu_a/Nu_s$ ) for Tube-Side Heat Transfer Enhancement for Two Sizes of Inner Tube (Enhancement Status: : Wire Coil,  $e=1$  mm,  $p=20$  mm).

$Re$ Inner tube	$U_0$ W/m <sup>2</sup> .C	Annulus (smooth) <sup>†</sup>				Inner Tube (augmented)						
		$Re_{s,c}$	$Pr_c$	$f_{s,o}$	$Nu_s$	$h_{s,o}$ W/m <sup>2</sup> .C	$Pr_h$	$f_a$	$h_{a,i}$ W/m <sup>2</sup> .C	$Nu_a$	Augmentation <sup>††</sup>	
Inner Tube Dimensions: L=1.245 m    d <sub>i</sub> = 0.011 m												
Experimental Conditions: Hot Water Inlet Temperature: $60 \pm 0.5^\circ\text{C}$ Cold Water Mass Flowrate: 0.1 kg/s												
5000	755.43	3242.6	6.7369	0.0533	28.34	1099.9	3.3471	0.1215	2754.4	47.02	2.8298	1.8353
10000	862.27	3293.8	6.6205	0.0533	28.82	1120.5	3.2062	0.1088	4284.1	72.85	3.1934	1.7848
15000	829.95	3293.8	6.6205	0.0503	27.78	1080.3	3.1344	0.1083	4099.8	69.57	3.4274	1.7559
20000	938.58	3303.6	6.5987	0.0533	28.91	1124.4	3.1155	0.1047	6528	110.7	3.6038	1.7358
25000	971.27	3293.8	6.6205	0.0533	28.82	1120.5	3.082	0.1025	8411.5	142.5	3.7468	1.7203
30000	998.66	3306.3	6.5926	0.0533	28.93	1125.5	3.0757	0.0991	10252	173.7	3.8678	1.7079
35000	983.87	3322.4	6.557	0.0503	28.04	1091.3	3.0525	0.0988	11594	196.3	3.9732	1.6974
40000	979.44	3305.5	6.5943	0.0503	27.89	1084.8	3.0589	0.0974	11699	198.1	4.0668	1.6884
Experimental Conditions: Hot Water Inlet Temperature: $60 \pm 0.5^\circ\text{C}$ Cold Water Mass Flowrate: 0.15 kg/s												
5000	1033.8	4854	6.7522	0.0474	45.2	1754	3.4104	0.1252	2875.3	49.17		
10000	1219.3	4896.7	6.6867	0.046	44.73	1737.5	3.2663	0.1128	4684.5	79.79		
15000	1206	4916.6	6.6566	0.0447	44.06	1712.1	3.1798	0.1104	4675.4	79.44		
20000	1384.2	4928.3	6.6389	0.0473	45.81	1780.6	3.1459	0.1061	7155.2	121.5		
25000	1437.5	4947.1	6.6109	0.046	45.13	1755.1	3.1187	0.1033	9174.1	155.6		
30000	1427.9	4923.1	6.6469	0.046	44.94	1746.7	3.1092	0.0994	9034.1	153.2		
35000	1490.1	4951.3	6.6048	0.046	45.16	1756.5	3.084	0.0993	11388	193		
40000	1508.6	4950.7	6.6056	0.046	45.16	1756.3	3.0685	0.0983	12422	210.4		
Experimental Conditions: Hot Water Inlet Temperature: $70 \pm 0.5^\circ\text{C}$ Cold Water Mass Flowrate: 0.1 kg/s												
5000	744.22	3298.1	6.6109	0.0503	27.82	1081.9	2.9266	0.1171	2722.5	45.92		1.8332
10000	842.93	3313	6.5778	0.0533	29	1128.2	2.7826	0.1122	3814	64.06		1.7825
15000	882.14	3315	6.5735	0.0503	27.97	1088.4	2.7081	0.1104	5339.6	89.49		1.7536
20000	960.98	3331.9	6.5364	0.0533	29.17	1135.7	2.6692	0.1048	7187.8	120.3		1.7335
25000	972.72	3354.3	6.4877	0.0533	29.38	1144.7	2.6452	0.1024	7454.9	124.7		1.718
30000	963.03	3361	6.4733	0.0503	28.38	1106	2.632	0.0997	8592.9	143.7		1.7055
35000	985.94	3365.4	6.464	0.0503	28.42	1107.7	2.6209	0.0989	10381	173.5		1.695
40000	1003.1	3361	6.4733	0.0503	28.38	1106	2.6039	0.0976	12515	209.1		1.6859
Experimental Conditions: Hot Water Inlet Temperature: $70 \pm 0.5^\circ\text{C}$ Cold Water Mass Flowrate: 0.15 kg/s												
5000	995.35	4869.7	6.7279	0.0447	43.69	1696.1	3.0298	0.1238	2751.1	46.55		
10000	1195.8	4940.7	6.6205	0.0473	45.91	1784.9	2.8598	0.1145	4146.8	69.81		
15000	1282.8	4954.8	6.5995	0.046	45.19	1757.7	2.7814	0.1092	5447.9	91.5		
20000	1391.1	4979.5	6.5631	0.0473	46.22	1798.7	2.7461	0.1044	7063.3	118.5		
25000	1405.4	5006.1	6.5244	0.0447	44.75	1742.5	2.6971	0.1021	8378.1	140.4		
30000	1431.4	4997.8	6.5364	0.0447	44.69	1739.7	2.6813	0.101	9331	156.3		
35000	1466.1	5023.8	6.4987	0.0447	44.89	1748.5	2.6586	0.099	10507	175.8		
40000	1491.4	5039.2	6.4767	0.0447	45	1753.7	2.634	0.0989	11562	193.4		
Inner Tube Dimensions: L=1.245 m    d <sub>i</sub> = 0.014 m												
Experimental Conditions: Hot Water Inlet Temperature: $60 \pm 0.5^\circ\text{C}$ Cold Water Mass Flowrate: 0.1 kg/s												
5000	709.83	3027	6.7171	0.0501	23.62	1137.3	3.3268	0.1267	2098.9	45.58	2.7579	1.9019
10000	833.44	3053.1	6.6553	0.0501	23.85	1149.3	3.2023	0.114	3377.5	73.09	3.1123	1.8495
15000	899.3	3086	6.5743	0.0519	24.68	1190.9	3.1403	0.1131	4095.9	88.48	3.3403	1.8197
20000	932.09	3100.6	6.5398	0.0501	24.26	1171.2	3.1047	0.1095	5101.8	110.1	3.5122	1.7989
25000	982.78	3118.6	6.4979	0.0501	24.42	1179.4	3.0809	0.1071	6604.8	142.4	3.6516	1.7829
30000	969.32	3121.9	6.4902	0.0465	23.3	1125.8	3.07	0.105	7830.9	168.8	3.7695	1.7699
35000	981	3138.4	6.4522	0.0465	23.44	1132.9	3.05	0.1034	8219.5	177.1	3.8722	1.759
40000	990.69	3137	6.4556	0.0465	23.42	1132.3	3.0418	0.1029	8911.4	192	3.9635	1.7497
Experimental Conditions: Hot Water Inlet Temperature: $60 \pm 0.5^\circ\text{C}$ Cold Water Mass Flowrate: 0.15 kg/s												
5000	953.9	4504.5	6.7766	0.0446	37.98	1826.9	3.4107	0.1262	2218.9	48.29		
10000	1159.7	4600.5	6.6196	0.0446	38.7	1866	3.2366	0.1166	3412.8	73.93		
15000	1287	4608.7	6.6065	0.0446	38.76	1869.4	3.1899	0.115	4611.6	99.76		
20000	1379.6	4633.4	6.5674	0.043	38.04	1835.5	3.1575	0.1091	6218.6	134.4		
25000	1352.1	4666.9	6.5149	0.0414	37.35	1803.8	3.1216	0.1067	6042.9	130.5		
30000	1406.7	4671.3	6.5081	0.0414	37.38	1805.5	3.0937	0.1038	7141.1	154.1		
35000	1458.9	4704.4	6.4573	0.0414	37.61	1818.1	3.084	0.1033	8296.5	178.9		
40000	1467.4	4672.9	6.5056	0.0398	36.45	1760.4	3.0742	0.1019	9937.8	214.3		
Experimental Conditions: Hot Water Inlet Temperature: $70 \pm 0.5^\circ\text{C}$ Cold Water Mass Flowrate: 0.1 kg/s												
5000	677.67	3069.5	6.6135	0.0501	23.99	1156.9	2.9066	0.1146	1817.2	38.99		1.8996
10000	841.41	3117.1	6.5013	0.0501	24.4	1178.7	2.7858	0.1134	3274.6	70.01		1.8473
15000	911.28	3120.1	6.4945	0.0501	24.43	1180	2.7202	0.109	4465.3	95.28		1.8174
20000	930.62	3155.4	6.4137	0.0465	23.57	1140.2	2.6712	0.1079	5661.9	120.6		1.7964
25000	980.19	3163.9	6.3945	0.0483	24.23	1172.2	2.647	0.1064	6705.7	142.8		1.7804
30000	977.16	3174.6	6.3705	0.0465	23.73	1148.5	2.6293	0.1048	7348.4	156.4		1.7675
35000	990.96	3171.6	6.3771	0.0465	23.7	1147.2	2.6107	0.1032	8173.7	173.9		1.7566
40000	1022.8	3180.1	6.3582	0.0465	23.77	1150.9	2.6008	0.1021	10368	220.5		1.7472
Experimental Conditions: Hot Water Inlet Temperature: $70 \pm 0.5^\circ\text{C}$ Cold Water Mass Flowrate: 0.15 kg/s												
5000	880.03	4529.5	6.7351	0.043	37.28	1794.4	2.9894	0.1235	1918.6	41.27		
10000	1155.7	4607.6	6.6083	0.043	37.85	1825.4	2.8476	0.1149	3509.8	75.18		
15000	1260	4647.6	6.545	0.043	38.14	1841.2	2.7782	0.1114	4454.4	95.21		
20000	1313.1	4685.6	6.486	0.0414	37.48	1810.9	2.7195	0.1087	5338.2	113.9		
25000	1383.9	4728.7	6.4203	0.0414	37.78	1827.3	2.6888	0.1058	6387	136.2		
30000	1450.8	4733.6	6.4128	0.0414	37.82	1829.2	2.6768	0.1046	7873.8	167.8		
35000	1495.4	4745.8	6.3945	0.0414	37.9	1833.9	2.6526	0.1032	9119.2	194.2		
40000	1516	4774.1	6.3524	0.0398	37.13	1797.7	2.6404	0.1021	10920	232.5		

**Table C-22:** Predicted Results ( $Re_{s,c}$ ,  $Pr$ ,  $f$ ,  $h$ ,  $Nu_s$ ,  $f_a/f_s$  and  $Nu_a/Nu_s$ ) for Tube-Side Heat Transfer Enhancement for Two Sizes of Inner Tube (Enhancement Status: : Wire Coil,  $e=1$  mm,  $p=30$  mm).

Re Inner tube	$U_0$ W/m <sup>2</sup> .C	Annulus (smooth) <sup>†</sup>				Inner Tube (augmented)						
		$Re_{s,c}$	$Pr_c$	$f_{s,o}$	$Nu_s$	$h_{s,o}$ W/m <sup>2</sup> .C	$Pr_h$	$f_a$	$h_{a,i}$ W/m <sup>2</sup> .C	$Nu_a$	$f_a/f_s$	$Nu_a/Nu_s$
Inner Tube Dimensions: L=1.245 m    d <sub>i</sub> = 0.011 m												
Experimental Conditions: Hot Water Inlet Temperature: 60 ± 0.5 °C    Cold Water Mass Flowrate: 0.1 kg/s												
5000	644.64	3220	6.7894	0.0474	26.09	1011.7	3.2976	0.0856	2026.2	34.54	2.0579	1.5902
10000	755.36	3256.2	6.7055	0.0474	26.4	1025.1	3.1765	0.0735	3280.7	55.74	2.3223	1.5465
15000	902.8	3266.8	6.6814	0.0503	27.54	1069.9	3.1465	0.0718	6647.4	112.8	2.4925	1.5216
20000	848.09	3269.5	6.6752	0.0474	26.51	1030	3.1013	0.0689	5509.1	93.4	2.6207	1.5042
25000	875.19	3291	6.6266	0.0473	26.7	1038	3.0817	0.0666	6413.5	108.7	2.7247	1.4908
30000	918.15	3299.7	6.6074	0.0503	27.84	1082.5	3.0742	0.0641	6956.1	117.8	2.8127	1.48
35000	915.12	3309.5	6.5856	0.0473	26.86	1044.7	3.0541	0.0632	8507.8	144	2.8894	1.4709
40000	928.33	3295.4	6.617	0.0473	26.73	1039.6	3.0662	0.0619	10034	169.9	2.9575	1.4631
Experimental Conditions: Hot Water Inlet Temperature: 60 ± 0.5 °C    Cold Water Mass Flowrate: 0.15 kg/s												
5000	913.34	4869.7	6.7279	0.0474	45.33	1759.7	3.3861	0.0902	2166.3	37.02		
10000	1081	4896.1	6.6876	0.0474	45.54	1769.1	3.2456	0.0775	3175.8	54.06		
15000	1202	4917.2	6.6557	0.0474	45.72	1776.6	3.1781	0.0723	4255.5	72.31		
20000	1329.1	4938.3	6.624	0.0447	44.23	1719.5	3.1518	0.0691	6732.2	114.3		
25000	1369.1	4951.8	6.6039	0.046	45.17	1756.7	3.1153	0.0674	7139.3	121.1		
30000	1315.6	4937.1	6.6258	0.0447	44.22	1719.1	3.1121	0.0648	6442.4	109.3		
35000	1414.5	4985.4	6.5544	0.0447	44.59	1735.5	3.0817	0.0633	8825.8	149.5		
40000	1445.3	4976	6.5683	0.0447	44.52	1732.3	3.0739	0.062	10091	170.9		
Experimental Conditions: Hot Water Inlet Temperature: 70 ± 0.5 °C    Cold Water Mass Flowrate: 0.1 kg/s												
5000	709.99	3250	6.7198	0.0533	28.41	1102.9	2.9107	0.0813	2273.9	38.34		1.5885
10000	777.32	3305.9	6.5934	0.0473	26.83	1043.5	2.7591	0.0753	3484.7	58.49		1.5446
15000	845.75	3313	6.5778	0.0503	27.95	1087.6	2.7	0.0715	4354.8	72.97		1.5196
20000	896.04	3337.8	6.5235	0.0503	28.18	1097.1	2.6659	0.0688	5610.3	93.91		1.5022
25000	905.69	3320.9	6.5605	0.0473	26.95	1048.9	2.6399	0.0667	7638.6	127.8		1.4888
30000	925.14	3355.5	6.4852	0.0473	27.25	1061.6	2.618	0.0648	8298.3	138.7		1.4779
35000	962.76	3356.7	6.4826	0.0503	28.34	1104.4	2.611	0.0633	8662.7	144.8		1.4688
40000	945.55	3342.1	6.5141	0.0473	27.13	1056.7	2.6072	0.0627	10402	173.8		1.461
Experimental Conditions: Hot Water Inlet Temperature: 70 ± 0.5 °C    Cold Water Mass Flowrate: 0.15 kg/s												
5000	951.76	4833	6.7848	0.0474	45.03	1746.5	3.0121	0.0834	2386.8	40.36		
10000	1095.9	4910.7	6.6654	0.0447	44.01	1710.1	2.8541	0.0775	3489.2	58.73		
15000	1178.5	4933.6	6.631	0.0447	44.19	1717.9	2.7757	0.0716	4297.5	72.17		
20000	1349.8	4963	6.5873	0.0473	46.09	1792.9	2.7321	0.0699	6275.7	105.3		
25000	1355.8	5010.8	6.5175	0.0447	44.79	1744.1	2.6931	0.0665	7006.2	117.4		
30000	1372.5	4975.4	6.5691	0.0447	44.51	1732.1	2.6746	0.0653	7615.3	127.5		
35000	1407	5015.5	6.5107	0.0447	44.82	1745.7	2.6595	0.0632	8362.6	140		
40000	1471.3	5050.5	6.4606	0.0447	45.09	1757.5	2.6359	0.0631	10455	174.9		
Inner Tube Dimensions: L=1.245 m    d <sub>i</sub> = 0.014 m												
Experimental Conditions: Hot Water Inlet Temperature: 60 ± 0.5 °C    Cold Water Mass Flowrate: 0.1 kg/s												
5000	682.13	3024.4	6.7234	0.0537	24.66	1187.2	3.3218	0.0911	1780.8	38.67	2.0057	1.6481
10000	801.92	3056.8	6.6442	0.0519	24.42	1177.2	3.1962	0.0822	2799.2	60.57	2.2634	1.6028
15000	875.53	3078.7	6.5917	0.0519	24.62	1187.5	3.1432	0.0812	3714.5	80.25	2.4292	1.5769
20000	904.54	3099.9	6.5415	0.0501	24.25	1170.8	3.1129	0.0752	4438.5	95.8	2.5542	1.5589
25000	948.1	3107.6	6.5235	0.0501	24.32	1174.3	3.082	0.0721	5502.4	118.7	2.6556	1.545
30000	970.31	3050.6	6.6592	0.0501	23.83	1148.2	3.0742	0.0714	7022.3	151.4	2.7414	1.5338
35000	963.77	3129.2	6.4733	0.0465	23.36	1128.9	3.0595	0.0698	7389.9	159.3	2.8161	1.5244
40000	983.52	3123.4	6.4868	0.0465	23.31	1126.4	3.0523	0.0686	8718.8	187.9	2.8824	1.5163
Experimental Conditions: Hot Water Inlet Temperature: 60 ± 0.5 °C    Cold Water Mass Flowrate: 0.15 kg/s												
5000	892.25	4507.8	6.7712	0.047	39.3	1890.7	3.3852	0.093	1876.9	40.82		
10000	1065	4553	6.6965	0.0462	39.22	1889	3.2304	0.0854	2716.4	58.83		
15000	1222.3	4594.5	6.6293	0.0446	38.66	1863.6	3.1746	0.0783	3960.8	85.64		
20000	1303.5	4606.5	6.61	0.0446	38.75	1868.5	3.1373	0.0754	4813.9	104		
25000	1358.8	4653.7	6.5355	0.043	38.19	1843.5	3.1198	0.0729	5781.6	124.8		
30000	1391.5	4659.2	6.5269	0.043	38.23	1845.7	3.0934	0.0706	6331.4	136.6		
35000	1469.1	4695	6.4716	0.043	38.48	1859.8	3.0778	0.0697	7851.9	169.3		
40000	1469.7	4697.7	6.4674	0.0414	37.57	1815.6	3.0659	0.0688	8673.1	187		
Experimental Conditions: Hot Water Inlet Temperature: 70 ± 0.5 °C    Cold Water Mass Flowrate: 0.1 kg/s												
5000	692	3049.5	6.6619	0.0537	24.89	1199.4	2.9032	0.0995	1817	38.98		1.6462
10000	793.88	3091.1	6.5622	0.0537	25.27	1219.5	2.7759	0.083	2529.8	54.07		1.6007
15000	860.6	3112.7	6.5115	0.0501	24.36	1176.7	2.7058	0.0792	3569.6	76.14		1.5748
20000	923.15	3152.1	6.4212	0.0501	24.7	1194.6	2.6643	0.076	4533.9	96.59		1.5567
25000	981.9	3159.8	6.4037	0.0501	24.77	1198.2	2.6426	0.0737	6088.5	129.6		1.5429
30000	1007.8	3170.1	6.3805	0.0501	24.86	1202.9	2.6289	0.0717	6968.7	148.3		1.5317
35000	1032.3	3180.5	6.3574	0.0501	24.94	1207.6	2.616	0.0696	7985.3	169.9		1.5222
40000	1050.4	3196	6.323	0.0501	25.08	1214.6	2.5999	0.0692	8737.8	185.8		1.5141
Experimental Conditions: Hot Water Inlet Temperature: 70 ± 0.5 °C    Cold Water Mass Flowrate: 0.15 kg/s												
5000	921.2	4533.9	6.7279	0.0446	38.2	1838.9	2.9866	0.0946	2051.2	44.11		
10000	1058.1	4616.4	6.5943	0.0446	38.82	1872.5	2.8118	0.077	2706.6	57.91		
15000	1200.5	4642.1	6.5536	0.0446	39.01	1882.9	2.7473	0.0799	3691.8	78.84		
20000	1347.8	4704.9	6.4564	0.043	38.56	1863.6	2.7126	0.0752	5444.1	116.1		
25000	1373.3	4708.2	6.4514	0.0446	39.5	1909.6	2.6897	0.0742	5466.3	116.5		
30000	1394.2	4732.5	6.4145	0.043	38.75	1874.5	2.6626	0.0728	6090.8	129.7		
35000	1473.6	4748	6.3912	0.043	38.87	1880.5	2.6466	0.0707	7643	162.7		
40000	1486.5	4741.9	6.4004	0.0414	37.88	1832.4	2.6317	0.0693	8858.1	188.5		

**Table C-23:** Predicted Results ( $Re_{s,c}$ ,  $Pr$ ,  $f$ ,  $h$ ,  $Nu_s$ ,  $f_a/f_s$  and  $Nu_a/Nu_s$ ) for Tube-Side Heat Transfer Enhancement for Two Sizes of Inner Tube (Enhancement Status: : Wire Coil,  $e=1$  mm,  $p=40$  mm).

Re Inner tube	U <sub>0</sub> W/m <sup>2</sup> .C	Annulus (smooth) <sup>†</sup>					Inner Tube (augmented)								
		Re <sub>s,c</sub>	Pr <sub>c</sub>	f <sub>s,o</sub>	Nu <sub>s</sub>	h <sub>s,o</sub> W/m <sup>2</sup> .C	Pr <sub>h</sub>	f <sub>a</sub>	h <sub>a,i</sub> W/m <sup>2</sup> .C	Nu <sub>a</sub>	Augmentation <sup>††</sup>				
Inner Tube Dimensions: L=1.245 m   d= 0.011 m															
Experimental Conditions: Hot Water Inlet Temperature: $60 \pm 0.5$ °C   Cold Water Mass Flowrate: 0.1 kg/s															
5000	637.34	3242.2	6.7378	0.0474	26.28	1019.9	3.3069	0.0682	1937.3	33.04	1.6416	1.4427			
10000	792.68	3237.5	6.7486	0.0474	26.24	1018.2	3.1713	0.0594	4096.2	69.59	1.8525	1.4035			
15000	785.94	3275.4	6.6619	0.0474	26.56	1032.2	3.1124	0.055	3768.4	63.91	1.9883	1.3811			
20000	844.35	3282	6.6469	0.0503	27.68	1075.7	3.0859	0.0499	4496.3	76.2	2.0906	1.3655			
25000	883.68	3275.4	6.6619	0.0474	26.56	1032.2	3.083	0.0493	7066.3	119.7	2.1735	1.3536			
30000	930.94	3315	6.5735	0.0503	27.97	1088.4	3.0517	0.0476	7408.4	125.4	2.2438	1.3439			
35000	870.53	3298.5	6.61	0.0444	25.67	998.21	3.0402	0.0461	7841.3	132.7	2.3049	1.3357			
40000	883.88	3298.9	6.6991	0.0444	25.67	998.35	3.0494	0.0445	8897.9	150.6	2.3592	1.3288			
Experimental Conditions: Hot Water Inlet Temperature: $60 \pm 0.5$ °C   Cold Water Mass Flowrate: 0.15 kg/s															
5000	898.01	4846.4	6.7639	0.046	44.33	1719.9	3.3701	0.0654	2143.6	36.62					
10000	1142.7	4889.6	6.6974	0.0474	45.49	1766.8	3.2399	0.0587	3700.1	62.98					
15000	1188.7	4916	6.6575	0.0474	45.71	1776.2	3.1675	0.0544	4113.9	69.88					
20000	1213.2	4930.1	6.6363	0.0447	44.16	1716.7	3.136	0.0526	4740.7	80.45					
25000	1366.6	4946.6	6.6118	0.0473	45.95	1787	3.1124	0.0493	6678.7	113.3					
30000	1347.6	4959.5	6.5926	0.0447	44.39	1726.7	3.1081	0.0475	7063.1	119.8					
35000	1389.6	4953.6	6.6013	0.0447	44.34	1724.7	3.0804	0.0461	8247.3	139.7					
40000	1414.5	4951.3	6.6048	0.0447	44.33	1723.9	3.082	0.0447	9101.2	154.2					
Experimental Conditions: Hot Water Inlet Temperature: $70 \pm 0.5$ °C   Cold Water Mass Flowrate: 0.1 kg/s															
5000	622.39	3250	6.7198	0.0474	26.35	1022.8	2.8896	0.0712	1812.4	30.54		1.441			
10000	743.12	3307.5	6.59	0.0473	26.84	1044	2.7582	0.0601	2945.3	49.43		1.4018			
15000	801.58	3301.2	6.6039	0.0473	26.79	1041.7	2.6862	0.0555	3979.3	66.65		1.3794			
20000	846.65	3312.2	6.5795	0.0473	26.88	1045.8	2.6577	0.0523	5098.8	85.33		1.3637			
25000	881.77	3349.2	6.4987	0.0473	27.19	1059.3	2.6466	0.0497	6042.8	101.1		1.3517			
30000	897.28	3354.3	6.4877	0.0473	27.24	1061.2	2.6191	0.0482	6679.5	111.7		1.342			
35000	945.67	3358.7	6.4784	0.0473	27.27	1062.8	2.6028	0.0461	9924.9	165.8		1.3338			
40000	922.83	3340.5	6.5175	0.0473	27.12	1056.1	2.6227	0.045	8432.1	141		1.3269			
Experimental Conditions: Hot Water Inlet Temperature: $70 \pm 0.5$ °C   Cold Water Mass Flowrate: 0.15 kg/s															
5000	838.83	4848.7	6.7603	0.0447	43.53	1688.8	2.9715	0.0641	1900.3	32.1					
10000	1052.2	4920.1	6.6513	0.0447	44.08	1713.3	2.8361	0.06	3116.2	52.42					
15000	1225.3	4957.1	6.596	0.0447	44.37	1725.9	2.7679	0.0544	4842.3	81.3					
20000	1272.1	5000.2	6.5329	0.0473	46.39	1806.1	2.709	0.0523	4931.6	82.66					
25000	1394	4987.2	6.5519	0.0473	46.28	1801.5	2.6846	0.0493	7091.4	118.8					
30000	1364.3	5000.2	6.5329	0.0447	44.7	1740.5	2.6601	0.0481	7265.8	121.6					
35000	1383.3	5041.6	6.4733	0.0447	45.02	1754.5	2.6402	0.0461	7528.7	125.9					
40000	1464	5059.9	6.4472	0.0447	45.16	1760.7	2.6388	0.0459	10049	168.1					
Inner Tube Dimensions: L=1.245 m   d= 0.014 m															
Experimental Conditions: Hot Water Inlet Temperature: $60 \pm 0.5$ °C   Cold Water Mass Flowrate: 0.1 kg/s															
5000	592.76	3042.9	6.6778	0.0537	24.83	1196.2	3.2592	0.0751	1303.9	28.26	1.5999	1.4886			
10000	813.28	3089.3	6.5665	0.0573	26.31	1269.8	3.1883	0.0696	2515.9	54.42	1.8055	1.4479			
15000	857.02	3086	6.5743	0.0537	25.22	1217	3.1309	0.0609	3226.2	69.67	1.9378	1.4245			
20000	927.1	3114.9	6.5064	0.0537	25.49	1231	3.1055	0.0572	4189.3	90.41	2.0375	1.4082			
25000	937.53	3115.7	6.5047	0.0501	24.39	1178	3.0698	0.0565	5130.9	110.6	2.1184	1.3957			
30000	964.42	3134	6.4623	0.0501	24.55	1186.4	3.0713	0.0546	5765.2	124.3	2.1868	1.3856			
35000	1000.5	3138.8	6.4514	0.0501	24.59	1188.6	3.0571	0.0533	7089.6	152.8	2.2464	1.3771			
40000	969	3138.1	6.453	0.0465	23.43	1132.8	3.0423	0.052	7521.6	162	2.2993	1.3697			
Experimental Conditions: Hot Water Inlet Temperature: $60 \pm 0.5$ °C   Cold Water Mass Flowrate: 0.15 kg/s															
5000	731.69	4518.7	6.7531	0.0462	38.96	1874.6	3.3156	0.0724	1331.9	28.91					
10000	1007.3	4584.1	6.646	0.0462	39.46	1902	3.2265	0.0713	2380.9	51.56					
15000	1145.1	4593.4	6.631	0.0462	39.54	1905.9	3.1743	0.0616	3194.3	69.07					
20000	1274.8	4644.9	6.5493	0.0462	39.93	1927.3	3.1443	0.0576	4200.2	90.74					
25000	1375	4633.4	6.5674	0.0446	38.95	1879.4	3.1198	0.0565	5730.8	123.7					
30000	1406.6	4656.4	6.5312	0.0446	39.12	1888.7	3.1095	0.0549	6167.6	133.1					
35000	1410.5	4672.9	6.5056	0.043	38.33	1851.1	3.0765	0.0537	6638.4	143.1					
40000	1458.7	4675.7	6.5013	0.043	38.35	1852.2	3.0664	0.0524	7707.5	166.1					
Experimental Conditions: Hot Water Inlet Temperature: $70 \pm 0.5$ °C   Cold Water Mass Flowrate: 0.1 kg/s															
5000	607.2	3037.9	6.6903	0.0537	24.79	1193.7	2.8732	0.0702	1371.6	29.4		1.4869			
10000	777.78	3106.9	6.5252	0.0537	25.41	1227.1	2.7523	0.0695	2361.7	50.44		1.4446			
15000	874.07	3131.5	6.4682	0.0537	25.64	1238.9	2.7081	0.0617	3305.6	70.51		1.4227			
20000	933.47	3153.5	6.4178	0.0537	25.83	1249.5	2.6621	0.0599	4116.5	87.69		1.4063			
25000	938.96	3156.1	6.412	0.0501	24.74	1196.5	2.6435	0.0562	4872	103.7		1.3938			
30000	982.2	3161.3	6.4004	0.0501	24.78	1198.8	2.6304	0.0557	6083.4	129.5		1.3837			
35000	985.56	3144.7	6.4379	0.0501	24.64	1191.3	2.6213	0.0535	6390.8	136		1.3752			
40000	1025.5	3173.1	6.3738	0.0501	24.88	1204.2	2.6096	0.0529	7755.7	165		1.3678			
Experimental Conditions: Hot Water Inlet Temperature: $70 \pm 0.5$ °C   Cold Water Mass Flowrate: 0.15 kg/s															
5000	746.43	4563.3	6.6796	0.0446	38.42	1850.9	2.9054	0.0765	1388.4	29.79					
10000	1073.1	4619.7	6.5891	0.0446	38.85	1873.8	2.8233	0.0644	2794.2	59.8					
15000	1201	4680.1	6.4945	0.0446	39.3	1898.3	2.7645	0.0632	3643.3	77.84					
20000	1304.9	4690.6	6.4784	0.0446	39.37	1902.5	2.7123	0.059	4637.4	98.93					
25000	1320.5	4697.7	6.4674	0.0446	39.43	1905.4	2.6931	0.0565	4803.4	102.4					
30000	1392.2	4720.4	6.4329	0.043	38.67	1869.7	2.6614	0.0555	6102	130					
35000	1412.6	4732	6.4153	0.043	38.75	1874.2	2.6421	0.0535	6422.2	136.7					
40000	1476.3	4750.2	6.3879	0.0414	37.93	1835.5	2.6309	0.0529	8478.9	180.5					

**Table C-24:** Predicted Results ( $Re_{s,h}$ ,  $Pr$ ,  $f$ ,  $h$ ,  $Nu$  and empirical values of  $f_{s,o}$ , and  $Nu_{s,o}$ ) for Annulus-Side Heat Transfer Enhancement for Two Annulus Sizes (Enhancement Status: Smooth Annulus).

Re Annul us	U <sub>0</sub> W/m <sup>2</sup> .C	Inner Tube (smooth) <sup>†</sup>				Annulus (smooth)						
		Re <sub>s,h</sub>	Pr <sub>h</sub>	f <sub>s,i</sub>	Nu <sub>s</sub>	h <sub>a,i</sub> W/m <sup>2</sup> .C	Pr <sub>c</sub>	f <sub>s,o</sub>	h <sub>a,i</sub> W/m <sup>2</sup> .C	Nu <sub>s,o</sub>	Empirical	
Annulus Dimensions: L=1.245 m D <sub>o</sub> =0.028 m D <sub>i</sub> =0.0125 m												
Experimental Conditions: Hot Water Inlet Temperature: 60 ± 0.5 °C Hot Water Mass Flowrate: 0.1125 kg/s												
3000	1031.8	27334	3.068	0.0248	146.1	8623	6.4733	0.052	1197	30.72	0.0456	
4000	1250.1	27043	3.1042	0.0248	145.2	8565.6	6.5132	0.0455	1503.2	38.6	0.0414	
5000	1474.6	26976	3.1126	0.0248	145	8552.4	6.5381	0.042	1840.8	47.28	0.0386	
6000	1639.4	26660	3.1532	0.0249	144.7	8519.4	6.6337	0.0391	2107.1	54.2	0.0365	
7000	1820.5	26507	3.1732	0.025	144.7	8518.2	6.6223	0.0393	2416.1	62.14	0.0349	
8000	1970.6	26433	3.1831	0.0251	145	8532.8	6.6021	0.0383	2686.2	69.07	0.0335	
9000	2108.1	26416	3.1852	0.0251	145	8529.4	6.6707	0.0383	2948.7	75.9	0.0324	
10000	2232.4	26348	3.1943	0.0252	145.3	8545	6.6389	0.039	3195.5	82.21	0.0315	
Experimental Conditions: Hot Water Inlet Temperature: 60 ± 0.5 °C Hot Water Mass Flowrate: 0.2 kg/s												
3000	1052	48851	3.0502	0.022	241	14235	6.5355	0.0475	1151.1	29.57	0.0456	
4000	1289.7	48866	3.0492	0.022	241	14238	6.5022	0.0435	1441.8	37.01	0.0414	
5000	1535	48631	3.0654	0.022	240.8	14216	6.5364	0.0394	1755.9	45.1	0.0386	
6000	1779.3	48541	3.0716	0.022	240.5	14200	6.5372	0.042	2083.4	53.51	0.0365	
7000	1960	48336	3.0859	0.022	240.1	14165	6.551	0.0394	2336.7	60.03	0.0349	
8000	2173.3	48140	3.0997	0.022	239.6	14131	6.5579	0.0418	2647.6	68.03	0.0335	
9000	2426.5	47813	3.123	0.0221	239.1	14093	6.557	0.0379	3035.2	77.99	0.0324	
10000	2539.4	47881	3.1181	0.0221	239.2	14105	6.5997	0.0381	3213.2	82.61	0.0315	
Experimental Conditions: Hot Water Inlet Temperature: 70 ± 0.5 °C Hot Water Mass Flowrate: 0.1125 kg/s												
3000	1078	31302	2.6461	0.0244	155.5	9297.4	6.4162	0.0528	1244.7	31.91	0.0456	
4000	1267.3	31242	2.6517	0.0244	155.4	9286.7	6.4312	0.0423	1504.5	38.58	0.0414	
5000	1463.6	30890	2.6844	0.0245	155.1	9258.3	6.5098	0.0397	1790.6	45.97	0.0386	
6000	1638	30592	2.7128	0.0244	153.7	9171	6.5882	0.0378	2063.6	53.05	0.0365	
7000	1819.2	30599	2.7121	0.0246	154.3	9205.9	6.5064	0.0365	2357.1	60.52	0.0349	
8000	1961.9	30608	2.7112	0.0245	154.3	9207.6	6.5141	0.0392	2602.3	66.82	0.0335	
9000	2097	30291	2.7421	0.0246	153.5	9150.2	6.6048	0.0366	2851.8	73.33	0.0324	
10000	2234	30211	2.75	0.0246	153.3	9135.6	6.6025	0.0361	3113.1	80.04	0.0315	
Experimental Conditions: Hot Water Inlet Temperature: 70 ± 0.5 °C Hot Water Mass Flowrate: 0.2 kg/s												
3000	1162.4	56541	2.601	0.0218	257.9	15433	6.359	0.0537	1274.5	32.65	0.0456	
4000	1394.6	56280	2.614	0.0218	257.3	15393	6.4162	0.0424	1559.5	39.98	0.0414	
5000	1643.7	56187	2.6187	0.0218	257.1	15379	6.4062	0.0395	1877.9	48.14	0.0386	
6000	1827.3	55739	2.6415	0.0218	256.4	15331	6.4329	0.0376	2122.6	54.43	0.0365	
7000	2005	55717	2.6426	0.0218	256.4	15327	6.4724	0.0368	2366.2	60.72	0.0349	
8000	2207.1	55468	2.6555	0.0219	256.2	15309	6.4741	0.0376	2653.6	68.09	0.0335	
9000	2347	55399	2.659	0.0219	256	15299	6.4843	0.037	2859	73.38	0.0324	
10000	2531.3	55098	2.6748	0.0219	255.7	15272	6.5332	0.0362	3138.5	80.61	0.0315	
Experimental Conditions: Hot Water Inlet Temperature: 70 ± 0.5 °C Hot Water Mass Flowrate: 0.2 kg/s												
3000	1043.7	21291	3.0974	0.0274	123.3	5713.8	6.4145	0.0515	1311.7	27.12	0.0456	
4000	1242.7	21140	3.1216	0.0275	122.8	5687.3	6.4547	0.0485	1644.5	34.02	0.0414	
5000	1472.1	21037	3.1384	0.0275	122.5	5669.2	6.4716	0.0449	2074.5	42.93	0.0386	
6000	1642.2	20908	3.1597	0.0275	122	5646.4	6.5141	0.0414	2433.8	50.4	0.0365	
7000	1762.8	20845	3.1702	0.0277	122.5	5664.7	6.5553	0.0385	2703.9	56.03	0.0349	
8000	1926.1	20754	3.1855	0.0278	122.8	5677.9	6.5709	0.0352	3103.6	64.32	0.0335	
9000	2115	20608	3.2103	0.0282	123.6	5709.8	6.5943	0.0341	3611.1	74.87	0.0324	
10000	2166.8	20541	3.2218	0.0284	124	5726.5	6.6114	0.0327	3756.8	77.91	0.0315	
Experimental Conditions: Hot Water Inlet Temperature: 60 ± 0.5 °C Hot Water Mass Flowrate: 0.1125 kg/s												
3000	1218.2	38374	3.051	0.0232	198.2	9199.1	6.3426	0.0525	1431.5	29.56	0.0456	
4000	1391.8	38222	3.0643	0.0232	197.4	9158.7	6.4145	0.049	1678.9	34.71	0.0414	
5000	1688.7	37923	3.0908	0.0232	196.6	9115.7	6.4187	0.0441	2133.4	44.11	0.0386	
6000	1903.5	37862	3.0963	0.0233	197.3	9143.3	6.4354	0.0428	2485.9	51.41	0.0365	
7000	2098	37661	3.1145	0.0234	197.5	9150.3	6.4716	0.0387	2827.5	58.51	0.0349	
8000	2303.6	37573	3.1224	0.0235	197.7	9155.5	6.5804	0.034	3213.5	66.61	0.0335	
9000	2532.5	37350	3.143	0.0236	197.5	9140.5	6.5039	0.0335	3679.9	76.19	0.0324	
10000	2588.4	37339	3.144	0.0236	197.4	9138.8	6.5509	0.0319	3799.3	78.72	0.0315	
Experimental Conditions: Hot Water Inlet Temperature: 70 ± 0.5 °C Hot Water Mass Flowrate: 0.1125 kg/s												
3000	1091.3	24566	2.6495	0.0266	130.4	6123.7	6.2671	0.0537	1363.2	28.12	0.0456	
4000	1257	24407	2.6681	0.0268	130.7	6133.4	6.345	0.0522	1631.1	33.69	0.0414	
5000	1462.1	24154	2.6985	0.0266	129.2	6059.7	6.3805	0.0461	2003	41.39	0.0386	
6000	1635.5	23920	2.7272	0.0271	130.7	6123.8	6.4212	0.04	2332.8	48.24	0.0365	
7000	1769.4	23874	2.7328	0.027	129.8	6083	6.4547	0.0381	2623.5	54.27	0.0349	
8000	1938.7	23709	2.7536	0.0273	130.8	6122.9	6.4902	0.0344	3003	62.16	0.0335	
9000	2114	23598	2.7677	0.0273	130.4	6104.8	6.4945	0.0331	3451.8	71.46	0.0324	
10000	2226.6	23508	2.7792	0.0274	130.2	6090.1	6.5131	0.0312	3768.9	78.04	0.0315	
Experimental Conditions: Hot Water Inlet Temperature: 70 ± 0.5 °C Hot Water Mass Flowrate: 0.2 kg/s												
3000	1211.2	44435	2.6003	0.0229	211.8	9962.4	6.1907	0.0506	1403.5	28.91	0.0456	
4000	1428.1	44030	2.6262	0.023	210.9	9910.4	6.2607	0.0488	1704.9	35.16	0.0414	
5000	1839.3	43579	2.6557	0.0231	210.7	9893	6.2615	0.0461	2326.8	47.99	0.0386	
6000	1872	43501	2.6608	0.0231	211	9903.4	6.3401	0.0455	2378.6	49.12	0.0365	
7000	2137.3	43248	2.6777	0.0231	210.3	9870.1	6.3524	0.0377	2827	58.39	0.0349	
8000	2336.2	43215	2.6799	0.0232	210.7	9886	6.3846	0.0359	3184	65.8	0.0335	
9000	2556.1	42761	2.7108	0.0233	210.5	9866.1	6.4028	0.0335	3610	74.62	0.0324	
10000	2633.3	42785	2.7091	0.0233	210.5	9869.3	6.4418	0.0311	3765.2	77.88	0.0315	

<sup>†</sup>Predicted values of smooth inner tube are used to complete calculations only.

**Table C-25:** Predicted Results ( $Re_{s,h}$ ,  $Pr_h$ ,  $f_s$ ,  $Nu_s$ ,  $f_a/f_s$  and  $Nu_a/Nu_s$ ) for Annulus-Side Heat Transfer Enhancement for Two Annulus Sizes (Enhancement Status: : Wire Coil,  $e=1$  mm,  $p=10$  mm).

Re Annul us	$U_0$ W/m <sup>2</sup> .C	Inner Tube (smooth) <sup>†</sup>				Annulus (augmented)					
		$Re_{s,h}$	$Pr_h$	$f_{s,i}$	$Nu_{s,i}$	$h_{s,i}$ W/m <sup>2</sup> .C	$Pr_c$	$f_a$	$h_{a,o}$ W/m <sup>2</sup> .C	$Nu_a$	
Annulus Dimensions: L=1.245 m D <sub>o</sub> =0.028 m D <sub>i</sub> =0.0125 m											
Experimental Conditions: Hot Water Inlet Temperature: 60 ± 0.5 °C Hot Water Mass Flowrate: 0.1125 kg/s											
3000	2153.4	26548	3.1678	0.0257	147.9	8704.4	6.1726	0.1537	3013.7	76.96	
4000	2479.8	26391	3.1885	0.0257	147.4	8671.6	6.1914	0.1357	3701	94.54	
5000	2738	26261	3.2059	0.0259	148	8702.8	6.2873	0.1239	4298.5	110	
6000	2948.2	25893	3.256	0.0259	146.9	8624.6	6.3524	0.1104	4868.1	124.7	
7000	3122.1	26000	3.2413	0.0262	148.2	8705.1	6.4212	0.1024	5326.5	136.6	
8000	3287.4	25699	3.2832	0.0262	147.2	8640.1	6.4463	0.0958	5859.6	150.3	
9000	3492.1	25733	3.2783	0.0263	147.8	8676.2	6.5631	0.0942	6520.2	167.5	
10000	3597.9	25572	3.3011	0.0263	147.3	8641.1	6.5393	0.0939	6924.1	177.9	
Experimental Conditions: Hot Water Inlet Temperature: 60 ± 0.5 °C Hot Water Mass Flowrate: 0.2 kg/s											
3000	2401	47932	3.1145	0.0224	242.1	14274	6.0887	0.1492	2986.2	76.15	
4000	2866	47691	3.1317	0.0224	241.5	14232	6.1522	0.1327	3744.6	95.6	
5000	3200.1	47617	3.1371	0.0224	241.9	14254	6.1978	0.1243	4333.6	110.7	
6000	3430.8	47414	3.1518	0.0225	241.4	14218	6.2808	0.1156	4772.4	122.1	
7000	3666.6	47252	3.1637	0.0225	241.6	14224	6.2986	0.1117	5240.3	134.1	
8000	3861.7	47135	3.1724	0.0225	241.3	14203	6.3311	0.1022	5651.9	144.7	
9000	4063.2	47094	3.1754	0.0225	241.2	14196	6.4062	0.0958	6095.7	156.3	
10000	4229.1	47013	3.1814	0.0226	241.3	14199	6.412	0.0979	6476.2	166	
Experimental Conditions: Hot Water Inlet Temperature: 70 ± 0.5 °C Hot Water Mass Flowrate: 0.1125 kg/s											
3000	2145.8	30511	2.7207	0.0254	158.6	9457.1	5.9758	0.1542	2908.2	74.03	
4000	2540.1	30255	2.7457	0.0256	158.7	9458.3	5.9953	0.1294	3682.8	93.77	
5000	2802.4	29780	2.7933	0.0257	157.7	9383.6	6.1071	0.1187	4278.5	109.1	
6000	3045	29789	2.7924	0.0258	158.2	9417.8	6.2287	0.1054	4860.7	124.2	
7000	3227.6	29632	2.8085	0.0258	157.8	9387.3	6.2921	0.1091	5354.4	137	
8000	3448.9	29443	2.8282	0.0258	157.3	9350.4	6.3475	0.0941	6009.4	153.9	
9000	3583.4	29317	2.8415	0.026	158	9389.6	6.453	0.0913	6409.2	164.4	
10000	3773.7	29056	2.8694	0.0261	157.2	9337.6	6.4359	0.0932	7078	181.5	
Experimental Conditions: Hot Water Inlet Temperature: 70 ± 0.5 °C Hot Water Mass Flowrate: 0.2 kg/s											
3000	2458.5	55575	2.6499	0.0221	258.4	15446	5.8251	0.1525	3019.7	76.67	
4000	2891.5	54853	2.6877	0.0222	257.5	15373	5.8727	0.1442	3704.9	94.14	
5000	3333.1	54832	2.6888	0.0222	257.4	15370	5.9915	0.1228	4462.9	113.6	
6000	3618.7	54548	2.7041	0.0222	257.3	15354	6.0611	0.1191	4992	127.3	
7000	3849.4	54122	2.7272	0.0223	256.8	15316	6.0956	0.1033	5447.4	138.9	
8000	4082.8	53591	2.7566	0.0223	255.6	15230	6.1569	0.0971	5941.6	151.7	
9000	4297.8	53790	2.7455	0.0223	256.2	15272	6.1938	0.092	6399.8	163.5	
10000	4431.2	53452	2.7644	0.0224	255.9	15246	6.2959	0.0948	6705.7	171.6	
Annulus Dimensions: L=1.245 m D <sub>o</sub> =0.028 m D <sub>i</sub> =0.0155 m											
Experimental Conditions: Hot Water Inlet Temperature: 60 ± 0.5 °C Hot Water Mass Flowrate: 0.1125 kg/s											
3000	2147.5	20676	3.1987	0.028	123.2	5693.1	6.0398	0.1587	3714.6	76.33	
4000	2385.1	20580	3.215	0.028	122.9	5675.6	6.1358	0.1423	4500.3	92.63	
5000	2556.5	20438	3.2396	0.0282	123	5678.5	6.2543	0.1342	5149.2	106.2	
6000	2748.8	20308	3.2626	0.0282	122.6	5654.3	6.314	0.1252	6024.2	124.4	
7000	2930.3	20224	3.2774	0.0282	122.3	5638.7	6.3681	0.1253	6996.7	144.5	
8000	3042	20096	3.3004	0.0286	123.1	5671.7	6.4281	0.1259	7602.6	157.2	
9000	3159	20026	3.3132	0.029	124.1	5714.7	6.4651	0.1228	8275.8	171.2	
10000	3265.5	19962	3.3249	0.029	123.8	5702.4	6.4964	0.1202	9083.7	188	
Experimental Conditions: Hot Water Inlet Temperature: 60 ± 0.5 °C Hot Water Mass Flowrate: 0.2 kg/s											
3000	2576	37620	3.1182	0.0233	196.6	9108	5.8373	0.164	3778.6	77.38	
4000	2976.3	37335	3.1443	0.0233	195.9	9066.2	5.9498	0.1452	4719.5	96.84	
5000	3270.3	37121	3.1643	0.0233	195.3	9034.7	6.0527	0.1392	5517.2	113.4	
6000	3555	36925	3.1828	0.0233	194.8	9005.6	6.1545	0.1279	6395.3	131.7	
7000	3757.2	36769	3.1976	0.0233	194.4	8982.5	6.2033	0.1235	7096.7	146.2	
8000	3944.9	36605	3.2134	0.0235	194.7	8993.5	6.2769	0.1256	7788	160.7	
9000	4113.7	36495	3.224	0.0235	194.4	8977.1	6.3207	0.1229	8491	175.3	
10000	4266.8	36389	3.2343	0.0236	194.9	8996.4	6.36	0.1205	9148.1	189	
Experimental Conditions: Hot Water Inlet Temperature: 70 ± 0.5 °C Hot Water Mass Flowrate: 0.1125 kg/s											
3000	2130	23746	2.7489	0.0277	132.3	6195.4	5.7703	0.1531	3462.7	70.83	
4000	2413.7	23394	2.794	0.0281	132.6	6202	5.9565	0.1399	4277.3	87.77	
5000	2650.2	23314	2.8044	0.0281	132.4	6188.5	6.0764	0.1382	5090.4	104.7	
6000	2814.4	23151	2.8259	0.0281	131.9	6160.8	6.1851	0.1257	5759.5	118.6	
7000	2963.4	23021	2.8434	0.0285	132.8	6202.5	6.2279	0.1227	6371.1	131.3	
8000	3125.4	22884	2.8619	0.0285	132.4	6178.8	6.2945	0.1163	7205.6	148.7	
9000	3205.8	22841	2.8678	0.0285	132.3	6171.2	6.3279	0.1177	7660.1	158.2	
10000	3366.2	22635	2.8964	0.0289	132.9	6198	6.3894	0.1202	8587.3	177.5	
Experimental Conditions: Hot Water Inlet Temperature: 70 ± 0.5 °C Hot Water Mass Flowrate: 0.2 kg/s											
3000	2520	43298	2.6744	0.0232	210.9	9897	5.5703	0.158	3534	72.03	
4000	2945.7	42872	2.7032	0.0231	209	9800.2	5.7618	0.1511	4454.1	91.1	
5000	3234.4	42534	2.7265	0.0232	209.1	9795.5	5.8503	0.1344	5150.2	105.5	
6000	3517.7	42155	2.7532	0.0232	208.1	9744.7	5.9587	0.1299	5928.6	121.7	
7000	3742.4	42031	2.762	0.0233	208.7	9767.6	6.0672	0.1245	6584.4	135.4	
8000	3894.4	41951	2.7677	0.0234	208.5	9756.8	6.1126	0.1184	7076.2	145.6	
9000	4122.6	41765	2.7812	0.0234	208	9731.4	6.1616	0.1182	7885.9	162.4	
10000	4263.1	41676	2.7876	0.0235	208.6	9758.8	6.2295	0.1183	8394.2	173	

<sup>†</sup>Predicted values of smooth inner tube are used to complete calculations only.

<sup>††</sup>Augmentation values are predicted by using the proposed correlations and not experimental results.

**Table C-26:** Predicted Results ( $Re_{s,h}$ ,  $Pr$ ,  $f$ ,  $h$ ,  $Nu$ ,  $f_a/f_s$  and  $Nu_a/Nu_s$ ) for Annulus-Side Heat Transfer Enhancement for Two Annulus Sizes (Enhancement Status: Wire Coil,  $e=1$  mm,  $p=20$  mm).

Re Annul us	$U_0$ W/m <sup>2</sup> .C	Inner Tube (smooth) <sup>†</sup>				Annulus (augmented)						
		$Re_{s,h}$	$Pr_h$	$f_{s,i}$	$Nu_{s,i}$	$h_{s,i}$ W/m <sup>2</sup> .C	$Pr_c$	$f_a$	$h_{a,o}$ W/m <sup>2</sup> .C	$Nu_a$	Augmentation <sup>††</sup>	
Annulus Dimensions: L=1.245 m D <sub>o</sub> =0.028 m D <sub>i</sub> =0.0125 m												
Experimental Conditions: Hot Water Inlet Temperature: 60 ± 0.5 °C Hot Water Mass Flowrate: 0.1125 kg/s												
3000	2050	26492	3.1751	0.0258	148.2	8722.2	6.1836	0.129	2812.9	71.85	1.876	2.8991
4000	2382.7	26298	3.2009	0.0257	147.1	8652.2	6.2727	0.1149	3492.3	89.33	1.9267	2.7025
5000	2648.9	26140	3.2223	0.0258	147.1	8648	6.3434	0.1054	4096.6	104.9	1.967	2.5594
6000	2810.9	26060	3.2332	0.0259	147.4	8660	6.4262	0.0997	4494	115.2	2.0006	2.4439
7000	3082.7	25889	3.2566	0.0263	148.3	8709.9	6.4371	0.0965	5210.7	133.6	2.0294	2.3562
8000	3181.3	25789	3.2706	0.0259	146.5	8602.3	6.4826	0.0886	5548.5	142.4	2.0547	2.2808
9000	3384	25699	3.2832	0.0263	147.7	8668.6	6.5398	0.0859	6157.4	158.2	2.0773	2.2151
10000	3492.4	25641	3.2912	0.0263	147.5	8656.2	6.5415	0.0859	6533.9	167.8	2.0977	2.1595
Experimental Conditions: Hot Water Inlet Temperature: 60 ± 0.5 °C Hot Water Mass Flowrate: 0.2 kg/s												
3000	2341.6	48050	3.106	0.0224	243	14331	6.0725	0.1249	2892.3	73.74		
4000	2768	47839	3.1211	0.0224	242.5	14293	6.1459	0.1146	3574.5	91.24		
5000	3154.9	47636	3.1357	0.0224	241.4	14222	6.1962	0.107	4254.3	108.7		
6000	3287.3	47352	3.1564	0.0225	241.2	14207	6.3598	0.0997	4500.3	115.3		
7000	3581.8	47433	3.1505	0.0225	242	14257	6.3459	0.0961	5064	129.7		
8000	3707.2	47138	3.1721	0.0225	241.3	14204	6.3722	0.0892	5326.8	136.5		
9000	4001.5	46984	3.1836	0.0226	241.2	14194	6.4237	0.087	5958.4	152.8		
10000	4108.4	46811	3.1965	0.0226	240.8	14162	6.4581	0.0866	6205.3	159.2		
Experimental Conditions: Hot Water Inlet Temperature: 70 ± 0.5 °C Hot Water Mass Flowrate: 0.1125 kg/s												
3000	2141.8	30543	2.7175	0.0252	157.5	9396.7	5.9594	0.1206	2907.4	73.99		2.9198
4000	2505.3	30257	2.7455	0.0252	156.8	9343.2	6.0239	0.1140	3629.5	92.46		2.7212
5000	2761.8	29997	2.7714	0.0254	156.6	9327.1	6.1639	0.1051	4197.4	107.2		2.5732
6000	3050.6	29814	2.7899	0.0254	156.1	9292.4	6.2191	0.0997	4914	125.6		2.4584
7000	3228.2	29635	2.8083	0.0254	155.6	9258.2	6.3116	0.0942	5404.9	138.3		2.3662
8000	3522.6	29348	2.8382	0.0255	155.4	9235.4	6.2752	0.0883	6296.3	161.1		2.2919
9000	3646.8	29297	2.8436	0.0255	155.2	9225.6	6.3271	0.0860	6710.3	171.8		2.2259
10000	3791.1	29099	2.8647	0.0256	155.2	9219	6.4321	0.0852	7220.3	185.2		2.1672
Experimental Conditions: Hot Water Inlet Temperature: 70 ± 0.5 °C Hot Water Mass Flowrate: 0.2 kg/s												
3000	2613.6	55391	2.6595	0.0221	258	15418	5.7309	0.1200	3258.5	82.59		
4000	3008.7	54673	2.6973	0.0221	256.4	15305	5.8359	0.1106	3904.6	99.15		
5000	3342.9	54531	2.7049	0.0222	256.8	15322	5.9328	0.1063	4485	114.1		
6000	3563.6	53953	2.7364	0.0222	255.5	15230	6.0703	0.0958	4902.3	125		
7000	3821.6	54056	2.7308	0.0222	256.4	15285	6.1141	0.0937	5396.2	137.7		
8000	4057.2	53713	2.7498	0.0223	255.9	15250	6.1686	0.0888	5884.3	150.3		
9000	4209.9	53558	2.7584	0.0223	255.5	15225	6.2223	0.0841	6215.7	158.9		
10000	4400.2	53461	2.7638	0.0223	255.3	15209	6.2631	0.0830	6643.2	169.9		
Annulus Dimensions: L=1.245 m D <sub>o</sub> =0.028 m D <sub>i</sub> =0.0155 m												
Experimental Conditions: Hot Water Inlet Temperature: 60 ± 0.5 °C Hot Water Mass Flowrate: 0.1125 kg/s												
3000	2114.9	20759	3.1847	0.0278	122.8	5678.8	6.0043	0.1292	3624.7	74.44	2.4011	2.7663
4000	2397.5	20569	3.217	0.028	122.8	5673.5	6.1459	0.125	4546	93.58	2.4661	2.6153
5000	2571.8	20449	3.2377	0.0282	123.1	5680.6	6.2519	0.1239	5209.9	107.4	2.5177	2.5036
6000	2673.3	20346	3.2558	0.0282	122.7	5661.4	6.3254	0.1208	5665	117	2.5607	2.4168
7000	2922.9	20176	3.286	0.0286	123.4	5686.8	6.3962	0.1213	6875.3	142.1	2.5975	2.3451
8000	2937.2	20208	3.2803	0.0286	123.5	5692.8	6.4262	0.1166	6945	143.6	2.6299	2.2862
9000	3012.6	20156	3.2895	0.0286	123.3	5683.1	6.4581	0.1148	7399.6	153.1	2.6588	2.2351
10000	3161.2	20024	3.3135	0.029	124	5714.4	6.5079	0.1132	8291.8	171.7	2.685	2.1898
Experimental Conditions: Hot Water Inlet Temperature: 60 ± 0.5 °C Hot Water Mass Flowrate: 0.2 kg/s												
3000	2559.6	37637	3.1166	0.0232	195.9	9074.2	5.8438	0.131	3749.6	76.8		
4000	2922.8	37335	3.1443	0.0232	195.1	9030.1	5.9639	0.1269	4596.7	94.34		
5000	3241.3	37141	3.1624	0.0233	195.4	9037.7	6.0741	0.1257	5433.9	111.7		
6000	3437.9	37023	3.1735	0.0232	194.3	8984.3	6.1498	0.1206	6036.6	124.3		
7000	3613.6	36714	3.2028	0.0233	194.2	8974.3	6.2279	0.1188	6605.9	136.2		
8000	3798.4	36654	3.2087	0.0235	194.8	9000.8	6.276	0.1164	7231.8	149.2		
9000	3940.6	36590	3.2148	0.0235	194.6	8991.3	6.3262	0.1132	7773.1	160.5		
10000	4073.1	36378	3.2354	0.0235	194.1	8959.4	6.3714	0.1133	8336.6	172.2		
Experimental Conditions: Hot Water Inlet Temperature: 70 ± 0.5 °C Hot Water Mass Flowrate: 0.1125 kg/s												
3000	2197.9	23655	2.7604	0.0277	132	6180.2	5.7443	0.1302	3651.6	74.66		2.7869
4000	2425.9	23415	2.7913	0.0277	131.3	6140.3	5.9498	0.1274	4349.3	89.24		2.6306
5000	2605.2	23262	2.8113	0.0281	132.2	6179.6	6.0596	0.1215	4933.6	101.4		2.5172
6000	2734.9	23132	2.8284	0.0281	131.8	6157.5	6.1624	0.1212	5439.3	112		2.4281
7000	2879.4	23092	2.8338	0.0285	133.1	6214.9	6.2343	0.1186	5982.3	123.3		2.3555
8000	2959.4	22981	2.8488	0.0285	132.7	6195.6	6.3091	0.1164	6360.6	131.3		2.2924
9000	3066	22933	2.8553	0.0285	132.6	6187.2	6.3549	0.1163	6885.5	142.2		2.2405
10000	3084.6	22905	2.8591	0.0287	133.1	6214.2	6.3962	0.1132	6942.6	143.5		2.1945
Experimental Conditions: Hot Water Inlet Temperature: 70 ± 0.5 °C Hot Water Mass Flowrate: 0.2 kg/s												
3000	2627.2	43155	2.6839	0.0231	209.7	9837.5	5.5317	0.129	3757.9	76.54		
4000	2994.1	42947	2.698	0.0231	209.2	9810.2	5.6989	0.1293	4563.3	93.23		
5000	3291.8	42592	2.7225	0.0232	209.2	9803.3	5.8294	0.1235	5294.9	108.4		
6000	3546.6	42434	2.7335	0.0232	208.8	9782.1	5.9298	0.1208	5995.4	123		
7000	3700.5	42251	2.7464	0.0233	209.2	9797.4	6.0224	0.1189	6441.5	132.3		
8000	3808.7	41761	2.7814	0.0234	208	9731	6.1671	0.1165	6812.2	140.3		
9000	3934	41837	2.7759	0.0234	208.2	9741.3	6.2247	0.1128	7217.6	148.8		
10000	4080.3	41595	2.7936	0.0234	207.6	9708.2	6.3018	0.1133	7749	159.9		

**Table C-27:** Predicted Results ( $Re_{s,h}$ ,  $Pr$ ,  $f$ ,  $h$ ,  $Nu$ ,  $f_a/f_s$  and  $Nu_a/Nu_s$ ) for Annulus-Side Heat Transfer Enhancement for Two Annulus Sizes (Enhancement Status: Wire Coil,  $e=1$  mm,  $p=30$  mm).

Re Annul us	$U_0$ W/m <sup>2</sup> .C	Inner Tube (smooth) <sup>†</sup>				Annulus (augmented)					
		$Re_{s,h}$	$Pr_h$	$f_{s,i}$	$Nu_{s,i}$	$h_{s,i}$ W/m <sup>2</sup> .C	$Pr_c$	$f_a$	$h_{a,o}$ W/m <sup>2</sup> .C	$Nu_a$	
Annulus Dimensions: L=1.245 m D <sub>o</sub> =0.028 m D <sub>i</sub> =0.0125 m											
Experimental Conditions: Hot Water Inlet Temperature: 60 ± 0.5 °C Hot Water Mass Flowrate: 0.1125 kg/s											
3000	1974.2	26644	3.1553	0.0256	147.6	8694.6	6.2375	0.0913	2675	68.39	
4000	2253	26232	3.2098	0.0256	146.4	8609.1	6.3871	0.0834	3227.4	82.71	
5000	2513.4	26164	3.2189	0.0257	146.7	8624.1	6.4237	0.0813	3786.6	97.09	
6000	2703.4	26189	3.2156	0.0257	146.8	8629.3	6.4178	0.0754	4233.5	108.5	
7000	2894.3	26131	3.2234	0.0256	146.1	8588	6.417	0.0734	4735.3	121.4	
8000	3016.2	26037	3.2363	0.0257	146.3	8597.3	6.4885	0.0692	5067.2	130.1	
9000	3203.8	25908	3.254	0.0258	146.4	8598.8	6.5813	0.0665	5619.1	144.4	
10000	3350.3	25838	3.2637	0.0259	146.7	8612.8	6.545	0.0669	6078	156.1	
Experimental Conditions: Hot Water Inlet Temperature: 60 ± 0.5 °C Hot Water Mass Flowrate: 0.2 kg/s											
3000	2254.7	47928	3.1147	0.0224	241.9	14265	6.1718	0.089	2763.6	70.57	
4000	2617.6	47569	3.1406	0.0224	241.2	14210	6.2792	0.0838	3332.8	85.26	
5000	2909.2	47359	3.1559	0.0224	240.7	14173	6.336	0.0806	3823.4	97.9	
6000	3209.5	47241	3.1645	0.0224	240.4	14152	6.3295	0.0754	4361.8	111.7	
7000	3463.1	47429	3.1508	0.0224	241.1	14203	6.3681	0.073	4837	123.9	
8000	3631	47282	3.1616	0.0224	240.8	14177	6.3689	0.0699	5175.1	132.6	
9000	3884.9	47142	3.1719	0.0225	240.7	14169	6.4287	0.0677	5708	146.4	
10000	4028.4	47068	3.1773	0.0225	240.5	14156	6.427	0.0677	6025.9	154.5	
Experimental Conditions: Hot Water Inlet Temperature: 70 ± 0.5 °C Hot Water Mass Flowrate: 0.1125 kg/s											
3000	1999	30497	2.722	0.025	156.3	9321.3	6.0787	0.0873	2657.3	67.76	
4000	2266	30388	2.7326	0.0252	157.1	9367.7	6.1048	0.0835	3144.8	80.22	
5000	2491.7	30004	2.7707	0.0252	156.1	9295.6	6.2112	0.0777	3609.2	92.23	
6000	2703.7	29879	2.7832	0.0252	155.7	9272.1	6.2671	0.0748	4076.7	104.3	
7000	2828.9	29812	2.7901	0.0252	155.6	9259.3	6.3246	0.0697	4371.5	111.9	
8000	3011.6	29700	2.8016	0.0254	155.8	9270.6	6.4103	0.0675	4820.1	123.6	
9000	3158.7	29528	2.8194	0.0254	155.3	9237.7	6.4004	0.0657	5220.4	133.8	
10000	3309.7	29443	2.8282	0.0254	155.1	9221.5	6.422	0.0644	5652.8	144.9	
Experimental Conditions: Hot Water Inlet Temperature: 70 ± 0.5 °C Hot Water Mass Flowrate: 0.2 kg/s											
3000	2362.2	55246	2.667	0.0219	256.4	15315	5.872	0.0884	2880.8	73.2	
4000	2729.8	55064	2.6766	0.0219	256	15286	5.9893	0.084	3448.6	87.8	
5000	3045.9	54627	2.6998	0.022	255.3	15238	6.1389	0.0794	3972.7	101.4	
6000	3313.2	54419	2.711	0.0221	255.5	15245	6.1922	0.0764	4439.1	113.4	
7000	3512.2	54510	2.7061	0.0221	256.4	15299	6.2152	0.0704	4797.7	122.6	
8000	3744.4	54287	2.7182	0.0222	256.2	15283	6.2287	0.0683	5243.9	134	
9000	3948.7	54076	2.7297	0.0222	255.7	15249	6.2727	0.0677	5658.9	144.7	
10000	4143.8	53953	2.7364	0.0222	255.8	15249	6.297	0.0653	6068.3	155.3	
Annulus Dimensions: L=1.245 m D <sub>o</sub> =0.028 m D <sub>i</sub> =0.0155 m											
Experimental Conditions: Hot Water Inlet Temperature: 60 ± 0.5 °C Hot Water Mass Flowrate: 0.1125 kg/s											
3000	1862.4	20827	3.1732	0.0278	123.1	5691.1	6.0894	0.0999	2937.6	60.42	
4000	2074.1	20608	3.2103	0.0279	122.3	5651.4	6.2223	0.0929	3518	72.51	
5000	2238.1	20521	3.2253	0.0279	122	5635.6	6.3124	0.0822	4026.2	83.11	
6000	2371.6	20519	3.2256	0.0282	123.3	5693.4	6.3763	0.079	4440.3	91.75	
7000	2509.1	20353	3.2546	0.0282	122.7	5662.6	6.4818	0.0735	4973.9	102.9	
8000	2588.3	20327	3.2592	0.0282	122.6	5657.9	6.4775	0.0744	5299.9	109.7	
9000	2685.6	20242	3.2743	0.0282	122.3	5642	6.5562	0.069	5742.5	119	
10000	2798.9	20149	3.2908	0.0282	122	5624.8	6.5541	0.0669	6310.5	130.8	
Experimental Conditions: Hot Water Inlet Temperature: 60 ± 0.5 °C Hot Water Mass Flowrate: 0.2 kg/s											
3000	2158.7	37614	3.1187	0.0232	195.8	9070.8	5.9706	0.0945	2948	60.51	
4000	2355.9	37457	3.1331	0.0233	195.8	9066.1	6.1397	0.0843	3329.4	68.53	
5000	2804.8	37289	3.1486	0.0233	195.7	9059.4	6.1522	0.0829	4304	88.61	
6000	3032.2	37182	3.1586	0.0233	195.5	9043.6	6.2311	0.0772	4868.9	100.4	
7000	3236.5	37060	3.17	0.0233	195.1	9025.7	6.301	0.0721	5425.2	112	
8000	3271.7	36841	3.1907	0.0235	195.3	9028.8	6.3598	0.0684	5523.7	114.1	
9000	3490.2	36861	3.1888	0.0235	195.4	9031.8	6.3722	0.0708	6174.8	127.6	
10000	3642.6	36649	3.2091	0.0235	194.8	9000.1	6.422	0.0676	6687.7	138.3	
Experimental Conditions: Hot Water Inlet Temperature: 70 ± 0.5 °C Hot Water Mass Flowrate: 0.1125 kg/s											
3000	1827.3	23958	2.7225	0.0275	132.2	6196.9	5.8975	0.092	2727.8	55.92	
4000	2105.1	23750	2.7484	0.0277	132.3	6196	6.0504	0.0828	3397.2	69.82	
5000	2290.4	23585	2.7693	0.0277	131.8	6168.7	6.1444	0.0801	3919.6	80.69	
6000	2448	23394	2.794	0.0277	131.2	6136.7	6.2615	0.0755	4422.8	91.22	
7000	2541.2	23309	2.8051	0.0277	131	6122.6	6.2913	0.0704	4746.1	97.93	
8000	2638	23211	2.818	0.0277	130.7	6106.1	6.3656	0.0655	5107.9	105.5	
9000	2779.1	23064	2.8376	0.0277	130.2	6081.3	6.4121	0.0643	5688.8	117.6	
10000	2875.9	22979	2.8491	0.0277	130	6067	6.4481	0.0635	6125.9	126.7	
Experimental Conditions: Hot Water Inlet Temperature: 70 ± 0.5 °C Hot Water Mass Flowrate: 0.2 kg/s											
3000	2163.2	43481	2.6621	0.023	210	9859.8	5.7226	0.0971	2873.6	58.73	
4000	2538.8	43162	2.6835	0.0231	209.7	9838.4	5.8409	0.0843	3579.5	73.31	
5000	2825.4	42882	2.7025	0.0231	209	9801.5	5.978	0.0808	4184.3	85.9	
6000	3069.4	42502	2.7288	0.0231	208.1	9751.1	6.084	0.0729	4755.8	97.8	
7000	3248.6	42308	2.7423	0.0232	208.5	9765.3	6.171	0.0701	5195.7	107	
8000	3440.4	42144	2.7539	0.0232	208.1	9743.2	6.2123	0.066	5713	117.7	
9000	3596.5	41991	2.7649	0.0232	207.7	9722.6	6.2626	0.0643	6165.6	127.2	
10000	3738.2	41855	2.7747	0.0232	207.4	9704.2	6.3054	0.0632	6603.6	136.3	

**Table C-28:** Predicted Results ( $Re_{s,h}$ ,  $Pr$ ,  $f$ ,  $h$ ,  $Nu$ ,  $f_a/f_s$  and  $Nu_a/Nu_s$ ) for Annulus-Side Heat Transfer Enhancement for Two Annulus Sizes (Enhancement Status: Wire Coil,  $e=1$  mm,  $p=40$  mm).

Re Annul us	$U_0$ W/m <sup>2</sup> .C	Inner Tube (smooth) <sup>†</sup>				Annulus (augmented)					
		$Re_{s,h}$	$Pr_h$	$f_{s,i}$	$Nu_{s,i}$	$h_{s,i}$ W/m <sup>2</sup> .C	$Pr_c$	$f_a$	$h_{a,o}$ W/m <sup>2</sup> .C	$Nu_a$	
Annulus Dimensions: L=1.245 m D <sub>o</sub> =0.028 m D <sub>i</sub> =0.0125 m											
Experimental Conditions: Hot Water Inlet Temperature: 60 ± 0.5 °C Hot Water Mass Flowrate: 0.1125 kg/s											
3000	1769.3	26669	3.1521	0.0253	146.7	8640.3	6.3108	0.0855	2316.7	59.29	
4000	2053.9	26464	3.179	0.0254	146.1	8598.2	6.3979	0.0725	2835.2	72.67	
5000	2255.6	26284	3.2028	0.0256	146.6	8619.8	6.5073	0.0662	3231.1	82.96	
6000	2411.5	26329	3.1968	0.0257	147.2	8658.7	6.4287	0.0658	3553.3	91.12	
7000	2542.5	26307	3.1998	0.0258	147.6	8683.2	6.5381	0.0603	3839.9	98.63	
8000	2722.4	26154	3.2203	0.0257	146.7	8621.9	6.5004	0.0581	4282.5	109.9	
9000	2860.9	26033	3.2368	0.0258	146.8	8625.4	6.5226	0.0537	4634.4	119	
10000	2982	25969	3.2456	0.0259	147.1	8640.8	6.6805	0.0518	4954.8	127.5	
Experimental Conditions: Hot Water Inlet Temperature: 60 ± 0.5 °C Hot Water Mass Flowrate: 0.2 kg/s											
3000	1990.2	48136	3.1	0.0221	240.2	14167	6.2343	0.0794	2379.6	60.83	
4000	2359.5	47813	3.123	0.0222	240.3	14164	6.3091	0.0700	2927.6	74.93	
5000	2616.4	47773	3.1259	0.0224	242.3	14282	6.3648	0.0661	3326.4	85.21	
6000	2865.4	47529	3.1435	0.0225	241.7	14238	6.35	0.0634	3743	95.86	
7000	3239.5	47370	3.1551	0.0225	241.3	14210	6.3738	0.0617	4410.9	113	
8000	3301.4	47569	3.1406	0.0225	242.4	14281	6.4379	0.057	4518.5	115.9	
9000	3458.7	47407	3.1524	0.0225	242	14252	6.4312	0.0543	4822	123.7	
10000	3706.9	47263	3.1629	0.0225	241.6	14226	6.5056	0.0537	5322.6	136.6	
Experimental Conditions: Hot Water Inlet Temperature: 70 ± 0.5 °C Hot Water Mass Flowrate: 0.1125 kg/s											
3000	1688.8	30808	2.6922	0.0247	155.4	9277.3	6.171	0.0809	2138.4	54.61	
4000	2056.5	30559	2.7159	0.0249	155.9	9299.4	6.1907	0.0679	2762	70.55	
5000	2164.1	30172	2.7539	0.0252	156.5	9327.3	6.3871	0.063	2956.6	75.76	
6000	2323.4	29988	2.7723	0.0252	156	9292.6	6.4128	0.0604	3266.8	83.75	
7000	2512.6	30042	2.7668	0.0252	156.2	9302.9	6.3987	0.0585	3651.9	93.6	
8000	2657.5	29758	2.7956	0.0256	157.1	9346.8	6.4254	0.0561	3957.2	101.5	
9000	2773	29738	2.7977	0.0255	156.5	9310.4	6.4657	0.0529	4227.3	108.5	
10000	2804.2	29886	2.7826	0.0258	158.5	9436.6	6.4767	0.0521	4270.4	109.6	
Experimental Conditions: Hot Water Inlet Temperature: 70 ± 0.5 °C Hot Water Mass Flowrate: 0.2 kg/s											
3000	1990	55653	2.6459	0.0218	255.6	15277	6.0542	0.0753	2346.8	59.82	
4000	2374.5	54903	2.685	0.0218	254.6	15202	6.1226	0.0692	2903.8	74.1	
5000	2621	54811	2.69	0.0218	254.4	15187	6.1812	0.0639	3281.9	83.82	
6000	2907.5	55165	2.6712	0.0219	255.9	15282	6.2104	0.062	3737.4	95.5	
7000	2971.4	54773	2.692	0.022	255.7	15261	6.345	0.058	3845.2	98.47	
8000	3308.3	54299	2.7175	0.022	254.6	15186	6.2776	0.0574	4435.9	113.5	
9000	3469.1	54134	2.7265	0.022	254.2	15160	6.323	0.0542	4732.9	121.2	
10000	3731.1	54307	2.7171	0.022	254.6	15188	6.4287	0.0521	5230.6	134.1	
Annulus Dimensions: L=1.245 m D <sub>o</sub> =0.028 m D <sub>i</sub> =0.0155 m											
Experimental Conditions: Hot Water Inlet Temperature: 60 ± 0.5 °C Hot Water Mass Flowrate: 0.1125 kg/s											
3000	1841.2	20803	3.1773	0.0282	124.2	5745.5	6.1218	0.0818	2869.9	59.06	
4000	2008	20728	3.1899	0.0282	124	5731.8	6.2327	0.0703	3301.9	68.07	
5000	2170.1	20652	3.2028	0.0282	123.7	5717.8	6.323	0.0644	3770.9	77.85	
6000	2281.1	20561	3.2184	0.0282	123.4	5701.2	6.3962	0.0597	4128.8	85.34	
7000	2399.9	20459	3.236	0.0286	124.3	5740.1	6.4455	0.0555	4508.3	93.25	
8000	2473.4	20375	3.2507	0.0288	124.7	5753	6.4919	0.0523	4764.8	98.63	
9000	2586.9	20324	3.2597	0.029	125.1	5771.8	6.5201	0.0500	5187.8	107.4	
10000	2634.2	20309	3.2623	0.029	125.1	5769.1	6.5553	0.0476	5384.3	111.6	
Experimental Conditions: Hot Water Inlet Temperature: 60 ± 0.5 °C Hot Water Mass Flowrate: 0.2 kg/s											
3000	2182.1	37751	3.1063	0.0232	196.2	9090.7	5.9439	0.0817	2989.6	61.34	
4000	2471.6	37512	3.128	0.0232	195.6	9056	6.0748	0.0712	3566.8	73.34	
5000	2670.1	37382	3.14	0.0233	196	9073.1	6.2191	0.0648	3991.8	82.27	
6000	2882	37188	3.158	0.0233	195.5	9044.5	6.2479	0.0591	4492.7	92.64	
7000	3023.5	37202	3.1567	0.0234	196.3	9082.6	6.3295	0.0559	4834.3	99.81	
8000	3178.4	37060	3.17	0.0235	195.9	9061.5	6.3508	0.0527	5250.5	108.4	
9000	3288.2	36890	3.1861	0.0235	195.5	9036.2	6.4087	0.0498	5567.6	115.1	
10000	3403.2	36890	3.1861	0.0236	196.2	9071.8	6.4455	0.0477	5889	121.8	
Experimental Conditions: Hot Water Inlet Temperature: 70 ± 0.5 °C Hot Water Mass Flowrate: 0.1125 kg/s											
3000	1818.3	24002	2.7171	0.027	130.2	6103.3	5.8975	0.0828	2727.8	55.92	
4000	2092.2	23761	2.7471	0.027	129.5	6064.8	6.0405	0.0719	3408.1	70.04	
5000	2242.4	23525	2.7771	0.027	128.8	6026.7	6.2088	0.0635	3842.5	79.18	
6000	2360.4	23369	2.7972	0.0274	129.8	6067.2	6.3189	0.059	4180.7	86.3	
7000	2496.5	23323	2.8032	0.0274	129.6	6059.6	6.4004	0.0555	4632.6	95.76	
8000	2580.9	23190	2.8208	0.0277	130.6	6102.6	6.3615	0.0526	4900.8	101.2	
9000	2664.2	23209	2.8182	0.0277	130.7	6105.8	6.4153	0.0493	5207.4	107.7	
10000	2751.4	23130	2.8287	0.0279	131.1	6125	6.4371	0.0475	5533.7	114.4	
Experimental Conditions: Hot Water Inlet Temperature: 70 ± 0.5 °C Hot Water Mass Flowrate: 0.2 kg/s											
3000	2147.2	43181	2.6821	0.0227	207.2	9718.7	5.7302	0.0824	2858.7	58.43	
4000	2496.5	43072	2.6895	0.0227	206.9	9704.6	5.8684	0.0705	3515	72.02	
5000	2718.1	42875	2.7029	0.0227	206.4	9679.1	5.99	0.0644	3975.7	81.63	
6000	2957.7	42602	2.7218	0.0228	206.2	9663.7	6.0695	0.059	4513.8	92.8	
7000	3103.7	42437	2.7333	0.0229	206.3	9662.2	6.1444	0.0558	4863.1	100.1	
8000	3242.3	42238	2.7473	0.0229	205.8	9635.9	6.2104	0.0525	5220.9	107.6	
9000	3350.6	42031	2.762	0.023	206.1	9648.3	6.4004	0.0499	5503	113.7	
10000	3434.9	42129	2.755	0.023	206.4	9661.5	6.4371	0.0475	5729.1	118.5	

**Table C-29:** Predicted Results ( $Re_{s,h}$ ,  $Pr$ ,  $f$ ,  $h$ ,  $Nu$ ,  $f_a/f_s$  and  $Nu_a/Nu_s$ ) for Annulus-Side Heat Transfer Enhancement for Two Annulus Sizes (Enhancement Status: Wire Coil,  $e=2.2$  mm,  $p=10$  mm).

Re	$U_0$ W/m <sup>2</sup> .C	Inner Tube (smooth) <sup>†</sup>				Annulus (augmented)							
		$Re_{s,h}$	$Pr_h$	$f_{s,i}$	$Nu_{s,i}$	$h_{s,i}$ W/m <sup>2</sup> .C	$Pr_c$	$f_a$	$h_{a,o}$ W/m <sup>2</sup> .C	$Nu_a$			
Annulus Dimensions: L=1.245 m D <sub>o</sub> =0.028 m D <sub>i</sub> =0.0125 m													
Experimental Conditions: Hot Water Inlet Temperature: 60 ± 0.5 °C Hot Water Mass Flowrate: 0.1125 kg/s													
3000	2184.6	26480	3.1768	0.0248	143.6	8453.3	6.1624	0.3082	3112.3	79.47	5.8418		
4000	2479.9	26257	3.2064	0.025	144	8467.5	6.3165	0.2706	3745	95.86	5.9999		
5000	2724.3	26099	3.2279	0.0249	143	8405.7	6.3631	0.2647	4350.3	111.4	6.1254		
6000	2924.5	26010	3.2399	0.0248	142.3	8358.4	6.4581	0.2424	4902.5	125.8	6.2299		
7000	3076.7	25852	3.2617	0.025	142.8	8384.5	6.4379	0.2452	5333.9	136.8	6.3197		
8000	3275.8	25762	3.2743	0.025	142.5	8365.9	6.4472	0.2188	5972.8	153.2	6.3985		
9000	3446.1	25809	3.2677	0.0253	143.7	8433.6	6.475	0.2244	6517.7	167.3	6.4688		
10000	3547.8	25721	3.28	0.0253	143.6	8429.7	6.4953	0.206	6894.4	177	6.5324		
Experimental Conditions: Hot Water Inlet Temperature: 60 ± 0.5 °C Hot Water Mass Flowrate: 0.2 kg/s													
3000	2492.8	47961	3.1124	0.0221	240	14154	6.0573	0.2927	3136.1	79.94			
4000	2920.7	47924	3.115	0.0221	240.1	14157	6.0894	0.2703	3844.7	98.05			
5000	3311.5	47580	3.1398	0.0222	239.4	14106	6.1773	0.2529	4557.8	116.4			
6000	3601.6	47101	3.1749	0.0222	238.5	14039	6.2271	0.2547	5136.2	131.3			
7000	3876.3	47065	3.1776	0.0222	238.6	14041	6.2719	0.2353	5713.2	146.1			
8000	4154.2	46819	3.1959	0.0223	238.4	14024	6.3091	0.2264	6342.2	162.3			
9000	4313.6	46416	3.2265	0.0223	237.4	13952	6.3574	0.2225	6740.1	172.6			
10000	4537.4	46753	3.2009	0.0223	238.5	14030	6.4648	0.2057	7279.1	186.8			
Experimental Conditions: Hot Water Inlet Temperature: 70 ± 0.5 °C Hot Water Mass Flowrate: 0.1125 kg/s													
3000	2128.5	30393	2.7321	0.0244	153.2	9135.1	5.9624	0.3011	2911.9	74.1	2.8868		
4000	2435	30255	2.7457	0.0245	153.1	9126.9	6.0649	0.2676	3519.2	89.71	2.7344		
5000	2707.2	30045	2.7666	0.0246	152.9	9105.2	6.1087	0.261	4122.6	105.2	2.6246		
6000	2973.2	29597	2.8122	0.0247	152.2	9055.6	6.2073	0.2502	4788.5	122.4	2.5358		
7000	3063.4	29706	2.8009	0.0249	153.6	9141.4	6.2953	0.2438	4997.2	127.9	2.4603		
8000	3280.1	29586	2.8134	0.025	153.9	9151.3	6.3238	0.2243	5596.4	143.3	2.4006		
9000	3400	29452	2.8273	0.0251	153.8	9142.3	6.3722	0.219	5959.3	152.7	2.3487		
10000	3546.8	29253	2.8483	0.0253	154	9152.8	6.4145	0.2052	6419.6	164.6	2.3024		
Experimental Conditions: Hot Water Inlet Temperature: 70 ± 0.5 °C Hot Water Mass Flowrate: 0.2 kg/s													
3000	2402.4	55799	2.6384	0.0219	257.3	15380	5.8051	0.2978	2938.2	74.57			
4000	2886.3	55123	2.6735	0.0219	256	15290	5.9202	0.2745	3701.9	94.14			
5000	3213.6	54962	2.6819	0.022	256.1	15293	5.9624	0.2602	4257.8	108.4			
6000	3720.5	54171	2.7245	0.022	254.3	15166	6.0103	0.2481	5212.7	132.8			
7000	4076.3	54081	2.7294	0.022	254.4	15171	6.1397	0.2354	5938	151.6			
8000	4264.6	53790	2.7455	0.0221	254.1	15145	6.1686	0.2266	6351.6	162.2			
9000	4534.3	53457	2.7641	0.0221	253.8	15121	6.1836	0.2096	6974.7	178.1			
10000	4707.2	53518	2.7607	0.0221	254.1	15140	6.2311	0.2133	7387	188.8			
Annulus Dimensions: L=1.245 m D <sub>o</sub> =0.028 m D <sub>i</sub> =0.0155 m													
Experimental Conditions: Hot Water Inlet Temperature: 60 ± 0.5 °C Hot Water Mass Flowrate: 0.1125 kg/s													
3000	2091.8	20653	3.2026	0.0294	127.5	5892.1	6.0994	0.3531	3470.1	71.38	7.5635		
4000	2245.5	20559	3.2187	0.0294	127.2	5874.1	6.2407	0.3392	3923.5	80.89	7.7681		
5000	2352.8	20477	3.2329	0.0294	126.9	5858.3	6.301	0.3311	4272.7	88.18	7.9307		
6000	2442.6	20430	3.2411	0.0297	128	5906.2	6.3656	0.3211	4546.4	93.92	8.066		
7000	2518.2	20403	3.2458	0.0299	128.5	5929.2	6.4615	0.3159	4798.5	99.28	8.1822		
8000	2594	20354	3.2543	0.0297	127.7	5891.4	6.5226	0.3137	5112.7	105.9	8.2842		
9000	2653.7	20197	3.2823	0.0298	127.1	5860.5	6.5141	0.306	5378.4	111.4	8.3753		
10000	2713	20176	3.286	0.0298	127	5856.5	6.5865	0.2991	5631.9	116.8	8.4576		
Experimental Conditions: Hot Water Inlet Temperature: 60 ± 0.5 °C Hot Water Mass Flowrate: 0.2 kg/s													
3000	2674.9	37008	3.1749	0.0237	197.3	9125.2	5.8895	0.3621	3991.5	81.82			
4000	2883.1	37107	3.1656	0.0234	196	9068.4	6.0405	0.3472	4489	92.25			
5000	3040.1	36904	3.1847	0.0235	195.5	9038.3	6.1374	0.3378	4891.2	100.7			
6000	3179.7	36818	3.1929	0.0235	195.3	9025.4	6.2889	0.32	5267.6	108.7			
7000	3281.4	36567	3.217	0.0237	196.1	9058.6	6.3238	0.3171	5538.8	114.3			
8000	3360.7	36579	3.2159	0.0236	195.4	9025	6.3805	0.3204	5783.7	119.5			
9000	3439.4	36769	3.1976	0.0235	195.1	9018.1	6.3945	0.3101	6024.3	124.5			
10000	3437	36488	3.2246	0.0236	195.1	9011.4	6.494	0.3008	6020.3	124.6			
Experimental Conditions: Hot Water Inlet Temperature: 70 ± 0.5 °C Hot Water Mass Flowrate: 0.1125 kg/s													
3000	2098.3	23676	2.7577	0.0288	136.3	6380.8	5.8575	0.3493	3321.5	68.05	2.4816		
4000	2303.7	23466	2.7846	0.0292	137	6409	6.0542	0.331	3855.9	79.26	2.388		
5000	2458.9	23413	2.7915	0.0289	135.5	6335.1	6.1164	0.3321	4349.1	89.49	2.3204		
6000	2549.4	23318	2.8039	0.0289	135.2	6318.5	6.3541	0.3262	4650.4	96.06	2.2591		
7000	2666.2	23216	2.8173	0.0292	136.2	6364.7	6.3262	0.3116	5022	103.7	2.2183		
8000	2784.1	23141	2.8273	0.0296	137.3	6415	6.3369	0.313	5416.9	111.9	2.1821		
9000	2870.3	23070	2.8368	0.0296	137.1	6402.1	6.4078	0.3063	5764.7	119.2	2.1478		
10000	2983.6	22822	2.8704	0.0298	136.9	6388.6	6.4741	0.3032	6254.7	129.4	2.1162		
Experimental Conditions: Hot Water Inlet Temperature: 70 ± 0.5 °C Hot Water Mass Flowrate: 0.2 kg/s													
3000	2441.3	43152	2.6842	0.0233	211	9898	5.7261	0.3493	3380.9	69.1			
4000	2934.8	42771	2.7101	0.0232	209.6	9827.1	5.8323	0.3432	4423.1	90.57			
5000	3213.1	42312	2.7421	0.0233	209.4	9805.7	5.9247	0.3303	5093.4	104.5			
6000	3515.4	42091	2.7577	0.0233	208.8	9775.8	6.081	0.3322	5909.4	121.5			
7000	3610.6	42283	2.7441	0.0232	208.4	9761.9	6.0864	0.3259	6189.7	127.3			
8000	3785.7	42117	2.7559	0.0233	208.9	9779.3	6.1087	0.3251	6713.7	138.1			
9000	3962.7	41844	2.7755	0.0234	208.2	9742.2	6.1796	0.3198	7314.2	150.7			
10000	4108.3	41580	2.7947	0.0234	207.6	9706.1	6.297	0.3113	7852	162			

**Table C-30:** Predicted Results ( $Re_{s,h}$ ,  $Pr$ ,  $f$ ,  $h$ ,  $Nu$ ,  $f_a/f_s$  and  $Nu_a/Nu_s$ ) for Annulus-Side Heat Transfer Enhancement for Two Annulus Sizes (Enhancement Status: Wire Coil,  $e=2.2$  mm,  $p=20$  mm).

Re Annul us	$U_0$ W/m <sup>2</sup> .C	Inner Tube (smooth) <sup>†</sup>					Annulus (augmented)					
		$Re_{s,h}$	$Pr_h$	$f_{s,i}$	$Nu_{s,i}$	$h_{s,i}$ W/m <sup>2</sup> .C	$Pr_c$	$f_a$	$h_{a,o}$ W/m <sup>2</sup> .C	$Nu_a$	Augmentation <sup>††</sup>	
Annulus Dimensions: L=1.245 m D <sub>o</sub> =0.028 m D <sub>i</sub> =0.0125 m												
Experimental Conditions: Hot Water Inlet Temperature: 60 ± 0.5 °C Hot Water Mass Flowrate: 0.1125 kg/s												
3000	2348.4	26435	3.1828	0.0251	145	8533.2	6.1288	0.2293	3440.8	87.81	4.1683	2.8552
4000	2626.6	26152	3.2206	0.0252	144.7	8504.7	6.2889	0.2068	4080.1	104.4	4.2811	2.7595
5000	2892.3	26008	3.2402	0.0253	144.3	8474.9	6.2591	0.2016	4769.8	122	4.3707	2.6949
6000	3133.7	25967	3.2458	0.0254	144.6	8495.5	6.3124	0.1884	5454.3	139.6	4.4453	2.6389
7000	3280.8	25750	3.276	0.0254	144	8450.1	6.3714	0.1881	5941.2	152.2	4.5093	2.5917
8000	3522	25701	3.2829	0.0255	144.6	8483	6.4153	0.1773	6758.5	173.3	4.5655	2.5519
9000	3653.5	25538	3.3059	0.0256	144.3	8462.9	6.4898	0.1766	7277	186.8	4.6157	2.5154
10000	3723.8	25434	3.3208	0.0256	144	8440.8	6.5209	0.1814	7581.3	194.7	4.6611	2.4852
Experimental Conditions: Hot Water Inlet Temperature: 60 ± 0.5 °C Hot Water Mass Flowrate: 0.2 kg/s												
3000	2698.5	47876	3.1185	0.0222	240.4	14175	6.0103	0.229	3467.5	88.31		
4000	3096.2	47470	3.1478	0.0222	239.7	14122	6.1118	0.2084	4158.1	106.1		
5000	3440.4	47308	3.1597	0.0222	239.3	14093	6.1172	0.1982	4807.3	122.7		
6000	3770	46973	3.1844	0.0223	239.1	14069	6.1828	0.1915	5480.4	140		
7000	3998.8	47135	3.1724	0.0224	239.8	14115	6.2471	0.1905	5968.1	152.6		
8000	4227.6	46815	3.1962	0.0224	239	14058	6.2986	0.1788	6506.4	166.5		
9000	4460.7	46563	3.2152	0.0224	238.8	14039	6.3744	0.1781	7080.7	181.4		
10000	4638.9	46446	3.2241	0.0225	238.9	14044	6.4084	0.1831	7539.1	193.3		
Experimental Conditions: Hot Water Inlet Temperature: 70 ± 0.5 °C Hot Water Mass Flowrate: 0.1125 kg/s												
3000	2388.1	30033	2.7677	0.0247	153.4	9136.3	5.9483	0.2246	3420.5	87.03		2.8719
4000	2693.2	29864	2.7848	0.0249	154	9170.8	6.0398	0.2034	4075.2	103.8		2.7757
5000	2948.1	29592	2.8127	0.025	153.9	9152.6	6.1726	0.1892	4694	119.9		2.7042
6000	3202.7	29673	2.8044	0.025	154.1	9167.7	6.2311	0.1849	5368.4	137.2		2.6474
7000	3388.8	29512	2.821	0.025	153.7	9137.5	6.2359	0.1896	5927.2	151.5		2.602
8000	3563.7	29137	2.8607	0.025	152.6	9066.2	6.3664	0.1722	6525.3	167.2		2.5589
9000	3714	28997	2.8758	0.025	152.2	9039.5	6.4176	0.1718	7065.8	181.2		2.5217
10000	3852.2	28861	2.8906	0.0251	151.9	9013.5	6.464	0.1756	7604.1	195.1		2.4906
Experimental Conditions: Hot Water Inlet Temperature: 70 ± 0.5 °C Hot Water Mass Flowrate: 0.2 kg/s												
3000	2801.3	55161	2.6715	0.0221	257.2	15362	5.7275	0.2219	3558.9	90.2		
4000	3180.6	54656	2.6982	0.0221	256.2	15292	5.8858	0.213	4200.1	106.7		
5000	3527	54163	2.7249	0.0221	255.3	15224	5.9247	0.2005	4834	122.9		
6000	3795.3	54444	2.7097	0.0221	256.2	15288	5.9975	0.1958	5343.6	136.1		
7000	4073.2	54163	2.7249	0.0222	255.9	15263	6.0527	0.1938	5915.6	150.8		
8000	4335.1	53778	2.7461	0.0222	255.1	15201	6.1195	0.1813	6497.5	165.8		
9000	4442.3	53501	2.7616	0.0222	254.9	15186	6.2336	0.1783	6744.7	172.4		
10000	4606.3	53331	2.7712	0.0223	254.7	15168	6.2809	0.182	7134.5	182.5		
Annulus Dimensions: L=1.245 m D <sub>o</sub> =0.028 m D <sub>i</sub> =0.0155 m												
Experimental Conditions: Hot Water Inlet Temperature: 60 ± 0.5 °C Hot Water Mass Flowrate: 0.1125 kg/s												
3000	2051.2	20553	3.2198	0.0292	126.5	5844.1	6.1343	0.3045	3377.4	69.51	5.3966	2.4381
4000	2212	20456	3.2366	0.0294	126.8	5854.2	6.2144	0.2805	3831.8	78.97	5.5426	2.3998
5000	2362.9	20327	3.2592	0.0294	126.3	5829.4	6.2953	0.2639	4323.6	89.22	5.6586	2.372
6000	2478.3	20375	3.2507	0.0301	129	5952.1	6.3664	0.2518	4640.2	95.86	5.7552	2.3505
7000	2569.4	20161	3.2886	0.029	124.5	5740.8	6.4741	0.2375	5145.4	106.5	5.8381	2.3309
8000	2701	20274	3.2686	0.0297	127.4	5875.6	6.4987	0.2138	5561.2	115.1	5.9109	2.3167
9000	2721	20131	3.2941	0.029	124.4	5734.9	6.497	0.2086	5798.2	120	5.9758	2.3029
10000	2812.8	20091	3.3012	0.0294	125.5	5783.7	6.5555	0.2033	6168.8	127.8	6.0345	2.2901
Experimental Conditions: Hot Water Inlet Temperature: 60 ± 0.5 °C Hot Water Mass Flowrate: 0.2 kg/s												
3000	2484.5	37518	3.1275	0.0233	196.4	9093.1	5.8735	0.3152	3587.4	73.51		
4000	2793.6	37199	3.157	0.0233	195.5	9046.2	6.0902	0.2835	4281	88.05		
5000	2966.6	36971	3.1784	0.0233	194.9	9012.4	6.1914	0.2718	4711.3	97.06		
6000	3149.3	36939	3.1814	0.0235	195.6	9043.5	6.2359	0.2561	5178.1	106.8		
7000	3297.4	36631	3.2109	0.0235	194.8	8997.4	6.2856	0.2421	5610.8	115.8		
8000	3422	36429	3.2304	0.0237	195.7	9037.7	6.301	0.2185	5961.7	123		
9000	3575.4	36572	3.2165	0.0236	195.4	9024	6.3879	0.2083	6451	133.3		
10000	3678.8	36500	3.2235	0.0236	195.2	9013.2	6.4254	0.2032	6802.4	140.7		
Experimental Conditions: Hot Water Inlet Temperature: 70 ± 0.5 °C Hot Water Mass Flowrate: 0.1125 kg/s												
3000	2158	23589	2.7689	0.0281	133.2	6235	5.8575	0.3167	3523.1	72.17		2.4526
4000	2359	23459	2.7855	0.0281	132.8	6213.1	6.0367	0.2855	4103	84.31		2.4142
5000	2545.2	23276	2.8095	0.0281	132.3	6182	6.1343	0.2671	4721.1	97.17		2.3846
6000	2639.8	23132	2.8284	0.0285	133.2	6221.9	6.2615	0.2491	5028	103.7		2.3602
7000	2745.6	23059	2.8382	0.0285	133	6209.2	6.3369	0.2341	5437.2	112.3		2.34
8000	2815.9	23004	2.8457	0.0285	132.8	6199.5	6.4037	0.2111	5729	118.4		2.3238
9000	2923.7	22795	2.8742	0.0281	130.7	6099.6	6.3829	0.2077	6307.6	130.3		2.3107
10000	2995.5	22789	2.875	0.0287	132.8	6193.7	6.486	0.1956	6531.7	135.2		2.2961
Experimental Conditions: Hot Water Inlet Temperature: 70 ± 0.5 °C Hot Water Mass Flowrate: 0.2 kg/s												
3000	2586.4	42667	2.7173	0.0231	208.5	9773	5.6851	0.3292	3685	75.27		
4000	2997.3	42589	2.7227	0.0231	208.3	9762.7	5.788	0.2998	4582.2	93.76		
5000	3238	42398	2.736	0.0231	207.9	9737.3	5.9188	0.2798	5177.6	106.2		
6000	3509.8	42206	2.7495	0.0232	208.3	9751.5	6.0013	0.2609	5903.3	121.2		
7000	3706.3	41996	2.7645	0.0232	207.7	9723.2	6.0971	0.2445	6495.3	133.6		
8000	3863.3	41882	2.7727	0.0233	207.9	9727.6	6.1382	0.2229	6990.7	143.9		
9000	3958.1	41802	2.7784	0.0234	208.1	9736.6	6.2144	0.2128	7302	150.5		
10000	4167.7	41532	2.7982	0.0234	207.4	9699.6	6.2679	0.2024	8076.8	166.6		

**Table C-31:** Predicted Results ( $Re_{s,h}$ ,  $Pr$ ,  $f$ ,  $h$ ,  $Nu$ ,  $f_a/f_s$  and  $Nu_a/Nu_s$ ) for Annulus-Side Heat Transfer Enhancement for Two Annulus Sizes (Enhancement Status: Wire Coil,  $e=2.2$  mm,  $p=30$  mm).

Re Annul us	$U_0$ W/m <sup>2</sup> .C	Inner Tube (smooth) <sup>†</sup>					Annulus (augmented)					
		$Re_{s,h}$	$Pr_h$	$f_{s,i}$	$Nu_{s,i}$	$h_{s,i}$ W/m <sup>2</sup> .C	$Pr_c$	$f_a$	$h_{a,o}$ W/m <sup>2</sup> .C	$Nu_a$	Augmentation <sup>††</sup>	
Annulus Dimensions: L=1.245 m D <sub>o</sub> =0.028 m D <sub>i</sub> =0.0125 m												
Experimental Conditions: Hot Water Inlet Temperature: 60 ± 0.5 °C Hot Water Mass Flowrate: 0.1125 kg/s												
3000	2274.1	26501	3.174	0.025	144.7	8517	6.1126	0.1893	3286.3	83.84	3.4214	2.6641
4000	2474.9	26393	3.1883	0.025	144.4	8495.2	6.2335	0.1609	3727.4	95.28	3.5139	2.6096
5000	2685	26222	3.2111	0.0252	144.9	8519.1	6.3238	0.1394	4218.7	108	3.5875	2.5667
6000	2833.1	26129	3.2237	0.0252	144.6	8500	6.3623	0.1302	4602.6	117.9	3.6487	2.5337
7000	3043.4	25928	3.2512	0.0254	144.5	8487.4	6.4287	0.134	5190	133.1	3.7013	2.5083
8000	3196.6	25862	3.2603	0.0254	144.3	8473.7	6.4455	0.121	5658.9	145.1	3.7474	2.484
9000	3298.1	25778	3.272	0.0255	144.6	8485	6.6004	0.1156	5978.5	153.7	3.7886	2.46
10000	3402.4	25733	3.2784	0.0256	144.9	8504.2	6.5466	0.1146	6318	162.3	3.8258	2.4447
Experimental Conditions: Hot Water Inlet Temperature: 60 ± 0.5 °C Hot Water Mass Flowrate: 0.2 kg/s												
3000	2738	47795	3.1243	0.0222	240.2	14161	5.9602	0.1894	3534	89.93		
4000	3128.4	47311	3.1594	0.0222	239.3	14094	6.068	0.1595	4219.2	107.6		
5000	3344.2	47544	3.1424	0.0223	240.2	14149	6.2033	0.1443	4614.6	117.9		
6000	3540.3	47363	3.1556	0.0223	239.8	14121	6.3018	0.1325	5000.6	128		
7000	3760.8	47285	3.1613	0.0223	239.6	14107	6.2752	0.1298	5454.5	139.5		
8000	3894.6	47028	3.1803	0.0223	239.4	14088	6.3829	0.1178	5744.3	147.2		
9000	3981.1	47065	3.1776	0.0224	239.6	14103	6.4346	0.1159	5931.2	152.1		
10000	4165.9	46819	3.1959	0.0224	239	14059	6.4634	0.1106	6361.2	163.2		
Experimental Conditions: Hot Water Inlet Temperature: 70 ± 0.5 °C Hot Water Mass Flowrate: 0.1125 kg/s												
3000	2292.5	30506	2.7211	0.0247	154.6	9222.7	5.9151	0.1745	3215.7	81.77		2.678
4000	2613.6	30015	2.7695	0.0247	153.3	9132.9	5.9803	0.1492	3903.6	99.37		2.6258
5000	2840.2	29956	2.7755	0.025	154.6	9204.5	6.1164	0.1361	4412.8	112.6		2.5813
6000	3024	29834	2.7878	0.0251	154.8	9214.5	6.2239	0.1275	4869.7	124.5		2.5472
7000	3221.3	29559	2.8162	0.0252	154.6	9195	6.3254	0.1265	5410.2	138.5		2.5178
8000	3342.9	29465	2.8259	0.0253	154.6	9193.4	6.3385	0.115	5762.8	147.6		2.4948
9000	3491.3	29297	2.8436	0.0253	154.2	9161.2	6.3995	0.1095	6235.3	159.8		2.4721
10000	3615	29167	2.8574	0.0253	154.1	9152.3	6.4455	0.1064	6646.8	170.5		2.4533
Experimental Conditions: Hot Water Inlet Temperature: 70 ± 0.5 °C Hot Water Mass Flowrate: 0.2 kg/s												
3000	2653.4	55220	2.6683	0.0219	256.2	15305	5.7471	0.1654	3326.5	84.34		
4000	3028.3	55102	2.6746	0.022	256.2	15302	5.8222	0.1464	3937.8	99.97		
5000	3372.1	54048	2.7312	0.022	254.4	15166	5.9446	0.1339	4555.4	115.8		
6000	3741.8	54291	2.718	0.022	254.9	15205	5.9983	0.1277	5249.4	133.7		
7000	4003.5	54134	2.7265	0.0221	254.9	15200	6.0634	0.1257	5780.1	147.3		
8000	4249.5	53941	2.7371	0.0221	254.4	15169	6.1257	0.1141	6313.3	161.1		
9000	4402.3	53491	2.7622	0.0221	253.7	15116	6.2158	0.1083	6668.1	170.4		
10000	4627.1	53233	2.7768	0.0222	253.5	15094	6.2622	0.1064	7203.6	184.2		
Annulus Dimensions: L=1.245 m D <sub>o</sub> =0.028 m D <sub>i</sub> =0.0155 m												
Experimental Conditions: Hot Water Inlet Temperature: 60 ± 0.5 °C Hot Water Mass Flowrate: 0.1125 kg/s												
3000	2124.6	20647	3.2037	0.029	126.2	5833.1	6.0733	0.227	3585.6	73.72	4.4296	2.2419
4000	2354.1	20504	3.2281	0.0294	127	5863.6	6.1452	0.2164	4273.7	87.98	4.5495	2.242
5000	2505	20235	3.2754	0.0297	127.2	5868.1	6.2575	0.2056	4795.3	98.89	4.6446	2.2379
6000	2691.4	20364	3.2526	0.0294	126.5	5836.5	6.3254	0.201	5559.2	114.8	4.7239	2.2376
7000	2795.3	20218	3.2786	0.0298	127.2	5864.6	6.3854	0.1921	5988.9	123.8	4.792	2.2374
8000	2935.5	20187	3.284	0.0298	127.1	5858.6	6.4589	0.1842	6680.4	138.2	4.8517	2.2361
9000	2979.4	20037	3.311	0.0298	126.5	5829.2	6.5016	0.1799	6958.1	144.1	4.905	2.2358
10000	3067.9	19980	3.3215	0.0298	126.3	5817.8	6.5332	0.1759	7481.1	155	4.9532	2.2346
Experimental Conditions: Hot Water Inlet Temperature: 60 ± 0.5 °C Hot Water Mass Flowrate: 0.2 kg/s												
3000	2549.8	37623	3.1179	0.0233	196.6	9108.4	5.8735	0.2318	3722.4	76.28		
4000	2940.1	37147	3.1618	0.0234	196.1	9074.4	5.9587	0.216	4626.7	94.95		
5000	3216.7	37159	3.1607	0.0233	195.4	9040.2	6.1226	0.2107	5364.2	110.4		
6000	3474.8	36841	3.1907	0.0233	194.5	8993.2	6.1733	0.2067	6146.8	126.6		
7000	3634.3	36760	3.1984	0.0235	195.1	9016.8	6.2136	0.2002	6649.9	137		
8000	3806.7	36636	3.2103	0.0235	194.8	8998.2	6.2679	0.1915	7263.9	149.8		
9000	3966.8	36507	3.2228	0.0232	192.9	8908	6.3051	0.1815	7948.1	164		
10000	4145.4	36357	3.2375	0.0235	194	8956.3	6.3827	0.1805	8648.4	178.7		
Experimental Conditions: Hot Water Inlet Temperature: 70 ± 0.5 °C Hot Water Mass Flowrate: 0.1125 kg/s												
3000	2179.6	23734	2.7505	0.0288	136.5	6390.7	5.7916	0.2282	3526.5	72.16		2.2587
4000	2431.3	23509	2.7791	0.0288	135.8	6351.7	5.9736	0.21	4255.2	87.34		2.2543
5000	2623.2	23265	2.8108	0.0292	136.4	6373.4	6.1273	0.2058	4866	100.1		2.2497
6000	2755	23083	2.835	0.0296	137.1	6404.6	6.2073	0.2016	5315.6	109.5		2.2457
7000	2869.2	23030	2.8422	0.0292	135.6	6331.5	6.2623	0.1936	5824.8	120.1		2.2438
8000	2987.4	22941	2.8541	0.0296	136.7	6378.9	6.3075	0.1899	6281.9	129.7		2.2422
9000	3079.6	22915	2.8577	0.03	137.9	6437	6.3459	0.1884	6634.3	137		2.2441
10000	3180.2	22737	2.8822	0.03	137.3	6404.1	6.4336	0.1765	7164.4	148.2		2.2407
Experimental Conditions: Hot Water Inlet Temperature: 70 ± 0.5 °C Hot Water Mass Flowrate: 0.2 kg/s												
3000	2619.1	43288	2.675	0.0231	210	9854.9	5.5756	0.2289	3738.6	76.21		
4000	3024.1	42830	2.7061	0.0231	208.9	9794.6	5.6962	0.2121	4637.2	94.73		
5000	3307.8	42498	2.729	0.0231	208.1	9750.6	5.8294	0.2114	5353.7	109.6		
6000	3512.3	41863	2.7741	0.0231	206.6	9665.5	5.996	0.201	5946.1	122.1		
7000	3688.2	42091	2.7577	0.0232	208	9736.1	6.0987	0.2014	6433.6	132.3		
8000	3879.5	41989	2.765	0.0232	207.7	9722.3	6.1891	0.1917	7047	145.2		
9000	4110.1	41604	2.7929	0.0234	207.6	9709.5	6.1483	0.1875	7856.3	161.7		
10000	4207.5	41506	2.8001	0.0233	207	9676.4	6.2525	0.1828	8246.2	170.1		

**Table C-32:** Predicted Results ( $Re_{s,h}$ ,  $Pr_h$ ,  $f_s$ ,  $h_s$ ,  $Nu_s$ ,  $f_a/f_s$  and  $Nu_a/Nu_s$ ) for Annulus-Side Heat Transfer Enhancement for Two Annulus Sizes (Enhancement Status: Wire Coil,  $e=2.2$  mm,  $p=40$  mm).

Re Annul us	$U_0$ W/m <sup>2</sup> .C	Inner Tube (smooth) <sup>†</sup>					Annulus (augmented)					
		$Re_{s,h}$	$Pr_h$	$f_{s,i}$	$Nu_{s,i}$	$h_{s,i}$ W/m <sup>2</sup> .C	$Pr_c$	$f_a$	$h_{a,o}$ W/m <sup>2</sup> .C	$Nu_a$	Augmentation <sup>††</sup>	
Annulus Dimensions: L=1.245 m   D <sub>o</sub> =0.028 m   D <sub>i</sub> =0.0125 m												
Experimental Conditions: Hot Water Inlet Temperature: 60 ± 0.5 °C   Hot Water Mass Flowrate: 0.1125 kg/s												
3000	2168.2	26459	3.1795	0.0247	143.1	8419.4	6.094	0.1489	3084.2	78.66	2.8334	
4000	2452.1	26352	3.1937	0.0248	143.3	8427.6	6.2009	0.1354	3690.5	94.29	2.9101	
5000	2670	26286	3.2026	0.0248	143.1	8414.3	6.3598	0.1269	4211.2	107.9	2.971	
6000	2822	26107	3.2267	0.0249	143	8407.4	6.3747	0.1241	4604.5	118	3.0217	
7000	3049.6	26047	3.2349	0.025	143.4	8424.5	6.4195	0.1177	5235.3	134.2	3.0652	
8000	3122.3	25953	3.2478	0.025	143.1	8405.2	6.4708	0.1129	5462.7	140.2	3.1035	
9000	3313.4	25760	3.2746	0.0253	143.5	8423.4	6.4902	0.1076	6064.7	155.7	3.1376	
10000	3426.6	25748	3.2763	0.0253	143.5	8420.8	6.5338	0.1052	6456.8	165.8	3.1684	
Experimental Conditions: Hot Water Inlet Temperature: 60 ± 0.5 °C   Hot Water Mass Flowrate: 0.2 kg/s												
3000	2486.4	48251	3.0919	0.0221	240.5	14187	6.0239	0.1394	3124.2	79.59		
4000	2760.1	47647	3.1349	0.0221	239	14082	6.1577	0.1279	3576.7	91.32		
5000	3095.8	47773	3.1259	0.0221	239.6	14121	6.1851	0.1218	4157.4	106.2		
6000	3315.3	47540	3.1427	0.0222	239.6	14116	6.2583	0.1183	4563.8	116.7		
7000	3593.5	47315	3.1591	0.0222	239.1	14077	6.3254	0.1081	5113.9	130.9		
8000	3850	47215	3.1664	0.0222	238.8	14059	6.3418	0.1116	5653	144.8		
9000	4056.3	47028	3.1803	0.0222	238.6	14044	6.3738	0.1069	6112.4	156.6		
10000	4315.3	46855	3.1932	0.0222	238.2	14013	6.4295	0.1015	6728.2	172.5		
Experimental Conditions: Hot Water Inlet Temperature: 70 ± 0.5 °C   Hot Water Mass Flowrate: 0.1125 kg/s												
3000	2134	30386	2.7328	0.0244	153.2	9133.9	5.9736	0.1329	2922.5	74.39	2.4415	
4000	2388.8	30287	2.7425	0.0245	153.2	9132.7	6.1102	0.1228	3422.5	87.31	2.4135	
5000	2606.4	30045	2.7666	0.0246	152.9	9105.2	6.1978	0.1142	3893.3	99.47	2.3944	
6000	2730.8	29970	2.7741	0.0247	153.2	9124.6	6.2495	0.1117	4172.8	106.7	2.3783	
7000	2927.4	29769	2.7945	0.0247	152.7	9087.5	6.2897	0.1048	4661.1	119.3	2.3648	
8000	3126.1	29568	2.8152	0.0249	153.3	9115.4	6.3492	0.0995	5175.8	132.6	2.3526	
9000	3189.2	29528	2.8194	0.025	153.7	9140.4	6.5047	0.0957	5341.4	137.1	2.3384	
10000	3310.3	29481	2.8243	0.025	153.6	9131.6	6.4463	0.095	5693.7	146	2.332	
Experimental Conditions: Hot Water Inlet Temperature: 70 ± 0.5 °C   Hot Water Mass Flowrate: 0.2 kg/s												
3000	2433.8	55043	2.6777	0.0217	253.9	15163	5.838	0.134	2994.8	76.05		
4000	2728.4	54866	2.6871	0.0217	253.5	15136	5.9721	0.1206	3455.1	87.94		
5000	3001.3	55005	2.6797	0.0217	253.8	15157	6.0193	0.1127	3903.2	99.43		
6000	3230	54874	2.6866	0.0218	254.2	15177	6.0987	0.1095	4297.2	109.6		
7000	3593.3	54415	2.7112	0.0218	253.2	15105	6.1671	0.1071	4973.8	127		
8000	3828.5	54295	2.7177	0.0218	253.1	15097	6.2247	0.1008	5437.4	139		
9000	3931.8	53865	2.7413	0.0219	252.6	15059	6.3025	0.0996	5654.2	144.7		
10000	4130.6	53666	2.7524	0.0219	252.2	15027	6.3392	0.0951	6080.4	155.7		
Annulus Dimensions: L=1.245 m   D <sub>o</sub> =0.028 m   D <sub>i</sub> =0.0155 m												
Experimental Conditions: Hot Water Inlet Temperature: 60 ± 0.5 °C   Hot Water Mass Flowrate: 0.1125 kg/s												
3000	2065.2	20564	3.2178	0.0282	123.4	5701.8	6.1796	0.182	3471.5	71.5	3.8505	
4000	2271.6	20451	3.2374	0.0282	123.1	5680.9	6.2065	0.1748	4109.6	84.68	3.9547	
5000	2429.7	20213	3.2794	0.0282	122.2	5636.6	6.2953	0.1621	4691.1	96.81	4.0375	
6000	2510.8	20211	3.2797	0.0286	123.5	5693.4	6.3755	0.1561	4954.5	102.4	4.1063	
7000	2651	20174	3.2863	0.0286	123.3	5686.4	6.4187	0.1467	5539.2	114.5	4.1655	
8000	2792	20232	3.276	0.029	124.8	5754.3	6.448	0.1434	6106.1	126.3	4.2174	
9000	2826.8	20020	3.3142	0.029	124	5713.7	6.5124	0.137	6328.9	131.1	4.2638	
10000	2900.7	19997	3.3183	0.0292	124.6	5737.4	6.5329	0.1362	6676.3	138.3	4.3057	
Experimental Conditions: Hot Water Inlet Temperature: 60 ± 0.5 °C   Hot Water Mass Flowrate: 0.2 kg/s												
3000	2445.8	37347	3.1432	0.0232	195.1	9031.8	5.9758	0.1843	3517.5	72.21		
4000	2693.9	37185	3.1583	0.0232	194.7	9008.1	6.0894	0.1711	4059.7	83.5		
5000	2963.1	36884	3.1866	0.0233	194.7	8999.6	6.1938	0.1593	4706.5	96.96		
6000	3178.1	36587	3.215	0.0235	194.6	8990.9	6.2945	0.1577	5276.4	108.9		
7000	3372.7	36582	3.2156	0.0235	194.6	8990.1	6.3459	0.152	5835.7	120.5		
8000	3537	36530	3.2206	0.0235	194.5	8982.3	6.4137	0.1415	6350.2	131.3		
9000	3727.4	36226	3.2504	0.0236	194.4	8971.6	6.3377	0.1421	6998.4	144.5		
10000	3901	36355	3.2377	0.0236	194.8	8991.2	6.4485	0.1373	7620.9	157.6		
Experimental Conditions: Hot Water Inlet Temperature: 70 ± 0.5 °C   Hot Water Mass Flowrate: 0.1125 kg/s												
3000	2110.5	23615	2.7654	0.0279	132.6	6206.6	5.8909	0.1844	3407.7	69.85	2.0343	
4000	2318	23376	2.7963	0.0277	131.2	6138.8	5.9923	0.1736	4017.3	82.49	2.0546	
5000	2485	23118	2.8303	0.0279	131.1	6122.9	6.1133	0.1631	4553.5	93.69	2.068	
6000	2654.6	22981	2.8488	0.0281	131.3	6131.6	6.1946	0.158	5150.4	106.1	2.0800	
7000	2769.4	22860	2.8652	0.0281	131	6110.9	6.2679	0.1516	5620.4	115.9	2.091	
8000	2874.4	22802	2.8732	0.0283	131.4	6132.6	6.3238	0.1457	6046.8	124.8	2.0999	
9000	2946.7	22728	2.8834	0.0289	133.2	6214.5	6.3966	0.1371	6280.4	129.8	2.1064	
10000	3035	22643	2.8953	0.0289	133	6199.3	6.4375	0.1363	6715.5	138.9	2.1147	
Experimental Conditions: Hot Water Inlet Temperature: 70 ± 0.5 °C   Hot Water Mass Flowrate: 0.2 kg/s												
3000	2470.2	42761	2.7108	0.023	207.9	9745.1	5.6865	0.1866	3457.5	70.62		
4000	2830.1	42402	2.7358	0.0229	206.2	9657.5	5.7951	0.1656	4224.4	86.45		
5000	3094.3	42492	2.7294	0.0229	206.4	9669.4	5.9365	0.1604	4838.3	99.25		
6000	3335	42248	2.7466	0.023	206.7	9677.2	6.0337	0.1601	5451	112		
7000	3459.1	42395	2.7362	0.023	207	9696.8	6.0833	0.1503	5782.8	118.9		
8000	3695.9	42148	2.7536	0.0231	207.3	9703.9	6.16	0.1443	6472.8	133.3		
9000	3857.9	41999	2.7643	0.0231	206.9	9683.9	6.2631	0.1382	6998.3	144.3		
10000	4029	41568	2.7955	0.0231	205.9	9625.8	6.2791	0.1403	7622.1	157.2		

**Table C-33:** Predicted Results ( $Re_{s,h}$ ,  $Pr$ ,  $f$ ,  $h$ ,  $Nu$ ,  $f_a/f_s$  and  $Nu_a/Nu_s$ ) for Annulus-Side Heat Transfer Enhancement for Two Annulus Sizes (Enhancement Status: Circular Ribs,  $e=2.2$  mm,  $p=10$  mm).

Re Annul us	$U_0$ W/m <sup>2</sup> .C	Inner Tube (smooth) <sup>†</sup>					Annulus (augmented)					
		$Re_{s,h}$	$Pr_h$	$f_{s,i}$	$Nu_{s,i}$	$h_{s,i}$ W/m <sup>2</sup> .C	$Pr_c$	$f_a$	$h_{a,o}$ W/m <sup>2</sup> .C	$Nu_a$	$f_a/f_s$	$Nu_a/Nu_s$
Annulus Dimensions: L=1.245 m   D <sub>o</sub> =0.028 m   D <sub>i</sub> =0.0125 m												
Experimental Conditions: Hot Water Inlet Temperature: 60 ± 0.5 °C   Hot Water Mass Flowrate: 0.1125 kg/s												
3000	2077.3	26397	3.1877	0.024	141.9	8347.5	6.2391	0.4272	2913.3	74.48	8.6658	2.5661
4000	2396.5	26294	3.2015	0.025	142.1	8356.7	6.2832	0.3966	3580.7	91.61	8.8494	2.5652
5000	2602.4	26224	3.2109	0.025	141.9	8342.7	6.3401	0.3719	4064.5	104.1	8.9946	2.566
6000	2821.3	26117	3.2253	0.025	142.1	8350.7	6.3995	0.3563	4622.1	118.5	9.1149	2.5645
7000	2966.9	25967	3.2458	0.025	141.9	8335	6.4775	0.342	5032.7	129.2	9.2179	2.5628
8000	3114	25883	3.2575	0.025	141.9	8332.5	6.4877	0.3298	5472.3	140.5	9.3081	2.5633
9000	3272	25764	3.274	0.025	142	8337.3	6.5149	0.319	5976.8	153.5	9.3884	2.5625
10000	3382.1	25781	3.2717	0.025	142.8	8384.2	6.5467	0.3112	6324	162.5	9.4607	2.5607
Experimental Conditions: Hot Water Inlet Temperature: 60 ± 0.5 °C   Hot Water Mass Flowrate: 0.2 kg/s												
3000	2405.5	47991	3.1103	0.022	238.8	14082	6.0413	0.4286	3002.9	76.52		
4000	2830.4	47617	3.1371	0.022	238.1	14032	6.1491	0.3939	3699.5	94.44		
5000	3178.6	47710	3.1304	0.022	238.8	14075	6.1678	0.3732	4313.1	110.1		
6000	3508	47370	3.1551	0.022	238.3	14033	6.2359	0.3553	4948.6	126.5		
7000	3795.7	47234	3.1651	0.022	238	14009	6.2808	0.3413	5545.4	141.9		
8000	4024.1	47109	3.1743	0.022	237.6	13987	6.3148	0.3297	6051.6	154.9		
9000	4200.6	46907	3.1894	0.022	237.3	13964	6.3681	0.3187	6465.4	165.6		
10000	4320.5	46661	3.2078	0.022	236.7	13921	6.4413	0.3102	6765.4	173.5		
Experimental Conditions: Hot Water Inlet Temperature: 70 ± 0.5 °C   Hot Water Mass Flowrate: 0.1125 kg/s												
3000	2074.9	30432	2.7283	0.024	151.3	9024.6	5.9788	0.4281	2824.7	71.9		2.5804
4000	2388.9	30177	2.7534	0.024	151	8996	6.1265	0.3965	3445.1	87.91		2.5784
5000	2677	30056	2.7654	0.024	150.7	8974.4	6.1538	0.3718	4082.9	104.2		2.5786
6000	2826.6	29864	2.7848	0.024	150.2	8939.8	6.2375	0.3532	4451.1	113.8		2.5763
7000	3044.6	29664	2.8053	0.024	150.2	8936.7	6.2962	0.3412	5018	128.4		2.5737
8000	3183.2	29530	2.8192	0.024	149.9	8912.3	6.3508	0.3296	5416.1	138.7		2.573
9000	3348.4	29481	2.8243	0.024	150.3	8936.1	6.3681	0.3195	5900.7	151.2		2.573
10000	3460.4	29341	2.8389	0.024	149.9	8910.4	6.4112	0.3094	6272	160.8		2.5714
Experimental Conditions: Hot Water Inlet Temperature: 70 ± 0.5 °C   Hot Water Mass Flowrate: 0.2 kg/s												
3000	2294.3	55429	2.6575	0.022	254.9	15233	5.8815	0.4232	2783.6	70.74		
4000	2845.5	55250	2.6668	0.022	254.6	15209	5.9151	0.3976	3640.3	92.56		
5000	3291.3	54836	2.6886	0.022	253.8	15151	5.9758	0.3733	4408.8	112.2		
6000	3707	54402	2.7119	0.022	252.8	15084	6.0413	0.3572	5197.3	132.4		
7000	3952.8	54011	2.7333	0.022	252.5	15054	6.1273	0.3416	5698.5	145.4		
8000	4171.9	53908	2.7389	0.022	252.4	15046	6.153	0.3305	6166.9	157.4		
9000	4449.7	53713	2.7498	0.022	252.3	15034	6.1883	0.3202	6796.5	173.6		
10000	4620.3	53546	2.7591	0.022	251.9	15008	6.2423	0.3089	7209.6	184.3		
Annulus Dimensions: L=1.245 m   D <sub>o</sub> =0.028 m   D <sub>i</sub> =0.0155 m												
Experimental Conditions: Hot Water Inlet Temperature: 60 ± 0.5 °C   Hot Water Mass Flowrate: 0.1125 kg/s												
3000	2015.7	20700	3.1946	0.029	126.4	5843.2	6.0994	0.6239	3282.4	67.52	12.2557	2.2648
4000	2138.2	20588	3.2136	0.0292	126.7	5850.9	6.2776	0.5787	3617.1	74.62	12.5154	2.1991
5000	2231.6	20511	3.227	0.0294	127	5864.8	6.3385	0.549	3885.9	80.24	12.7207	2.1527
6000	2337.8	20477	3.2329	0.0297	128.1	5915.3	6.3929	0.5209	4191.2	86.62	12.8909	2.1139
7000	2353.7	20461	3.2357	0.0297	128.1	5912.2	6.4928	0.4996	4244.1	87.85	13.0366	2.0821
8000	2447.4	20404	3.2456	0.0297	127.9	5901.2	6.5415	0.4796	4566.3	94.6	13.1641	2.055
9000	2552.7	20277	3.2628	0.0297	127.4	5876.3	6.5278	0.4682	4966.7	102.9	13.2776	2.0348
10000	2568.6	20274	3.2685	0.0299	128	5903.9	6.5949	0.4554	5004.9	103.8	13.38	2.0128
Experimental Conditions: Hot Water Inlet Temperature: 60 ± 0.5 °C   Hot Water Mass Flowrate: 0.2 kg/s												
3000	2015.7	20700	3.1946	0.029	126.4	5843.2	6.0994	0.6239	3762.1	77.15		
4000	2138.2	20588	3.2136	0.0292	126.7	5850.9	6.2776	0.5787	4077.5	83.85		
5000	2231.6	20511	3.227	0.0294	127	5864.8	6.3385	0.549	4472.5	92.12		
6000	2337.8	20477	3.2329	0.0297	128.1	5915.3	6.3929	0.5209	4761.8	98.3		
7000	2353.7	20461	3.2357	0.0297	128.1	5912.2	6.4928	0.4996	5045	104.2		
8000	2447.4	20404	3.2456	0.0297	127.9	5901.2	6.5415	0.4796	5187.7	107.3		
9000	2552.7	20277	3.2628	0.0297	127.4	5876.3	6.5278	0.4682	5470.8	113.1		
10000	2568.6	20274	3.2685	0.0299	128	5903.9	6.5949	0.4554	5710.2	118.2		
Experimental Conditions: Hot Water Inlet Temperature: 70 ± 0.5 °C   Hot Water Mass Flowrate: 0.1125 kg/s												
3000	2039.3	23732	2.7507	0.0281	133.7	6259.1	5.8727	0.6166	3210.3	65.79		2.2781
4000	2206.3	23489	2.7816	0.0281	132.9	6218.2	6.1211	0.5885	3660.2	75.32		2.2108
5000	2389.6	23422	2.7903	0.0285	134.1	6271.8	6.1428	0.5514	4167.2	85.78		2.1649
6000	2480.6	23328	2.8025	0.0285	133.8	6255.7	6.3623	0.5203	4461	92.15		2.1203
7000	2564.1	23202	2.8192	0.0289	134.8	6298.2	6.3483	0.4964	4711.8	97.32		2.0928
8000	2686.8	23148	2.8264	0.0289	134.6	6288.7	6.3738	0.4787	5150.6	106.4		2.0672
9000	2774.1	23075	2.8361	0.0292	135.7	6339.6	6.4388	0.4698	5439.3	112.5		2.0428
10000	2884.4	22955	2.8523	0.0292	135.3	6318.2	6.4892	0.458	5900.5	122.1		2.0205
Experimental Conditions: Hot Water Inlet Temperature: 70 ± 0.5 °C   Hot Water Mass Flowrate: 0.2 kg/s												
3000	2429.7	43168	2.683	0.0231	209.7	9839.3	5.7107	0.6239	3366.3	68.79		
4000	2862.8	42843	2.7052	0.0231	208.9	9796.3	5.8373	0.5694	4267.9	87.4		
5000	3154.7	42386	2.7369	0.0233	209.6	9815.6	5.9431	0.5425	4945.4	101.5		
6000	3356.6	42216	2.7489	0.0231	207.4	9712.9	6.111	0.529	5496.1	113.1		
7000	3535.9	42244	2.7468	0.0232	208.4	9756.7	6.1025	0.4985	5975.4	122.9		
8000	3734.8	42117	2.7559	0.0233	208.5	9759.4	6.1366	0.4942	6565	135.1		
9000	3910.3	41793	2.7791	0.0234	208.1	9735.3	6.2025	0.4625	7141.7	147.2		
10000	4028	41652	2.7894	0.0234	207.7	9716	6.2997	0.4424	7557.3	156		

**Table C-34:** Predicted Results ( $Re_{s,h}$ ,  $Pr$ ,  $f$ ,  $h$ ,  $Nu$ ,  $f_a/f_s$  and  $Nu_a/Nu_s$ ) for Annulus-Side Heat Transfer Enhancement for Two Annulus Sizes (Enhancement Status: Circular Ribs,  $e=2.2$  mm,  $p=20$  mm).

Re Annul us	$U_0$ W/m <sup>2</sup> .C	Inner Tube (smooth) <sup>†</sup>				Annulus (augmented)						
		$Re_{s,h}$	$Pr_h$	$f_{s,i}$	$Nu_{s,i}$	$h_{s,i}$ W/m <sup>2</sup> .C	$Pr_c$	$f_a$	$h_{a,o}$ W/m <sup>2</sup> .C	$Nu_a$	Augmentation <sup>††</sup>	
Annulus Dimensions: L=1.245 m D <sub>o</sub> =0.028 m D <sub>i</sub> =0.0125 m												
Experimental Conditions: Hot Water Inlet Temperature: 60 ± 0.5 °C Hot Water Mass Flowrate: 0.1125 kg/s												
3000	2348.5	26311	3.1993	0.0251	144.6	8507.9	6.1203	0.3531	3445.7	87.92	6.2044	
4000	2662.8	26144	3.2217	0.0252	144.7	8503	6.2136	0.3192	4168.5	106.5	6.3359	
5000	2921.5	26060	3.2332	0.0254	144.9	8514.7	6.2776	0.3107	4835.1	123.7	6.4398	
6000	3120.1	25916	3.2529	0.0254	144.5	8484.8	6.3747	0.2958	5418.4	138.8	6.5259	
7000	3326.1	25756	3.2751	0.0255	144.5	8480.3	6.3854	0.2824	6074.1	155.6	6.5997	
8000	3455.7	25695	3.2837	0.0255	144.5	8481.7	6.4522	0.2732	6519.5	167.2	6.6642	
9000	3615	25529	3.3072	0.0257	144.8	8489.5	6.4801	0.2644	7104.4	182.3	6.7217	
10000	3726.5	25458	3.3174	0.0258	145	8502.7	6.5278	0.2575	7536.6	193.6	6.7735	
Experimental Conditions: Hot Water Inlet Temperature: 60 ± 0.5 °C Hot Water Mass Flowrate: 0.2 kg/s												
3000	2667.5	47799	3.124	0.0222	240.3	14162	5.9803	0.3509	3417.3	86.99		
4000	3125.1	47355	3.1562	0.0223	239.8	14119	6.0987	0.33	4210.7	107.4		
5000	3458.1	47514	3.1446	0.0223	240.3	14158	6.1172	0.3107	4833.3	123.3		
6000	3778.8	47153	3.1711	0.0223	239.5	14101	6.2152	0.2956	5493.4	140.4		
7000	4014.2	46987	3.1833	0.0224	239.7	14107	6.2663	0.2834	6004.2	153.6		
8000	4203.9	46672	3.207	0.0224	238.6	14033	6.3483	0.2736	6456.6	165.4		
9000	4436.9	46533	3.2175	0.0224	238.6	14025	6.3738	0.2647	7025.1	180		
10000	4610.6	46493	3.2206	0.0225	239.1	14053	6.4078	0.2573	7461.8	191.3		
Experimental Conditions: Hot Water Inlet Temperature: 70 ± 0.5 °C Hot Water Mass Flowrate: 0.1125 kg/s												
3000	2370.4	30161	2.755	0.025	155.1	9242.5	5.9357	0.3469	3368	85.67	2.6281	
4000	2732	29877	2.7835	0.0251	154.9	9222.5	6.0535	0.3297	4152.7	105.8	2.5957	
5000	2957.1	29684	2.8032	0.0251	154.7	9202.5	6.1616	0.3096	4702.1	120.1	2.5708	
6000	3248.8	29397	2.8331	0.0251	153.9	9148	6.2239	0.2948	5507.3	140.8	2.5502	
7000	3412.2	29350	2.838	0.0251	153.8	9139.1	6.28	0.2837	5998.5	153.5	2.5339	
8000	3575	29218	2.852	0.0252	153.4	9113.8	6.336	0.2735	6534.9	167.3	2.5209	
9000	3704.6	29077	2.8671	0.0252	153.3	9102.9	6.397	0.2647	6988.6	179.1	2.5063	
10000	3877.4	28933	2.8827	0.0252	152.9	9075.1	6.448	0.2558	7652.6	196.3	2.4961	
Experimental Conditions: Hot Water Inlet Temperature: 70 ± 0.5 °C Hot Water Mass Flowrate: 0.2 kg/s												
3000	2789.7	54996	2.6801	0.0221	257.6	15380	5.7107	0.3531	3539	89.67		
4000	3173.5	54794	2.6909	0.0221	257.2	15354	5.8402	0.3264	4182.6	106.2		
5000	3542.1	54569	2.7029	0.0222	256.9	15328	5.9291	0.3097	4850.5	123.4		
6000	3853.9	53912	2.7387	0.0222	255.4	15223	6.0436	0.296	5469.9	139.4		
7000	4085.2	53843	2.7425	0.0222	255.2	15212	6.1079	0.283	5949.8	151.8		
8000	4313.6	53753	2.7475	0.0222	255.3	15217	6.1273	0.2719	6445.9	164.5		
9000	4417	53599	2.7561	0.0222	255.1	15202	6.2295	0.2661	6683.1	170.8		
10000	4623.4	53554	2.7586	0.0223	255.2	15204	6.2423	0.2575	7166.5	183.2		
Experimental Conditions: Hot Water Inlet Temperature: 70 ± 0.5 °C Hot Water Mass Flowrate: 0.2 kg/s												
3000	2028.4	20595	3.2126	0.029	126.1	5823.3	6.128	0.4839	3323.6	68.4	8.7743	
4000	2203.2	20490	3.2307	0.0294	126.9	5860.8	6.2215	0.4493	3802.5	78.37	8.9602	
5000	2359.1	20370	3.2516	0.0296	127.1	5866.1	6.3067	0.4232	4288.8	88.52	9.1072	
6000	2479.6	20360	3.2534	0.0294	126.5	5835.7	6.3689	0.4031	4726.3	97.64	9.229	
7000	2560.9	20224	3.2774	0.0297	127.2	5865.9	6.4733	0.3792	5006	103.6	9.3333	
8000	2643.1	20207	3.2804	0.0301	128.4	5918.7	6.5321	0.3735	5282.6	109.4	9.4246	
9000	2781.7	20044	3.3099	0.0301	127.8	5886.1	6.5484	0.3621	5902.9	122.3	9.5059	
10000	2793	20062	3.3066	0.0298	126.6	5834	6.5794	0.3559	6014.1	124.7	9.5792	
Experimental Conditions: Hot Water Inlet Temperature: 60 ± 0.5 °C Hot Water Mass Flowrate: 0.1125 kg/s												
3000	2510.7	37495	3.1296	0.0232	195.5	9053.4	5.8887	0.4983	3649.5	74.8		
4000	2755.4	37250	3.1522	0.0232	194.9	9017.7	6.0902	0.4594	4198.9	86.36		
5000	2938.7	37071	3.169	0.0233	194.8	9009.3	6.1938	0.4295	4642.3	95.64		
6000	3153.6	36904	3.1847	0.0233	194.7	9002.5	6.2247	0.4074	5204.8	107.3		
7000	3313.9	36677	3.2064	0.0233	194.1	8968.8	6.2848	0.3847	5671.3	117		
8000	3496	36431	3.2302	0.0233	193.4	8932.1	6.3344	0.3759	6245.9	129		
9000	3563.2	36576	3.2162	0.0235	194.6	8989.2	6.407	0.3637	6431.2	132.9		
10000	3652.4	36563	3.2174	0.0235	194.6	8987.3	6.4379	0.3544	6728.8	139.2		
Experimental Conditions: Hot Water Inlet Temperature: 70 ± 0.5 °C Hot Water Mass Flowrate: 0.1125 kg/s												
3000	2183.3	23578	2.7703	0.0281	133.2	6233.1	5.8546	0.4802	3591.7	73.58	2.3928	
4000	2382.2	23406	2.7924	0.0284	133.6	6249.6	6.0352	0.4396	4155.6	85.39	2.3022	
5000	2540.5	23296	2.8068	0.0281	132.3	6185.4	6.1405	0.4007	4702.7	96.8	2.2346	
6000	2635.8	23116	2.8307	0.0285	133.1	6219	6.2551	0.3987	5015.5	103.4	2.1807	
7000	2733.4	23059	2.8382	0.0289	134.3	6273.1	6.3492	0.3904	5336.9	110.2	2.1357	
8000	2808.6	22989	2.8477	0.0289	134.1	6260.8	6.3929	0.3714	5642.5	116.6	2.0998	
9000	2976.5	22768	2.878	0.0285	132	6158.3	6.392	0.3551	6485	134	2.0685	
10000	2981.4	22796	2.874	0.0285	132.1	6163.3	6.4876	0.344	6502.4	134.6	2.0385	
Experimental Conditions: Hot Water Inlet Temperature: 70 ± 0.5 °C Hot Water Mass Flowrate: 0.2 kg/s												
3000	2588.7	42821	2.7066	0.0232	209.3	9813.7	5.6624	0.4652	3683.4	75.2		
4000	3021	42539	2.7262	0.0231	208.2	9756	5.788	0.4336	4639.3	94.93		
5000	3255.8	42364	2.7384	0.0232	208.6	9772.7	5.9144	0.4153	5211.9	106.9		
6000	3507.6	42231	2.7478	0.0233	209.2	9794.8	5.9983	0.4074	5879.7	120.7		
7000	3722.7	42047	2.7609	0.0233	208.7	9769.8	6.091	0.4005	6522.6	134.2		
8000	3919.6	41865	2.7739	0.0233	207.9	9725.4	6.1242	0.3823	7178.6	147.7		
9000	4046.8	41743	2.7827	0.0234	208	9728.5	6.1985	0.3597	7615.1	156.9		
10000	4208.5	41525	2.7987	0.0234	207.4	9698.6	6.2607	0.3495	8232.2	169.8		

**Table C-35:** Predicted Results ( $Re_{s,h}$ ,  $Pr_h$ ,  $f$ ,  $h$ ,  $Nu$ ,  $f_a/f_s$  and  $Nu_a/Nu_s$ ) for Annulus-Side Heat Transfer Enhancement for Two Annulus Sizes (Enhancement Status: Circular Ribs,  $e=2.2$  mm,  $p=30$  mm).

Re Annul us	$U_0$ W/m <sup>2</sup> .C	Inner Tube (smooth) <sup>†</sup>				Annulus (augmented)					
		$Re_{s,h}$	$Pr_h$	$f_{s,i}$	$Nu_{s,i}$	$h_{s,i}$ W/m <sup>2</sup> .C	$Pr_c$	$f_a$	$h_{a,o}$ W/m <sup>2</sup> .C	$Nu_a$	
Annulus Dimensions: $L=1.245$ m $D_o=0.028$ m $D_i=0.0125$ m											
Experimental Conditions: Hot Water Inlet Temperature: $60 \pm 0.5$ °C   Hot Water Mass Flowrate: 0.1125 kg/s											
3000	2274	26518	3.1718	0.0248	143.7	8460.9	6.0794	0.2626	3295.6	84.03	
4000	2520.2	26357	3.1931	0.0249	143.8	8458.1	6.2367	0.2456	3839.9	98.16	
5000	2729.2	26200	3.2141	0.0248	142.8	8396.9	6.3173	0.2262	4365.6	111.7	
6000	2893.6	26064	3.2326	0.0252	144.4	8486.5	6.4112	0.2173	4769.4	122.3	
7000	3065.5	25973	3.2451	0.0253	144.1	8467.6	6.4203	0.2063	5263.3	134.9	
8000	3218.9	25826	3.2653	0.0253	143.7	8437.2	6.4741	0.2026	5748.1	147.5	
9000	3315.5	25810	3.2676	0.0254	144.2	8462.6	6.5022	0.1965	6048.9	155.3	
10000	3445.2	25675	3.2865	0.0255	144.2	8463.2	6.5484	0.1899	6494.6	166.8	
Experimental Conditions: Hot Water Inlet Temperature: $60 \pm 0.5$ °C   Hot Water Mass Flowrate: 0.2 kg/s											
3000	2825.2	47978	3.1112	0.0222	240.7	14193	5.9041	0.2627	3678.2	93.51	
4000	3171.5	47672	3.1332	0.0222	239.6	14122	6.071	0.2437	4295	109.5	
5000	3440.1	47532	3.1433	0.0222	239.6	14115	6.1405	0.2292	4803.8	122.6	
6000	3668.6	47372	3.1549	0.0222	239.5	14104	6.2271	0.2169	5263	134.5	
7000	3839.7	47078	3.1766	0.0222	238.8	14052	6.3156	0.2096	5632	144.2	
8000	3981.5	47031	3.1801	0.0223	238.9	14062	6.3697	0.2021	5940.5	152.2	
9000	4102.8	46919	3.1884	0.0223	239	14059	6.4087	0.1949	6215.2	159.3	
10000	4258	46731	3.2026	0.0224	238.8	14043	6.4665	0.1895	6582.4	168.9	
Experimental Conditions: Hot Water Inlet Temperature: $70 \pm 0.5$ °C   Hot Water Mass Flowrate: 0.1125 kg/s											
3000	2385.6	30397	2.7317	0.0249	155.5	9269.6	5.8366	0.2503	3394.7	86.2	
4000	2675.9	30067	2.7643	0.0249	154.6	9208.6	6.0156	0.2382	4027.6	102.6	
5000	2925.3	29774	2.7939	0.0249	153.8	9154.1	6.1452	0.226	4636.2	118.3	
6000	3096.3	29452	2.8273	0.0249	152.9	9093.7	6.2808	0.2175	5102.2	130.5	
7000	3273	29535	2.8187	0.0249	153.2	9109.2	6.2873	0.2084	5593.9	143.1	
8000	3449.2	29386	2.8343	0.0251	153.9	9145.8	6.3336	0.202	6110.1	156.4	
9000	3580.4	29254	2.8482	0.0253	154	9152.9	6.3763	0.1942	6530.3	167.3	
10000	3711.6	29140	2.8604	0.0254	154.3	9163	6.4187	0.1893	6973.6	178.8	
Experimental Conditions: Hot Water Inlet Temperature: $70 \pm 0.5$ °C   Hot Water Mass Flowrate: 0.2 kg/s											
3000	2730.6	55068	2.6764	0.0219	255.3	15247	5.6913	0.2711	3452.1	87.44	
4000	3202.6	54653	2.6984	0.0218	254	15160	5.8258	0.2421	4250.3	107.9	
5000	3562.2	54506	2.7063	0.0219	254.1	15159	5.9012	0.2335	4907.9	124.8	
6000	3944.6	53872	2.7441	0.0219	252.6	15059	6.0201	0.222	5680.6	144.7	
7000	4183	53693	2.7509	0.0219	252.6	15051	6.094	0.2128	6190.1	157.9	
8000	4399.1	53664	2.7525	0.022	253.2	15085	6.1195	0.2033	6667.6	170.1	
9000	4625.7	53493	2.7621	0.022	253.1	15078	6.1647	0.1954	7204.5	184	
10000	4790.9	53231	2.7769	0.0221	253.2	15074	6.2287	0.1818	7614.3	194.6	
Annulus Dimensions: $L=1.245$ m $D_o=0.028$ m $D_i=0.0155$ m											
Experimental Conditions: Hot Water Inlet Temperature: $60 \pm 0.5$ °C   Hot Water Mass Flowrate: 0.1125 kg/s											
3000	2168.8	20597	3.2122	0.0294	127.3	5881.4	6.0618	0.3839	3692	75.9	
4000	2414.3	20422	3.2425	0.0294	126.7	5847.7	6.1561	0.3548	4486.8	92.38	
5000	2622.2	20194	3.2828	0.0298	127.1	5859.9	6.2567	0.3353	5251.1	108.3	
6000	2748.7	20291	3.2655	0.0297	127.4	5879	6.3271	0.3186	5763.8	119	
7000	2875.8	20153	3.2901	0.0298	126.9	5851.9	6.3887	0.3062	6387.9	132	
8000	2958.4	20123	3.2955	0.0298	126.8	5846.1	6.4514	0.3004	6819.1	141.1	
9000	3062	20016	3.3115	0.0298	126.4	5824.9	6.5141	0.2863	7433.8	153.9	
10000	3142.9	19936	3.3296	0.0301	127.4	5864.6	6.5631	0.2743	7849	162.7	
Experimental Conditions: Hot Water Inlet Temperature: $60 \pm 0.5$ °C   Hot Water Mass Flowrate: 0.2 kg/s											
3000	2629.1	37491	3.13	0.0234	197.1	9125.3	5.8793	0.3933	3890.4	79.73	
4000	3043.6	37066	3.1694	0.0235	195.9	9062.4	5.9617	0.3605	4892.3	100.4	
5000	3283.4	37097	3.1665	0.0234	196	9067	6.1187	0.3428	5541.1	114	
6000	3535.4	36768	3.1977	0.0235	195.5	9035.7	6.1757	0.321	6315.6	130.1	
7000	3788.3	36576	3.2162	0.0236	195.4	9024.6	6.212	0.3081	7178.5	147.9	
8000	3925.4	36553	3.2184	0.0236	195.3	9021.1	6.2727	0.2927	7690.1	158.6	
9000	4106.2	36390	3.2342	0.0236	194.9	8996.5	6.3222	0.2912	8439.9	174.2	
10000	4253.6	36306	3.2424	0.0236	194.6	8983.8	6.3763	0.2791	9101.4	188.1	
Experimental Conditions: Hot Water Inlet Temperature: $70 \pm 0.5$ °C   Hot Water Mass Flowrate: 0.1125 kg/s											
3000	2291.3	23568	2.7715	0.0288	136	6362	5.7887	0.3711	3840.1	78.57	
4000	2504	23417	2.7909	0.0289	135.5	6335.8	5.9609	0.3479	4491.7	92.18	
5000	2707	23168	2.8236	0.0289	134.7	6292.3	6.1218	0.3115	5222.7	107.5	
6000	2868.7	22964	2.8511	0.0289	134	6256.3	6.1875	0.3115	5894.7	121.4	
7000	2973.8	22917	2.8574	0.0293	135.2	6311.4	6.2695	0.3038	6294.5	129.8	
8000	3116.7	22790	2.8748	0.0296	136.1	6351.4	6.31	0.2925	6917.8	142.8	
9000	3228.2	22758	2.8792	0.0296	136	6345.6	6.3508	0.2889	7501.6	154.9	
10000	3312.3	22650	2.8942	0.0296	135.7	6325.8	6.4194	0.2708	8006.4	165.5	
Experimental Conditions: Hot Water Inlet Temperature: $70 \pm 0.5$ °C   Hot Water Mass Flowrate: 0.2 kg/s											
3000	2717.4	43106	2.6872	0.023	208.7	9790.4	5.5763	0.3865	3953.7	80.6	
4000	3128.2	42678	2.7165	0.023	207.7	9734.2	5.6969	0.3717	4903.1	100.2	
5000	3443.9	42295	2.7432	0.0231	207.6	9723.6	5.8294	0.3298	5729.9	117.3	
6000	3813.7	41821	2.7771	0.0231	206.5	9660	5.8997	0.3219	6867.3	140.8	
7000	3952.2	41977	2.7658	0.0231	206.9	9681	6.0277	0.3089	7316.6	150.3	
8000	4037.3	41681	2.7873	0.0232	207	9680.5	6.2041	0.2837	7614.2	156.9	
9000	4320.5	41321	2.8138	0.0232	206.1	9631.5	6.1569	0.2949	8732.5	179.8	
10000	4365.1	41339	2.8124	0.0232	206.1	9634	6.2443	0.2655	8913.9	183.8	

**Table C-36:** Predicted Results ( $Re_{s,h}$ ,  $Pr$ ,  $f$ ,  $h$ ,  $Nu$ ,  $f_a/f_s$  and  $Nu_a/Nu_s$ ) for Annulus-Side Heat Transfer Enhancement for Two Annulus Sizes (Enhancement Status: Circular Ribs,  $e=2.2$  mm,  $p=40$  mm).

Re	$U_0$ W/m <sup>2</sup> .C	Inner Tube (smooth) <sup>†</sup>					Annulus (augmented)					
		$Re_{s,h}$	$Pr_h$	$f_{s,i}$	$Nu_{s,i}$	$h_{s,i}$ W/m <sup>2</sup> .C	$Pr_c$	$f_a$	$h_{a,o}$ W/m <sup>2</sup> .C	$Nu_a$	Augmentation <sup>††</sup>	
Annulus Dimensions: L=1.245 m   D <sub>o</sub> =0.028 m   D <sub>i</sub> =0.0125 m												
Experimental Conditions: Hot Water Inlet Temperature: 60 ± 0.5 °C   Hot Water Mass Flowrate: 0.1125 kg/s												
3000	2232	26539	3.169	0.0247	143.5	8450.3	6.0917	0.2236	3209.8	81.86	4.2339	2.6937
4000	2532.7	26278	3.2037	0.0248	143	8412.6	6.2367	0.192	3879.9	99.19	4.3236	2.6327
5000	2773	26190	3.2155	0.0248	142.8	8394.8	6.2792	0.1751	4479.4	114.6	4.3945	2.5905
6000	2988.8	25956	3.2473	0.0253	144.1	8464.2	6.3937	0.1614	5042.5	129.2	4.4533	2.5523
7000	3128.9	25942	3.2494	0.0251	143.6	8432	6.3979	0.1546	5470	140.2	4.5036	2.5236
8000	3352.4	25705	3.2823	0.0253	143.3	8411.9	6.4564	0.1459	6204	159.2	4.5477	2.4988
9000	3405.2	25763	3.2741	0.0254	144	8452.9	6.4928	0.1445	6360.7	163.3	4.5869	2.4767
10000	3544.2	25622	3.294	0.0254	143.6	8423.3	6.5269	0.1449	6885.6	176.8	4.6223	2.4565
Experimental Conditions: Hot Water Inlet Temperature: 60 ± 0.5 °C   Hot Water Mass Flowrate: 0.2 kg/s												
3000	2568.3	48142	3.0996	0.0221	240.6	14193	5.9498	0.2245	3254.3	82.8		
4000	2970	47772	3.126	0.0222	239.9	14139	6.0817	0.1962	3932.1	100.3		
5000	3385.2	47582	3.1396	0.0222	239.7	14124	6.1366	0.1765	4696.4	119.9		
6000	3649.4	47382	3.1542	0.0222	239.5	14106	6.2303	0.165	5223.3	133.5		
7000	3841.3	47054	3.1784	0.0222	238.7	14048	6.3051	0.1559	5636.1	144.2		
8000	4071.6	47052	3.1786	0.0222	238.7	14048	6.3213	0.1493	6146.3	157.3		
9000	4303.7	46840	3.1943	0.0223	238.5	14028	6.3639	0.1472	6696.3	171.5		
10000	4492.8	46629	3.2103	0.0223	237.9	13990	6.4228	0.1478	7176.7	184		
Experimental Conditions: Hot Water Inlet Temperature: 70 ± 0.5 °C   Hot Water Mass Flowrate: 0.1125 kg/s												
3000	2227.3	30465	2.7251	0.0247	154.5	9215.2	5.9026	0.2278	3089.8	78.55		2.7076
4000	2506.5	30187	2.7524	0.0247	153.8	9164.5	6.0634	0.1926	3663.7	93.39		2.6446
5000	2740.6	29906	2.7805	0.0249	154.2	9178.7	6.1843	0.1712	4183	106.8		2.5988
6000	2959.7	29566	2.8154	0.025	153.5	9131.4	6.2816	0.1587	4730	121		2.5602
7000	3079.7	29595	2.8124	0.025	153.6	9136.9	6.3213	0.1566	5042.2	129.1		2.5304
8000	3228.7	29489	2.8234	0.0249	153	9100.6	6.3664	0.1485	5469.1	140.1		2.5063
9000	3362.9	29412	2.8315	0.025	153.4	9118.5	6.402	0.1448	5857.3	150.1		2.4836
10000	3463	29321	2.8411	0.025	153.1	9101.3	6.427	0.1435	6176.9	158.4		2.464
Experimental Conditions: Hot Water Inlet Temperature: 70 ± 0.5 °C   Hot Water Mass Flowrate: 0.2 kg/s												
3000	2550.6	55142	2.6724	0.0218	254.6	15207	5.7555	0.2199	3171.4	80.42		
4000	2955.4	54831	2.6889	0.0218	254.2	15176	5.9136	0.1915	3824.4	97.25		
5000	3300.4	54795	2.6908	0.0219	254.7	15205	5.984	0.1785	4420	112.5		
6000	3648.2	54097	2.7285	0.0219	253.1	15095	6.101	0.1672	5080.9	129.6		
7000	3841	53937	2.7373	0.0219	253.1	15090	6.1686	0.1591	5463.7	139.5		
8000	4041.8	53974	2.7353	0.022	253.9	15135	6.1726	0.1524	5871.4	149.9		
9000	4225.1	53767	2.7467	0.022	253.4	15102	6.2343	0.1483	6272.7	160.4		
10000	4452	53533	2.7598	0.022	252.9	15064	6.2784	0.1469	6794.8	173.8		
Annulus Dimensions: L=1.245 m   D <sub>o</sub> =0.028 m   D <sub>i</sub> =0.0155 m												
Experimental Conditions: Hot Water Inlet Temperature: 60 ± 0.5 °C   Hot Water Mass Flowrate: 0.1125 kg/s												
3000	2098.2	20612	3.2096	0.0288	125.5	5797.6	6.1242	0.2965	3525.6	72.55	6.2818	2.5253
4000	2338.3	20474	3.2335	0.0286	124.4	5742.8	6.1694	0.2722	4293.8	88.43	6.4149	2.414
5000	2519.8	20219	3.2783	0.029	124.7	5751.8	6.2727	0.2596	4941.2	101.9	6.5202	2.3276
6000	2639	20191	3.2833	0.029	124.6	5746.4	6.345	0.2473	5426.5	112.1	6.6074	2.2583
7000	2711.7	20173	3.2865	0.029	124.6	5743.1	6.417	0.2435	5747.1	118.8	6.6821	2.204
8000	2782.7	20182	3.2849	0.0286	123.4	5687.9	6.4792	0.2292	6145.3	127.2	6.7474	2.1557
9000	2926.2	20070	3.3051	0.0286	123	5666.7	6.4919	0.2179	6926.4	143.4	6.8056	2.1174
10000	3045.8	19994	3.3189	0.0286	122.7	5652.3	6.5192	0.2164	7665.3	158.7	6.8581	2.0817
Experimental Conditions: Hot Water Inlet Temperature: 60 ± 0.5 °C   Hot Water Mass Flowrate: 0.2 kg/s												
3000	2465.1	37444	3.1343	0.0233	196.2	9082.2	5.9379	0.2955	3549	72.81		
4000	2879	37203	3.1566	0.0233	195.5	9046.7	6.0133	0.275	4484.8	92.12		
5000	3135.1	36950	3.1803	0.0233	194.8	9009.4	6.118	0.256	5152.2	106		
6000	3312.1	36591	3.2147	0.0238	196.9	9097.5	6.2511	0.2384	5610.5	115.7		
7000	3591.6	36620	3.2119	0.0236	195.5	9031.3	6.2623	0.2429	6499.9	134.1		
8000	3667	36593	3.2145	0.0236	195.4	9027.2	6.3565	0.2281	6753.7	139.5		
9000	3928.6	36172	3.2556	0.0238	195.8	9033.5	6.3541	0.2242	7692.7	158.9		
10000	4004.4	36411	3.2321	0.0237	195.7	9034.9	6.4109	0.2158	7987.2	165.1		
Experimental Conditions: Hot Water Inlet Temperature: 70 ± 0.5 °C   Hot Water Mass Flowrate: 0.1125 kg/s												
3000	2195.4	23646	2.7615	0.0277	132	6178.8	5.8179	0.297	3645.3	74.63		2.5468
4000	2428.5	23365	2.7977	0.0277	131.1	6132	5.9565	0.2517	4362.2	89.52		2.4295
5000	2642.1	23076	2.8359	0.0281	131.6	6147.9	6.0764	0.256	5091.3	104.7		2.3394
6000	2771.6	22924	2.8566	0.0285	132.5	6185.6	6.182	0.2464	5560.9	114.5		2.2688
7000	2855.1	22813	2.8717	0.0285	132.2	6166.2	6.2695	0.2349	5927.3	122.3		2.2141
8000	3037.2	22755	2.8797	0.0285	132	6156.1	6.3026	0.231	6783.4	140		2.1665
9000	3100.4	22729	2.8833	0.0281	130.5	6088.1	6.3541	0.226	7210	148.9		2.124
10000	3145.4	22630	2.8971	0.0285	131.6	6134.2	6.4162	0.2169	7382.8	152.6		2.0885
Experimental Conditions: Hot Water Inlet Temperature: 70 ± 0.5 °C   Hot Water Mass Flowrate: 0.2 kg/s												
3000	2573.7	42824	2.7065	0.0227	206.3	9672.4	5.6215	0.2908	3675.3	74.98		
4000	3002.3	42438	2.7332	0.0229	206.3	9662.3	5.7485	0.2791	4618.9	94.44		
5000	3275.1	42276	2.7446	0.0229	205.9	9640.9	5.9276	0.2462	5304.8	108.8		
6000	3565.6	41797	2.7788	0.023	205.6	9617.1	6.0542	0.2393	6121.9	125.8		
7000	3757.8	42057	2.7601	0.023	206.2	9651.9	6.0535	0.242	6692.7	137.6		
8000	4047.9	41750	2.7822	0.0231	206.3	9650.4	6.1374	0.2302	7672.8	157.9		
9000	4156.8	41656	2.7891	0.0231	206.1	9637.7	6.2439	0.2212	8083.6	166.7		
10000	4327.8	41316	2.8141	0.0231	205.2	9591.5	6.2562	0.2106	8799.2	181.5		

**Table C-37:** Isothermal Pressure Drop and Friction Factor for Smooth and Augmented Tubes (Using a Wire Coil of  $e = 1$  mm and  $p = 10, 20, 30, \text{ and } 40$  mm) for Water Flowing at 20, 40, 60, and 70 °C.

Re	$Q \times 10^{-4} (\text{m}^3/\text{s})$	Smooth Tube		Augmented Tube, Wire coil, $e = 1$ mm										
		$\Delta p_{(\text{mm H}_2\text{O})}$	$f_s$	$p = 10 \text{ mm}$		$p = 20 \text{ mm}$		$p = 30 \text{ mm}$		$p = 40 \text{ mm}$				
				Exp.	Theo.	$\Delta p_{(\text{mm H}_2\text{O})}$	$f_a$	$\Delta p_{(\text{mm H}_2\text{O})}$	$f_a$	$\Delta p_{(\text{mm H}_2\text{O})}$	$f_a$			
Inner Tube Dimensions: $L=1.245 \text{ m}$ $d_i=0.011 \text{ m}$														
Experimental Conditions: Isothermal $T = 20^\circ\text{C}$														
5000	0.4336	51	0.0425	0.0386	241	0.2009	143	0.1189	99	0.0824	79	0.0658		
10000	0.8671	162	0.0338	0.0315	899	0.1873	524	0.1092	352	0.0733	272	0.0567		
15000	1.3007	326	0.0302	0.0282	1961	0.1816	1131	0.1047	746	0.0691	566	0.0524		
20000	1.7343	537	0.028	0.0262	3419	0.1781	1957	0.1019	1269	0.0661	950	0.0495		
25000	2.1679	793	0.0264	0.0247	5267 *	0.1756	2989	0.0997	1918	0.0639	1424	0.0475		
30000	2.6014	1093	0.0253	0.0236	7506 *	0.1738	4222	0.0977	2684	0.0621	1972	0.0457		
35000	3.035	1433	0.0244	0.0228	10131 *	0.1723	5653 *	0.0962	3561	0.0606	2598	0.0442		
40000	3.4686	1813	0.0236	0.0221	13128 *	0.171	7263 *	0.0946	4538	0.0591	3297	0.0429		
Experimental Conditions: Isothermal $T = 40^\circ\text{C}$														
5000	0.2843	21	0.0412	0.0386	105	0.2027	62	0.1206	42	0.0829	34	0.066		
10000	0.5685	70	0.0341	0.0315	390	0.1891	227	0.1107	151	0.0736	115	0.0561		
15000	0.8528	140	0.0303	0.0282	850	0.1831	491	0.1064	320	0.0694	240	0.052		
20000	1.1371	230	0.028	0.0262	1483	0.1797	849	0.1035	545	0.0664	405	0.0494		
25000	1.4213	339	0.0265	0.0247	2284	0.1771	1296	0.1011	825	0.0644	607	0.0474		
30000	1.7056	466	0.0252	0.0236	3255	0.1753	1831	0.0992	1154	0.0625	842	0.0456		
35000	1.9899	611	0.0243	0.0228	4393	0.1738	2452	0.0976	1531	0.0609	1110	0.0442		
40000	2.2741	773	0.0236	0.0221	5693 *	0.1725	3149	0.096	1951	0.0595	1409	0.0429		
Experimental Conditions: Isothermal $T = 60^\circ\text{C}$														
5000	0.2049	11	0.0423	0.0386	55	0.2067	32	0.1223	22.5	0.0847	18	0.0675		
10000	0.4097	35	0.0332	0.0315	203	0.1924	119	0.1128	80	0.0758	63	0.0597		
15000	0.6146	72	0.0303	0.0282	444	0.187	256	0.1078	169	0.0712	130	0.0547		
20000	0.8195	120	0.0284	0.0262	773	0.1831	443	0.1049	287	0.068	218	0.0516		
25000	1.0243	178	0.027	0.0247	1192	0.1807	676	0.1025	434	0.0658	326	0.0494		
30000	1.2292	242	0.0255	0.0236	1698	0.1788	955	0.1005	607	0.0639	451	0.0475		
35000	1.434	318	0.0246	0.0228	2292	0.1773	1279	0.0989	806	0.0623	595	0.046		
40000	1.6389	405	0.024	0.0221	2970	0.1759	1643	0.0973	1027	0.0608	753	0.0446		
Experimental Conditions: Isothermal $T = 70^\circ\text{C}$														
5000	0.1767	8	0.0418	0.0386	39.5	0.2033	23.5	0.1203	16.5	0.0841	13	0.067		
10000	0.3535	28	0.0358	0.0315	148	0.1895	86	0.1101	58	0.0743	47	0.0602		
15000	0.5302	55	0.0313	0.0282	323	0.1838	186	0.1058	124	0.0706	92	0.0523		
20000	0.7069	89	0.0285	0.0262	563	0.1802	322	0.1031	211	0.0675	160	0.0512		
25000	0.8837	132	0.027	0.0247	867	0.1776	492	0.1008	319	0.0653	235	0.0481		
30000	1.0604	181	0.0257	0.0236	1236	0.1758	695	0.0989	446	0.0634	330	0.0469		
35000	1.2371	235	0.0246	0.0228	1668	0.1743	931	0.0973	592	0.0619	430	0.0449		
40000	1.4139	297	0.0238	0.0221	2162	0.173	1196	0.0957	754	0.0603	550	0.044		
Inner Tube Dimensions: $L=1.245 \text{ m}$ $d_i=0.014 \text{ m}$														
Experimental Conditions: Isothermal $T = 20^\circ\text{C}$														
5000	0.5518	23	0.0395	0.0386	106	0.1821	71	0.122	52	0.0894	42	0.0722		
10000	1.1036	79	0.0339	0.0315	394	0.1693	261	0.1121	188	0.0808	148	0.0636		
15000	1.6555	159	0.0304	0.0282	855	0.1632	563	0.1075	401	0.0766	311	0.0594		
20000	2.2073	263	0.0282	0.0262	1488	0.1598	974	0.1046	688	0.0739	527	0.0566		
25000	2.7591	387	0.0266	0.0247	2292	0.1575	1491	0.1025	1044	0.0718	792	0.0544		
30000	3.3109	535	0.0255	0.0236	3265	0.1558	2109	0.1007	1468	0.0701	1106	0.0528		
35000	3.8627	702	0.0246	0.0228	4405	0.1545	2829	0.0992	1957	0.0686	1463	0.0513		
40000	4.4146	888	0.0238	0.0221	5716 *	0.1535	3645	0.0979	2504	0.0672	1865	0.0501		
Experimental Conditions: Isothermal $T = 40^\circ\text{C}$														
5000	0.3618	10	0.0402	0.0386	46	0.1839	29	0.1166	22	0.0885	17	0.0684		
10000	0.7236	33	0.0332	0.0315	172	0.1719	113	0.1136	81	0.0814	63	0.0633		
15000	1.0854	69	0.0308	0.0282	373	0.1657	246	0.1099	172	0.0769	133	0.0594		
20000	1.4472	113	0.0284	0.0262	650	0.1624	426	0.1071	296	0.0744	226	0.0568		
25000	1.809	169	0.0272	0.0247	1002	0.1602	652	0.1049	449	0.0722	340	0.0547		
30000	2.1708	232	0.0259	0.0236	1428	0.1586	922	0.103	631	0.0705	475	0.0531		
35000	2.5325	304	0.0249	0.0228	1927	0.1572	1237	0.1015	841	0.069	628	0.0515		
40000	2.8943	381	0.0239	0.0221	2500	0.1561	1594	0.1002	1076	0.0676	798	0.0501		
Experimental Conditions: Isothermal $T = 60^\circ\text{C}$														
5000	0.2607	5	0.0391	0.0386	24	0.1875	15	0.1172	11	0.086	9	0.0703		
10000	0.5215	16	0.0313	0.0315	89	0.1739	58	0.1133	42	0.082	33	0.0645		
15000	0.7822	35	0.0304	0.0282	194	0.1684	126	0.1094	90	0.0781	70	0.0608		
20000	1.0429	58	0.0283	0.0262	338	0.1651	220	0.1074	155	0.0757	119	0.0581		
25000	1.3037	85	0.0266	0.0247	520	0.1625	337	0.1053	236	0.0738	179	0.0559		
30000	1.5644	117	0.0254	0.0236	741	0.1608	477	0.1035	332	0.0721	250	0.0543		
35000	1.8252	155	0.0247	0.0228	997	0.159	640	0.1021	442	0.0705	331	0.0528		
40000	2.0859	196	0.0239	0.0221	1298	0.1585	825	0.1007	566	0.0691	421	0.0514		
Experimental Conditions: Isothermal $T = 70^\circ\text{C}$														
5000	0.2249	4	0.0422	0.0386	17	0.1795	11	0.1161	9	0.095	7	0.0739		
10000	0.4499	12	0.0317	0.0315	65	0.1716	42	0.1108	31	0.0818	24	0.0633		
15000	0.6748	27	0.0317	0.0282	143	0.1677	91	0.1067	68	0.0798	51	0.0598		
20000	0.8997	42	0.0277	0.0262	249	0.1643	159	0.1049	117	0.0772	87	0.0574		
25000	1.1247	65	0.0274	0.0247	384	0.1622	243	0.1026	178	0.0752	131	0.0553		
30000	1.3496	85	0.0249	0.0236	548	0.1607	344	0.1009	250	0.0733	183	0.0537		
35000	1.5745	116	0.025	0.0228	741	0.1596	461	0.0993	330	0.0711	243	0.0524		
40000	1.7995	143	0.0236	0.0221	960	0.1584	594	0.098	423	0.0698	309	0.051		

\* Values of pressure drop larger than 5000 mm H<sub>2</sub>O are obtained via extrapolation and not by experimental work.

**Table C-38:** Isothermal Pressure Drop and Friction Factor for Smooth and Augmented Annuli (Using a Wire Coil of  $e = 1$  mm and  $p = 10, 20, 30, \text{ and } 40$  mm) for Water Flowing at 20, 40, 60, and 70 °C.

Re Annul us	Q $\times 10^{-4}$ (m <sup>3</sup> /s)	Smooth Annulus		Augmented Annulus, Wire coil, $e = 1$ mm								
				$p = 10$ mm		$p = 20$ mm		$p = 30$ mm		$p = 40$ mm		
		Exp.	Theo.	$\Delta p$ (mm H <sub>2</sub> O)	$f_a$	$\Delta p$ (mm H <sub>2</sub> O)	$f_a$	$\Delta p$ (mm H <sub>2</sub> O)	$f_a$	$\Delta p$ (mm H <sub>2</sub> O)	$f_a$	
Annulus Dimensions: L=1.245 m   D <sub>o</sub> = 0.028 m   D <sub>i</sub> = 0.0125 m												
Experimental Conditions: Isothermal T = 20 °C												
3000	0.9578	7	0.0453	0.0456	21	0.136	18	0.1166	15	0.0972	10	0.0648
4000	1.2771	11	0.0401	0.0414	32	0.1166	27	0.0984	23	0.0838	18	0.0656
5000	1.5963	17	0.0396	0.0386	42	0.0979	41	0.0956	37	0.0863	27	0.063
6000	1.9156	24	0.0389	0.0365	61	0.0988	59	0.0955	49	0.0794	39	0.0632
7000	2.2349	32	0.0381	0.0349	80	0.0952	70	0.0833	64	0.0761	51	0.0607
8000	2.5541	42	0.0383	0.0335	99	0.0902	90	0.082	81	0.0738	63	0.0574
9000	2.8734	52	0.0374	0.0324	123	0.0885	118	0.0849	102	0.0734	80	0.0576
10000	3.1927	65	0.0379	0.0315	150	0.0874	150	0.0874	135	0.0787	102	0.0595
Experimental Conditions: Isothermal T = 40 °C												
3000	0.628	3	0.0455	0.0456	9	0.1356	7.5	0.1137	6	0.091	5	0.0758
4000	0.8373	5	0.0426	0.0414	13	0.1102	12	0.1023	9	0.0767	7	0.0597
5000	1.0466	7.5	0.0409	0.0386	20	0.1085	15	0.0819	13	0.0709	11	0.0600
6000	1.2559	10	0.0379	0.0365	25	0.0942	20	0.0758	18	0.0682	17	0.0644
7000	1.4653	14	0.039	0.0349	35	0.0969	29	0.0807	24	0.0668	21	0.0585
8000	1.6746	18	0.0384	0.0335	42	0.089	35	0.0746	30	0.0664	29	0.0618
9000	1.8839	22	0.0371	0.0324	53	0.0887	46	0.0775	39	0.0657	34	0.0573
10000	2.0932	28	0.0382	0.0315	62	0.0841	56	0.0764	49	0.0669	41	0.0559
Experimental Conditions: Isothermal T = 60 °C												
3000	0.4526	1.5	0.0442	0.0456	5	0.1473	4	0.1178	3	0.0884	2.5	0.0736
4000	0.6034	2.5	0.0414	0.0414	7	0.116	5	0.0828	4	0.0663	4	0.0663
5000	0.7543	3.5	0.0371	0.0386	10	0.106	8	0.0848	7	0.0742	5	0.053
6000	0.9051	5.5	0.0405	0.0365	14	0.1031	12	0.0884	9	0.0663	7	0.0515
7000	1.056	7.5	0.0406	0.0349	18	0.0974	15	0.0812	12	0.0649	11	0.0595
8000	1.2068	9.5	0.0394	0.0335	22	0.0911	19	0.0787	15	0.0621	13	0.0539
9000	1.3577	12	0.0393	0.0324	26	0.0851	23	0.0753	19	0.0622	16	0.0524
10000	1.5085	14	0.0371	0.0315	33	0.0875	30	0.0795	25	0.0663	20	0.053
Experimental Conditions: Isothermal T = 70 °C												
3000	0.3904	1.5	0.0597	0.0456	3	0.1194	3	0.1194	2.5	0.0995	2	0.0796
4000	0.5206	2	0.0448	0.0414	5	0.1119	4	0.0895	4	0.0895	3	0.0672
5000	0.6507	3	0.043	0.0386	8	0.1146	6	0.086	6	0.086	4	0.0573
6000	0.7808	4	0.0398	0.0365	11	0.1094	8	0.0796	7	0.0696	6	0.0597
7000	0.911	5	0.0365	0.0349	14	0.1023	11	0.0804	9	0.0658	8	0.0585
8000	1.0411	7	0.0392	0.0335	17	0.0951	13	0.0728	11	0.0616	10	0.056
9000	1.1713	9	0.0398	0.0324	21	0.0929	17	0.0752	15	0.0663	12	0.0531
10000	1.3014	10	0.0358	0.0315	24	0.086	21	0.0752	17	0.0609	15	0.0537
Annulus Dimensions: L=1.245 m   D <sub>o</sub> = 0.028 m   D <sub>i</sub> = 0.0155 m												
Experimental Conditions: Isothermal T = 20 °C												
3000	1.0288	15	0.051	0.0456	45	0.1529	41	0.1393	28	0.0951	24	0.0815
4000	1.3717	24	0.0459	0.0414	75	0.1433	69	0.1319	43	0.0822	37	0.0707
5000	1.7146	36	0.044	0.0386	110	0.1345	100	0.1223	63	0.0771	52	0.0636
6000	2.0575	46	0.0391	0.0365	150	0.1274	141	0.1198	82	0.0696	72	0.0612
7000	2.4004	61	0.0381	0.0349	198	0.1236	181	0.1129	107	0.0668	85	0.053
8000	2.7433	78	0.0373	0.0335	240	0.1147	230	0.1099	136	0.065	107	0.0511
9000	3.0863	94	0.0355	0.0324	305	0.1151	287	0.1083	171	0.0646	133	0.0502
10000	3.4292	113	0.0346	0.0315	372	0.1137	343	0.1049	203	0.0621	161	0.0492
Experimental Conditions: Isothermal T = 40 °C												
3000	0.6745	6	0.0477	0.0456	20	0.1581	17	0.1352	12	0.0954	11	0.0875
4000	0.8993	10	0.0447	0.0414	33	0.1467	29	0.1297	18	0.0805	17	0.076
5000	1.1241	15	0.0429	0.0386	47	0.1337	43	0.1231	25	0.0716	25	0.0716
6000	1.349	20	0.0398	0.0365	64	0.1265	59	0.1173	34	0.0676	33	0.0656
7000	1.5738	25	0.0365	0.0349	88	0.1277	80	0.1168	45	0.0657	43	0.0628
8000	1.7986	31	0.0347	0.0335	114	0.1267	103	0.1152	59	0.066	55	0.0615
9000	2.0234	39	0.0345	0.0324	141	0.1238	132	0.1166	70	0.0618	67	0.0592
10000	2.2483	48	0.0343	0.0315	175	0.1245	163	0.1166	87	0.0623	78	0.0558
Experimental Conditions: Isothermal T = 60 °C												
3000	0.4861	3	0.0463	0.0456	11	0.1699	9	0.139	6	0.0927	6	0.0927
4000	0.6481	5	0.0435	0.0414	18	0.1564	15	0.1304	10	0.0869	9	0.0782
5000	0.8101	7	0.0389	0.0386	24	0.1335	22	0.1224	15	0.0834	13	0.0723
6000	0.9722	10	0.0386	0.0365	34	0.1313	31	0.1197	20	0.0772	17	0.0657
7000	1.1342	13	0.0369	0.0349	45	0.1277	41	0.1163	26	0.0738	20	0.0568
8000	1.2962	17	0.0369	0.0335	59	0.1282	52	0.113	32	0.0695	24	0.0521
9000	1.4583	21	0.036	0.0324	71	0.1219	65	0.1116	38	0.0652	33	0.0566
10000	1.6203	25	0.0348	0.0315	87	0.121	76	0.1057	45	0.0626	37	0.0514
Experimental Conditions: Isothermal T = 70 °C												
3000	0.4193	2	0.0417	0.0456	8	0.167	6.5	0.1357	5	0.1044	4	0.0835
4000	0.5591	3.5	0.0411	0.0414	14	0.1644	11	0.1292	8	0.0939	7	0.0822
5000	0.6989	5.5	0.0413	0.0386	20	0.1503	15	0.1127	11	0.0827	10	0.0751
6000	0.8387	8	0.0417	0.0365	27	0.1409	21	0.1096	14	0.0731	13	0.0678
7000	0.9785	10.5	0.0403	0.0349	35	0.1342	28	0.1073	19	0.0728	17	0.0652
8000	1.1182	13	0.0382	0.0335	43	0.1262	35	0.1027	23	0.0675	21	0.0616
9000	1.258	16	0.0371	0.0324	53	0.1229	44	0.102	27	0.0626	25	0.058
10000	1.3978	17	0.0319	0.0315	70	0.1315	55	0.1033	34	0.0639	30	0.0564

**Table C-39:** Isothermal Pressure Drop and Friction Factor for Smooth and Augmented Annuli (Using a Wire Coil of  $e = 2.2$  mm and  $p = 10, 20, 30,$  and  $40$  mm) for Water Flowing at  $20, 40, 60,$  and  $70^\circ\text{C}$ .

Re Annul us	$Q \times 10^{-4}$ ( $\text{m}^3/\text{s}$ )	Smooth Annulus		Augmented Annulus, Wire coil, $e = 2.2$ mm								
				$p = 10 \text{ mm}$		$p = 20 \text{ mm}$		$p = 30 \text{ mm}$		$p = 40 \text{ mm}$		
		$\Delta p$ (mm H <sub>2</sub> O)	$f_a$	$\Delta p$ (mm H <sub>2</sub> O)	$f_a$	$\Delta p$ (mm H <sub>2</sub> O)	$f_a$	$\Delta p$ (mm H <sub>2</sub> O)	$f_a$	$\Delta p$ (mm H <sub>2</sub> O)	$f_a$	
Annulus Dimensions: $L=1.245 \text{ m}$ $D_o=0.028 \text{ m}$ $D_i=0.0125 \text{ m}$												
Experimental Conditions: Isothermal $T = 20^\circ\text{C}$												
3000	0.9578	7	0.0453	0.0456	47	0.2639	34	0.1909	29	0.1628	22	0.1235
4000	1.2771	11	0.0401	0.0414	76	0.24	56	0.1769	43	0.1358	37	0.1169
5000	1.5963	17	0.0396	0.0386	110	0.2224	85	0.1718	62	0.1253	55	0.1112
6000	1.9156	24	0.0389	0.0365	142	0.1993	117	0.1642	85	0.1193	75	0.1053
7000	2.2349	32	0.0381	0.0349	188	0.1939	154	0.1588	115	0.1186	100	0.1031
8000	2.5541	42	0.0383	0.0335	241	0.1903	199	0.1571	139	0.1098	125	0.0987
9000	2.8734	52	0.0374	0.0324	302	0.1884	244	0.1522	165	0.1029	157	0.0979
10000	3.1927	65	0.0379	0.0315	360	0.1819	300	0.1516	200	0.1011	183	0.0925
Experimental Conditions: Isothermal $T = 40^\circ\text{C}$												
3000	0.628	3	0.0455	0.0456	19	0.2863	13	0.1971	12	0.1819	9	0.1364
4000	0.8373	5	0.0426	0.0414	29	0.2458	23	0.1961	17	0.145	13	0.1109
5000	1.0466	7.5	0.0409	0.0386	44	0.2387	35	0.191	24	0.131	22	0.1201
6000	1.2559	10	0.0379	0.0365	60	0.226	48	0.1819	35	0.1326	31	0.1175
7000	1.4653	14	0.039	0.0349	80	0.2214	63	0.1754	45	0.1253	41	0.1142
8000	1.6746	18	0.0384	0.0335	102	0.2161	81	0.1727	56	0.1194	54	0.1151
9000	1.8839	22	0.0371	0.0324	129	0.216	101	0.1701	70	0.1179	67	0.1129
10000	2.0932	28	0.0382	0.0315	158	0.2143	124	0.1692	84	0.1146	83	0.1132
Experimental Conditions: Isothermal $T = 60^\circ\text{C}$												
3000	0.4526	1.5	0.0442	0.0456	9	0.2651	7	0.2062	6	0.1767	4.5	0.1326
4000	0.6034	2.5	0.0414	0.0414	16	0.2651	12	0.1988	9	0.1491	7	0.116
5000	0.7543	3.5	0.0371	0.0386	25	0.2651	17	0.1803	12	0.1273	10	0.106
6000	0.9051	5.5	0.0405	0.0365	32	0.2357	25	0.1841	17	0.1252	15	0.1105
7000	1.056	7.5	0.0406	0.0349	40	0.2164	32	0.1731	24	0.1298	20	0.1082
8000	1.2068	9.5	0.0394	0.0335	51	0.2113	40	0.1657	29	0.1201	23	0.0953
9000	1.3577	12	0.0393	0.0324	64	0.2095	52	0.1702	35	0.1146	29	0.0949
10000	1.5085	14	0.0371	0.0315	77	0.2041	62	0.1644	42	0.1113	38	0.1007
Experimental Conditions: Isothermal $T = 70^\circ\text{C}$												
3000	0.3904	1.5	0.0597	0.0456	7	0.2786	5	0.199	4.5	0.1791	3.5	0.1393
4000	0.5206	2	0.0448	0.0414	12	0.2686	9	0.2015	7	0.1567	5	0.1119
5000	0.6507	3	0.043	0.0386	18	0.2579	13	0.1863	10	0.1433	8	0.1146
6000	0.7808	4	0.0398	0.0365	25	0.2487	20	0.199	13	0.1293	11	0.1094
7000	0.911	5	0.0365	0.0349	34	0.2485	25	0.1827	18	0.1316	15	0.1096
8000	1.0411	7	0.0392	0.0335	42	0.2351	32	0.1791	23	0.1287	19	0.1063
9000	1.1713	9	0.0398	0.0324	53	0.2344	40	0.1769	27	0.1194	25	0.1105
10000	1.3014	10	0.0358	0.0315	61	0.2185	48	0.1719	33	0.1182	30	0.1075
Annulus Dimensions: $L=1.245 \text{ m}$ $D_o=0.028 \text{ m}$ $D_i=0.0155 \text{ m}$												
Experimental Conditions: Isothermal $T = 20^\circ\text{C}$												
3000	1.0288	15	0.051	0.0456	105	0.3567	88	0.299	65	0.2208	54	0.1835
4000	1.3717	24	0.0459	0.0414	179	0.3421	145	0.2771	110	0.2102	90	0.172
5000	1.7146	36	0.044	0.0386	261	0.3192	215	0.263	171	0.2091	132	0.1614
6000	2.0575	46	0.0391	0.0365	375	0.3185	301	0.2557	230	0.1954	185	0.1571
7000	2.4004	61	0.0381	0.0349	509	0.3176	387	0.2415	312	0.1947	239	0.1491
8000	2.7433	78	0.0373	0.0335	661	0.3158	504	0.2408	402	0.1921	305	0.1457
9000	3.0863	94	0.0355	0.0324	836	0.3156	634	0.2393	508	0.1918	390	0.1472
10000	3.4292	113	0.0346	0.0315	1023	0.3128	767	0.2345	622	0.1902	475	0.1452
Experimental Conditions: Isothermal $T = 40^\circ\text{C}$												
3000	0.6745	6	0.0477	0.0456	42	0.332	34	0.2703	27	0.2147	22	0.1749
4000	0.8993	10	0.0447	0.0414	72	0.3201	60	0.2683	46	0.2057	37	0.1655
5000	1.1241	15	0.0429	0.0386	110	0.313	88	0.2519	68	0.1946	56	0.1603
6000	1.349	20	0.0398	0.0365	151	0.2984	121	0.2405	93	0.1849	75	0.1491
7000	1.5738	25	0.0365	0.0349	212	0.3078	162	0.2366	130	0.1899	100	0.146
8000	1.7986	31	0.0347	0.0335	270	0.3001	211	0.2359	167	0.1867	131	0.1465
9000	2.0234	39	0.0345	0.0324	339	0.2977	263	0.2323	211	0.1864	166	0.1467
10000	2.2483	48	0.0343	0.0315	430	0.3059	322	0.2304	258	0.1846	196	0.1403
Experimental Conditions: Isothermal $T = 60^\circ\text{C}$												
3000	0.4861	3	0.0463	0.0456	23	0.3553	18	0.2781	15	0.2317	12	0.1854
4000	0.6481	5	0.0435	0.0414	40	0.3476	31	0.2694	22	0.1912	18	0.1564
5000	0.8101	7	0.0389	0.0386	56	0.3115	46	0.2558	33	0.1835	28	0.1557
6000	0.9722	10	0.0386	0.0365	79	0.3051	64	0.2472	46	0.1777	40	0.1545
7000	1.1342	13	0.0369	0.0349	103	0.2923	81	0.2299	62	0.1759	52	0.1476
8000	1.2962	17	0.0369	0.0335	139	0.302	105	0.2281	81	0.176	63	0.1369
9000	1.4583	21	0.036	0.0324	174	0.2987	130	0.2232	103	0.1768	78	0.1339
10000	1.6203	25	0.0348	0.0315	215	0.2989	158	0.2197	123	0.171	95	0.1321
Experimental Conditions: Isothermal $T = 70^\circ\text{C}$												
3000	0.4193	2	0.0417	0.0456	17	0.3548	14	0.2922	11	0.2296	9	0.1879
4000	0.5591	3.5	0.0411	0.0414	30	0.3522	25	0.2935	16	0.1879	15	0.1761
5000	0.6989	5.5	0.0413	0.0386	45	0.3381	37	0.278	26	0.1954	22	0.1653
6000	0.8387	8	0.0417	0.0365	60	0.3131	51	0.2661	36	0.1879	29	0.1513
7000	0.9785	10.5	0.0403	0.0349	83	0.3182	67	0.2569	47	0.1802	39	0.1495
8000	1.1182	13	0.0382	0.0335	105	0.3082	82	0.2407	59	0.1732	48	0.1409
9000	1.258	16	0.0371	0.0324	134	0.3108	102	0.2366	74	0.1716	62	0.1438
10000	1.3978	17	0.0319	0.0315	160	0.3006	122	0.2292	90	0.1691	75	0.1409

**Table C-40:** Isothermal Pressure Drop and Friction Factor for Smooth and Augmented Annuli (Using Circular Ribs of  $e = 2.2$  mm and  $p = 10, 20, 30, \text{ and } 40$  mm) for Water Flowing at 20, 40, 60, and 70 °C.

Re Annul us	$Q$ $\times 10^{-4}$ ( $\text{m}^3/\text{s}$ )	Smooth Annulus		Augmented Annulus, Circular ribs, $e = 2.2$ mm										
		$\Delta p$ (mm H <sub>2</sub> O)	$f_s$	$p = 10 \text{ mm}$		$p = 20 \text{ mm}$		$p = 30 \text{ mm}$		$p = 40 \text{ mm}$				
				Exp.	Theo.	$\Delta p$ (mm H <sub>2</sub> O)	$f_a$	$\Delta p$ (mm H <sub>2</sub> O)	$f_a$	$\Delta p$ (mm H <sub>2</sub> O)	$f_a$			
Annulus Dimensions: $L=1.245 \text{ m}$ $D_o=0.028 \text{ m}$ $D_i=0.0125 \text{ m}$														
Experimental Conditions: Isothermal $T = 20^\circ\text{C}$														
3000	0.9578	7	0.0453	0.0456	79	0.4436	64	0.3594	43	0.2414	41	0.2302		
4000	1.2771	11	0.0401	0.0414	127	0.4011	103	0.3253	69	0.2179	65	0.2053		
5000	1.5963	17	0.0396	0.0386	177	0.3578	143	0.2891	96	0.1941	91	0.1839		
6000	1.9156	24	0.0389	0.0365	244	0.3425	197	0.2765	132	0.1853	125	0.1755		
7000	2.2349	32	0.0381	0.0349	314	0.3238	254	0.262	170	0.1753	161	0.166		
8000	2.5541	42	0.0383	0.0335	396	0.3127	320	0.2527	214	0.169	203	0.1603		
9000	2.8734	52	0.0374	0.0324	485	0.3026	392	0.2446	262	0.1635	249	0.1553		
10000	3.1927	65	0.0379	0.0315	582	0.2941	471	0.238	315	0.1592	299	0.1511		
Experimental Conditions: Isothermal $T = 40^\circ\text{C}$														
3000	0.628	3	0.0455	0.0456	30	0.4521	24	0.3638	16.5	0.2501	15	0.2274		
4000	0.8373	5	0.0426	0.0414	50	0.4238	40	0.3411	27	0.2302	26	0.2217		
5000	1.0466	7.5	0.0409	0.0386	74	0.4014	59	0.322	40	0.2183	37	0.2019		
6000	1.2559	10	0.0379	0.0365	102	0.3843	81	0.307	55	0.2084	52	0.1971		
7000	1.4653	14	0.039	0.0349	134	0.3709	106	0.2951	72	0.2005	68	0.1893		
8000	1.6746	18	0.0384	0.0335	168	0.356	133	0.2835	91	0.194	85	0.1812		
9000	1.8839	22	0.0371	0.0324	207	0.3466	164	0.2762	112	0.1887	105	0.1769		
10000	2.0932	28	0.0382	0.0315	249	0.3377	197	0.2688	134	0.1828	125	0.1705		
Experimental Conditions: Isothermal $T = 60^\circ\text{C}$														
3000	0.4526	1.5	0.0442	0.0456	14.5	0.4271	12	0.3535	8.5	0.2504	7	0.2062		
4000	0.6034	2.5	0.0414	0.0414	24	0.3977	20	0.3314	14	0.232	12	0.1988		
5000	0.7543	3.5	0.0371	0.0386	35	0.3712	29	0.3075	20	0.2121	17	0.1803		
6000	0.9051	5.5	0.0405	0.0365	48	0.3535	40	0.2946	28	0.2062	24	0.1767		
7000	1.056	7.5	0.0406	0.0349	63	0.3409	52	0.2813	37	0.2002	31	0.1677		
8000	1.2068	9.5	0.0394	0.0335	80	0.3314	66	0.2734	46	0.1905	39	0.1616		
9000	1.3577	12	0.0393	0.0324	98	0.3207	81	0.2651	57	0.1866	48	0.1571		
10000	1.5085	14	0.0371	0.0315	117	0.3102	97	0.2572	68	0.1803	58	0.1538		
Experimental Conditions: Isothermal $T = 70^\circ\text{C}$														
3000	0.3904	1.5	0.0597	0.0456	12	0.4776	9	0.3582	6.5	0.2587	5.5	0.2189		
4000	0.5206	2	0.0448	0.0414	21	0.4701	16	0.3582	11	0.2462	9	0.2015		
5000	0.6507	3	0.043	0.0386	30	0.4298	23	0.3295	16	0.2292	14	0.2006		
6000	0.7808	4	0.0398	0.0365	42	0.4179	32	0.3184	22	0.2189	19	0.189		
7000	0.911	5	0.0365	0.0349	56	0.4093	42	0.307	29	0.212	25	0.1827		
8000	1.0411	7	0.0392	0.0335	69	0.3862	52	0.291	36	0.2015	31	0.1735		
9000	1.1713	9	0.0398	0.0324	85	0.3759	64	0.283	44	0.1946	38	0.168		
10000	1.3014	10	0.0358	0.0315	102	0.3653	77	0.2758	53	0.1898	46	0.1648		
Annulus Dimensions: $L=1.245 \text{ m}$ $D_o=0.028 \text{ m}$ $D_i=0.0155 \text{ m}$														
Experimental Conditions: Isothermal $T = 20^\circ\text{C}$														
3000	1.0288	15	0.051	0.0456	184	0.6251	142	0.4824	113	0.3839	87	0.2956		
4000	1.3717	24	0.0459	0.0414	304	0.581	234	0.4472	186	0.3555	144	0.2752		
5000	1.7146	36	0.044	0.0386	448	0.5479	345	0.422	275	0.3363	212	0.2593		
6000	2.0575	46	0.0391	0.0365	615	0.5224	474	0.4026	377	0.3202	291	0.2472		
7000	2.4004	61	0.0381	0.0349	805	0.5023	620	0.3869	494	0.3083	381	0.2377		
8000	2.7433	78	0.0373	0.0335	1014	0.4844	781	0.3731	622	0.2972	480	0.2293		
9000	3.0863	94	0.0355	0.0324	1241	0.4685	956	0.3609	761	0.2873	587	0.2216		
10000	3.4292	113	0.0346	0.0315	1494	0.4568	1151	0.3519	916	0.2801	707	0.2162		
Experimental Conditions: Isothermal $T = 40^\circ\text{C}$														
3000	0.6745	6	0.0477	0.0456	77	0.6086	60	0.4771	48	0.3816	37	0.2942		
4000	0.8993	10	0.0447	0.0414	133	0.5913	103	0.4607	81	0.3623	63	0.2818		
5000	1.1241	15	0.0429	0.0386	195	0.5548	152	0.4336	119	0.3406	93	0.2662		
6000	1.349	20	0.0398	0.0365	252	0.4979	196	0.3886	155	0.3081	121	0.2405		
7000	1.5738	25	0.0365	0.0349	333	0.4834	259	0.3782	205	0.2994	160	0.2337		
8000	1.7986	31	0.0347	0.0335	425	0.4724	331	0.3695	262	0.2929	205	0.2292		
9000	2.0234	39	0.0345	0.0324	533	0.4681	415	0.3662	327	0.2889	257	0.227		
10000	2.2483	48	0.0343	0.0315	643	0.4574	500	0.3578	396	0.2834	310	0.2218		
Experimental Conditions: Isothermal $T = 60^\circ\text{C}$														
3000	0.4861	3	0.0463	0.0456	41	0.6334	32	0.4944	25	0.3862	20	0.309		
4000	0.6481	5	0.0435	0.0414	68	0.5909	52	0.4519	40	0.3476	32	0.2781		
5000	0.8101	7	0.0389	0.0386	101	0.5617	77	0.4283	59	0.3281	47	0.2614		
6000	0.9722	10	0.0386	0.0365	139	0.5369	106	0.4094	81	0.3129	65	0.2511		
7000	1.1342	13	0.0369	0.0349	180	0.5108	138	0.3916	106	0.3008	84	0.2384		
8000	1.2962	17	0.0369	0.0335	227	0.4932	174	0.378	133	0.289	106	0.2303		
9000	1.4583	21	0.036	0.0324	280	0.4807	214	0.3674	164	0.2815	130	0.2232		
10000	1.6203	25	0.0348	0.0315	336	0.4672	257	0.3573	197	0.2739	157	0.2183		
Experimental Conditions: Isothermal $T = 70^\circ\text{C}$														
3000	0.4193	2	0.0417	0.0456	30	0.6262	23	0.4801	17	0.3548	14	0.2922		
4000	0.5591	3.5	0.0411	0.0414	49	0.5753	39	0.4579	28	0.3288	23	0.27		
5000	0.6989	5.5	0.0413	0.0386	72	0.541	57	0.4283	41	0.3081	34	0.2555		
6000	0.8387	8	0.0417	0.0365	100	0.5218	79	0.4122	57	0.2974	47	0.2453		
7000	0.9785	10.5	0.0403	0.0349	131	0.5022	103	0.3949	74	0.2837	62	0.2377		
8000	1.1182	13	0.0382	0.0335	165	0.4843	130	0.3816	93	0.273	78	0.229		
9000	1.258	16	0.0371	0.0324	201	0.4662	159	0.3688	114	0.2644	95	0.2203		
10000	1.3978	17	0.0319	0.0315	242	0.4546	191	0.3588	137	0.2574	114	0.2142		

**Table C-41:** Description of Turbulence Promoters (Inserts) in Terms of the Dimensionless Parameters ( $e/d_i$ ) and ( $p/d_i$ ) or ( $e/D_e$ ) and ( $p/D_e$ )

Type of Insert			Wire coil inside the inner tube			Wire coil on the outer surface of the inner tube			Circular rib on the outer surface of the inner tube			
			Param- eter	$d_i = 11.0$	$d_i = 14.0$	Param- eter	$D_i = 12.5$ $D_o = 28.0$	$D_i = 15.5$ $D_o = 28.0$	$D_i = 12.5$ $D_o = 28.0$	$D_i = 15.5$ $D_o = 28.0$		
Wire or circular rib diameter  $e = 1 \text{ mm}$	Coiling or ribbing pitch, $p$ (mm)	10		$e/d_i$	0.0909	0.0714	$e/D_e$	0.0645	0.0800	—	—	
				$p/d_i$	0.9091	0.7143	$p/D_e$	0.6452	0.8000	—	—	
		20		$e/d_i$	0.0909	0.0714	$e/D_e$	0.0645	0.0800	—	—	
				$p/d_i$	1.8182	1.4286	$p/D_e$	1.2903	1.6000	—	—	
		30		$e/d_i$	0.0909	0.0714	$e/D_e$	0.0645	0.0800	—	—	
				$p/d_i$	2.7273	2.1429	$p/D_e$	1.9355	2.4000	—	—	
		40		$e/d_i$	0.0909	0.0714	$e/D_e$	0.0645	0.0800	—	—	
				$p/d_i$	3.6364	2.8571	$p/D_e$	2.5806	3.2000	—	—	
Wire or circular rib diameter  $e = 2.2 \text{ mm}$	Coiling or ribbing pitch, $p$ (mm)	10		$e/d_i$	—	—	$e/D_e$	0.1419	0.1760	0.1419	0.1760	
				$p/d_i$	—	—	$p/D_e$	0.6452	0.8000	0.6452	0.8000	
		20		$e/d_i$	—	—	$e/D_e$	0.1419	0.1760	0.1419	0.1760	
				$p/d_i$	—	—	$p/D_e$	1.2903	1.6000	1.2903	1.6000	
		30		$e/d_i$	—	—	$e/D_e$	0.1419	0.1760	0.1419	0.1760	
				$p/d_i$	—	—	$p/D_e$	1.9355	2.4000	1.9355	2.4000	
		40		$e/d_i$	—	—	$e/D_e$	0.1419	0.1760	0.1419	0.1760	
				$p/d_i$	—	—	$p/D_e$	2.5806	3.2000	2.5806	3.2000	

**Table C-42:** Application of FG-2a Criterion to the Tube-Side Heat Transfer Enhancement for all Geometrical Characteristics and Conditions.

Re Inner tube	FG-2a Criterion, Wire Coil, $e = 1 \text{ mm}$							
	$p = 10 \text{ mm}$		$p = 20 \text{ mm}$		$p = 30 \text{ mm}$		$p = 40 \text{ mm}$	
	$Re_o$	$q_a/q_o$	$Re_o$	$q_a/q_o$	$Re_o$	$q_a/q_o$	$Re_o$	$q_a/q_o$
Inner Tube Dimensions: $L=1.245 \text{ m}$ $d_i=0.011 \text{ m}$								
$\Delta T_f = 40 \text{ }^\circ\text{C}$ , $Pr=3.14$								
5000	8936.1	1.4505	7319.8	1.3408	6513.4	1.2806	5995.8	1.2395
10000	18682	1.3605	15303	1.2576	13617	1.2011	12535	1.1625
15000	28758	1.3104	23556	1.2114	20961	1.1569	19296	1.1198
20000	39055	1.2761	31991	1.1796	28467	1.1266	26205	1.0904
25000	49520	1.25	40563	1.1555	36095	1.1036	33226	1.0681
30000	60121	1.2291	49246	1.1362	43821	1.0851	40339	1.0503
35000	70835	1.2117	58023	1.1201	51631	1.0698	47528	1.0354
40000	81649	1.1969	66880	1.1064	59513	1.0566	54783	1.0227
$\Delta T_f = 50 \text{ }^\circ\text{C}$ , $Pr=2.72$								
5000	8936.1	1.4486	7319.8	1.3391	6513.4	1.2789	5995.8	1.2378
10000	18682	1.3587	15303	1.256	13617	1.1995	12535	1.161
15000	28758	1.3087	23556	1.2098	20961	1.1554	19296	1.1183
20000	39055	1.2744	31991	1.178	28467	1.1251	26205	1.089
25000	49520	1.2484	40563	1.154	36095	1.1021	33226	1.0667
30000	60121	1.2275	49246	1.1347	43821	1.0837	40339	1.0489
35000	70835	1.2101	58023	1.1187	51631	1.0684	47528	1.0341
40000	81649	1.1953	66880	1.1049	59513	1.0553	54783	1.0214
Inner Tube Dimensions: $L=1.245 \text{ m}$ $d_i=0.014 \text{ m}$								
$\Delta T_f = 40 \text{ }^\circ\text{C}$ , $Pr=3.14$								
5000	8852.2	1.5151	7251.1	1.4005	6452.3	1.3376	5939.5	1.2947
10000	18506	1.4211	15159	1.3136	13489	1.2546	12417	1.2143
15000	28488	1.3688	23335	1.2653	20765	1.2084	19114	1.1696
20000	38689	1.3329	31691	1.2321	28200	1.1767	25959	1.139
25000	49056	1.3057	40183	1.2069	35756	1.1527	32914	1.1157
30000	59557	1.2838	48784	1.1868	43410	1.1334	39960	1.0971
35000	70170	1.2657	57478	1.17	51146	1.1174	47082	1.0815
40000	80882	1.2501	66252	1.1556	58954	1.1037	54269	1.0683
$\Delta T_f = 50 \text{ }^\circ\text{C}$ , $Pr=2.71$								
5000	8852.2	1.5131	7251.1	1.3987	6452.3	1.3358	5939.5	1.293
10000	18506	1.4192	15159	1.3119	13489	1.2529	12417	1.2127
15000	28488	1.367	23335	1.2636	20765	1.2068	19114	1.1681
20000	38689	1.3311	31691	1.2305	28200	1.1752	25959	1.1375
25000	49056	1.304	40183	1.2054	35756	1.1512	32914	1.1142
30000	59557	1.2822	48784	1.1852	43410	1.1319	39960	1.0956
35000	70170	1.264	57478	1.1685	51146	1.1159	47082	1.0801
40000	80882	1.2485	66252	1.1541	58954	1.1022	54269	1.0669

**Table C-43:** Application of FG-3 Criterion to the Tube-Side Heat Transfer Enhancement for all Geometrical Characteristics and Conditions.

Re Inner tube	FG-3 Criterion, Wire Coil, e = 1 mm							
	p = 10 mm		p = 20 mm		p = 30 mm		p = 40 mm	
	Re <sub>o</sub>	P <sub>a</sub> /P <sub>o</sub>	Re <sub>o</sub>	P <sub>a</sub> /P <sub>o</sub>	Re <sub>o</sub>	P <sub>a</sub> /P <sub>o</sub>	Re <sub>o</sub>	P <sub>a</sub> /P <sub>o</sub>
Inner Tube Dimensions: L=1.245 m d <sub>i</sub> = 0.011 m								
$\Delta T_f = 40^\circ\text{C}, \text{Pr}=3.14$								
5000	13965.3	0.2957	10409	0.3825	8764.86	0.4447	7758.35	0.4949
10000	27034.1	0.3647	20149.9	0.4719	16967.1	0.5486	15018.7	0.6105
15000	39784.8	0.4124	29653.6	0.5335	24969.7	0.6203	22102.3	0.6903
20000	52333.1	0.4499	39006.5	0.5821	32845.3	0.6768	29073.5	0.7531
25000	64733.1	0.4814	48248.8	0.6228	40627.7	0.7241	35962.3	0.8058
30000	77016	0.5087	57403.9	0.6581	48336.7	0.7652	42786	0.8515
35000	89202.6	0.533	66487.2	0.6896	55985.2	0.8017	49556.2	0.8922
40000	101307	0.555	75509.4	0.7181	63582.3	0.8348	56280.9	0.929
$\Delta T_f = 50^\circ\text{C}, \text{Pr}=2.72$								
5000	13943.4	0.2969	10392.7	0.3842	8751.12	0.4467	7746.19	0.497
10000	26991.8	0.3663	20118.3	0.4739	16940.5	0.551	14995.2	0.6131
15000	39722.5	0.4141	29607.1	0.5358	24930.6	0.623	22067.7	0.6932
20000	52251.1	0.4518	38945.4	0.5846	32793.8	0.6797	29027.9	0.7563
25000	64631.6	0.4834	48173.2	0.6255	40564	0.7272	35905.9	0.8092
30000	76895.3	0.5109	57313.9	0.661	48261	0.7685	42719	0.8552
35000	89062.8	0.5353	66383	0.6926	55897.5	0.8052	49478.6	0.896
40000	101148	0.5574	75391	0.7211	63482.7	0.8384	56192.7	0.933
Inner Tube Dimensions: L=1.245 m d <sub>i</sub> = 0.014 m								
$\Delta T_f = 40^\circ\text{C}, \text{Pr}=3.14$								
5000	14576.8	0.2564	10864.8	0.3317	9148.65	0.3856	8098.2	0.4291
10000	28217.9	0.3162	21032.2	0.4091	17710.1	0.4757	15676.6	0.5293
15000	41526.9	0.3575	30952.1	0.4626	26063.1	0.5378	23070.5	0.5985
20000	54624.7	0.3901	40714.5	0.5047	34283.5	0.5868	30347	0.6529
25000	67567.6	0.4174	50361.5	0.54	42406.7	0.6278	37537.5	0.6986
30000	80388.4	0.441	59917.5	0.5706	50453.3	0.6634	44660.2	0.7382
35000	93108.6	0.4621	69398.5	0.5979	58436.7	0.6951	51727	0.7735
40000	105743	0.4812	78815.8	0.6226	66366.5	0.7238	58746.2	0.8054
$\Delta T_f = 50^\circ\text{C}, \text{Pr}=2.71$								
$\Delta T_f = 40^\circ\text{C}, \text{Pr}=3.14$								
5000	14553.9	0.2575	10847.8	0.3331	9134.31	0.3873	8085.5	0.4309
10000	28173.7	0.3176	20999.3	0.4109	17682.3	0.4777	15652	0.5316
15000	41461.8	0.3591	30903.6	0.4646	26022.2	0.5401	23034.3	0.601
20000	54539.1	0.3918	40650.7	0.5069	34229.7	0.5893	30299.5	0.6557
25000	67461.7	0.4191	50282.6	0.5423	42340.2	0.6305	37478.7	0.7016
30000	80262.4	0.4429	59823.6	0.5731	50374.2	0.6663	44590.2	0.7414
35000	92962.7	0.4641	69289.7	0.6005	58345.1	0.6981	51645.9	0.7768
40000	105578	0.4833	78692.2	0.6252	66262.4	0.7269	58654.1	0.8089

**Table C-44:** Application of FN-1 Criterion to the Tube-Side Heat Transfer Enhancement for all Geometrical Characteristics and Conditions.

Re Inner tube	FN-1 Criterion, Wire Coil, $e = 1 \text{ mm}$							
	$p = 10 \text{ mm}$		$p = 20 \text{ mm}$		$p = 30 \text{ mm}$		$p = 40 \text{ mm}$	
	$\text{Re}_o$	$A_a/A_o$	$\text{Re}_o$	$A_a/A_o$	$\text{Re}_o$	$A_a/A_o$	$\text{Re}_o$	$A_a/A_o$
Inner Tube Dimensions: $L=1.245 \text{ m}$ $d_i=0.011 \text{ m}$								
$\Delta T_f = 40^\circ \text{C}, \text{Pr}=3.14$								
5000	7344.63	0.5855	6270.82	0.6556	5717.02	0.7005	5354.01	0.7342
10000	15882.2	0.6421	13560.1	0.719	12362.6	0.7682	11577.6	0.8051
15000	24936.6	0.6776	21290.8	0.7588	19410.5	0.8108	18178	0.8497
20000	34343.9	0.7041	29322.7	0.7884	26733.1	0.8424	25035.6	0.8829
25000	44022.6	0.7253	37586.4	0.8122	34267	0.8678	32091.2	0.9095
30000	53923.3	0.7431	46039.6	0.8321	41973.6	0.8891	39308.5	0.9318
35000	64012.5	0.7585	54653.7	0.8494	49827	0.9075	46663.2	0.9511
40000	74265.9	0.7721	63408	0.8646	57808.2	0.9238	54137.6	0.9682
$\Delta T_f = 50^\circ \text{C}, \text{Pr}=2.72$								
5000	7349.69	0.5866	6275.14	0.6569	5720.96	0.7018	5357.7	0.7356
10000	15893.1	0.6433	13569.5	0.7203	12371.1	0.7696	11585.6	0.8066
15000	24953.8	0.6789	21305.5	0.7603	19423.9	0.8123	18190.5	0.8513
20000	34367.6	0.7054	29342.9	0.7899	26751.5	0.844	25052.9	0.8846
25000	44053	0.7267	37612.3	0.8137	34290.6	0.8694	32113.3	0.9112
30000	53960.5	0.7445	46071.3	0.8337	42002.6	0.8907	39335.6	0.9336
35000	64056.6	0.7599	54691.4	0.851	49861.3	0.9092	46695.3	0.9529
40000	74317.1	0.7735	63451.7	0.8662	57848	0.9255	54174.9	0.97
Inner Tube Dimensions: $L=1.245 \text{ m}$ $d_i=0.014 \text{ m}$								
$\Delta T_f = 40^\circ \text{C}, \text{Pr}=3.14$								
5000	7110.46	0.5499	6070.89	0.6158	5534.74	0.6579	5183.27	0.6896
10000	15375.8	0.603	13127.8	0.6753	11968.4	0.7215	11208.4	0.7562
15000	24141.5	0.6365	20612	0.7127	18791.6	0.7615	17598.3	0.7981
20000	33248.9	0.6613	28387.8	0.7405	25880.8	0.7912	24237.3	0.8292
25000	42619.1	0.6812	36388	0.7628	33174.4	0.815	31067.8	0.8542
30000	52204.1	0.6979	44571.7	0.7816	40635.4	0.835	38054.9	0.8752
35000	61971.6	0.7124	52911.2	0.7978	48238.3	0.8523	45175.1	0.8933
40000	71898.1	0.7252	61386.4	0.8121	55965.1	0.8676	52411.2	0.9093
$\Delta T_f = 50^\circ \text{C}, \text{Pr}=2.71$								
$\Delta T_f = 40^\circ \text{C}, \text{Pr}=3.14$								
5000	7115.36	0.551	6075.07	0.617	5538.56	0.6592	5186.85	0.6909
10000	15386.4	0.6042	13136.9	0.6766	11976.7	0.7229	11216.1	0.7576
15000	24158.2	0.6377	20626.2	0.7141	18804.6	0.7629	17610.5	0.7996
20000	33271.8	0.6625	28407.4	0.7419	25898.6	0.7927	24254	0.8308
25000	42648.4	0.6825	36413.1	0.7643	33197.3	0.8166	31089.2	0.8558
30000	52240.1	0.6993	44602.4	0.783	40663.4	0.8366	38081.2	0.8768
35000	62014.3	0.7137	52947.6	0.7993	48271.6	0.854	45206.3	0.895
40000	71947.6	0.7265	61428.7	0.8136	56003.6	0.8693	52447.3	0.911

**Table C-45:** Application of FG-2a Criterion to the Annulus-Side Heat Transfer Enhancement for all Geometrical Characteristics and Conditions.

Re	FG-2a Criterion, Wire Coil, e = 1 mm								
	Annulus	p = 10 mm		p = 20 mm		p = 30 mm		p = 40 mm	
		Re <sub>o</sub>	q <sub>a</sub> /q <sub>o</sub>						
Annulus Dimensions: L=1.245 m D <sub>o</sub> =0.028 m D <sub>i</sub> =0.0125 m									
3000	4314.35	2.3679	3800.3	2.3669	3528.44	2.2033	3347.46	2.0056	
4000	5810.48	2.1562	5118.17	2.1921	4752.04	2.0626	4508.29	1.8927	
5000	7319.85	2.0051	6447.71	2.0654	5986.46	1.9597	5679.4	1.8094	
6000	8839.86	1.8896	7786.61	1.9674	7229.58	1.8794	6858.76	1.7442	
7000	10368.8	1.7971	9133.35	1.8882	8479.98	1.8141	8045.02	1.6908	
8000	11905.3	1.7206	10486.8	1.8221	9736.65	1.7594	9237.24	1.6459	
9000	13448.6	1.6559	11846.3	1.7657	10998.8	1.7125	10434.7	1.6073	
10000	14998	1.6001	13211	1.7168	12265.9	1.6716	11636.8	1.5736	
Annulus Dimensions: L=1.245 m D <sub>o</sub> =0.028 m D <sub>i</sub> =0.0155 m									
3000	4733.81	2.1126	4169.72	2.0804	3871.45	1.8978	3672.86	1.7009	
4000	6375.39	1.9507	5615.7	1.9567	5214	1.806	4946.53	1.6328	
5000	8031.51	1.8337	7074.48	1.8659	6568.42	1.7378	6231.48	1.5818	
6000	9699.3	1.7433	8543.53	1.7948	7932.39	1.684	7525.48	1.5414	
7000	11376.9	1.6704	10021.2	1.7368	9304.35	1.6398	8827.07	1.5079	
8000	13062.8	1.6097	11506.3	1.688	10683.2	1.6025	10135.2	1.4796	
9000	14756.2	1.558	12997.8	1.6462	12068.1	1.5703	11449	1.455	
10000	16456.1	1.5132	14495.2	1.6097	13458.3	1.542	12768	1.4334	
Re	FG-2a Criterion, Wire Coil, e = 2.2 mm								
	Annulus	p = 10 mm		p = 20 mm		p = 30 mm		p = 40 mm	
		Re <sub>o</sub>	q <sub>a</sub> /q <sub>o</sub>						
Annulus Dimensions: L=1.245 m D <sub>o</sub> =0.028 m D <sub>i</sub> =0.0125 m									
3000	5824.29	1.6344	5130.34	1.8074	4763.33	1.7938	4519.01	1.7129	
4000	7844.04	1.5393	6909.44	1.7376	6415.16	1.7472	6086.11	1.6848	
5000	9881.66	1.4694	8704.28	1.6854	8081.61	1.7119	7667.08	1.6632	
6000	11933.6	1.4147	10511.8	1.6439	9759.8	1.6836	9259.19	1.6459	
7000	13997.6	1.37	12329.9	1.6096	11447.8	1.6601	10860.6	1.6313	
8000	16072	1.3324	14157.1	1.5804	13144.3	1.6399	12470.1	1.6188	
9000	18155.4	1.3001	15992.3	1.5552	14848.2	1.6223	14086.6	1.6078	
10000	20247	1.2719	17834.6	1.5329	16558.8	1.6068	15709.4	1.5981	
Annulus Dimensions: L=1.245 m D <sub>o</sub> =0.028 m D <sub>i</sub> =0.0155 m									
3000	6390.55	1.2978	5629.05	1.4266	5226.39	1.3955	4958.29	1.3175	
4000	8606.67	1.2431	7581.09	1.3975	7038.8	1.3865	6677.73	1.323	
5000	10842.4	1.2023	9550.41	1.3753	8867.25	1.3796	8412.39	1.3273	
6000	13093.9	1.17	11533.6	1.3575	10708.6	1.374	10159.3	1.3308	
7000	15358.6	1.1433	13528.4	1.3425	12560.7	1.3693	11916.4	1.3338	
8000	17634.6	1.1207	15533.2	1.3297	14422.1	1.3652	13682.3	1.3364	
9000	19920.6	1.1012	17546.8	1.3186	16291.7	1.3616	15456	1.3387	
10000	22215.5	1.084	19568.3	1.3086	18168.5	1.3584	17236.5	1.3407	
Re	FG-2a Criterion, Circular Ribs, e = 2.2 mm								
	Annulus	p = 10 mm		p = 20 mm		p = 30 mm		p = 40 mm	
		Re <sub>o</sub>	q <sub>a</sub> /q <sub>o</sub>						
Annulus Dimensions: L=1.245 m D <sub>o</sub> =0.028 m D <sub>i</sub> =0.0125 m									
3000	6754.83	1.277	5957.6	1.4423	5535.55	1.5593	5254.4	1.6529	
4000	9077.71	1.2701	8006.34	1.4193	7439.14	1.5253	7061.31	1.6101	
5000	11416.7	1.2649	10069.3	1.4018	9355.96	1.4994	8880.77	1.5777	
6000	13768.7	1.2606	12143.7	1.3876	11283.4	1.4786	10710.3	1.5517	
7000	16131.5	1.2569	14227.6	1.3758	13219.7	1.4613	12548.2	1.53	
8000	18503.5	1.2538	16319.7	1.3656	15163.6	1.4464	14393.4	1.5115	
9000	20883.8	1.251	18419	1.3566	17114.2	1.4334	16244.9	1.4954	
10000	23271.3	1.2486	20524.7	1.3487	19070.7	1.4218	18102.1	1.4811	
Annulus Dimensions: L=1.245 m D <sub>o</sub> =0.028 m D <sub>i</sub> =0.0155 m									
3000	7694.74	1.035	6786.49	1.2078	6305.75	1.3302	5985.45	1.4282	
4000	10340.9	1.0025	9120.27	1.1589	8474.2	1.2695	8043.76	1.3579	
5000	13005.3	0.978	11470.3	1.1223	10657.7	1.2243	10116.4	1.3058	
6000	15684.6	0.9585	13833.2	1.0933	12853.3	1.1885	12200.4	1.2647	
7000	18376.1	0.9423	16207.1	1.0693	15059	1.1592	14294.1	1.231	
8000	21078.3	0.9284	18590.3	1.049	17273.4	1.1343	16396	1.2025	
9000	23789.7	0.9164	20981.7	1.0314	19495.4	1.1128	18505.1	1.1779	
10000	26509.4	0.9058	23380.4	1.0159	21724.1	1.0939	20620.7	1.1564	

**Table C-46:** Application of FG-3 Criterion to the Annulus-Side Heat Transfer Enhancement for all Geometrical Characteristics and Conditions.

Re	FG-3 Criterion, Wire Coil, e = 1 mm								
	Annulus	p = 10 mm		p = 20 mm		p = 30 mm		p = 40 mm	
		Re <sub>o</sub>	P <sub>a</sub> /P <sub>o</sub>						
Annulus Dimensions: L=1.245 m D <sub>o</sub> = 0.028 m D <sub>i</sub> = 0.0125 m									
3000	11995	0.0658	10560.4	0.0659	9006.28	0.0827	7642.77	0.1112	
4000	14455.9	0.0885	12985.3	0.084	11216.3	0.1018	9609.15	0.1335	
5000	16707.5	0.1113	15243.4	0.1014	13297.5	0.1196	11476.6	0.1539	
6000	18805.1	0.1342	17377	0.1182	15281.7	0.1365	13268.7	0.1728	
7000	20782.7	0.1573	19412.3	0.1345	17188.5	0.1526	15000.6	0.1906	
8000	22663.2	0.1804	21367.1	0.1505	19031.5	0.1681	16682.6	0.2075	
9000	24462.7	0.2036	23254.1	0.1662	20820.6	0.1831	18322	0.2236	
10000	26193.1	0.2269	25082.8	0.1816	22563	0.1976	19924.6	0.2391	
Annulus Dimensions: L=1.245 m D <sub>o</sub> = 0.028 m D <sub>i</sub> = 0.0155 m									
3000	11495.2	0.0944	9942.94	0.0991	8278.59	0.1324	6896.85	0.1871	
4000	14084.3	0.1214	12451.7	0.1202	10512.2	0.1548	8848.8	0.2128	
5000	16487.7	0.1476	14826	0.1397	12652	0.1748	10735.9	0.2352	
6000	18753	0.1731	17098.2	0.1579	14719.8	0.193	12572.8	0.2553	
7000	20909.4	0.1981	19289	0.1751	16729.7	0.2099	14369	0.2735	
8000	22976.7	0.2226	21412.4	0.1916	18691.3	0.2258	16131.1	0.2904	
9000	24969.3	0.2467	23478.5	0.2074	20611.5	0.2407	17863.9	0.3062	
10000	26897.7	0.2706	25495.2	0.2226	22495.9	0.2549	19571.1	0.321	
Re	FG-3 Criterion, Wire Coil, e = 2.2 mm								
	Annulus	p = 10 mm		p = 20 mm		p = 30 mm		p = 40 mm	
		Re <sub>o</sub>	P <sub>a</sub> /P <sub>o</sub>						
Annulus Dimensions: L=1.245 m D <sub>o</sub> = 0.028 m D <sub>i</sub> = 0.0125 m									
3000	10431.2	0.2122	10353.2	0.1544	9527.06	0.1581	8556.88	0.1829	
4000	13084.6	0.2563	13307.4	0.1749	12436.5	0.1718	11299.8	0.1928	
5000	15599.3	0.2968	16168	0.1925	15292.3	0.1833	14019.6	0.2008	
6000	18008.7	0.3346	18956.1	0.2083	18106	0.1932	16721.2	0.2075	
7000	20334	0.3703	21685.3	0.2227	20885.3	0.202	19407.6	0.2134	
8000	22589.6	0.4043	24365.1	0.2359	23635.4	0.2099	22081.2	0.2187	
9000	24786	0.4368	27002.5	0.2482	26360.2	0.2172	24743.5	0.2234	
10000	26931	0.4681	29602.7	0.2597	29062.7	0.2239	27396	0.2277	
Annulus Dimensions: L=1.245 m D <sub>o</sub> = 0.028 m D <sub>i</sub> = 0.0155 m									
3000	8706.04	0.4393	8580.1	0.3258	7760.2	0.3494	6877.05	0.4188	
4000	11141.8	0.5032	11276.1	0.3477	10371.8	0.3565	9307.73	0.4133	
5000	13491.3	0.559	13938.2	0.3658	12988.9	0.3622	11770.6	0.4092	
6000	15774.4	0.6093	16573.4	0.3812	15610.4	0.3669	14259.4	0.4058	
7000	18003.6	0.6552	19186.6	0.3947	18235.6	0.3709	16770	0.4029	
8000	20187.7	0.6979	21781.1	0.4068	20863.9	0.3744	19299.4	0.4005	
9000	22333.2	0.7377	24359.3	0.4178	23495	0.3775	21845.3	0.3983	
10000	24444.9	0.7754	26923.1	0.4279	26128.5	0.3804	24406	0.3964	
Re	FG-3 Criterion, Circular Ribs, e = 2.2 mm								
	Annulus	p = 10 mm		p = 20 mm		p = 30 mm		p = 40 mm	
		Re <sub>o</sub>	P <sub>a</sub> /P <sub>o</sub>						
Annulus Dimensions: L=1.245 m D <sub>o</sub> = 0.028 m D <sub>i</sub> = 0.0125 m									
3000	9027.7	0.4622	9199.1	0.3148	9376.2	0.2461	9537.1	0.2047	
4000	12055	0.4702	12130	0.3311	12275	0.2638	12424	0.2224	
5000	15086	0.4764	15032	0.3444	15128	0.2785	15253	0.2372	
6000	18121	0.4815	17911	0.3556	17945	0.291	18036	0.2499	
7000	21158	0.4859	20772	0.3654	20731	0.3021	20782	0.2613	
8000	24198	0.4898	23617	0.3741	23493	0.312	23496	0.2715	
9000	27239	0.4932	26448	0.3819	26232	0.321	26183	0.2809	
10000	30283	0.4963	29267	0.389	28953	0.3293	28845	0.2895	
Annulus Dimensions: L=1.245 m D <sub>o</sub> = 0.028 m D <sub>i</sub> = 0.0155 m									
3000	8014.8	0.8972	8490.4	0.551	8845.5	0.4064	9135.1	0.3247	
4000	10371	0.9922	10864	0.6279	11246	0.471	11563	0.3807	
5000	12667	1.0726	13153	0.6948	13549	0.528	13883	0.4308	
6000	14915	1.1432	15377	0.7547	15776	0.5798	16120	0.4765	
7000	17124	1.2065	17548	0.8094	17943	0.6274	18291	0.519	
8000	19301	1.2641	19675	0.8599	20058	0.6719	20406	0.5588	
9000	21449	1.3173	21764	0.9071	22131	0.7137	22473	0.5964	
10000	23573	1.3667	23821	0.9516	24165	0.7533	24499	0.6322	

**Table C-47:** Application of FN-1 Criterion to the Annulus-Side Heat Transfer Enhancement for all Geometrical Characteristics and Conditions.

Re	FN-1 Criterion, Wire Coil, e = 1 mm								
	Annulus	p = 10 mm		p = 20 mm		p = 30 mm		p = 40 mm	
		Re <sub>o</sub>	A <sub>a</sub> /A <sub>o</sub>						
Annulus Dimensions: L=1.245 m D <sub>o</sub> =0.028 m D <sub>i</sub> =0.0125 m									
3000	2684.96	0.2831	2365.62	0.2833	2284.67	0.3146	2282.54	0.361	
4000	3807.28	0.3247	3323.34	0.317	3190.71	0.3465	3173.7	0.393	
5000	4991.87	0.3612	4325.99	0.3458	4134.36	0.3735	4098.26	0.4198	
6000	6228.59	0.394	5365.96	0.3714	5109.09	0.3971	5050.35	0.443	
7000	7510.41	0.424	6438.03	0.3944	6110.46	0.4182	6025.94	0.4636	
8000	8832.14	0.4519	7538.37	0.4155	7135.22	0.4373	7022.13	0.4822	
9000	10189.8	0.4779	8664.03	0.4351	8180.87	0.455	8036.68	0.4992	
10000	11580.2	0.5026	9812.68	0.4533	9245.44	0.4714	9067.82	0.515	
Annulus Dimensions: L=1.245 m D <sub>o</sub> =0.028 m D <sub>i</sub> =0.0155 m									
3000	3136.87	0.3346	2786.49	0.3422	2721.29	0.3915	2742.08	0.4595	
4000	4414.14	0.376	3881.52	0.3743	3766.4	0.4209	3777	0.4879	
5000	5753.28	0.4117	5019.43	0.4013	4846.32	0.4453	4841.89	0.5111	
6000	7143.87	0.4433	6192.72	0.4248	5954.82	0.4663	5931.3	0.5308	
7000	8578.77	0.4719	7396.27	0.4457	7087.67	0.4848	7041.53	0.5481	
8000	10052.7	0.4981	8626.34	0.4647	8241.77	0.5014	8169.89	0.5636	
9000	11561.7	0.5225	9880.09	0.4821	9414.8	0.5166	9314.36	0.5775	
10000	13102.5	0.5454	11155.2	0.4982	10604.9	0.5305	10473.3	0.5903	
Re	FN-1 Criterion, Wire Coil, e = 2.2 mm								
	Annulus	p = 10 mm		p = 20 mm		p = 30 mm		p = 40 mm	
		Re <sub>o</sub>	A <sub>a</sub> /A <sub>o</sub>						
Annulus Dimensions: L=1.245 m D <sub>o</sub> =0.028 m D <sub>i</sub> =0.0125 m									
3000	4444.81	0.4872	3704.36	0.4205	3453.64	0.4251	3360.76	0.4548	
4000	6186.83	0.5318	5098.17	0.4454	4719.13	0.4418	4567.68	0.466	
5000	7995.86	0.5693	6531.3	0.4657	6012.16	0.4552	5795.07	0.4749	
6000	9860.13	0.6018	7996.56	0.4831	7327.55	0.4665	7039.03	0.4822	
7000	11771.6	0.6308	9489.09	0.4982	8661.84	0.4762	8296.93	0.4885	
8000	13724.6	0.657	11005.4	0.5117	10012.5	0.4848	9566.89	0.4941	
9000	15714.4	0.681	12542.7	0.5239	11377.7	0.4925	10847.5	0.499	
10000	17737.6	0.7033	14099.1	0.5351	12755.9	0.4995	12137.6	0.5034	
Annulus Dimensions: L=1.245 m D <sub>o</sub> =0.028 m D <sub>i</sub> =0.0155 m									
3000	5536.74	0.6828	4629.44	0.5944	4350.88	0.614	4260.26	0.6679	
4000	7635.37	0.7272	6306.02	0.6127	5880.46	0.6198	5724.51	0.6638	
5000	9797.01	0.7636	8014.37	0.6272	7428.38	0.6243	7198.74	0.6607	
6000	12010.2	0.7947	9748.49	0.6393	8991.08	0.6281	8680.99	0.6581	
7000	14267.3	0.8219	11504.3	0.6497	10566.2	0.6313	10169.9	0.656	
8000	16562.6	0.8463	13279	0.6589	12152	0.634	11664.6	0.6541	
9000	18891.8	0.8684	15070.2	0.6671	13747.2	0.6365	13164.4	0.6525	
10000	21251.6	0.8887	16876.3	0.6745	15350.8	0.6387	14668.6	0.651	
Re	FN-1 Criterion, Circular Ribs, e = 2.2 mm								
	Annulus	p = 10 mm		p = 20 mm		p = 30 mm		p = 40 mm	
		Re <sub>o</sub>	A <sub>a</sub> /A <sub>o</sub>						
Annulus Dimensions: L=1.245 m D <sub>o</sub> =0.028 m D <sub>i</sub> =0.0125 m									
3000	5904.58	0.6991	4870.34	0.585	4335.18	0.5219	3985.13	0.4792	
4000	7958.58	0.7047	6603.18	0.5989	5897.11	0.539	5433.39	0.498	
5000	10032.2	0.709	8361.61	0.6099	7486.72	0.5527	6910.31	0.513	
6000	12121.7	0.7125	10140.7	0.6191	9098.75	0.5641	8410.47	0.5257	
7000	14224.3	0.7155	11937.2	0.6269	10729.7	0.5739	9930.23	0.5366	
8000	16338.4	0.7181	13748.7	0.6338	12376.9	0.5826	11467	0.5462	
9000	18462.4	0.7205	15573.5	0.6399	14038.6	0.5904	13018.7	0.5549	
10000	20595.4	0.7225	17410	0.6454	15713.2	0.5974	14584	0.5627	
Annulus Dimensions: L=1.245 m D <sub>o</sub> =0.028 m D <sub>i</sub> =0.0155 m									
3000	7550.65	0.951	6116.79	0.7585	5389.65	0.6586	4919.6	0.5935	
4000	10326.6	0.9964	8409.48	0.8058	7431.69	0.7052	6797.46	0.639	
5000	13165.3	1.0331	10764.7	0.8446	9534.84	0.7436	8734.98	0.6766	
6000	16054.8	1.064	13170.9	0.8776	11688	0.7766	10721.4	0.7091	
7000	18987.4	1.091	15620.4	0.9066	13883.7	0.8056	12749.5	0.7377	
8000	21957.4	1.1148	18107.6	0.9324	16116.4	0.8316	14813.9	0.7634	
9000	24960.4	1.1363	20628.2	0.9558	18382	0.8552	16910.6	0.7868	
10000	27993.1	1.1559	23178.8	0.9772	20677.3	0.8769	19036.4	0.8084	

## الخلاصة

تم استخدام ثلاثة طرق لتعزيز انتقال الحرارة باستخدام مسببات شدة الاضطراب وذلك من أجل زيادة الكفاءة الحرارية لمبادل حراري من نوع الانابيب المترنكة بطول 1245 ملم وبقطر خارجي 28 ملم وانبوب داخلي قابل للتغيير بقطرتين 11 و 14 ملم. محلزنات سلكية بقطر 1 ملم وفواصل لف بمقدار 10، 20، 30 و 40 ملم استخدمت كمسببات شدة الاضطراب داخل الانبوب الداخلي للمبادل الحراري في مدى رقم رينولدرز بين 5000 و 40000. كما تم استخدام نوعين جديدين من مسببات شدة الاضطراب لزيادة انتقال الحرارة في الجانب الخارجي لنفس المبادل الحراري في مدى رقم رينولدرز بين 3000 و 10000. النوع الاول تم باستخدام محلزنات سلكية بقطر 1 و 2.2 ملم وفواصل لف بمقدار 10، 20، 30 و 40 ملم تم تركيبها على السطح الخارجي للانبوب الداخلي. أما الطريقة الثانية فكانت باستخدام نتوءات دائرية المقطع بقطر 2.2 ملم ركبت بنفس الفواصل والموقع. استخدام الماء في جانبي المبادل الحراري كما تم تنويع الظروف التجريبية وذلك بتغيير معدل الجريان الكتلي للجانب الغير المراد رفع كفائه وكذلك بتغيير درجة حرارة الدخول للمائع الساخن. الهدف من تغيير الظروف التجريبية هو الحصول على اكبر قدر من النقااط التجريبية للحصول على معادلات تجريبية بأدق ما يمكن بالإضافة الى معرفة مدى تأثير تغير تلك الظروف.

تم زيادة انتقال الحرارة في داخل الانبوب الداخلي بمقدار 2.43 ضعف ما هو عليه في حالة استخدام انبوب املس بنفس رقم رينولدرز وكان ذلك مصحوبا بازدياد معامل الاحتاك بمقدار 4.75 اضعاف. اما في الجانب الخارجي للمبادل فقد تم زيادة انتقال الحرارة بمقدار 3.25 اضعاف مقارنة بالجانب الخارجي الاملس وكان ذلك مصحوباً بزيادة معامل الاحتاك بمقدار 2.63 اضعاف.

تم الحصول على معادلات تجريبية جديدة لرقم نسلت ومعامل الاحتاك لجانبي المبادل الحراري وذلك كدوال لرقمي رينولدرز وبرانتل بالإضافة للخواص الهندسية للمضافات والانابيب. كما تم تطبيق معايير تقييم الانجاز (PEC) الموضوعة من قبل وب وبيرجلز وذلك لتحديد الطريقة الاكثر فائدة.

## **شكر وتقدير**

بعد شكر الباري عز وجل والثناء عليه، اود ان اتقدم بالشكر الجليل الى استاذى الفاضل والمشرف على هذه الرسالة الاستاذ الدكتور قاسم جبار السليمان والذي لولا توجيهاته لما خرج هذا العمل بهذه الصورة البهية، كما أتقدم بوافر الشكر والامتنان للسيد عميد كلية الهندسة لما ابداه من دعم معنوي لي اثناء العمل التجربى، وأشكرا السيد رئيس قسم الهندسة الكيمياوية والساسة التدريسيين والكادر العامل في قسم الهندسة الكيمياوية.

ولا انسى ان أشكرا جميع زملائي وزميلاتي في جامعة النهرین لما كان لهم من دور كبير في التخفيف من معاناة التعب والانتظار.

**عباس نوار**

# تعزيز إنتقال الحرارة

## باستخدام مسبب شدة الإضطراب

رسالة

مقدمة إلى كلية الهندسة في جامعة النهرين  
وهي جزء من متطلبات نيل درجة ماجستير علوم  
في الهندسة الكيميائية

من قبل

عباس نوار زناد  
(بكالوريوس علوم في الهندسة الكيميائية ، 1995)

1432 هـ  
2011 م

ربيع الأول  
شباط